Universität Bremen

Synthesis and Characterization of Iron Oxide Nanoparticles and Investigation of their Biocompatibility on Astrocyte Cultures

DISSERTATION

zur Erlangung des Grades eines
Doktors der Naturwissenschaften (Dr. rer. nat.)
des Fachbereichs 2 Biologie/Chemie der Universität Bremen

2012

vorgelegt von
MARK GEPPERT

Dekan: Prof. Dr. Sørge Kelm

1. Gutachter: Prof. Dr. Ralf Dringen
2. Gutachter: Prof. Dr. Sørge Kelm

Hiermit versichere ich, die vorliegende Dissertationsarbeit selbstständig und nur unter Verwendung der angegebenen Hilfsmittel angefertigt zu haben. Diese Arbeit wurde zuvor nicht an anderer Stelle eingereicht.

Bremen, 15. März 2012

(Mark Geppert)

Table of contents

I   Acknowledgements

First I would like to gratefully thank Prof. Dr. Ralf Dringen for offering me this highly interesting topic and giving me the opportunity to work under his guidance. I am very thankful to his enormous encouragement he gave me all the time during the work on this thesis. His huge spectrum of knowledge regarding brain cells, metabolism and nanoparticles was a great help for me during all the discussions I had with him. I further like to thank him for giving me the opportunity to visit national and international conferences.

My second acknowledge goes to Prof. Dr. Sørge Kelm for being the second referee on this thesis.

I would like to thank all co-authors of my publications and manuscripts of this thesis for the very good and always goal-oriented cooperation. Especially I like to thank Dr. Michaela Hohnholt for all her contributions and Dr. Ingo Grunwald for giving me the opportunity to work at the Fraunhofer Institute thereby using methods which were essential for improving the quality of this thesis.

I would like to thank all the members of the working group of Prof. Dr. Dringen for the constant help and support. I especially want to mention the always very good working atmosphere in the group. Yvonne Köhler and Monica Cox get my special thanks for always excellently managing the laboratory.

I acknowledge the graduate school nanoToxCom under the guidance of Prof. Dr. Juliane Filser which gave me the opportunity to always critically discuss aspects of my thesis in a broader scientific field. I would like to thank very much the Hans-Böckler-Stiftung for financially supporting my thesis in the connection with the graduate school nanoToxCom and for giving me the opportunity to visit their meetings.

Finally, I would like to thank very much my beloved parents and my dear brother. Without your endless encouragement, writing such a thesis would not have been possible.

II   Information on the structure of the thesis

This thesis is divided into three main chapters (1) Introduction, (2) Results and (3) Summarizing discussion.

The first chapter introduces the reader into the basic knowledge about iron oxide nanoparticles and brain astrocytes and gives a short review on the current scientific research status.

The second part presents the results obtained during the laboratory work of this thesis. This chapter is divided into six sub-chapters containing publications/manuscripts that describe uptake, reactivity and biocompatibility of iron oxide nanoparticles in brain astrocyte cultures. The sub-chapters 2.1 to 2.4 contain already published articles which are embedded as portable document format in this thesis. The sub-chapters 2.5 and 2.6 contain two manuscripts that were submitted for publication. These manuscripts were included in the thesis in the style as they were submitted for publication. However, the running text of the manuscripts was adjusted to the layout of this thesis and the figures and tables were positioned together with their legends directly after the respective results parts.

The third part of the thesis presents a summarizing discussion of the key-findings of the investigations performed. Furthermore, it presences an outlook for future studies on the topic.

III   Summary

Magnetic iron oxide nanoparticles (IONPs) are used as tools for a wide range of biomedical and (neuro)biological applications, for example as contrast agent in magnetic resonance imaging, as transporter for drug delivery across biological barriers or for cancer treatment by magnetic field-induced hyperthermia. However, the knowledge on the effects of such particles on brain cells have only recently been addressed. This thesis describes the synthesis and characterization of citrate- and dimercaptosuccinate (DMSA)-coated IONPs. In addition, the uptake, reactivity and biocompatibility of such particles were investigated for astrocyte-rich primary cultures as a model system for brain astrocytes. Citrate- and DMSA-coated IONPs were accumulated by viable cultured astrocytes in a time- and concentration-dependent process leading to more than 100fold elevated specific cellular iron contents. Electron microscopy revealed that IONPs were present in intracellular vesicles as well as attached extracellularly to the cell membrane. Lowering the incubation temperature to 4°C reduced the iron accumulation to about 50% which represented almost exclusively membrane associated extracellular IONPs. Presence of an external magnetic field increased the amount of cellular iron by 2-4fold, while presence of serum strongly reduced IONP-accumulation by up to 90% compared with the respective controls. Application of endocytosis inhibitors revealed that clathrin-mediated endocytosis and macropinocytosis contributed to IONP-uptake in serum-containing conditions. However, additional mechanisms are responsible for IONP-uptake under serum-free conditions. Prolonged presence of IONPs in cultured astrocytes for up to 7 d after a transient loading period of 4 h neither compromised cell viability nor affected basic metabolic pathways. However, a transient formation of reactive oxygen species and a delayed upregulation of cellular ferritin indicate that iron ions were liberated from the accumulated particles. In summary, this thesis revealed that viable astrocytes efficiently take up and safely store IONPs and IONP-derived iron, supporting the view that such particles can be used as save tools for diagnostic or therapeutic approaches in the brain.

IV Zusammenfassung

Magnetische Eisenoxid-Nanopartikel (IONPs) werden für ein breites Spektrum an biomedizinischen und (neuro)biologischen Anwendungen eingesetzt, wie zum Beispiel als Kontrastmittel in der Kernspinresonanztomographie, als Transporter für Pharmazeutika über biologische Barrieren oder zur Bekämpfung von Krebs mittels Magnetfeld-induzierter Hyperthermie. Kenntnisse über die Effekte solcher Partikel auf Gehirnzellen wurden allerdings erst kürzlich erworben. Diese Arbeit beschreibt die Synthese und Charakterisierung von Citrat- und Dimercaptosuccinat (DMSA)-umhüllten IONPs. Außerdem wurden Aufnahme, Reaktivität und Biokompatibilität solcher Partikel in Astrozyten-reichen Primärkulturen als Modellsystem für die Astrozyten des Gehirns untersucht. Citrat- und DMSA-umhüllte IONPs wurden von vitalen Astrozyten in einem zeit- und konzentrationsabhängigen Prozess akkumuliert, welcher zu einem mehr als 100fach gesteigerten spezifischen zellulären Eisengehalt führte. Elektronenmikroskopie zeigte die Präsenz von IONPs in intrazellulären Vesikeln sowie IONPs, die extrazellulär an die Zellmembran gebunden waren. Absenken der Inkubationstemperatur auf 4°C verringerte die Eisenakkumulation auf etwa 50%, welche fast ausschließlich extrazellulär membrangebundene IONPs darstellen. Präsenz eines externen Magnetfeldes führte zu einer 2-4fachen Erhöhung des zellulären Eisengehaltes, während die Gegenwart von Serum die IONP-Akkumulation um bis zu 90% im Vergleich zur jeweiligen Kontrolle verringerte. Der Einsatz von Endozytose-Inhibitoren zeigte, dass Clathrin-vermittelte Endozytose und Makropinozytose an der IONP-Aufnahme unter Serum-haltigen Inkubationsbedingungen beteiligt sind. Darüber hinaus sind noch weitere Mechanismen an der IONP-Aufnahme unter Serum-freien Bedingungen beteiligt. Eine längere Präsenz von IONPs in Astrozyten für bis zu 7 Tage nach einer 4-stündigen Beladung führte weder zu einem Verlust an Zellvitalität noch zu Veränderungen in basalen Stoffwechselleistungen. Jedoch wiesen eine transiente Bildung reaktiver Sauerstoffspezies sowie eine verzögerte Hochregulation von zellulärem Ferritin die Freisetzung von Eisen-Ionen aus den akkumulierten Partikeln nach. Zusammenfassend zeigte diese Arbeit, dass vitale Astrozyten IONPs effizient aufnehmen und die Partikel und deren Eisen sicher speichern. Diese Befunde stützen die Ansicht, dass IONPs einen sicheren Einsatz für diagnostische und therapeutische Zwecke im Gehirn erlauben.

V   List of abbreviations

ANOVA	analysis of variance
ATP	adenosine triphosphate
BPS	bathophenanthroline disulfonate
BSA	bovine serum albumin
cm	centimeter
CNS	central nervous system
Cp	ceruloplasmin
d	day(s)
DAPI	4'-6-diamidino-2-phenylindole
Dcyt*b*	duodenal cytochrome *b*
D-Fe-NP	DMSA-coated iron oxide nanoparticles
DFX	deferoxamine
DLS	dynamic light scattering
DMEM	Dulbecco's modified Eagle's medium
DMSA	dimercaptosuccinic acid
DMSA-IONP(s)	dimercaptosuccinic acid-coated iron oxide nanoparticles
DMSO	dimethyl sulfoxide
DMT1	divalent metal transporter 1
EDX	energy dispersive X-ray spectroscopy
EGFR	epidermal growth factor receptor
EIPA	5-(N-ethyl-N-isopropyl)amiloride
et al.	and others (latin: *et alii*)
eV	electronvolts
FAC	ferric ammonium citrate
FCS	fetal calf serum
Fe-NP(s)	iron oxide nanoparticles
Fig(s).	figure(s)
FZ	ferrozine
GABA	γ-aminobutyric acid
GFAP	glial fibrillary acidic protein
GLUT	glucose transporter
GPI	glycosylphosphatidylinositol
g	gram
g	gravity force
gr.	greek
GSH	glutathione
GSx	total glutathione
GSSG	glutathione disulfide
h	hour(s)
H	heavy (chain of ferritin)
HAADF	high angle annular dark field
HEPES	N-(2-hydroxyethyl)-piperazinyl-N'-2-ethansulfonic acid

HCP-1	heme carrier protein 1
HO-1	heme oxygenase 1
HR-TEM	high resolution transmission electron microscopy
i.e.	in example
IB	incubation buffer
IgG	immunoglobulin G
IONP(s)	iron oxide nanoparticle(s)
IR	infrared
IRE	iron-responsive element
IRP	iron-responsive protein
keV	kiloelectronvolts
kg	kilogram
kHz	kilohertz
K_M	Michaelis-constant
kV	kilovolts
L	light (chain of ferritin)
LDH	lactate dehydrogenase
M	molar
MFH	magnetic fluid hyperthermia
mg	milligram
min	minute(s)
mL	milliliter
mm	millimeter
mM	millimolar
MRI	magnetic resonance imaging
mRNA	messenger ribonucleic acid
mV	millivolts
n	number of individual experiments
N	Newton
NADH	nicotinamide adenine dinucleotide (reduced)
NdFeB	neodymium-iron-boron
NGF	nerve growth factor
nm	nanometer
nmol	nanomol
NP(s)	nanoparticle(s)
NR	Neutral Red
OVA	ovalbumin
p	probability
PB	phosphate buffer
PBMC	periphery blood mononuclear cells
PBS	phosphate-buffered saline
PEG	polyethylene glycol
pH	*pondus hydrogenii*
Ph.D.	Doctor of philosophy
PVA	polyvinyl alcohol

PVAP	polyvinyl alcohol phosphate
PVP	polyvinyl pyrrolidone
ROS	reactive oxygen species
SAED	selected area electron diffraction
SCB	sodium cacodylate buffer
SD	standard deviation
SDR2	stromal cell-derived receptor 2
STEM	scanning transmission electron microscopy
T	Tesla
T_1/T_2	longitudinal/transversal relaxation
Tab.	table
TBST	Tris-buffered saline containing 0.1% (w/v) Tween 20
TEM	transmission electron microscopy
TfR	transferrin receptor
Tris	Tris-(hydroxymethyl)-aminomethan
U	units
v/v	volume per volume
V_{max}	maximal velocity
VSOP C184	very small iron oxide particle (184th variant)
w/v	weight per volume
XRD	X-ray diffraction
ΔFe	difference of cellular iron content at 37°C and 4°C
µg	microgram
µL	microliter
µm	micrometer
µM	micromolar
°C	degree Celsius

<u>Part 1</u>

Introduction

1.   Introduction

Nanotechnology gained a huge interest in the last decades and is expected to be one of the major industries of the 21st century (Mangematin & Walsh 2012). By some estimates, it will become a $2.5 trillion market by 2015 (Invernizzi 2011). Nanoparticles (NPs) are defined as particles which have a size of 1 to 100 nm in two or three dimensions (Auffan *et al*. 2009). Due to their small size, physical and chemical properties of NPs are likely to differ from the respective bulk/macroscopic material (Auffan *et al*. 2009).

NPs can consist of various materials. One important type of NP which became popular in the 1980s was the by Sir Harold W. Kroto and colleagues discovered C_{60}-Fullerene, a carbon NP made of 60 C-Atoms (Kroto *et al*. 1985). Another interesting type of carbon-based nanostructures are the so-called carbon nanotubes (Iijiama 1991), which have been considered for applications in neurobiology (Malarkey & Parpura 2010). Furthermore, also the industrially produced carbon black contains NPs (Berg *et al*. 2010).

Besides carbon, there is a wide range of metal or metal-oxide containing NPs. Such NPs usually consist of a core of the respective metal/metal oxide which is surrounded by a ligand shell. Due to their size, NPs show different properties compared to the respective bulk material or metal in solution. This gives them a wide range of possible applications for example as catalysts (Jia & Schuth 2011), antibacterial agents (Rai *et al.* 2009, Dastjerdi & Montazer 2010) or in cosmetic products (Kokura *et al.* 2010).

1.1   Iron oxide nanoparticles

Iron oxide nanoparticles (IONPs) contain a core of iron oxide which is surrounded by a shell of ligands (Lu *et al.* 2007, Laurent *et al.* 2008). Although there are more than ten described iron oxides, hydroxides and oxidohydroxides (Cornell & Schwertmann 1996), the core of the most IONPs contains either magnetite (Fe_3O_4) or maghemite (γ-Fe_2O_3). Due to the magnetism of these iron oxide modifications, magnetic IONPs have gained

high interest and a wide range of technical, biological and clinical applications (see 1.1.4). However, also hematite (α-Fe$_2$O$_3$) or even zero-valent iron NPs have been described (Zhang 2003, Rosicka & Sembera 2011, Xu *et al.* 2011).

Various types of molecules have been used as ligands for IONPs. The type of ligand determines the surface chemistry and thus the behavior of the particles. Possible ligands (coatings) for IONPs can be divided into four groups: inorganic compounds, small organic molecules, polymers and proteins. Examples for these ligand-types and a description of the importance of the coating for the properties of IONPs are given in chapter 1.1.2.

1.1.1 Synthesis

There is a large number of methods described for the synthesis of IONPs (Gupta & Gupta 2005, Laurent *et al.* 2008, Mahmoudi *et al.* 2011). Besides numerous chemical or physical methods for the synthesis of IONPs, also bacterial synthesis involving biomineralization have been described. An overview on important methods used to synthesize IONPs is given in Table 1.1.

Table 1.1: Selected methods for synthesis of IONPs.

Type of method	Description	Selected reference
Chemical	Co-precipitation	Massart 1982
	Microemulsions	Chin & Yaacob 2007
	Thermal decomposition	Kwon *et al.* 2007
	Sol-gel reactions	Ennas *et al.* 1998
	Polyol methods	Cai & Wan 2007
	Sonochemical methods	Abu Mukh-Qasem & Gedanken 2005
	Electrochemical methods	Pascal *et al.* 1999
Physical	Flow injection	Salazar-Alvarez *et al.* 2006
	Aerosol / Vapor	Pecharroman *et al.* 1995
	Pulsed laser ablation	Wang *et al.* 2006
Biological	Biomineralization	Lisy *et al.* 2007

Since the synthesis via co-precipitation of ferrous and ferric iron in an alkaline environment is one of the most common methods and has also been used in this thesis, it will be described here in more detail. This method was originally described by René Massart about three decades ago (Massart 1982). In the co-precipitation technique, IONPs are produced by adding a base (NaOH, NH_4OH or $N(CH_3)_4OH$) to an aqueous solution containing Fe^{2+} and Fe^{3+} ions, usually in a 1:2 stoichiometric ratio. Magnetite (Fe_3O_4) NPs are then generated by the following reaction scheme (Schwertmann & Cornell 1991):

$$Fe^{2+} + 2\,Fe^{3+} + 8\,OH^- \rightarrow Fe_3O_4 + 4\,H_2O$$

Since magnetite is not very stable and sensitive to oxidation (Laurent *et al.* 2008), the generated NPs will be oxidized to maghemite ($\gamma\text{-}Fe_2O_3$) or ferric hydroxide ($Fe(OH)_3$) according to the following reaction schemes (Mahmoudi *et al.* 2011):

$$Fe_3O_4 + 2\,H^+ \rightarrow \gamma\text{-}Fe_2O_3 + Fe^{2+} + H_2O$$
$$Fe_3O_4 + O_2 + H_2O \rightarrow 3\,Fe(OH)_3$$
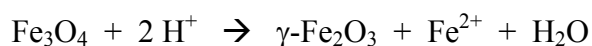
As seen from the equations, oxidation of magnetite can occur by either oxygen or by proton transfer depending on the pH of the suspension. At acidic pH values, Fe^{2+} ions desorb from the NPs surface as hexa-aqua complexes in solution leading to the formation of maghemite (Laurent *et al.* 2008). It should be noticed here, that IONPs prepared by the co-precipitation method often contain mixtures of both magnetite and maghemite (Maity & Agrawal 2007). The size, shape and composition of the IONPs formed depend on the experimental parameters applied, like the types of salts used, the Fe^{2+}/Fe^{3+}-ratio, the reaction temperature, the pH value and the ionic strength of the reaction medium (Lu *et al.* 2007). However, the synthesis of IONPs via the co-precipitation method is highly reproducible as long as identical experimental conditions are used (Lu *et al.* 2007).

Both iron oxides, Fe_3O_4 and $\gamma\text{-}Fe_2O_3$ are ferrimagnetic (Cornell & Schwertmann 1996). Thus, the synthesized NPs can easily be separated from the reaction mixture by decantation in the presence of an external magnetic field. When dispersed into a

solution, IONPs behave like a magnetic fluid in an external magnetic field, also called ferrofluid. Due to their small size, the IONPs are superparamagnetic (see. 1.1.3).

1.1.2 Coating

The stabilization of IONPs by surface coating is an important issue because these particles tend to aggregate/agglomerate when dispersed into high ionic strength solvents like biological media. This aggregation is a result of attractive forces between the particles, such as van der Waals forces and magnetic dipole interactions. On the other hand, IONPs can be stabilized in solution by electrostatic or steric repulsion forces (Laurent *et al*. 2008). The function of a proper surface coating for IONPs is to stabilize the particles in solutions (like biological media) by optimization of the two repulsive forces (Cornell & Schwertmann 1996, Laurent *et al.* 2008).

Coatings for IONPs consist of various types of molecules and can be divided into four groups of coating material: inorganic molecules (atoms, ions), small organic molecules, polymers and proteins. Examples for coatings of IONPs are given in Table 1.2.

Table 1.2: Selected coatings for stabilization of IONPs.

Type of coating	**Example**	**Selected references**
Inorganic	Silica	Bumb *et al*. 2008
	Gold	Lim *et al*. 2009
Organic (monomer)	Citric acid	Bee *et al*. 1995 Taupitz *et al*. 2004
	Gluconic acid	Fauconnier *et al*. 1999
	Dimercaptosuccinic acid	Fauconnier *et al*. 1997
Organic (polymer)	Dextran	Bautista *et al*. 2005
	Polyethlene glycol	Zhang *et al*. 2002 Barrera *et al*. 2009
	Polyvinyl alcohol	Petri-Fink *et al*. 2008
	Polyvinyl pyrrolidone	Lee *et al*. 2008
Protein	Fetal bovine serum	Wiogo *et al*. 2011

Inorganic coatings

Various types of inorganic coatings have been described for IONPs. The most important materials are gold and silica. These IONPs thus have a core of iron oxide which is surrounded by a shell of the inorganic material (Laurent *et al*. 2008).

Gold-iron oxide core/shell NPs can be synthesized via reduction of Au^{3+} ions on an IONP surface. For example, Cui *et al*. synthesized Au-coated IONPs via mixing $HAuCl_4 \cdot 4\,H_2O$ with an aqueous dispersion of IONPs and subsequent addition of NH_2OH as a reducing agent. These NPs were used for immobilization of immunoglobulin G (IgG) and for detection of the hepatitis B antigen in blood (Cui *et al*. 2005). Another report by Lim and colleagues described the synthesis of Au-coated IONPs by attachment of very small gold nanoparticles (1.5-3 nm in diameter) onto the surface of IONPs that had been modified with mercaptoundecanoic acid (Lim *et al*. 2009).

Another important inorganic coating material for IONPs is silica. Silica-coated IONPs are stabilized in two different ways: on the one hand sterically and on the other hand electrostatically, because of the negative charges of the coating (Sun *et al*. 2005, Laurent *et al*. 2008). Silica as coating-material is considered to generate IONPs which show a high biocompatibility (Mahmoudi *et al*. 2011). For example, it has been shown recently that silica-coated IONPs are less toxic than citrate-coated IONPs (Narayanan *et al*. 2011). Ferumoxsil (Leung 2004) is a commercially available silica-coated IONP that was already used for clinical investigations two decades ago (Hahn *et al*. 1990). The commercial product NanoTherm® contains 15 nm aminosilane-coated IONPs which are used for cancer treatment by magnetic field-mediated hyperthermia (Thiesen & Jordan 2008, Rivera Gil *et al.* 2010).

Organic monomeric coatings

Different types of functional groups like carboxylates, phosphates or sulfates are known to bind to the surface of iron oxides or IONPs (Cornell & Schwertmann 1996, Sahoo *et al.* 2001, Lu *et al.* 2007). Best described in the literature are carboxylates as coating material.

Citric acid has frequently been used for coating of IONPs. It is assumed, that this acid adsorbs to the surface of the IONPs by coordinating with one or two of its carboxylate groups to the particles surface. The other one or two carboxylate group(s) are thus exposed to the solvent leading to a negative surface charge and also to electrostatic stabilization of the NPs (Lu *et al.* 2007). An important example for such NP which also had been used for clinical investigations is the so-called VSOP C184: a citrate-coated IONP with a core-diameter of 4 nm (Wagner *et al.* 2002, Taupitz *et al.* 2004). Bee and colleagues reported that the presence of citric acid during the synthesis of IONPs affects the diameter of the obtained particles (Bee *et al.* 1995). Newer reports show that citric acid not only affects the particle size but also the crystallinity of the iron oxides formed (Liu & Huang 1999, Lu *et al.* 2007).

Besides citric acid, other small organic molecules containing carboxyl-groups have been described as coating material for IONPs. Gluconic acid, tartaric acid or dimercaptosuccinic acid (DMSA) have been shown to affect the colloidal stability of IONPs in aqueous solution at different pH values (Fauconnier *et al.* 1999). An interesting role plays hereby the compound DMSA. In addition to the two carboxylate groups, this compound contains two thiol (SH) groups. These SH groups can be oxidized to form disulfides, thereby leading to the formation of poly-DMSA-molecules that are assumed to form a cage-like structure around the core of the IONPs (Fauconnier *et al.* 1997, Valois *et al.* 2010). Free carboxylate groups exposed to the solvent give these DMSA-IONPs a negative charge at physiological pH and thus lead to electrostatic stabilization. A further advantage of DMSA-IONPs is that solvent-exposed SH groups can be used for coupling of thiol reagents (for example fluorescent compounds) onto the NPs surface.

Other monomeric coatings for IONPs contain sulfate or phosphate groups (Portet *et al.* 2001). For example Yee *et al.* functionalized IONPs with alkanesulfonic or alkanephosphonic acids (Yee *et al.* 1999). Characterization of these particles via infrared (IR) spectroscopy suggested a binding of these ligands to the IONP-core via the sulfate- or phosphate-groups, respectively. For the phosphate ligands, a monodentate and a bidentate binding to the iron oxide surface is discussed, while sulfate ligands bind only via one oxygen atom to the surface of IONPs (Yee *et al.* 1999).

Organic polymeric coatings

A wide range of polymers has been used for coating and stabilization of IONPs. Frequently used polymer coatings are based on polyethylene glycol (PEG), polyvinyl alcohol (PVA), polyvinyl pyrrolidone (PVP) or dextran. The coating of IONPs with polymers can either occur during the particle synthesis (*in situ* coating) or after synthesis in an individual second coating step (post-synthesis coating) (Laurent *et al.* 2008).

In 1993, Palmacci and Josephson described a method for *in situ* coating of IONPs with dextran during a co-precipitation process (Palmacci & Josephson 1993). The size of the obtained NPs varied between 10 and 50 nm, depending on the conditions applied for synthesis (Palmacci & Josephson 1993). A more recent publication by Jarrett and colleagues described the synthesis of 30 nm dextran sulfate-coated IONPs and their applications in magnetic resonance imaging (MRI) (Jarrett *et al.* 2007). Nowadays, several methods for synthesis of dextran-coated IONPs exist and such nanoparticles have a wide range of biomedical applications (Tassa *et al.* 2011). The commercial available products "Endorem" and "Resovist" contain dextran- or carboxydextran-coated IONPs, respectively (Soenen & De Cuyper 2010).

Because of its hydrophilicity, polyethylene glycol (PEG) is frequently used as coating material for the generation of water-soluble IONPs. Due to the terminal hydroxyl groups, PEG-coating can also be used to conjugate additional (biological) molecules to the NP surface (Mahmoudi *et al.* 2011). Tong and colleagues synthesized PEG-coated IONPs by preparing an iron oxide core via thermal decomposition and by subsequent ligand exchange with a PEG-derivative (Tong *et al.* 2010). A similar approach was described earlier by Barrera *et al.* using PEG-silane as coating material (Barrera *et al.* 2009). PEGylation of IONPs has also been discussed to facilitate their blood-brain barrier permeability (Winer *et al.* 2011).

Further polymers, which are often used as coating materials for IONPs are polyvinyl alcohol (PVA) or polyvinyl pyrrolidone (PVP). A study of Petri-Fink and colleagues investigated the colloidal stability of PVA-coated IONPs in cell culture media. Long-time colloidal stability was observed for PVA-coated IONPs in serum-containing

culture media. In contrast, in serum-free media the IONPs were only stable for about 30 min (Petri-Fink *et al.* 2008). PVA-coated IONPs are taken up by HeLa cells and appear to cause no toxicity (Petri-Fink *et al.* 2008). Liu *et al.* synthesized PVP-coated IONPs by the polyol process that had an average diameter of less than 5 nm and were superparamagnetic (Liu *et al.* 2007). In addition, phosphate-containing polymers like polyvinyl alcohol phosphate (PVAP) have been described as coating materials for IONPs (Mohapatra *et al.* 2006).

Protein coatings

Formation of protein-coated IONPs is often observed after dispersion of IONPs in a protein-containing (i.e. serum-containing) cell culture medium. This formation of a protein-corona around the NP core (Nel *et al.* 2009) is important, since it affects the interactions between the particles and cell-membranes. Literature data clearly show that the uptake of IONPs into cells strongly depends on the presence of serum in the medium (Chen *et al.* 2008). Besides this 'spontaneous' protein-coating, also the controlled stabilization of IONPs with proteins has been described. Wiogo and co-workers stabilized carboxyl-functionalized IONPs in cell-culture media by adding fetal calf serum (FCS) to the medium (Wiogo *et al.* 2011). In another report, Lim *et al.* stabilized Au-coated IONPs by additional coating with bovine serum albumin (BSA) (Lim *et al.* 2009).

1.1.3 Characterization

Physical and chemical characterization of IONPs is a crucial issue, since small alterations in the particle properties might have large influences on their possible technical, biological or biomedical applications (Laurent *et al.* 2008). IONPs can be characterized by a wide range of physical and (physico)chemical methods. Frequently used methods to characterize properties of IONPs are given in Table 1.3.

Table 1.3: Methods to characterize IONPs.

Method	Parameter/properties investigated
Electron microscopy	Core size and morphology
Energy dispersive X-ray spectroscopy	Elemental composition
Mößbauer spectroscopy	Discrimination between Fe(II) and Fe(III)
X-ray diffraction	Crystal structure
IR spectroscopy	Detection of functional groups (surface coating)
Dynamic light scattering	Hydrodynamic particle size in dispersion
Zeta-potential measurement	Surface charge
Magnetic susceptibility measurement	Magnetism
Magnetic resonance	T_1 / T_2 – Relaxation times

Size and shape of IONPs

By definition, NPs have a size of less than 100 nm in two or three dimensions (Auffan *et al.* 2009). NPs with only two dimensions smaller that 100 nm and a third dimension that is much longer are called nanorods or nanowires (Cao & Wang 2004). The most suitable method to get information about the size and shape of NPs is electron microscopy. Mostly, transmission electron microscopy (TEM) is used for size determination. However, also X-ray diffraction, which is normally used to obtain information about the crystal structure, is suitable to investigate the particle size by using the Scherrer equation (Holzwarth & Gibson 2011). The frequently used photon correlation spectroscopy or dynamic light scattering (DLS) determines hydrodynamic diameters of NPs in dispersion and thus gives information about their colloidal stability (Aberle *et al.* 2002).

IONPs that were synthesized by the classical co-precipitation route have a typical size of around 10 nm in diameter (Kang *et al.* 1996). However, the particle size can be modulated. For example, Bee *et al.* showed that the size of IONPs obtained in the co-precipitation process can be lowered to ~2 nm when citric acid is added to the reaction mixture (Bee *et al.* 1995). Nowadays, numerous methods have been described for size controlled synthesis of IONPs (Lu *et al.* 2007). Besides the size, also the shape of the IONPs can be controlled during the synthesis. Classical synthesis routes lead to particles

that are roughly spherical in shape and have a polydisperse size distribution. However, methods have also been described to obtain monodisperse spherical IONPs (Hyeon *et al.* 2001, Park *et al.* 2007), iron oxide nanocubes (Yang *et al.* 2008, Kim *et al.* 2009, Wang & Yang 2009), nanorods (Li *et al.* 2009, Wang & Yang 2009) or even octahedral shaped IONPs (Li *et al*. 2010).

Crystal structure of IONPs

More than ten different iron oxides, hydroxides or oxidohydroxides have been described (Cornell & Schwertmann 1996). The most common iron oxides are the ferrous oxide Wüstite (FeO), the ferrous/ferric iron oxide magnetite (Fe_3O_4), the ferric oxides hematite (α-Fe_2O_3) and maghemite (γ-Fe_2O_3). Magnetite and maghemite are both ferrimagnetic iron oxides (Cornell & Schwertmann 1996). This is the base for the magnetic properties of nanoparticular forms of these iron oxides.

The crystal structure of IONPs can be determined via X-ray diffraction (XRD) (Brown 1980). Since the distances between the atoms in a crystal structure are comparable to the wavelengths of X-rays, crystals diffract X-rays (Cornell & Schwertmann 1996). The diffraction pattern allows to determine the crystal structure and thus, the type of iron oxide. Typically IONPs consist of one of the magnetic iron oxides, either magnetite (Fe_3O_4) or maghemite (γ-Fe_2O_3), which both crystallize in the cubic structure (Cornell & Schwertmann 1996). Thus, it is difficult to distinguish between these two types of iron oxides via XRD. Since magnetite contains both – ferrous and ferric iron – whereas maghemite is fully oxidized to ferric iron, these oxides can de distinguished by Mößbauer spectroscopy (Woo *et al.* 2004). In addition to magnetite and maghemite IONPs, also hematite (α-Fe_2O_3) IONPs have been described (Xu *et al*. 2011). α-Fe_2O_3 has a hexagonal (rhombohedral) crystal structure and is thus easily distinguishable from the other iron oxides by XRD (Cornell & Schwertmann 1996). The ferrous oxide Wüstite (FeO) is very sensitive to oxidation processes and thus is rarely found in IONPs. Wüstite IONPs often consist of FeO/Fe_3O_4 core-shell structures as determined by high resolution TEM (HR-TEM) and selected area electron diffraction (SAED) (Sharma *et al*. 2011).

Magnetism of IONPs

Magnetite (Fe_3O_4) and maghemite (γ-Fe_2O_3) are both ferrimagnetic iron oxides (Cornell & Schwertmann 1996). In a ferrimagnetic compound, the single particles (atoms, ions, molecules) carry a magnetic moment and these magnetic moments align to an ordering of two oppositely directed magnetic sublattices (Koksharov 2009). Since the sublattices are not identical and one has a higher magnetic moment than the other, the total magnetic moment does not vanish (Koksharov 2009). Thus, magnetic domains (so-called Weiss domains) are formed which have a typical size ranging from a few nanometers up to one micrometer (Lu *et al.* 2007). When such a ferrimagnetic compound is exposed to an external magnetic field, the magnetic domains align and the compound gets magnetized. Ferro- and ferrimagnetic materials retain some of this magnetization which can be macroscopically measured.

When the particle size of a compound is in the nanometer range, each particle will contain only one Weiss domain. They are randomly ordered, but will align when an external magnetic field is applied. When the field is removed, they will spontaneously randomize again due to the so called Brownian and Néel relaxation (Gittlema *et al.* 1974). Thus, no retaining magnetization will be observed. The compound behaves like a paramagnet, which consists of magnetic moments and increases a magnetic field in its interior but looses it when the field is removed. This phenomenon is called superparamagetism. Superparamagnetic IONPs dispersed in an appropriate solvent behave like a magnetic fluid (Lu *et al.* 2007).

1.1.4 Applications

There are many applications of IONPs which take advantage of their different properties, such as their small size, surface chemistry or their magnetism. Applications of IONPs range from technical and engineering fields (i.e. their function as pigments, in catalysis or for magnetic storage media) to medical and (neuro)biological fields. In this thesis, only a short review about their most prominent applications in medicine and biology (especially related to the brain) will be given. A summary of these applications is shown in Table 1.4.

Table 1.4: Biomedical and (neuro)biological applications of IONPs.

Application	Selected references
MRI contrast enhancement	Weinstein *et al.* 2010 Winer *et al.* 2011
Targeted drug delivery	Chertok *et al.* 2008
Magnetic field-induced hyperthermia	Thiesen & Jordan 2008 Maier-Hauff *et al.* 2011
Cell labeling / cell tracking	Cromer Berman *et al.* 2011
Magnetic transfection (magnetofection)	Kamau *et al.* 2006 Pickard & Chari 2010a

The most common application of IONPs is their use as contrast agent in magnetic resonance imaging (MRI) (Weinstein *et al.* 2010, Winer *et al.* 2011). Iron oxide based contrast agents constitute the counterpart to the classical gadolinium (Gd)-based agents. While the latter ones affect the longitudinal (T_1) relaxation processes, the IONP-based contrast agents reduce transverse (T_2) relaxation times. This leads to contrast enhancement in T_2/T_2*-weighted MRI acquisitions by IONP-based contrast agents compared to Gd-based contrast agents which are used in T_1-weighted MRI acquisitions (Weinstein *et al*. 2010). IONP-based contrast agents have a longer half-life which is an advantage for repeated imaging without subsequent administration of contrast agent (Winer *et al.* 2011). Furthermore they seem to be less toxic than Gd-based contrast agents, since the latter ones are known to cause nephrogenic systemic fibrosis in patients with renal insufficiency (Marckmann *et al*. 2006). Another advantage of IONP-based contrast agents in brain tumor imaging is that IONPs which have penetrated the defective blood-brain barrier are endocytosed by reactive astrocytes or macrophages and remain there for several days (Murillo *et al*. 2005). Thus, repeated imaging of the brain without subsequent administration of contrast agent is possible.

Due to their MRI contrast enhancing effect, IONPs have been used for effective cell labeling and cell tracking with the advantage of a high image resolution that did not require exposure to ionizing radiation for imaging (Cromer Berman *et al.* 2011). Cells can be labeled by various techniques, such as simple incubation of the cells with the particles or by application of transfection agents (Cromer Berman *et al.* 2011). The transfection efficiency of cells with IONPs can be facilitated with the aid of magnetic

fields (Kamau *et al.* 2006, Pickard & Chari 2010a). This magnetofection has also been successfully applied to cultured astrocytes (Pickard & Chari 2010a).

Another large field of applications of NPs is the targeted delivery of drugs across the blood-brain barrier (Yang 2010). This barrier is formed by the endothelial cells of the brain capillaries which are connected via tight junctions (Abbott *et al.* 2010). Since more that 98% of small molecular weight drugs and almost 100% of large molecular weight drugs are not able to penetrate the blood-brain barrier (Pardridge 2002, Yang 2010), targeted drug delivery is a big challenge for the future. Already more than ten years ago, it was shown that the anticancer drug doxorubicin could be successfully delivered to the brain by using polysorbate-80-coated poly(butyl-cyanoacrylate) NPs (Kreuter 2001). Also IONPs have been used as drug delivery vehicle for targeting of brain tumors with the aid of magnetic fields (Chertok *et al.* 2008). The magnetic drug targeting with IONPs is considered as promising technology for therapy challenges in the 21st century (Kempe *et al.* 2011).

Besides the delivery of drugs with the aid of IONPs, the particles themselves are a promising tool in anti-tumor treatment. In magnetic fluid hyperthermia (MFH), IONPs are injected into a tumor and the patient is then exposed to a high frequency (100 kHz) altering magnetic field. This treatment induces fast movements of the NPs and thus heating of NPs and the surrounding tumor tissue. The potential of small magnetite or ferrite particles as tool for MFH has already been described in 1993 (Jordan *et al.* 1993). In 2003, the first clinical study for treatment of brain glioblastoma multiforme by MFH with aminosilane-coated IONPs was started (Maier-Hauff *et al.* 2007, Thiesen & Jordan 2008). Post-mortem studies of the brains of glioblastoma patients revealed the presence of remaining IONPs in the regions of instillation. The particles were mainly phagocytosed by macrophages and only a minority was taken up by glioma cells (van Landeghem *et al.* 2009). Nowadays, there are several reports on clinical studies about treatments of glioblastoma or prostate carcinoma with MFH or with combinations of MFH and classical radiation therapy (Johannsen *et al.* 2005, Maier-Hauff *et al.* 2007, Thiesen & Jordan 2008, Maier-Hauff *et al.* 2011).

1.2   Astrocytes

The mammalian brain is a highly complex organ containing different cell types (Figure 1.1) which can be mainly divided into two groups: the neurons and the glia cells. Although, glia cells make up most of the cells of the brain, they were considered for long times only to have a passive supporting role (Allen & Barres 2009). However, nowadays it has become clear, that glia cells have a huge variety of important functions in the brain.

Astrocytes, which are strategically located between blood vessels and other brain cells, have various functions in metabolic support, signal transduction, protection of neurons and detoxification of xenobiotics (Parpura *et al.* 2012). Oligodendrocytes form the myelin sheaths around the neuronal axons which are important to protect the axons and to facilitate signal transduction (Bradl & Lassmann 2010, Miron *et al.* 2011). Microglia represent the immune cells in the brain which show phagocytotic activity (Graeber & Streit 2010, Tremblay *et al.* 2011) and ependymal cells cover the ventricles that are filled with cerebrospinal fluid in the brain (Del Bigio 2010).
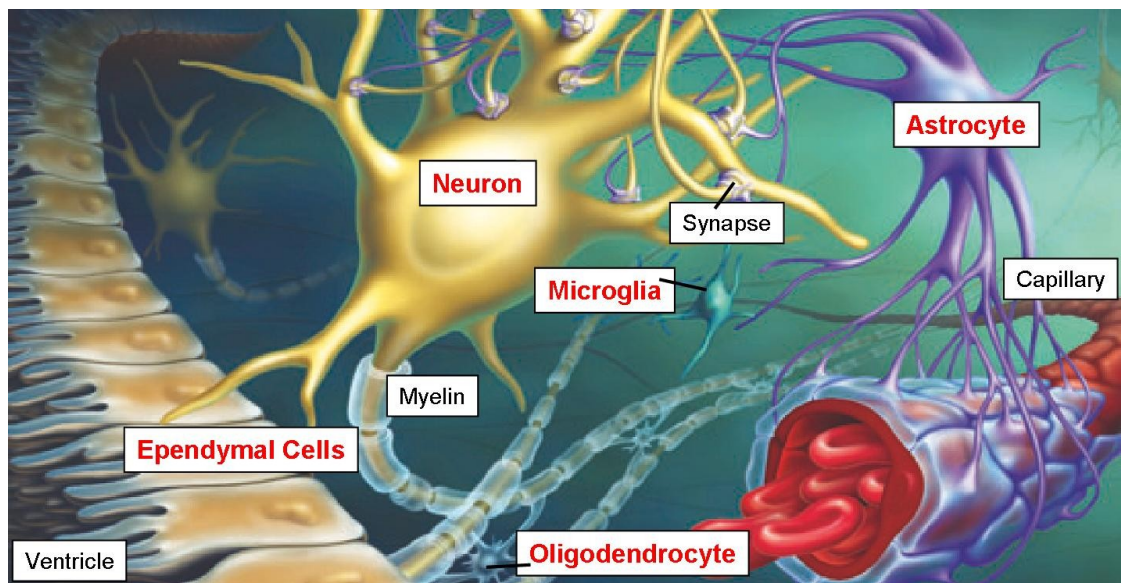

Figure 1.1: Different types of cells in the brain. The picture shows the neurons, which are responsible for signal transduction via the synapses, and the different types of glia cells. Astrocytes connect blood vessels and neurons, oligodendrocytes form the myelin sheaths around the neuronal axons and microglia cells are the phagocytes of the brain. The ependymal cells cover the ventricles in the brain. (Modified from Pfrieger & Steinmetz 2003).

1.2.1 Properties and functions

Astrocytes belong to the glia cells and represent the most abundant cell type in the brain outnumbering the neurons by over fivefold (Sofroniew & Vinters 2010). Astrocytes got their name from their star-shaped morphology (gr. *astron (αστρον):* star), containing a cell body which extends several processes (Oberheim *et al.* 2012). Astrocytes can be divided into mainly two groups: the protoplasmatic astrocytes found throughout the grey matter and the fibrous astrocytes which are present in the white matter of the brain (Kimelberg 2010, Sofroniew & Vinters 2010). Via their endfeet processes, both types of astrocytes stand in contact with the blood vessels of the brain (Mathiisen *et al.* 2010, Sofroniew & Vinters 2010). Furthermore, astrocytes are in contact with synapses and nodes of Ranvier and are also connected by gap junctions with neighboring astrocytes (Peters *et al.* 1991, Sofroniew & Vinters 2010). Thus, astrocytes have a strategically very important position in the brain, being the first cells that encounter substances which have passed the blood-brain barrier and standing in contact with all other types of brain cells.

A characteristic marker for astrocytes is the glial fibrillary acidic protein (GFAP), which was first isolated in multiple sclerosis plaques around 40 years ago (Eng *et al.* 1971, Eng *et al.* 2000). GFAP is the main intermediate filament protein of astrocytes (Middeldorp & Hol 2011). It is expressed in healthy astrocytes, but its expression is strongly enhanced in reactive astrocytes. Thus it is also considered as marker for reactive astrogliosis and CNS injuries (Sofroniew & Vinters 2010). Also astrocytes in cell culture express GFAP (Bock *et al.* 1977, Schmidt 2010).

Brain energy metabolism is of great importance, since this organ consumes about 20% of the energy used by the human body, but accounts only for 2% of the body mass (Sokoloff 1960, Attwell & Laughlin 2001, McKenna *et al.* 2006). With their contacts to the blood vessels, neighboring astrocytes, neuronal axons and synapses, astrocytes have an ideal position to fulfill a variety of important metabolic functions in the brain (Barros & Deitmer 2010, Sofroniew & Vinters 2010). Via the GLUT1 transporter, astrocytes take up glucose from the blood, which can be metabolized into lactate via glycolysis and than exported and taken up by neurons, as described by the astrocyte-neuron lactate shuttle hypothesis (Pellerin & Magistretti 1994, Pellerin *et al.* 2007). Nevertheless, it

has been shown that in the brain neurons take up about half of the glucose directly via the transporter GLUT3 (Nehlig *et al.* 2004). In cell culture experiments neurons preferentially use either glucose or lactate as their main source of energy, depending on their stimulated or resting physiological state (Bouzier-Sore *et al.* 2006, Bak *et al.* 2009).

Besides their important metabolic functions in the brain, astrocytes also take up and release neurotransmitters (Eulenburg & Gomeza 2010, Parpura & Zorec 2010, Parpura *et al.* 2012). The astrocyte processes, which have contact to the synapses, express high levels of transporters for the uptake of neurotransmitters like glutamate, γ-aminobutyric acid (GABA) and glycine (Sattler & Rothstein 2006, Seifert *et al.* 2006, Sofroniew & Vinters 2010). Furthermore, astrocytes release neurotransmitters (=gliotransmitters) like glutamate, purines, GABA and D-serine depending on synaptic activity and astrocytic intracellular Ca^{2+} concentration (Sofroniew & Vinters 2010), thereby modulating synaptic transmission. The importance of astrocytes in neurotransmission is underlined by their inclusion into the concept of the so-called tripartite synapse that is composed of a pre- and post-synaptic neuron and an astrocyte (Araque *et al.* 1999, Halassa *et al.* 2007).

Astrocytes have important functions in the detoxification of peroxides in the brain. Since the brain consumes about 20% of the oxygen used by the body, generation and disposal of peroxides is a crucial issue (Dringen *et al.* 2005). By mainly use of both, catalase and the glutathione (GSH) system, cultured astrocytes are able to clear hydrogen peroxide efficiently with half times in the minute range (Dringen *et al.* 1999, Dringen *et al.* 2005). In addition, astrocytes provide neighboring neurons with precursors for neuronal GSH synthesis (Dringen 2009, Hirrlinger & Dringen 2010, Schmidt & Dringen 2012) thus playing an important protective role for neurons against oxidative stress.

In addition to all these functions in metabolism, signal transduction and protection of neurons, astrocytes have important functions in the regulation of metal homeostasis (Tiffany-Castiglioni & Qian 2001, Dringen *et al.* 2007, Tiffany-Castiglioni *et al.* 2011). Quite a large number of information is now available about uptake, metabolism and

release of metals such as iron and copper in cultured astrocytes (Hoepken *et al.* 2004, Bishop *et al.* 2010, Scheiber *et al.* 2010, Bishop *et al.* 2011, Dang *et al.* 2011, Scheiber *et al.* 2012). Since the metabolism of iron is highly important for this thesis, the following chapter will summarize the iron metabolism of astrocytes.

1.2.2 Iron metabolism

Metal ions have a wide range of important functions in numerous biological processes such as energy production, neurotransmission, muscle contraction and oxygen transport (Crichton *et al.* 2011). For the central nervous system, iron plays a key role in many metabolic processes, including oxidative phosphorylation, myelin synthesis, neurotransmitter production, nitric oxide metabolism and oxygen transport (Crichton 2009, Crichton *et al.* 2011). On the other hand, iron can be toxic to cells since low molecular weight ferrous (Fe^{2+}) iron can catalyze the Fenton reaction in which hydrogen peroxide (H_2O_2) in converted to a hydroxyl anion (OH^-) and the highly reactive hydroxyl radical ($OH\cdot$) (Dringen *et al.* 2007).

$$Fe^{2+} + H_2O_2 \;\rightarrow\; Fe^{3+} + OH\cdot + OH^-$$

Thus, the amount of free cellular ferrous iron has to be tightly regulated.

<u>Iron uptake into the brain</u>

In the blood circulation, up to two ferric (Fe^{3+}) iron ions are bound to the iron transport protein transferrin. The diferric transferrin binds to the transferrin receptor (TfR) – which is expressed on the luminal side of the brain capillaries – and is then internalized into the endothelial cells by receptor mediated endocytosis (Crichton 2009, Crichton *et al.* 2011). Due to the lower endosomal pH value, the iron is liberated from transferrin and the apotransferrin gets recycled (Crichton *et al.* 2011). However, the exact mechanism of iron release from the endosomes of the capillary endothelial cells and of the entrance of iron into the brain is still under discussion since it is not clear if the divalent metal transporter 1 (DMT1) is expressed in brain capillary endothelial cells

(Burdo *et al.* 2001, Moos & Morgan 2004, Moos & Rosengren Nielsen 2006, Crichton *et al.* 2011). Nevertheless, the endothelial cells of the brain capillaries have to be able to release at least some iron to provide this essential metal to parenchymal brain cells.

Iron metabolism of astrocytes

Astrocytes, which cover with their endfeet the brain capillaries (Mathiisen *et al.* 2010), are the first cells which encounter substances released from endothelial cells into the brain parenchyma. It has been suggested, that astrocytes play an important role in the release of iron from the endothelial cells by providing citrate or adenosine triphosphate (ATP) to complex the released iron (Moos *et al.* 2007). Complexed iron will then circulate in the brain extracellular fluid before it is bound to transferrin and/or taken up by astrocytes or other types of brain cells. Uptake, metabolism, storage and export of iron have been quite well investigated for cultured astrocytes. A summary of the most important pathways involved in iron metabolism of astrocytes is given in Figure 1.2.

Different pathways have been suggested for the uptake of iron into astrocytes. Transferrin bound iron can be taken up by receptor-mediated endocytosis via TfR as shown for cultured rat astrocytes (Qian *et al.* 2000, Hoepken *et al.* 2004, Dringen *et al.* 2007). However, it has to be noticed that TfR appears not to be expressed in astrocytes *in vivo* (Moos *et al.* 1999, Jeong & David 2006), suggesting different routes for iron uptake into astrocytes in brain. Also, non-transferrin-bound ferric iron is taken up by cultured astrocytes (Keenan *et al.* 2010, Lane *et al.* 2010, Tulpule *et al.* 2010, Bishop *et al.* 2011). However, the mechanism of uptake of non-transferrin-bound ferric iron is still under debate. The divalent metal transporter 1 (DMT1) appears to be a suitable transporter for non-transferrin-bound ferrous iron. DMT1 is a proton co-transporter which is expressed in astrocytic endfeet *in vivo* as well as in cultured astrocytes (Burdo *et al.* 2001, Tulpule *et al.* 2010). Indeed, DMT1 contributes to the uptake of ferrous iron in cultured rat astrocytes (Lane *et al.* 2010, Tulpule *et al.* 2010). Since ferrous iron is rapidly oxidized to ferric iron at physiological pH, it is discussed that cultured astrocytes possess extracellular ferric reductase activity. Indeed, the mRNA of the ferric reductases duodenal cytochrome *b* (Dcyt*b*) and stromal cell-derived receptor 2 (SDR2) were detected in cultured astrocytes (Tulpule *et al.* 2010). Another pathway of iron

uptake into astrocytes is the uptake of hemin, which contains ferric iron. The uptake is mediated by the heme carrier protein 1 (HCP1) which is expressed by cultured astrocytes (Dang *et al.* 2010). Hemin is then intracellular degraded in astrocytes by the heme oxygenase 1 (HO-1), leading to liberation of the iron (Dang *et al.* 2011).
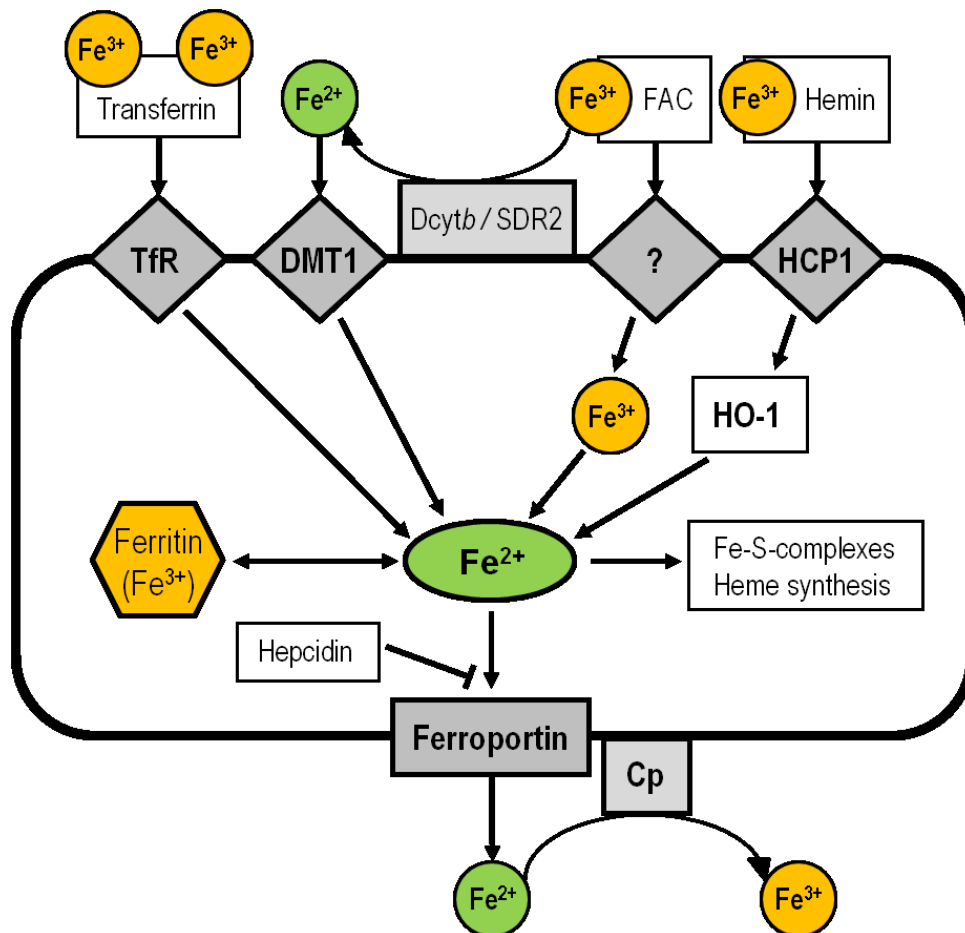

Figure 1.2: Iron metabolism of cultured astrocytes. Transferrin-bound iron can be taken up by transferrin receptor (TfR)-mediated endocytosis. Non-transferrin-bound iron can enter the cell by different pathways. Cultured astrocytes express the divalent metal transporter 1 (DMT1) that allows the uptake of ferrous iron into the cell. Ferric iron (for example as ferric ammonium citrate, FAC) can either be taken up directly or be reduced to ferrous iron by the extracellular ferric reductases duodenal cytochrome *b* (Dcyt*b*) or stromal cell-derived receptor 2 (SDR2). Heme iron enters the cell via the heme carrier protein 1 (HCP1). Internalized iron enters the labile cellular iron pool of Fe^{2+}. This can either be used for metabolism or can be stored as Fe^{3+} in ferritin in redox-inactive form. Ferroportin functions as iron exporter and is modulated by hepcidin. Exported ferrous iron will be immediately oxidized to ferric iron by the glycosylphosphatidylinositol (GPI)-anchored ceruloplasmin (Cp). (Modified from Dringen *et al.* 2007).

Intracellular low molecular iron represents the labile iron pool which is used for the synthesis of heme or iron sulfur clusters (Dringen *et al.* 2007). However, since an excess of intracellular ferrous iron is cell-toxic, the amount of low molecular weight ferrous iron has to be tightly regulated. A safe storage for iron is the iron storage protein ferritin. This protein consists of 24 heavy (H) or light (L) subunits which form a spherical structure that accommodates about 4000 Fe atoms (Arosio *et al.* 2009, Arosio & Levi 2010). Since the H subunits of the ferritin possess ferroxidase activity, the iron is stored as ferric iron in a structure similar to the mineral ferrihydrite (Harrison & Arosio 1996, Arosio *et al.* 2009). The ferritin expression is regulated by the iron-responsive protein (IRP). Low molecular weight iron incorporated in the iron-sulfur cluster of the IRP prevents its binding to the iron-responsive element (IRE) in the ferritin mRNA and thus allows the translation (Arosio *et al.* 2009). The upregulation of ferritin therefore requires the presence of intracellular low molecular weight iron.

Iron is exported from cultured astrocytes by the iron exporter ferroportin (Wu *et al.* 2004, Dringen *et al.* 2007, Garrick & Garrick 2009) which is modulated by hepcidin (Zechel *et al.* 2006, Du *et al.* 2011). Ferroportin is coupled to the glycosyl-phosphatidylinositol (GPI)-anchored ceruloplasmin (Cp) which is a ferroxidase that oxidizes released ferrous iron to ferric iron (Patel & David 1997, Jeong & David 2003).

1.3   Iron oxide nanoparticles and brain cells

Several routes were discussed for NPs to enter the brain and various types of NPs have been considered for the delivery of drugs to the brain (reviewed in Hu & Gao 2010, Yang 2010). For IONPs, recent studies by Wang and colleagues showed the presence of IONPs in rat brain after peripheral administration, demonstrating that IONPs are able to cross the blood-brain barrier and to enter the brain (Wang *et al.* 2010). Furthermore fluorescent IONPs were found in the brain of mice after inhalation, suggesting that IONPs can also enter the brain via the olfactory neuronal pathway (Kwon *et al.* 2008), as earlier demonstrated for inhaled ultrafine carbon particles (Oberdorster *et al.* 2004). Nevertheless, data on consequences of IONPs on brain cells are rather limited so far. Table 1.5 summarizes the currently available studies on the consequences of a treatment of cultured primary brain cells with IONPs.

Table 1.5: Studies describing the consequences of an exposure of cultured primary brain cells to IONPs.

Cell-type	IONP-coating	Observation(s)	Reference(s)
Human astrocytes	Epidermal growth factor receptor (EGFR) antibody	No toxicity to astrocytes	Hadjipanayis *et al.* 2010
Primary rat astrocytes	Citrate	Uptake, membrane association, no toxicity	Geppert *et al.* 2009* Hohnholt *et al.* 2010b*
	DMSA	Uptake, membrane association, no toxicity, increased uptake in magnetic field	Geppert *et al.* 2011* Lamkowsky *et al.* 2012*
Secondary rat astrocytes	Not specified	Mitochondrial uncoupling, inhibition of cell adherence	Au *et al.* 2007
	Dextran	Uptake, toxicity dependent on cell-type (not toxic to astrocytes)	Ding *et al.* 2010
	Not specified	Uptake, no toxicity, magnetic field-induced transfection	Pickard & Chari 2010a Pickard *et al.* 2011 Yiu *et al.* 2011
Secondary microglia	Not specified	Uptake, concentration dependent toxicity	Pickard & Chari 2010b
Oligodendrocyte precursor cells	Not specified	Magnetic field-induced transfection	Jenkins *et al.* 2011
Cortical neurons	Polydimethylamine, aminosilane, dextran	Effects on metabolic activity and cell viability, effects of concentration and coating	Rivet *et al.* 2012

* These articles are part of this thesis.

The first study on the effects of IONPs on astrocyte cultures was reported by Au and co-workers (Au *et al*. 2007). Treatment of the cells with 10 µg/mL magnetic nanoparticles (iron oxide core, coating not specified) for 6 h did not cause any loss of membrane integrity but altered the mitochondrial function of the cells (Au *et al*. 2007). Furthermore, presence of IONPs inhibited adhesion of cells to the culture plate (Au *et al*. 2007). In another report, Ding and colleagues investigated the cytotoxicity of dextan-stabilized IONPs on various cell types, including astrocyte cultures (Ding *et al*. 2010). Their study revealed that IONPs are not toxic to astrocytes even in concentrations of up to 500 µg/mL. Also for human astrocytes a treatment for 1 h with IONPs was not toxic for up to 3 d (Hadjipanayis *et al*. 2010). In contrast, IONPs in a concentration of 128 µg/µL caused apoptosis in periphery blood mononuclear cells (PBMC) (Ding *et al*. 2010).

Uptake of IONPs by cultured astrocytes was demonstrated by TEM and fluorescence microscopy (Ding *et al*. 2010, Pickard *et al*. 2011). Experiments with endocytosis inhibitors suggest that macropinocytosis is the main mechanism of uptake of carboxyl-modified fluorescent IONPs (0.2-0.39 µm in diameter) into astrocytes, at least in serum-containing cell culture medium (Pickard *et al*. 2011). In addition, IONPs were successfully used for transfection of cultured astrocytes (Pickard & Chari 2010a). The transfection efficiency was enhanced by the application of static and oscillating magnetic fields while the latter effect was frequency dependent (Pickard & Chari 2010a).

In contrast to astrocytes, there is only a limited number of studies considering the effects of IONPs on other types of brain cells. Pickard and Chari incubated cultured microglial cells with commercial available carboxyl-modified fluorescent IONPs and observed particle uptake and concentration-dependent toxicity (Pickard & Chari 2010b). Jenkins *et al*. used another type of commercial available IONPs for gene-transfer to oligodendrocyte precursor cells (Jenkins *et al*. 2011). This transfection worked successfully. Its efficiency was increased by static or oscillating magnetic fields, but the treatment did not affect the cells ability to proliferate and to differentiate (Jenkins *et al*. 2011). A very recent report by Rivet and co-workers investigated the effects of IONPs on cortical neurons. They demonstrated that toxicity of the IONPs strongly depends on

their surface coating. While polydimethylamine-coated IONPs were toxic at all concentrations tested, aminosilane and dextran-coated IONPs had at best low effects on metabolic activity and membrane integrity at higher NP concentrations (Rivet *et al.* 2012).

Different cell-lines of neuronal origin have frequently been used as model systems to study the effects of IONPs on brain cells. Important results about the effects of citrate- and DMSA-coated IONPs were gained on the oligodendroglial cell-line OLN93 (Hohnholt *et al.* 2010a, Hohnholt *et al.* 2011, Hohnholt & Dringen 2011). OLN93-cells accumulated IONPs and remained viable for up to 48 h of incubation time. The particles were able to provide iron for cell-proliferation under iron-restricting conditions (Hohnholt *et al.* 2010a). Furthermore, IONP-accumulation by OLN93-cells led to a delayed upregulation in cellular ferritin levels (Hohnholt *et al.* 2011) and – depending on the incubation conditions – also to the formation of reactive oxygen species (ROS) (Hohnholt & Dringen 2011). The rat pheochromocytoma cell-line PC12M is often used as a model system for studying neurons. Exposure of PC12-cells to DMSA-coated IONPs revealed particle uptake, concentration-dependent toxicity and a diminished capacity of the cells to extend neurites in response to nerve growth factor (NGF) (Pisanic *et al.* 2007). In contrast, Kim *et al.* showed recently, that PEG-encapsulated IONPs lead to an enhanced neurite outgrowth in PC12-cells that were exposed to both, IONPs and NGF (Kim *et al.* 2011).

1.4   Aim of the thesis

This thesis aims to synthesize and characterize IONPs that can be used as tools to investigate the uptake, reactivity and biocompatibility of IONPs on cultured astrocytes. A method for a reproducible synthesis of water-dispersable IONPs will be established based on previously published protocols (Bee *et al.* 1995, Geppert 2008). Of special interest are IONPs that are stable in commonly used biological buffer systems and media. This stabilization will be achieved by using proper biocompatible surface coatings for the IONPs, such as citrate and DMSA. The coated IONPs will be characterized by use of a large spectrum of physical and chemical methods. Important parameters that will be investigated are the size, shape and elemental composition of the

IONPs, the total iron content, the hydrodynamic size, surface charge and stability of IONPs in different buffer systems and media, and the effects of the presence of cultured astrocytes on the size and stability of the IONPs.

Rat primary astrocyte cultures will be used as a model system to study the consequences of a treatment of brain cells with the synthesized IONPs. The uptake of the particles by viable cells will be investigated by modulating parameters such as the incubation time, temperature, IONP-concentration, the surface coating of the IONPs and the incubation medium (serum-free or serum-containing). In addition the effects of an external magnetic field on the particle uptake into astrocytes will be investigated. Iron uptake will be confirmed by measurement of the cellular iron content, by cellular staining for iron and by electron microscopy. Furthermore, co-incubations of cells with IONPs and endocytosis inhibitors will be performed to investigate an involvement of endocytotic mechanisms in IONP-uptake. Finally, after transient loading of the cells with IONPs, the long-time consequences of the presence of IONPs in astrocytes will be investigated by measuring several metabolic parameters like lactate export, cellular GSH/GSSG-ratio, presence of ROS and upregulation of cellular ferritin. These investigations will provide experimental data on the reactivity and biocompatibility of IONPs in astrocytes and whether cultured astrocytes are able to liberate low molecular weight iron from accumulated IONPs.

1.5   References

Abbott, N. J., Patabendige, A. A., Dolman, D. E., Yusof, S. R. and Begley, D. J. (2010) Structure and function of the blood-brain barrier. *Neurobiol Dis, 37,* 13-25.

Aberle, L. B., Kleemeier, M., Hennemann, O. D. and Burchard, W. (2002) Selection of single scattering from multiple scattering systems by 3D cross-correlation. 2. Concentrated polymer solutions. *Macromolecules, 35,* 1877-1886.

Abu Mukh-Qasem, R. and Gedanken, A. (2005) Sonochemical synthesis of stable hydrosol of Fe_3O_4 nanoparticles. *J Colloid Interface Sci, 284,* 489-494.

Allen, N. J. and Barres, B. A. (2009) Neuroscience: Glia - more than just brain glue. *Nature, 457,* 675-677.

Araque, A., Parpura, V., Sanzgiri, R. P. and Haydon, P. G. (1999) Tripartite synapses: glia, the unacknowledged partner. *Trends Neurosci,* **22,** 208-215.

Arosio, P., Ingrassia, R. and Cavadini, P. (2009) Ferritins: a family of molecules for iron storage, antioxidation and more. *Biochim Biophys Acta,* **1790,** 589-599.

Arosio, P. and Levi, S. (2010) Cytosolic and mitochondrial ferritins in the regulation of cellular iron homeostasis and oxidative damage. *Biochim Biophys Acta,* **1800,** 783-792.

Attwell, D. and Laughlin, S. B. (2001) An energy budget for signaling in the grey matter of the brain. *J Cereb Blood Flow Metab,* **21,** 1133-1145.

Au, C., Mutkus, L., Dobson, A., Riffle, J., Lalli, J. and Aschner, M. (2007) Effects of nanoparticles on the adhesion and cell viability on astrocytes. *Biol Trace Elem Res,* **120,** 248-256.

Auffan, M., Rose, J., Bottero, J. Y., Lowry, G. V., Jolivet, J. P. and Wiesner, M. R. (2009) Towards a definition of inorganic nanoparticles from an environmental, health and safety perspective. *Nat Nanotechnol,* **4,** 634-641.

Bak, L. K., Walls, A. B., Schousboe, A., Ring, A., Sonnewald, U. and Waagepetersen, H. S. (2009) Neuronal glucose but not lactate utilization is positively correlated with NMDA-induced neurotransmission and fluctuations in cytosolic Ca^{2+} levels. *J Neurochem,* **109 Suppl 1,** 87-93.

Barrera, C., Herrera, A. P. and Rinaldi, C. (2009) Colloidal dispersions of monodisperse magnetite nanoparticles modified with poly(ethylene glycol). *J Colloid Interf Sci,* **329,** 107-113.

Barros, L. F. and Deitmer, J. W. (2010) Glucose and lactate supply to the synapse. *Brain Res Rev,* **63,** 149-159.

Bautista, M. C., Bomati-Miguel, O., Morales, M. D., Serna, C. J. and Veintemillas-Verdaguer, S. (2005) Surface characterisation of dextran-coated iron oxide nanoparticles prepared by laser pyrolysis and coprecipitation. *J Magn Magn Mater,* **293,** 20-27.

Bee, A., Massart, R. and Neveu, S. (1995) Synthesis of very fine maghemite particles. *J Magn Magn Mater,* **149,** 6-9.

Berg, J. M., Ho, S., Hwang, W., Zebda, R., Cummins, K., Soriaga, M. P., Taylor, R., Guo, B. and Sayes, C. M. (2010) Internalization of carbon black and maghemite iron oxide nanoparticle mixtures leads to oxidant production. *Chem Res Toxicol,* **23,** 1874-1882.

Bishop, G. M., Dang, T. N., Dringen, R. and Robinson, S. R. (2011) Accumulation of non-transferrin-bound iron by neurons, astrocytes, and microglia. *Neurotox Res,* **19,** 443-451.

Bishop, G. M., Scheiber, I. F., Dringen, R. and Robinson, S. R. (2010) Synergistic accumulation of iron and zinc by cultured astrocytes. *J Neural Transm,* **117,** 809-817.

Bock, E., Moller, M., Nissen, C. and Sensenbrenner, M. (1977) Glial fibrillary acidic protein in primary astroglial cell cultures derived from newborn rat brain. *FEBS letters,* **83,** 207-211.

Bouzier-Sore, A. K., Voisin, P., Bouchaud, V., Bezancon, E., Franconi, J. M. and Pellerin, L. (2006) Competition between glucose and lactate as oxidative energy substrates in both neurons and astrocytes: a comparative NMR study. *Eur J Neurosci,* **24,** 1687-1694.

Bradl, M. and Lassmann, H. (2010) Oligodendrocytes: biology and pathology. *Acta Neuropathol,* **119,** 37-53.

Brown, G. (1980) Associated minerals. In: *Crystal structures of clay minerals and their X-ray identification*, (G. W. Brindley and G. Brown eds.)*,* pp. 361-410. Mineralogical Society, London.

Bumb, A., Brechbiel, M. W., Choyke, P. L., Fugger, L., Eggeman, A., Prabhakaran, D., Hutchinson, J. and Dobson, P. J. (2008) Synthesis and characterization of ultra-small superparamagnetic iron oxide nanoparticles thinly coated with silica. *Nanotechnology,* **19,** 335601.

Burdo, J. R., Menzies, S. L., Simpson, I. A., Garrick, L. M., Garrick, M. D., Dolan, K. G., Haile, D. J., Beard, J. L. and Connor, J. R. (2001) Distribution of divalent metal transporter 1 and metal transport protein 1 in the normal and Belgrade rat. *J Neurosci Res,* **66,** 1198-1207.

Cai, W. and Wan, J. Q. (2007) Facile synthesis of superparamagnetic magnetite nanoparticles in liquid polyols. *J Colloid Interf Sci,* **305,** 366-370.

Cao, G. and Wang, Y. (2004) *Nanostructures and nanomaterials: synthesis, properties and applications*. Imperial College Press, London, UK.

Chen, Z. P., Zhang, Y., Xu, K., Xu, R. Z., Liu, J. W. and Gu, N. (2008) Stability of hydrophilic magnetic nanoparticles under biologically relevant conditions. *J Nanosci Nanotechnol,* **8,** 6260-6265.

Chertok, B., Moffat, B. A., David, A. E., Yu, F. Q., Bergemann, C., Ross, B. D. and Yang, V. C. (2008) Iron oxide nanoparticles as a drug delivery vehicle for MRI monitored magnetic targeting of brain tumors. *Biomaterials,* **29,** 487-496.

Chin, A. B. and Yaacob, I. I. (2007) Synthesis and characterization of magnetic iron oxide nanoparticles via w/o microemulsion and Massart's procedure. *J Mater Process Tech,* **191,** 235-237.

Cornell, R. M. and Schwertmann, U. (1996) *The iron oxides: structure, properties, reactions, occurences and uses*. Wiley-VCH, Weinheim, Germany.

Crichton, R. R. (2009) *Iron metabolism - from molecular mechanisms to clinical consequences*. Wiley, Chichester.

Crichton, R. R., Dexter, D. T. and Ward, R. J. (2011) Brain iron metabolism and its perturbation in neurological diseases. *J Neural Transm,* **118,** 301-314.

Cromer Berman, S. M., Walczak, P. and Bulte, J. W. (2011) Tracking stem cells using magnetic nanoparticles. *Wiley Interdiscip Rev Nanomed Nanobiotechnol,* **3,** 343-355.

Cui, Y. L., Wang, Y. N., Hui, W. L., Zhang, Z. F., Xin, X. F. and Chen, C. (2005) The synthesis of GoldMag nano-particles and their application for antibody immobilization. *Biomed Microdevices,* **7,** 153-156.

Dang, T. N., Bishop, G. M., Dringen, R. and Robinson, S. R. (2010) The putative heme transporter HCP1 is expressed in cultured astrocytes and contributes to the uptake of hemin. *Glia,* **58,** 55-65.

Dang, T. N., Bishop, G. M., Dringen, R. and Robinson, S. R. (2011) The metabolism and toxicity of hemin in astrocytes. *Glia,* **59,** 1540-1550.

Dastjerdi, R. and Montazer, M. (2010) A review on the application of inorganic nano-structured materials in the modification of textiles: focus on anti-microbial properties. *Colloids Surf B Biointerfaces,* **79,** 5-18.

Del Bigio, M. R. (2010) Ependymal cells: biology and pathology. *Acta Neuropathol,* **119,** 55-73.

Ding, J., Tao, K., Li, J., Song, S. and Sun, K. (2010) Cell-specific cytotoxicity of dextran-stabilized magnetite nanoparticles. *Colloids Surf B,* **79,** 184-190.

Dringen, R. (2009) Neuron-glia coupling in glutathione metabolism. In: *The New Encyclopedia of Neuroscience*, (L. Squire, T. Albright, F. Bloom, F. Gage and N. Spitzer eds.)*,* pp. 733-737. Elsevier, Oxford, OK.

Dringen, R., Bishop, G. M., Koeppe, M., Dang, T. N. and Robinson, S. R. (2007) The pivotal role of astrocytes in the metabolism of iron in the brain. *Neurochem Res,* **32,** 1884-1890.

Dringen, R., Kussmaul, L., Gutterer, J. M., Hirrlinger, J. and Hamprecht, B. (1999) The glutathione system of peroxide detoxification is less efficient in neurons than in astroglial cells. *J Neurochem,* **72,** 2523-2530.

Dringen, R., Pawlowski, P. G. and Hirrlinger, J. (2005) Peroxide detoxification by brain cells. *J Neurosci Res,* **79,** 157-165.

Du, F., Qian, C., Qian, Z. M., Wu, X. M., Xie, H., Yung, W. H. and Ke, Y. (2011) Hepcidin directly inhibits transferrin receptor 1 expression in astrocytes via a cyclic AMP-protein kinase a pathway. *Glia,* **59,** 936-945.

Eng, L. F., Ghirnikar, R. S. and Lee, Y. L. (2000) Glial fibrillary acidic protein: GFAP-thirty-one years (1969-2000). *Neurochem Res,* **25,** 1439-1451.

Eng, L. F., Vanderhaeghen, J. J., Bignami, A. and Gerstl, B. (1971) An acidic protein isolated from fibrous astrocytes. *Brain Res,* **28,** 351-354.

Ennas, G., Musinu, A., Piccaluga, G., Zedda, D., Gatteschi, D., Sangregorio, C., Stanger, J. L., Concas, G. and Spano, G. (1998) Characterization of iron oxide nanoparticles in an Fe_2O_3-SiO_2 composite prepared by a sol-gel method. *Chem Mater,* **10,** 495-502.

Eulenburg, V. and Gomeza, J. (2010) Neurotransmitter transporters expressed in glial cells as regulators of synapse function. *Brain Res Rev,* **63,** 103-112.

Fauconnier, N., Bee, A., Roger, J. and Pons, J. N. (1999) Synthesis of aqueous magnetic liquids by surface complexation of maghemite nanoparticles. *J Mol Liq,* **83,** 233-242.

Fauconnier, N., Pons, J. N., Roger, J. and Bee, A. (1997) Thiolation of maghemite nanoparticles by dimercaptosuccinic acid. *J Colloid Interface Sci,* **194,** 427-433.

Garrick, M. D. and Garrick, L. M. (2009) Cellular iron transport. *Biochim Biophys Acta,* **1790,** 309-325.

Geppert, M. (2008) *Synthese und Charakterisierung von Eisenoxid-Nanopartikeln und Untersuchung ihrer Biokompatibilität an Zellkulturen*, Diploma Thesis, University of Bremen.

Geppert, M., Hohnholt, M., Gaetjen, L., Grunwald, I., Bäumer, M. and Dringen, R. (2009) Accumulation of iron oxide nanoparticles by cultured brain astrocytes. *J Biomed Nanotechnol,* **5,** 285-293.

Geppert, M., Hohnholt, M. C., Thiel, K., Nürnberger, S., Grunwald, I., Rezwan, K. and Dringen, R. (2011) Uptake of dimercaptosuccinate-coated magnetic iron oxide nanoparticles by cultured brain astrocytes. *Nanotechnology,* **22,** 145101.

Gittlema, J. I., Abeles, B. and Bozowski, S. (1974) Superparamagnetism and relaxation effects in granular Ni-SiO_2 and Ni-Al_2O_3 Films. *Phys Rev B,* **9,** 3891-3897.

Graeber, M. B. and Streit, W. J. (2010) Microglia: biology and pathology. *Acta Neuropathol,* **119,** 89-105.

Gupta, A. K. and Gupta, M. (2005) Synthesis and surface engineering of iron oxide nanoparticles for biomedical applications. *Biomaterials,* **26,** 3995-4021.

Hadjipanayis, C. G., Machaidze, R., Kaluzova, M., Wang, L., Schuette, A. J., Chen, H., Wu, X. and Mao, H. (2010) EGFRvIII antibody-conjugated iron oxide nanoparticles for magnetic resonance imaging-guided convection-enhanced delivery and targeted therapy of glioblastoma. *Cancer Res,* **70,** 6303-6312.

Hahn, P. F., Stark, D. D., Lewis, J. M., Saini, S., Elizondo, G., Weissleder, R., Fretz, C. J. and Ferrucci, J. T. (1990) First clinical trial of a new superparamagnetic iron oxide for use as an oral gastrointestinal contrast agent in MR imaging. *Radiology,* **175,** 695-700.

Halassa, M. M., Fellin, T. and Haydon, P. G. (2007) The tripartite synapse: roles for gliotransmission in health and disease. *Trends Mol Med,* **13,** 54-63.

Harrison, P. M. and Arosio, P. (1996) The ferritins: molecular properties, iron storage function and cellular regulation. *Biochim Biophys Acta,* **1275,** 161-203.

Hirrlinger, J. and Dringen, R. (2010) The cytosolic redox state of astrocytes: Maintenance, regulation and functional implications for metabolite trafficking. *Brain Res Rev,* **63,** 177-188.

Hoepken, H. H., Korten, T., Robinson, S. R. and Dringen, R. (2004) Iron accumulation, iron-mediated toxicity and altered levels of ferritin and transferrin receptor in cultured astrocytes during incubation with ferric ammonium citrate. *J Neurochem,* **88,** 1194-1202.

Hohnholt, M., Geppert, M. and Dringen, R. (2010a) Effects of iron chelators, iron salts, and iron oxide nanoparticles on the proliferation and the iron content of oligodendroglial OLN-93 cells. *Neurochem Res,* **35,** 1259-1268.

Hohnholt, M. C. and Dringen, R. (2011) Iron-dependent formation of reative oxygen species and glutathione depletion after accumulation of magnetic iron oxide nanoparticles by oligodendroglial cells. *J Nanopart Res*, **13,** 6761-6774

Hohnholt, M. C., Geppert, M. and Dringen, R. (2011) Treatment with iron oxide nanoparticles induces ferritin synthesis but not oxidative stress in oligodendroglial cells. *Acta Biomater,* **7,** 3946-3954.

Hohnholt, M. C., Geppert, M., Nürnberger, S., von Byern, J., Grunwald, I. and Dringen, R. (2010b) Advanced Biomaterials: Accumulation of citrate-coated magnetic iron oxide nanoparticles by cultured brain astrocytes. *Adv Eng Mater,* **12,** B690-B694.

Holzwarth, U. and Gibson, N. (2011) The Scherrer equation versus the 'Debye-Scherrer equation'. *Nat Nanotechnol,* **6,** 534.

Hu, Y. L. and Gao, J. Q. (2010) Potential neurotoxicity of nanoparticles. *Int J Pharm,* **394,** 115-121.

Hyeon, T., Lee, S. S., Park, J., Chung, Y. and Bin Na, H. (2001) Synthesis of highly crystalline and monodisperse maghemite nanocrystallites without a size-selection process. *Journal of the American Chemical Society,* **123,** 12798-12801.

Iijiama, S. (1991) Helical microtubules of graphitic carbon. *Nature,* **354,** 56-58.

Invernizzi, N. (2011) Nanotechnology between the lab and the shop floor: what are the effects on labor? *J Nanopart Res,* **13,** 2249-2268.

Jarrett, B. R., Frendo, M., Vogan, J. and Louie, A. Y. (2007) Size-controlled synthesis of dextran sulfate coated iron oxide nanoparticles for magnetic resonance imaging. *Nanotechnology,* **18,** 035603.

Jenkins, S. I., Pickard, M. R., Granger, N. and Chari, D. M. (2011) Magnetic nanoparticle-mediated gene transfer to oligodendrocyte precursor cell transplant populations is enhanced by magnetofection strategies. *ACS Nano,* **5,** 6527-6538.

Jeong, S. Y. and David, S. (2003) Glycosylphosphatidylinositol-anchored ceruloplasmin is required for iron efflux from cells in the central nervous system. *J Biol Chem,* **278,** 27144-27148.

Jeong, S. Y. and David, S. (2006) Age-related changes in iron homeostasis and cell death in the cerebellum of ceruloplasmin-deficient mice. *J Neurosci,* **26,** 9810-9819.

Jia, C. J. and Schuth, F. (2011) Colloidal metal nanoparticles as a component of designed catalyst. *Phys Chem Chem Phys,* **13,** 2457-2487.

Johannsen, M., Gneveckow, U., Eckelt, L., Feussner, A., Waldofner, N., Scholz, R., Deger, S., Wust, P., Loening, S. A. and Jordan, A. (2005) Clinical hyperthermia of prostate cancer using magnetic nanoparticles: presentation of a new interstitial technique. *Int J Hyperthermia,* **21,** 637-647.

Jordan, A., Wust, P., Fahling, H., John, W., Hinz, A. and Felix, R. (1993) Inductive heating of ferrimagnetic particles and magnetic fluids: physical evaluation of their potential for hyperthermia. *Int J Hyperthermia,* **9,** 51-68.

Kamau, S. W., Hassa, P. O., Steitz, B., Petri-Fink, A., Hofmann, H., Hofmann-Amtenbrink, M., von Rechenberg, B. and Hottiger, M. O. (2006) Enhancement of the efficiency of non-viral gene delivery by application of pulsed magnetic field. *Nucleic Acids Res,* **34,** e40.

Kang, Y. S., Risbud, S., Rabolt, J. F. and Stroeve, P. (1996) Synthesis and characterization of nanometer-size Fe_3O_4 and γ-Fe_2O_3 particles. *Chem Mater,* **8,** 2209-2211.

Keenan, B. M., Robinson, S. R. and Bishop, G. M. (2010) Effects of carboxylic acids on the uptake of non-transferrin-bound iron by astrocytes. *Neurochem Int,* **56,** 843-849.

Kempe, H., Kates, S. A. and Kempe, M. (2011) Nanomedicine's promising therapy: magnetic drug targeting. *Exp Rev Med Devices,* **8,** 291-294.

Kim, D., Lee, N., Park, M., Kim, B. H., An, K. and Hyeon, T. (2009) Synthesis of uniform ferrimagnetic magnetite nanocubes. *J Am Chem Soc,* **131,** 454-455.

Kim, J. A., Lee, N., Kim, B. H., Rhee, W. J., Yoon, S., Hyeon, T. and Park, T. H. (2011) Enhancement of neurite outgrowth in PC12 cells by iron oxide nanoparticles. *Biomaterials,* **32,** 2871-2877.

Kimelberg, H. K. (2010) Functions of mature mammalian astrocytes: a current view. *Neuroscientist,* **16,** 79-106.

Koksharov, Y. A. (2009) Magnetism of nanoparticles: Effects of size, shape and interactions. In: *Magnetic Nanoparticles*, (S. P. Gubin ed.)*,* pp. 197-254. Wiley-VCH, Weinheim.

Kokura, S., Handa, O., Takagi, T., Ishikawa, T., Naito, Y. and Yoshikawa, T. (2010) Silver nanoparticles as a safe preservative for use in cosmetics. *Nanomedicine,* **6,** 570-574.

Kreuter, J. (2001) Nanoparticulate systems for brain delivery of drugs. *Adv Drug Deliv Rev,* **47,** 65-81.

Kroto, H. W., Heath, J. R., O'Brien, S. C., Curl, R. F. and Smalley, R. E. (1985) C60: Buckminsterfullerene. *Nature,* **314,** 162-163.

Kwon, J. T., Hwang, S. K., Jin, H., Kim, D. S., Minai-Tehrani, A., Yoon, H. J., Choi, M., Yoon, T. J., Han, D. Y., Kang, Y. W., Yoon, B. I., Lee, J. K. and Cho, M. H. (2008) Body distribution of inhaled fluorescent magnetic nanoparticles in the mice. *J Occup Health,* **50,** 1-6.

Kwon, S. G., Piao, Y., Park, J., Angappane, S., Jo, Y., Hwang, N. M., Park, J. G. and Hyeon, T. (2007) Kinetics of monodisperse iron oxide nanocrystal formation by "heating-up" process. *J Am Chem Soc,* **129,** 12571-12584.

Lamkowsky, M. C., Geppert, M., Schmidt, M. M. and Dringen, R. (2012) Magnetic field-induced acceleration of the accumulation of magnetic iron oxide nanoparticles by cultured brain astrocytes. *J Biomed Mater Res A,* **100,** 323-334.

Lane, D. J., Robinson, S. R., Czerwinska, H., Bishop, G. M. and Lawen, A. (2010) Two routes of iron accumulation in astrocytes: ascorbate-dependent ferrous iron uptake via the divalent metal transporter (DMT1) plus an independent route for ferric iron. *Biochem J,* **432,** 123-132.

Laurent, S., Forge, D., Port, M., Roch, A., Robic, C., Elst, L. V. and Muller, R. N. (2008) Magnetic iron oxide nanoparticles: Synthesis, stabilization, vectorization, physicochemical characterizations, and biological applications. *Chem Rev,* **108,** 2064-2110.

Lee, H. Y., Lee, S. H., Xu, C. J. *et al.* (2008) Synthesis and characterization of PVP-coated large core iron oxide nanoparticles as an MRI contrast agent. *Nanotechnology,* **19,** 165101.

Leung, K. (2004) Ferumoxsil. In: *Molecular Imaging and Contrast Agent Database (MICAD)*. Bethesda (MD).

Li, L., Yang, Y., Ding, J. and Xue, J. M. (2010) Synthesis of magnetite nanooctahedra and their magnetic field-induced two-/three-dimensional superstructure. *Chem Mater,* **22,** 3183-3191.

Li, Z. M., Lai, X. Y., Wang, H., Mao, D., Xing, C. J. and Wang, D. (2009) Direct hydrothermal synthesis of single-crystalline hematite nanorods assisted by 1,2-propanediamine. *Nanotechnology,* **20,** 245603.

Lim, J. K., Majetich, S. A. and Tilton, R. D. (2009) Stabilization of superparamagnetic iron oxide core-gold shell nanoparticles in high ionic strength media. *Langmuir,* **25,** 13384-13393.

Lisy, M. R., Hartung, A., Lang, C., Schuler, D., Richter, W., Reichenbach, J. R., Kaiser, W. A. and Hilger, I. (2007) Fluorescent bacterial magnetic nanoparticles as bimodal contrast agents. *Invest Radiol,* **42,** 235-241.

Liu, C. and Huang, P. M. (1999) Atomic force microscopy and surface characteristics of iron oxides formed in citrate solutions. *Soil Sci Soc Am J,* **63,** 65-72.

Liu, H. L., Ko, S. P., Wu, J. H., Jung, M. H., Min, J. H., Lee, J. H., An, B. H. and Kim, Y. K. (2007) One-pot polyol synthesis of monosize PVP-coated sub-5nm Fe_3O_4 nanoparticles for biomedical applications. *J Magn Magn Mater,* **310,** E815-E817.

Lu, A. H., Salabas, E. L. and Schuth, F. (2007) Magnetic nanoparticles: Synthesis, protection, functionalization, and application. *Angew Chem Int Ed,* **46,** 1222-1244.

Mahmoudi, M., Stroeve, P., Milani, A. S. and Arbab, A. S. (2011) *Superparamagnetic iron oxide nanoparticles: synthesis, surface engineering, cytotoxicity and biomedical applications*. Nova Science Publishers, Inc., New York.

Maier-Hauff, K., Rothe, R., Scholz, R., Gneveckow, U., Wust, P., Thiesen, B., Feussner, A., von Deimling, A., Waldoefner, N., Felix, R. and Jordan, A. (2007) Intracranial thermotherapy using magnetic nanoparticles combined with external beam radiotherapy: results of a feasibility study on patients with glioblastoma multiforme. *J Neurooncol,* **81,** 53-60.

Maier-Hauff, K., Ulrich, F., Nestler, D., Niehoff, H., Wust, P., Thiesen, B., Orawa, H., Budach, V. and Jordan, A. (2011) Efficacy and safety of intratumoral thermotherapy using magnetic iron-oxide nanoparticles combined with external beam radiotherapy on patients with recurrent glioblastoma multiforme. *J Neurooncol,* **103,** 317-324.

Maity, D. and Agrawal, D. C. (2007) Synthesis of iron oxide nanoparticles under oxidizing environment and their stabilization in aqueous and non-aqueous media. *J Magn Magn Mater,* **308,** 46-55.

Malarkey, E. B. and Parpura, V. (2010) Carbon nanotubes in neuroscience. *Acta Neurochir Suppl,* **106,** 337-341.

Mangematin, V. and Walsh, S. (2012) The future of nanotechnologies. *Technovation,* **32,** 157-160.

Marckmann, P., Skov, L., Rossen, K., Dupont, A., Damholt, M. B., Heaf, J. G. and Thomsen, H. S. (2006) Nephrogenic systemic fibrosis: suspected causative role of gadodiamide used for contrast-enhanced magnetic resonance imaging. *J Am Soc Nephrol,* **17,** 2359-2362.

Massart, R. (1982) *Magnetic fluids and process for obtaining them.* US-Patent 4329241.

Mathiisen, T. M., Lehre, K. P., Danbolt, N. C. and Ottersen, O. P. (2010) The perivascular astroglial sheath provides a complete covering of the brain microvessels: an electron microscopic 3D reconstruction. *Glia,* **58,** 1094-1103.

McKenna, M. C., Gruetter, R., Sonnewald, U., Waagepetersen, H. S. and Schousboe, A. (2006) Energy metabolism of the brain. In: *Basic Neurochemistry,* (G. J. Siegel, R. W. Albers, S. T. Brady and D. L. Price eds.), Vol. 7, pp. 531-557. Alsevier Academic Press, Burlington, MA, USA.

Middeldorp, J. and Hol, E. M. (2011) GFAP in health and disease. *Prog Neurobiol,* **93,** 421-443.

Miron, V. E., Kuhlmann, T. and Antel, J. P. (2011) Cells of the oligodendroglial lineage, myelination, and remyelination. *Biochim Biophys Acta,* **1812,** 184-193.

Mohapatra, S., Pramanik, N., Ghosh, S. K. and Pramanik, P. (2006) Synthesis and characterization of ultrafine poly(vinylalcohol phosphate) coated magnetite nanoparticles. *J Nanosci Nanotechnol,* **6,** 823-829.

Moos, T. and Morgan, E. H. (2004) The significance of the mutated divalent metal transporter (DMT1) on iron transport into the Belgrade rat brain. *J Neurochem,* **88,** 233-245.

Moos, T., Oates, P. S. and Morgan, E. H. (1999) Iron-independent neuronal expression of transferrin receptor mRNA in the rat. *Brain Res Mol Brain Res,* **72,** 231-234.

Moos, T. and Rosengren Nielsen, T. (2006) Ferroportin in the postnatal rat brain: implications for axonal transport and neuronal export of iron. *Semin Pediatr Neurol,* **13,** 149-157.

Moos, T., Rosengren Nielsen, T., Skjorringe, T. and Morgan, E. H. (2007) Iron trafficking inside the brain. *J Neurochem,* **103,** 1730-1740.

Murillo, T. P., Sandquist, C., Jacobs, P. M., Nesbit, G., Manninger, S. and Neuwelt, E. A. (2005) Imaging brain tumors with ferumoxtran-10, a nanoparticle magnetic resonance contrast agent. *Therapy,* **2,** 871-882.

Narayanan, T. N., Mary, A. P., Swalih, P. K., Kumar, D. S., Makarov, D., Albrecht, M., Puthumana, J., Anas, A. and Anantharaman, M. R. (2011) Enhanced bio-compatibility of ferrofluids of self-assembled superparamagnetic iron oxide-silica core-shell nanoparticles. *J Nanosci Nanotechnol,* **11,** 1958-1967.

Nehlig, A., Wittendorp-Rechenmann, E. and Lam, C. D. (2004) Selective uptake of [14C]2-deoxyglucose by neurons and astrocytes: high-resolution microautoradiographic imaging by cellular 14C-trajectography combined with immunohistochemistry. *J Cereb Blood Flow Metab,* **24,** 1004-1014.

Nel, A. E., Madler, L., Velegol, D., Xia, T., Hoek, E. M., Somasundaran, P., Klaessig, F., Castranova, V. and Thompson, M. (2009) Understanding biophysicochemical interactions at the nano-bio interface. *Nat Mater,* **8,** 543-557.

Oberdorster, G., Sharp, Z., Atudorei, V., Elder, A., Gelein, R., Kreyling, W. and Cox, C. (2004) Translocation of inhaled ultrafine particles to the brain. *Inhal Toxicol,* **16,** 437-445.

Oberheim, N. A., Goldman, S. A. and Nedergaard, M. (2012) Heterogeneity of astrocytic form and function. *Methods Mol Biol,* **814,** 23-45.

Palmacci, S. and Josephson, L. (1993) *Synthesis of polysaccharide covered superparamagnetic oxide colloids*. US-Patent 5262176.

Pardridge, W. M. (2002) Drug and gene delivery to the brain: the vascular route. *Neuron,* **36,** 555-558.

Park, J., Joo, J., Kwon, S. G., Jang, Y. and Hyeon, T. (2007) Synthesis of monodisperse spherical nanocrystals. *Angew Chem Int Edit,* **46,** 4630-4660.

Parpura, V., Heneka, M. T., Montana, V., Oliet, S. H. R., Schousboe, A., Haydon, P. G., Stout Jr, R. F., Spray, D. C., Reichenbach, A., Pannicke, T., Pekny, M., Pekna, M., Zorec, R. and Verkhratsky, A. (2012) Glial cells in (patho)physiology. *J Neurochem, in press*.

Parpura, V. and Zorec, R. (2010) Gliotransmission: Exocytotic release from astrocytes. *Brain Res Rev,* **63,** 83-92.

Pascal, C., Pascal, J. L., Favier, F., Moubtassim, M. L. E. and Payen, C. (1999) Electrochemical synthesis for the control of γ-Fe_2O_3 nanoparticle size. Morphology, microstructure, and magnetic behavior. *Chem Mater,* **11,** 141-147.

Patel, B. N. and David, S. (1997) A novel glycosylphosphatidylinositol-anchored form of ceruloplasmin is expressed by mammalian astrocytes. *J Biol Chem,* **272,** 20185-20190.

Pecharroman, C., Gonzalezcarreno, T. and Iglesias, J. E. (1995) The infrared dielectric-properties of maghemite, γ-Fe_2O_3, from reflectance measurement on pressed powders. *Phys Chem Miner,* **22,** 21-29.

Pellerin, L., Bouzier-Sore, A. K., Aubert, A., Serres, S., Merle, M., Costalat, R. and Magistretti, P. J. (2007) Activity-dependent regulation of energy metabolism by astrocytes: an update. *Glia,* **55,** 1251-1262.

Pellerin, L. and Magistretti, P. J. (1994) Glutamate uptake into astrocytes stimulates aerobic glycolysis: a mechanism coupling neuronal activity to glucose utilization. *Proc Natl Acad Sci U S A,* **91,** 10625-10629.

Peters, A., Palay, S. L. and Webster, H. D. (1991) *The fine structure of the nervous system*. Oxford University Press, New York.

Petri-Fink, A., Steitz, B., Finka, A., Salaklang, J. and Hofmann, H. (2008) Effect of cell media on polymer coated superparamagnetic iron oxide nanoparticles (SPIONs): Colloidal stability, cytotoxicity, and cellular uptake studies. *Eur J Pharm Biopharm,* **68,** 129-137.

Pfrieger, F. W. and Steinmetz, C. (2003) Les astrocytes, nouvelles stars du cerveau. *La Recherche,* **361,** 50-54.

Pickard, M. and Chari, D. (2010a) Enhancement of magnetic nanoparticle-mediated gene transfer to astrocytes by 'magnetofection': effects of static and oscillating fields. *Nanomedicine,* **5,** 217-232.

Pickard, M. R. and Chari, D. M. (2010b) Robust uptake of magnetic nanoparticles (MNPs) by central nervous system (CNS) microglia: Implications for particle uptake in mixed neural cell populations. *Int J Mol Sci,* **11,** 967-981.

Pickard, M. R., Jenkins, S. I., Koller, C. J., Furness, D. N. and Chari, D. M. (2011) Magnetic nanoparticle labeling of astrocytes derived for neural transplantation. *Tissue Eng Part C Methods,* **17,** 89-99.

Pisanic, T. R., 2nd, Blackwell, J. D., Shubayev, V. I., Finones, R. R. and Jin, S. (2007) Nanotoxicity of iron oxide nanoparticle internalization in growing neurons. *Biomaterials,* **28,** 2572-2581.

Portet, D., Denizot, B., Rump, E., Lejeune, J. J. and Jallet, P. (2001) Nonpolymeric coatings of iron oxide colloids for biological use as magnetic resonance imaging contrast agents. *J Colloid Interface Sci,* **238,** 37-42.

Qian, Z. M., Liao, Q. K., To, Y., Ke, Y., Tsoi, Y. K., Wang, G. F. and Ho, K. P. (2000) Transferrin-bound and transferrin free iron uptake by cultured rat astrocytes. *Cell Mol Biol (Noisy-le-grand),* **46,** 541-548.

Rai, M., Yadav, A. and Gade, A. (2009) Silver nanoparticles as a new generation of antimicrobials. *Biotechnol Adv,* **27,** 76-83.

Rivera Gil, P., Huhn, D., del Mercato, L. L., Sasse, D. and Parak, W. J. (2010) Nanopharmacy: Inorganic nanoscale devices as vectors and active compounds. *Pharmacol Res,* **62,** 115-125.

Rivet, C. J., Yuan, Y., Borca-Tasciuc, D. A. and Gilbert, R. J. (2012) Altering iron oxide nanoparticle surface properties induce cortical neuron cytotoxicity. *Chem Res Toxicol,* **25,** 153-161.

Rosicka, D. and Sembera, J. (2011) Influence of structure of iron nanoparticles in aggregates on their magnetic properties. *Nanoscale Res Lett,* **6,** 527.

Sahoo, Y., Pizem, H., Fried, T., Golodnitsky, D., Burstein, L., Sukenik, C. N. and Markovich, G. (2001) Alkyl phosphonate/phosphate coating on magnetite nanoparticles: A comparison with fatty acids. *Langmuir,* **17,** 7907-7911.

Salazar-Alvarez, G., Muhammed, M. and Zagorodni, A. A. (2006) Novel flow injection synthesis of iron oxide nanoparticles with narrow size distribution. *Chem Eng Sci,* **61,** 4625-4633.

Sattler, R. and Rothstein, J. D. (2006) Regulation and dysregulation of glutamate transporters. *Handb Exp Pharmacol***, 175,** 277-303.

Scheiber, I. F., Mercer, J. F. and Dringen, R. (2010) Copper accumulation by cultured astrocytes. *Neurochem Int,* **56,** 451-460.

Scheiber, I. F., Schmidt, M. M. and Dringen, R. (2012) Copper export from cultured astrocytes. *Neurochem Int*, **60,** 292-300.

Schmidt, M. and Dringen, R. (2012) Glutathione synthesis and metabolism. In: *Advances in Neurobiology*, (G. I-YCR ed.)*,* Springer Science, New York, *in press.*

Schmidt, M. M. (2010) *Effects of xenobiotics on the glutathione and glucose metabolism of cultured astrocytes*, PhD Thesis, University of Bremen.

Schwertmann, U. and Cornell, R. M. (1991) *Iron oxides in the laboratory: preparation and characterization*. Wiley-VCH, Weinheim, Germany.

Seifert, G., Schilling, K. and Steinhauser, C. (2006) Astrocyte dysfunction in neurological disorders: a molecular perspective. *Nat Rev Neurosci,* **7,** 194-206.

Sharma, S. K., Vargas, J. M., Pirota, K. R., Kumar, S., Lee, C. G. and Knobel, M. (2011) Synthesis and ageing effect in FeO nanoparticles: Transformation to core-shell FeO/Fe_3O_4 and their magnetic characterization. *J Alloy Compd,* **509,** 6414-6417.

Soenen, S. J. and De Cuyper, M. (2010) Assessing iron oxide nanoparticle toxicity in vitro: current status and future prospects. *Nanomedicine (Lond),* **5,** 1261-1275.

Sofroniew, M. V. and Vinters, H. V. (2010) Astrocytes: biology and pathology. *Acta Neuropathol,* **119,** 7-35.

Sokoloff, L. (1960) The metabolism of the central nervous system. In: *Handbook of Physiology, Section I, Neurophysiology*, (J. Field, H. W. Magoun and V. E. Hall eds.), Vol. 3*,* pp. 1843-1864. American Physiological Society, Washington D.C.

Sun, Y. K., Duan, L., Guo, Z. R., Yun, D. M., Ma, M., Xu, L., Zhang, Y. and Gu, N. (2005) An improved way to prepare superparamagnetic magnetite-silica core-shell nanoparticles for possible biological application. *J Magn Magn Mater,* **285,** 65-70.

Tassa, C., Shaw, S. Y. and Weissleder, R. (2011) Dextran-coated iron oxide nanoparticles: a versatile platform for targeted molecular imaging, molecular diagnostics, and therapy. *Accounts of chemical research,* **44,** 842-852.

Taupitz, M., Wagner, S., Schnorr, J., Kravec, I., Pilgrimm, H., Bergmann-Fritsch, H. and Hamm, B. (2004) Phase I clinical evaluation of citrate-coated monocrystalline very small superparamagnetic iron oxide particles as a new contrast medium for magnetic resonance imaging. *Invest Radiol,* **39,** 394-405.

Thiesen, B. and Jordan, A. (2008) Clinical applications of magnetic nanoparticles for hyperthermia. *Int J Hyperther,* **24,** 467-474.

Tiffany-Castiglioni, E., Hong, S. and Qian, Y. (2011) Copper handling by astrocytes: Insights into neurodegenerative diseases. *Int J Dev Neurosci,* **29,** 811-818.

Tiffany-Castiglioni, E. and Qian, Y. C. (2001) Astroglia as metal depots: Molecular mechanisms for metal accumulation, storage and release. *Neurotoxicology,* **22,** 577-592.

Tong, S., Hou, S. J., Zheng, Z. L., Zhou, J. and Bao, G. (2010) Coating optimization of superparamagnetic iron oxide nanoparticles for high T_2 relaxivity. *Nano Lett,* **10,** 4607-4613.

Tremblay, M. E., Stevens, B., Sierra, A., Wake, H., Bessis, A. and Nimmerjahn, A. (2011) The role of microglia in the healthy brain. *J Neurosci,* **31,** 16064-16069.

Tulpule, K., Robinson, S. R., Bishop, G. M. and Dringen, R. (2010) Uptake of ferrous iron by cultured rat astrocytes. *J Neurosci Res,* **88,** 563-571.

Valois, C. R., Braz, J. M., Nunes, E. S., Vinolo, M. A., Lima, E. C., Curi, R., Kuebler, W. M. and Azevedo, R. B. (2010) The effect of DMSA-functionalized magnetic nanoparticles on transendothelial migration of monocytes in the murine lung via a β_2 integrin-dependent pathway. *Biomaterials,* **31,** 366-374.

van Landeghem, F. K., Maier-Hauff, K., Jordan, A., Hoffmann, K. T., Gneveckow, U., Scholz, R., Thiesen, B., Bruck, W. and von Deimling, A. (2009) Post-mortem studies in glioblastoma patients treated with thermotherapy using magnetic nanoparticles. *Biomaterials,* **30,** 52-57.

Wagner, S., Schnorr, J., Pilgrimm, H., Hamm, B. and Taupitz, M. (2002) Monomer-coated very small superparamagnetic iron oxide particles as contrast medium for magnetic resonance imaging: preclinical in vivo characterization. *Invest Radiol,* **37,** 167-177.

Wang, J., Chen, Y., Chen, B. *et al.* (2010) Pharmacokinetic parameters and tissue distribution of magnetic Fe_3O_4 nanoparticles in mice. *Int J Nanomedicine,* **5,** 861-866.

Wang, Y. and Yang, H. (2009) Synthesis of iron oxide nanorods and nanocubes in an imidazolium ionic liquid. *Chem Eng J,* **147,** 71-78.

Wang, Z. M., Liu, Y. and Zeng, X. Y. (2006) One-step synthesis of γ-Fe$_2$O$_3$ nanoparticles by laser ablation. *Powder Technol,* **161,** 65-68.

Weinstein, J. S., Varallyay, C. G., Dosa, E., Gahramanov, S., Hamilton, B., Rooney, W. D., Muldoon, L. L. and Neuwelt, E. A. (2010) Superparamagnetic iron oxide nanoparticles: diagnostic magnetic resonance imaging and potential therapeutic applications in neurooncology and central nervous system inflammatory pathologies, a review. *J Cereb Blood Flow Metab,* **30,** 15-35.

Winer, J. L., Kim, P. E., Law, M., Liu, C. Y. and Apuzzo, M. L. (2011) Visualizing the future: enhancing neuroimaging with nanotechnology. *World Neurosurg,* **75,** 626-637.

Wiogo, H. T. R., Lim, M., Bulmus, V., Yun, J. and Amal, R. (2011) Stabilization of magnetic iron oxide nanoparticles in biological media by fetal bovine serum (FBS). *Langmuir,* **27,** 843-850.

Woo, K., Hong, J., Choi, S., Lee, H. W., Ahn, J. P., Kim, C. S. and Lee, S. W. (2004) Easy synthesis and magnetic properties of iron oxide nanoparticles. *Chem Mater,* **16,** 2814-2818.

Wu, L. J., Leenders, A. G., Cooperman, S., Meyron-Holtz, E., Smith, S., Land, W., Tsai, R. Y., Berger, U. V., Sheng, Z. H. and Rouault, T. A. (2004) Expression of the iron transporter ferroportin in synaptic vesicles and the blood-brain barrier. *Brain Res,* **1001,** 108-117.

Xu, Y. Y., Yang, S., Zhang, G. Y., Sun, Y. Q., Gao, D. Z. and Sun, Y. X. (2011) Uniform hematite alpha-Fe(2)O(3) nanoparticles: Morphology, size-controlled hydrothermal synthesis and formation mechanism. *Mater Lett,* **65,** 1911-1914.

Yang, H. (2010) Nanoparticle-mediated brain-specific drug delivery, imaging, and diagnosis. *Pharm Res,* **27,** 1759-1771.

Yang, H. T., Ogawa, T., Hasegawa, D. and Takahashi, M. (2008) Synthesis and magnetic properties of monodisperse magnetite nanocubes. *J Appl Phys,* **103**. 07D526/1-07D526/3.

Yee, C., Kataby, G., Ulman, A., Prozorov, T., White, H., King, A., Rafailovich, M., Sokolov, J. and Gedanken, A. (1999) Self-assembled monolayers of alkanesulfonic and -phosphonic acids on amorphous iron oxide nanoparticles. *Langmuir,* **15,** 7111-7115.

Yiu, H. H., Pickard, M. R., Olariu, C. I., Williams, S. R., Chari, D. M. and Rosseinsky, M. J. (2011) Fe$_3$O$_4$-PEI-RITC magnetic nanoparticles with imaging and gene transfer capability: development of a tool for neural cell transplantation therapies. *Pharm Res, in press*.

Zechel, S., Huber-Wittmer, K. and von Bohlen und Halbach, O. (2006) Distribution of the iron-regulating protein hepcidin in the murine central nervous system. *J Neurosci Res,* **84,** 790-800.

Zhang, M. Q., Zhang, Y. and Kohler, N. (2002) Surface modification of superparamagnetic magnetite nanoparticles and their intracellular uptake. *Biomaterials,* **23,** 1553-1561.

Zhang, W. X. (2003) Nanoscale iron particles for environmental remediation: An overview. *J Nanopart Res,* **5,** 323-332.

Part 2

Results

2.1 Publication 1

Geppert, M., Hohnholt, M., Gaetjen, L., Grunwald, I., Bäumer, M. and Dringen, R. (2009) Accumulation of iron oxide nanoparticles by cultured brain astrocytes. *J Biomed Nanotechnol* **5,** 285-293.

Contributions of M. Geppert:

- Synthesis of iron oxide nanoparticles
- Performance of experiments for Table 1* and Figures 1*, 2*, 3* and 6
- Preparation of the first draft of the manuscript

M. Hohnholt obtained the data given in Figure 4. L. Gaetjen performed the electron microscopy and provided Figure 5.

*Note: The data given in Table 1 and in Figures 1-3 were obtained during the diploma thesis of M. Geppert.

Accumulation of Iron Oxide Nanoparticles by Cultured Brain Astrocytes

Mark Geppert[1,2], Michaela Hohnholt[1,2], Linda Gaetjen[3], Ingo Grunwald[3],
Marcus Bäumer[4], and Ralf Dringen[1,2,5,*]

[1] Center for Biomolecular Interactions Bremen, University of Bremen, PO. Box 330440, D-28334 Bremen, Germany
[2] Center for Environmental Research and Sustainable Technology, Leobener Strasse, D-28359 Bremen, Germany
[3] Fraunhofer Institute for Manufacturing Technology and Applied Materials Research,
Wiener Strasse 12, D-28395 Bremen, Germany
[4] Institute for Applied and Physical Chemistry, University of Bremen, PO. Box 330440, D-28359 Bremen, Germany
[5] School of Psychology, Psychiatry, and Psychological Medicine, Monash University,
Wellington Rd., Clayton, Victoria 3800, Australia

Magnetic iron oxide nanoparticles are considered for various diagnostic and therapeutic applications in brain including their use as contrast agent for magnetic resonance imaging or as tool for magnetic drug delivery. However, little is known so far on the consequences of a treatment of brain cells with such nanoparticles. In order to study the biocompatibility of iron oxide nanoparticles and the accumulation of iron from such particles in brain cells, we have used astrocyte-rich primary cultures as model system. Iron oxide nanoparticles were chemically synthesized with a yield of about 80% regarding the iron content. Transmission electron microscopy revealed that the synthesized iron oxide nanoparticles had a diameter of about 10 nm. Exposure of astrocyte cultures to 100 μM iron that were supplied as citrate-coated iron oxide nanoparticles did not cause any acute loss in cell viability but resulted in an almost linear increase in the cellular iron content that reached after 6 h of incubation at 37 °C a total cellular iron content of about 300 nmol/mg protein. The rate of iron accumulation from iron oxide nanoparticles was significantly higher than that from the low molecular weight iron complex ferric ammonium citrate (FAC). Lowering the incubation temperature from 37 °C to 4 °C reduced the iron accumulation rate from iron oxide nanoparticles or FAC by about 60%. In addition, presence of ferric or ferrous iron chelators did not affect the cellular iron accumulation from iron oxide nanoparticles. These data suggest that cultured astrocytes are able to accumulate intact iron oxide nanoparticles.

Keywords: Accumulation, Astrocytes, Brain, Iron, Nanoparticles, Oxidative Stress, Uptake.

1. INTRODUCTION

Magnetic iron oxide nanoparticles are considered for a wide range of biomedical applications, for example for targeted drug delivery, as contrast agents in magnetic resonance imaging or for the elimination of tumors by magnetically mediated hyperthermia.[1–4] Magnetic iron oxide nanoparticles consist of an iron oxide core (Fe_3O_4 or γ-Fe_2O_3) and are surrounded by a ligand shell of polymers, proteins or small organic molecules.[4,5] This coating with ligands is important for the stability and for the chemical properties of the nanoparticles.[5] Typical diameters of chemically synthesized magnetic iron oxide nanoparticles are around 10 nm, but methods have also been described

to obtain iron oxide nanoparticles of other sizes.[6,7] The magnetic behaviour of aqueous dispersions of iron oxide nanoparticles relies on the small size of the particles and the resulting superparamagnetism.[5]

Astrocytes are the most abundant cell type of the brain.[8] These cells cover with their endfeet almost completely the brain capillaries.[9] In addition, astrocytes have contact with neurons and other types of brain cells. This strategic important localization of astrocytes in the brain allows a controlled transport of nutrients from blood to the brain parenchyma and a controlled export of waste products from the brain. Astrocytes have important functions for the brain in the supply of nutrients to neurons,[10,11] in the detoxification of reactive oxygen species and xenobiotics[12–14] as well as in the metabolism of iron and other metals in the brain.[15–17]

*Author to whom correspondence should be addressed.

Little information is currently available on the consequences of a treatment of brain cells with iron oxide nanoparticles. Exposure of cultured astrocytes with iron oxide nanoparticles did not lower cell viability but affected cell adhesion after exposure of the cells for days to nanoparticles.[18] In contrast, when PC12 cells—a frequently used model system for neurons–were exposed to iron oxide nanoparticles for days, a severe loss in cell viability was observed.[19]

Quantitative data on the biocompatibility and accumulation of iron oxide nanoparticles in brain cells are currently not available. Since astrocytes cover the endothelial cells of the brain capillaries, these cells would have the first contact to iron oxide nanoparticles after entering the brain from blood. Astrocytes have the capacity to effectively accumulate iron from various extracellular iron sources, are able to store large amounts of iron and are able to release iron.[16] Thus, this cell type is of especial interest to study the consequences of a treatment of brain cells with iron oxide nanoparticles. Therefore, we have synthesized and characterised iron oxide nanoparticles and have studied the consequences of an exposure of astrocyte-rich primary cultures to the synthesized nanoparticles. Incubation of cultured astrocytes with iron oxide nanoparticles caused a time dependent increase in cellular iron content that depended on the incubation temperature and was not prevented by the presence of iron chelators. In addition, no acute cell toxicity was observed, if cultured astrocytes were exposed to iron oxide nanoparticles.

2. MATERIALS AND METHODS

2.1. Materials

Fetal calf serum (FCS) and penicillin/streptomycin solution were obtained from Biochrom (Berlin, Germany). Dulbecco's modified Eagle's medium (DMEM) was from Gibco (Karlsruhe, Germany). Acetonitrile, bathophenanthroline disulfonate (BPS), deferoxamine (DFX), diaminobenzidine, glutaraldehyde, lead citrate, neocuproine, osmium tetroxide, paraformaldehyde, sodium ascorbate, sodium cacodylate, Trizma base and uranyl acetate were purchased from Sigma (Steinheim, Germany). Bovine serum albumin and NADH were purchased from Applichem (Darmstadt, Germany). All other chemicals of the highest purity available were from either Fluka (Buchs, Switzerland), Merck (Darmstadt, Germany), or Riedel-deHaen (Seelze, Germany). 96-well microtiter plates were from Nunc (Wiesbaden, Germany) and 24-well cell culture plates from Sarstedt (Nümbrecht, Germany).

2.2. Synthesis of Iron Oxide Nanoparticles

Iron oxide nanoparticles were prepared using a modification of a published method.[6] Briefly, 380 mL of an aqueous solution containing 8.89 g $FeCl_3 \cdot 6\ H_2O$, 3.28 g $FeCl_2 \cdot 4\ H_2O$ and 1 mL 37% HCl was mixed under vigorous stirring with 25 mL 25% (w/v) ammonium hydroxide solution. The resulting black magnetic precipitate was isolated with the aid of a permanent magnet (S-30-10-N, Webcraft (Uster, Switzerland)) and washed twice with 100 mL deionized water. The precipitate was then boiled with 40 mL 2 M HNO_3 for 5 min, isolated from the supernatant by magnetic separation and incubated with 60 mL 0.34 M $Fe(NO_3)_3$ in water for 30 min at 90 °C. After magnetic separation from the supernatant, the particles were dispersed with deionized water to a final volume of 50 mL. The iron content of this aqueous dispersion was determined and the dispersion was diluted with water to a final concentration of 20 mM of total iron.

2.3. Citrate-Coating of Iron Oxide Nanoparticles

The synthesized iron oxide nanoparticles were coated with citrate to stabilize them in incubation buffer at physiological pH. Ten milliliter of the aqueous dispersion of iron oxide nanoparticles (total iron concentration of 20 mM) were mixed with 10 mL sodium citrate solution (200 mM) in water. The mixture was incubated for 10 min at 80 °C and then cooled down to room temperature. Before application to the cells the coated iron oxide nanoparticles were filtered through a 200 nm syringe filter (Renner, Darmstadt, Germany).

2.4. Transmission Electron Microscopy of Iron Oxide Nanoparticles

The transmission electron microscopy (TEM) of the synthesized iron oxide nanoparticles was performed using a Tecnai F20 STwin (FEI, Hillsboro, Oregon, USA) at 200 kV. The particles were analyzed in the bright-field imaging mode and in high angle annular dark-field (HAADF) STEM mode. The point resolution in TEM mode is 0.24 nm and 0.19 nm in HAADF-STEM mode. Samples were spotted on carbon-copper grids (Plano, Wetzlar, Germany), washed with ultrapure water and were dried to completeness before the analysis.

2.5. Cell Cultures

Astrocyte-rich primary cultures were prepared from the brains of newborn Wistar rats.[20] The cells were seeded in culture medium (90% DMEM, 10% FCS, 1 mM pyruvate, 20 units/mL penicillin G and 20 μg/mL streptomycin sulfate) in wells of 24-well plates (300,000 cells in 1 mL) and incubated in the humidified atmosphere of a Sanyo (Osaka, Japan) incubator with 10% CO_2. The cultures were maintained by renewing the culture medium every seventh day. The cultures were used for experiments at an age between 15 and 27 days.

2.6. Experimental Incubation

Cells in wells of 24-well plates were washed twice with 1 mL pre-warmed (37 °C) or cold (4 °C) incubation buffer (IB: 20 mM HEPES, 145 mM NaCl, 1.8 mM CaCl$_2$, 5.4 mM KCl, 1 mM MgCl$_2$, 0.8 mM Na$_2$HPO$_4$, 5 mM glucose) that had been adjusted to pH 7.4 at the desired temperature. Different concentrations of iron as iron oxide nanoparticles or as ferric ammonium citrate (FAC, a soluble ferric iron complex) in the incubation buffer were attained by diluting stock solutions (10 mM) to the desired final iron concentration in IB. The main incubation of the cells was started by application of 1 mL incubation buffer of the desired temperature with or without iron oxide nanoparticles, FAC and/or iron chelators. After incubation of cells for the indicated incubation time at 4 °C or 37 °C the media were collected and the cells were washed twice with 1 mL ice-cold phosphate-buffered saline (PBS, 10 mM potassium phosphate buffer pH 7.4, containing 150 mM NaCl) and stored frozen until further analysis of protein and iron contents.

2.7. Quantification of Total Iron

The total iron content of incubation buffers or cells was determined by a modification of the ferrozine (FZ) method previously described.[21] For estimation of iron in solutions, 100 μL of the sample was mixed with 100 μL 50 mM NaOH and 100 μL freshly prepared iron-releasing reagent (1:1 mixture of 1.4 M HCl and 4.5% KMnO$_4$ in water). After incubation over night at 60 °C, 30 μL freshly prepared iron-detection reagent (6.5 mM ferrozine, 6.5 mM neocuproine, 2.5 M ammonium acetate, 1 M ascorbate) was added. For estimation of the total iron content in cells, 200 μL 50 mM NaOH, 200 μL 10 mM HCl and 200 μL iron-releasing reagent was added to each well of a 24-well plate and incubated over night at 60 °C in a water-saturated environment. Thereafter, 60 μL iron-detection reagent was added to each well. As iron standards, 100 μL of FeCl$_3$ (0 to 300 μM FeCl$_3$ in 10 mM HCl) were mixed with 100 μL 50 mM NaOH, 100 μL iron-releasing reagent and 30 μL iron-detection reagent. After 30 min incubation with the iron-detection reagent at room temperature the absorbance at 540 nm of the ferrous iron-FZ complex in 280 μL reaction mixture was recorded in wells of a microtiter plate using a Sunrise RC microtiterplate photometer (Tecan, Crailsheim, Germany). Iron contents were determined by comparison of absorbance of reaction mixtures containing samples to those containing iron standards.

2.8. Perls' Staining of Cultured Cells for Iron

Ferric iron was visualized in cells by a modification of the histochemical Perls' stain.[22, 23] Following incubation, cells were washed thrice with 1 mL ice cold PBS, fixed

in 300 μL 4% paraformaldehyde in phosphate buffer (PB; 0.1 M potassium phosphate buffer pH 7.4) for 30 min and then washed thrice with 1 mL PB for 10 min. The Perls' reaction was performed by incubating cells with 500 μL 5% (w/v) potassium ferrocyanide in PB for 30 min, followed by incubation with 500 μL of a solution that contains 5% (w/v) potassium ferrocyanide and 5% HCl in PB for 30 min. Cells were washed once with 1 mL PB for 20 min and the Perls' reaction was intensified by incubation with 500 μL of a solution that contained 0.05% (w/v) 3'3'-diaminobenzidine and 0.1% (w/v) nickel sulphate for 15 min and subsequent incubation with 500 μL of a solution that contained 0.05% (w/v) 3'3'-diaminobenzidine, 0.1% (w/v) nickel sulphate and 0.002% H$_2$O$_2$ for 15 min. The stained cells were washed twice with 1 mL of PB for 10 min and incubated at 4 °C over night in 1 mL PB to obtain a clear staining. The cellular staining was visualized using the Eclipse TS2000U microscope (Nikon, Düsseldorf, Germany) with a DS-Qi1Mc digital camera (Nikon, Düsseldorf, Germany).

2.9. TEM of Iron Oxide Nanoparticles in Cultured Astrocytes

To obtain TEM images of cultured astrocytes that had been exposed to iron oxide nanoparticles the cells were washed twice with 1 mL PBS. The cells were scratched of the culture dish with a rubber policemen and the cell suspension was centrifuged at 500 g for 3 minutes. The cell pellet was fixed using a modification of a published method.[24] Briefly, the cells were fixed with 2.5% (w/v) glutaraldehyde in 0.1 M sodium cacodylate buffer pH 7.3 (SCB) at 4 °C over night, washed with SCB and post-fixed in 2% (w/v) osmium tetroxide in SCB for 2 h at room temperature. After washing with SCB, the fixed cells were dehydrated by incubation in solutions of increasing ethanol concentration (up to 100%), washed in acetonitrile, embedded in the Agar low viscosity resin R1078 (Agar Scientific, Stansted, England) and sliced with a microtome (Ultracut UCT, Leica, Germany). The slices were stained with uranyl acetate and lead citrate before they were analysed using the FEI Tecnai F20 S-Twin.

2.10. Determination of Cell Viability and Protein Content

Cell viability was analyzed by determining the activity of lactate dehydrogenase (LDH) in the incubation buffers using the microtiter plate assay described previously[25] with the modification that 20 μL of lysates or incubation buffers were used. The protein content was determined after solubilization of the cells in 200 μL 0.5 M NaOH according to the Lowry method,[26] using bovine serum albumin as a standard.

2.11. Presentation of Data

With the exception of the TEM analysis and the Perls' staining, the data presented are means $\pm$ SD of triplicate values obtained in a representative experiment or they represent means $\pm$ SD of data that were obtained in n independent experiments that were performed in triplicates. All cell culture experiments were performed on at least three independently prepared cultures with comparable results. Significance of differences between two sets of data was analyzed by paired t-test, analysis of significance between groups of data was performed by ANOVA followed by the Bonferroni *post-hoc* tests. $p > 0.05$ was considered as not significant.

3. RESULTS

Magnetic iron oxide nanoparticles were synthesized by coprecipitation of ferrous and ferric iron and subsequent oxidation as described in Methods. The product obtained was a concentrated ferrofluid which showed strong magnetic properties in an external magnetic field (Fig. 1). The yield of the synthesis was determined by measuring the iron content of the ferrofluid. In three independent syntheses the amount of iron quantified in the iron oxide nanoparticles was $78 \pm 10\%$ of the amount of total iron that was used as substrate of the reaction.

Transmission electron microscopy (TEM) revealed that the ferrofluid contained spherical particles that were polydisperse and had diameters between 5 and 20 nm (Fig. 2). The average particle diameter was about 10 nm. The agglomerates of the particles observed by TEM (Fig. 2) are likely to be a direct consequence of the drying process that was required for the sample preparation for the TEM, since the synthesized nanoparticle solution was filtered through
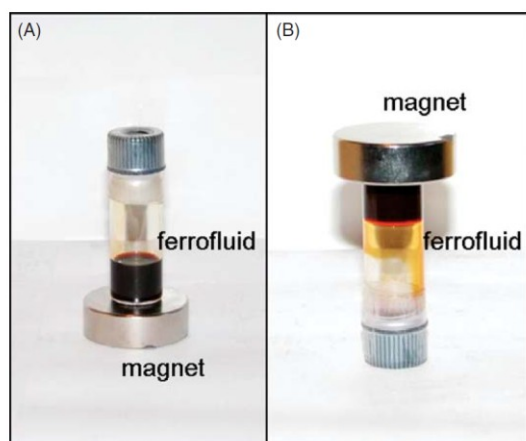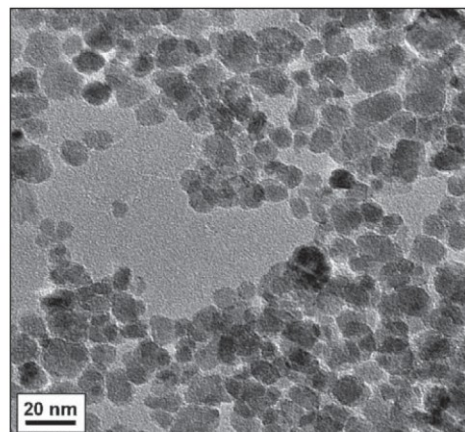

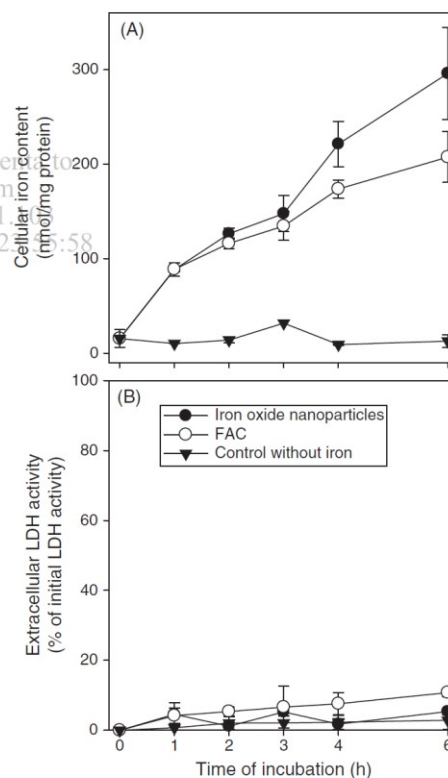**Fig. 2.** TEM image of the synthesized iron oxide nanoparticles.

Fig. 3. Time-dependent accumulation of iron from iron oxide nanoparticles or FAC. Cultured astrocytes were incubated for up to 6 hours without or with iron (100 μM) as iron oxide nanoparticles or FAC. For the given incubation periods the cellular iron content (A) and the extracellular LDH activity (B) was measured. The data represent mean values $\pm$ SD of a representative experiment that was performed in triplicates on a 20-day-old culture that contained 143 ± 18 μg protein per well.

Fig. 1. Aqueous dispersion of iron oxide nanoparticles (ferrofluid) in a magnetic field.

Geppert et al.   Accumulation of Iron Oxide Nanoparticles by Cultured Brain Astrocytes

Table I. Temperature dependency of iron accumulation of iron from iron oxide nanoparticles or FAC.

Iron source	Temperature (°C)	Iron accumulation rate (nmol/(h×mg))	Extracellular LDH activity (% of initial LDH activity)
Iron oxide	37	36.1 ± 4.1	4.7 ± 3.3
nanoparticles	4	13.9 ± 1.2***	3.2 ± 1.5
FAC	37	26.1 ± 1.7**	11.5 ± 3.8
	4	7.4 ± 1.9***	6.7 ± 2.4

Notes: Astrocyte-rich primary cultures were incubated with 100 μM iron as iron oxide nanoparticles or as FAC for up to 4 h. The cellular iron accumulation was calculated from the linear increase in the values of the cellular iron contents between 1 and 4 h of incubation. The extracellular LDH activity was measured after 4 h of incubation. The data represent means ± SD of values that were obtained in 3 individual experiments performed in triplicates. Indicated is the significance of differences between the data obtained for cells that were incubated at 4 °C or 37 °C with one extracellular iron source (*** $p < 0.001$) or the difference between the data that were obtained for the incubation at 37 °C with iron oxide nanoparticles or FAC (** $p < 0.05$).

a 200 nm filter. Dilution of the ferrofluid in the physiological incubation buffer caused immediate aggregation and precipitation of the particles (data not shown). In order to disperse the synthesized iron oxide nanoparticles in such a buffer, the particles were coated with citrate.

To test for the ability of cultured astrocytes to accumulate iron from iron oxide nanoparticles, astrocyte-rich primary cultures were incubated without iron (control), with 100 μM iron in the form of iron oxide nanoparticles or with 100 μM iron supplied as FAC for up to 6 h (Fig. 3). In the absence of exogenous iron, the cellular iron content remained unchanged during the incubation. In contrast, after application of iron as iron oxide nanoparticles

or as FAC, the cellular iron content increased almost linearly during incubation for up to 6 h (Fig. 3(A)). The cellular iron content after 6 h of incubation with iron oxide nanoparticles and FAC was about 300 and 200 nmol/mg protein, respectively (Fig. 3(A)). None of these conditions caused a significant loss in cell viability as indicated by the almost complete absence of extracellular LDH activity (Fig. 3(B)).
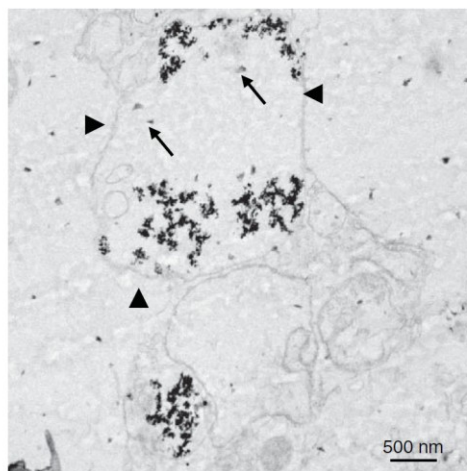

Fig. 4. TEM image of cultured astrocytes that had been exposed for 4 h to 100 μM iron as iron oxide nanoparticles. Small aggregates of iron oxide nanoparticles of a diameter of about 50 nm (arrows) as well as large agglomerates of particles are located in a membrane (arrowheads)-surrounded compartment.
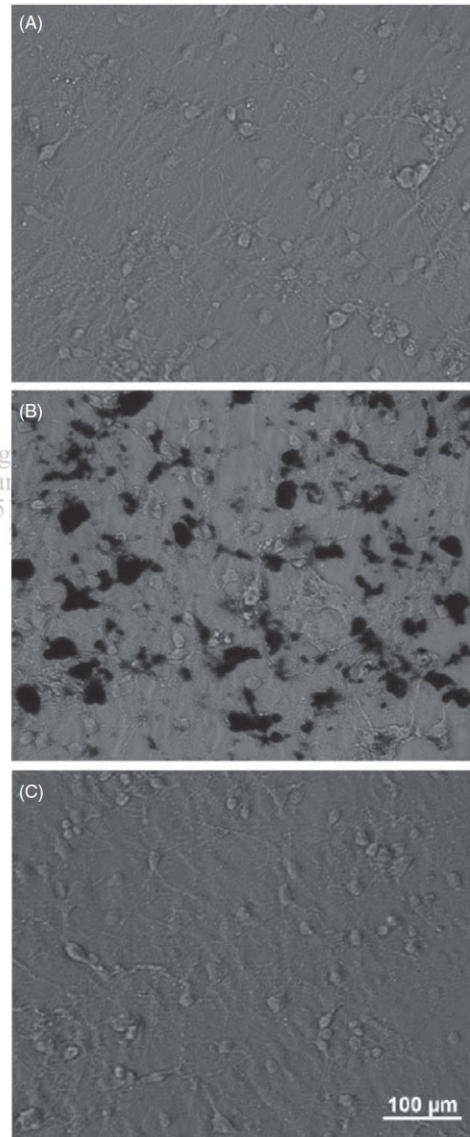
Fig. 5. Perls' staining of cultured astrocytes for ferric iron after exposure to iron oxide nanoparticles. Cultured astrocytes were incubated for 4 h without (A) or with (B, C) iron oxide nanoparticles (100 μM total iron) at 37 °C (A, B) or 4 °C (C). The size bar in (C) applies to all panels.

The linear increase in cellular iron content after application of iron oxide nanoparticles or FAC was used to calculate specific accumulation rates for iron. The specific accumulation rate of iron after application of iron oxide nanoparticles was with 36.1 ± 4.1 nmol/(h × mg protein) significantly ($p < 0.05$) higher than that calculated for cells that were exposed to equimolar amounts of low molecular iron in form of FAC (26.1 ± 1.7 nmol/(h × mg protein)) (Table I).

To confirm that the iron accumulation from exogenous iron oxide nanoparticles or FAC was due to membrane-dependent uptake mechanisms, iron accumulation by astrocytes was compared for incubation temperatures of 37 °C and 4 °C. When astrocyte cultures were incubated for up to 4 h at 4 °C with iron oxide nanoparticles and FAC,

the iron accumulation rate was significantly decreased to approximately 40% and 30%, respectively, of the values obtained for incubations at 37 °C (Table I). Also for these conditions the viability of the cells was not compromised as indicated by the absence of any substantial increase in extracellular LDH activity (Table I).

TEM pictures of astrocyte cultures that had been exposed for 4 h with 100 μM iron as iron oxide nanoparticles revealed the presence of small aggregates (diameter of about 50 nm) and of large agglomerates of iron oxide nanoparticles in compartments that appeared to be surrounded by a membrane (Fig. 4). Cellular accumulation of iron from iron oxide nanoparticles was also demonstrated by the cytochemical Perls' staining for iron of astrocyte cultures that have been exposed for 4 h to iron oxide nanoparticles (100 μM of total iron). While no staining for iron was observed for cultures that were incubated in the absence of iron oxide nanoparticles (Fig. 5(A)), many but not all cells in the cultures that were exposed to iron oxide nanoparticles were intensively stained for iron as indicated by the very dark colour (Fig. 5(B)). In contrast, if cells were incubated with iron oxide nanoparticles (100 μM total iron) for 4 h at 4 °C, hardly any cellular iron was detected by the cytochemical Perls' staining (Fig. 5(C)).

In order to investigate whether the accumulation of iron by astrocyte cultures from exogenous iron oxide nanoparticles was due to uptake of intact iron oxide nanoparticles or a consequence of uptake of low molecular weight iron that was released from the iron oxide nanoparticles, the iron chelators deferoxamine, ferrozine or bathophenanthroline disulfonate (BPS) were applied to the cells together with iron oxide nanoparticles. Under the conditions used, none of the chelators affected significantly the iron accumulation (Fig. 6(A)) or the viability of the cells (Fig. 6(B)).
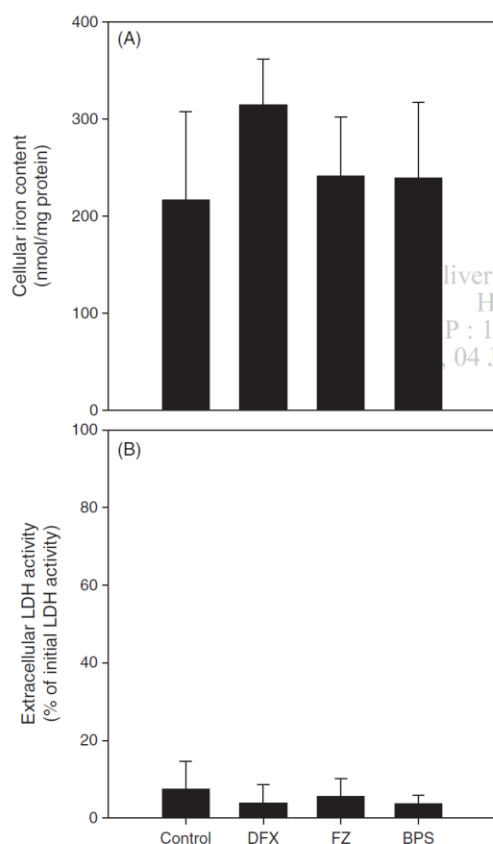
4. DISCUSSION

Iron oxide nanoparticles were synthesized by coprecipitation of ferric and ferrous iron and subsequent oxidation using a modification of a published method[6] to obtain maghemite iron oxide nanoparticles. The yield of the synthesis was about 80% regarding the amount of iron used as substrate for the synthesis and we obtained spherical polydisperse iron oxide nanoparticles with a mean diameter of around 10 nm. It can be assumed that the iron oxide nanoparticles produced contain predominately maghemite,[6] since oxygen was not excluded during synthesis. However, we can not preclude that the particles may also have contained some magnetite, since iron oxide nanoparticles can contain mixtures of the two magnetic iron oxides.[27]

The uncoated iron oxide nanoparticles aggregated and precipitated quickly in incubation buffer at physiological pH. To avoid this process, iron oxide nanoparticles have to be coated with low molecular weight compounds

Fig. 6. Effects of iron chelators on the iron accumulation (A) and viability (B) of cultured astrocytes after exposure to iron oxide nanoparticles. The cells were incubated with 100 μM iron as iron oxide nanoparticles in the absence (control) or presence of 500 μM of the ferric iron chelator deferoxamine (DFX) or the ferrous iron chelators ferrozine (FZ) or bathophenanthroline disulfonate (BPS). After 4 h of incubation the cellular iron content (A) and the extracellular LDH activity (B) were measured. The data represent mean values $\pm$ SD of three individual experiments performed in triplicates.

such as sodium oleate,[28] dimercaptosuccinic acid[19, 29] or citrate[6, 30, 31] or with organic polymers.[32] Since citrate is a physiological compound that is produced and release in substantial amounts by astrocytes[33] we have used citrate as coating ligand for the iron oxide nanoparticles that were applied to cultured astrocytes.

Application of citrate-coated iron oxide nanoparticles to cultured astrocytes did not cause any acute cell toxicity, if the cells were incubated for up to 6 h with iron amounts of 100 μM. This result confirms literature data.[18] Thus, the conditions used were considered suitable to investigate the accumulation of iron from iron oxide nanoparticles by viable astrocytes.

During an incubation of astrocytes with iron oxide nanoparticles, the cellular iron content increased strongly from about 10 nmol/mg protein to about 300 nmol/mg protein within 6 h. This increase was even stronger than that observed after application of ferric ammonium citrate (FAC), a compound that has previously been reported as a good extracellular iron source for astrocytes.[21, 34] The accumulation of iron in cultured astrocytes after exposure to iron oxide nanoparticles was confirmed by TEM and by cytochemical Perls' staining. TEM revealed that most of the cell-associated particles were present in small aggregates or in large agglomerates that were surrounded by a membrane.

The Perls' iron staining has already been used before to demonstrate the presence of iron oxide nanoparticles in cells.[35] Interestingly, not all cells in astrocyte cultures were Perls' positive after exposure to iron oxide nanoparticles and several cells appeared not to be stained. However, it should be noted here that the sensitivity of the Perls' staining for fixed cells is still a matter of debate.[36] Even cells in brain sections are very heterogeneously stained for iron,[37,38] although the brain contains large amounts of iron.[38] The differences in the intensity of the observed cellular Perls' iron staining could be a consequence of the presence of different types of astrocytes in the total brain cultures used that differ in the expression level of proteins that are involved in the accumulation of iron oxide nanoparticles.

To further investigate whether the cellular accumulation of iron after exposure of astrocytes to iron oxide nanoparticles was completely caused by the accumulation of particles and not in part by the known uptake of ferrous or ferric iron ions into astrocytes,[16] the cells were exposed to iron oxide nanoparticles in the presence of iron chelators. Presence of the ferric iron chelator deferoxamine and the ferrous iron chelators ferrozine or bathophenanthroline disulfonate prevent almost completely the uptake by cultured astrocytes of iron from FAC[34] or from ferrous iron (K. Tulpule and R. Dringen, unpublished results), respectively. Since none of these iron chelators prevented the cellular accumulation of iron from iron oxide nanoparticles, an extracellular liberation of ferric or ferrous iron

ions from the iron oxide nanoparticles during the incubation with the cells and subsequent uptake of low molecular weight iron can be excluded.

Since the method used to quantify iron does not allow discriminating between intracellular iron and iron that is bound extracellularly to the cells, the temperature dependency of the iron accumulation was investigated. The accumulation of iron by astrocyte-rich primary cultures after exposure to iron oxide nanoparticles (or FAC) was strongly attenuated by lowering the incubation temperature to 4 °C. This finding confirms that the accumulation of iron from iron oxide nanoparticles at 37 °C is due to a membrane-dependent uptake process rather than being due to the non-specific extracellular binding of the nanoparticles. The strong reduction by lowering the temperature on the ability of astrocytes to accumulate iron from iron oxide nanoparticles or FAC confirms literature data that report that lowering the incubation temperature reduces cellular accumulation of iron[39–42] or of silica-coated nanoparticles.[43]

The effects of the magnetic properties of the citrate-coated iron oxide particles on the accumulation of the nanoparticles was not investigated here and the cultured astrocytes were exposed to the nanoparticles in the absence of an exogenous high magnetic field. However, it should be noted that the uptake of polymer-coated superparamagnetic iron oxide nanoparticles by HELA cells was strongly accelerated by an exogenous magnetic field.[44] Whether such a magnetic field will also enhance the accumulation of citrate-coated iron oxide nanoparticles in cultured brain astrocytes under the conditions used here remains to be elucidated.

Iron in redox active form catalyses the generation of hydroxyl radicals by the Fenton reaction. The iron-dependent generation of cell-damaging reactive oxygen species has also been reported for cultured astrocytes. Exposure of astrocytes to low molecular weight iron in the form of FAC causes radical formation and moderate toxicity[34] which was severely increased by subsequent application of hydrogen peroxide.[45] In contrast, iron chelators completely prevented the iron-mediated toxicity of astrocytes in the absence or presence of peroxides.[34, 45, 46] Although cultured astrocytes efficiently accumulated the nanoparticles, the cells were not acutely damaged by iron oxide nanoparticles under the conditions used. Thus, cellular damage by iron-mediated production of radicals[34] appears not to occur after exposure to the iron oxide nanoparticles. This suggests that for the conditions used an increased formation of reactive oxygen species by a catalytic action of iron in the nanoparticles,[47] or a quick intracellular mobilization of iron from the particles and subsequent formation of radicals by low molecular weight iron[34] does not take place.

In summary, we report that cultured astrocytes rapidly accumulate iron oxide nanoparticles in a temperature-dependent process. It would be interesting to study the

Accumulation of Iron Oxide Nanoparticles by Cultured Brain Astrocytes   *Geppert et al.*

accumulation of iron oxide nanoparticles in astrocytes in the brain to demonstrate the *in vivo* relevance of the data that were obtained on cultured astrocytes. Further studies will also be necessary to test whether the iron accumulated in astrocytes after exposure to iron oxide nanoparticles is bioavailable and can be mobilized from the particles to serve as source for cellular iron metabolism. If iron in cellular iron oxide nanoparticles is bioavailable, the delivery of iron in redox-inactive form as iron oxide nanoparticles could be an interesting approach to load cells with a depot of iron without risking a quick mobilisation of iron that would subsequently lead to iron-catalyzed generation of reactive oxygen species and to oxidative cell damage.

References and Notes

1. S. Laurent, D. Forge, M. Port, A. Roch, C. Robic, L. V. Elst, and R. N. Muller, Magnetic iron oxide nanoparticles: Synthesis, stabilization, vectorization, physicochemical characterizations and biological applications. *Chem. Rev.* 108, 2064 (**2008**).
2. J. Kreuter, Application of nanoparticles for the delivery of drugs to the brain. *Int. Congr. Ser.* 1277, 85 (**2005**).
3. C. Corot, P. Robert, J. M. Idée, and M. Port, Recent advances in iron oxide nanocrystal technology for medical imaging, *Adv. Drug Deliv. Rev.* 58, 1471 (**2006**).
4. B. Samanta, H. Van, N. O. Fischer, J. Shi, D. J. Jerry, and V. M. Rotello, Protein-passivated Fe_3O_4-nanoparticles: Low toxicity and rapid heating for thermal therapy, *J. Mater. Chem.* 18, 1204 (**2008**).
5. F. Schüth, A. H. Lu, and E. L. Salabas, Magnetische nanopartikel: Synthese, stabilisierung, funktionalisierung und anwendung. *Angew. Chem.* 119, 1242 (**2007**).
6. A. Bee, R. Massart, and S. Neveu, Synthesis of very fine maghemite particles. *J. Magn. Magn. Mater.* 149, 6 (**1995**).
7. S. Sun, H. Zeng, Size-controlled synthesis of magnetite nanoparticles. *J. Am. Chem. Soc.* 124, 8204 (**2002**).
8. I. Markiewicz and B. Lukomska, The role of astrocytes in the physiology and pathology of the central nervous system. *Acta Neurobiol. Exp.* 66, 343 (**2006**).
9. M. Nedergaard, B. Ransom, and S. A. Goldman, New roles for astrocytes: Redefining the functional architecture of the brain. *Trends Neurosci.* 26, 532 (**2003**).
10. F. Kirchhoff, R. Dringen, and C. Giaume, Pathways of neuron-astrocyte interactions and their possible role in neuroprotection. *Eur. Arch. Psychiatr. Clin. Neurosci.* 251, 159 (**2001**).
11. E. E. Benarroch, Neuron-astrocyte interactions: Partnership for normal function and disease in the central nervous system. *Mayo Clin. Proc.* 80, 1326 (**2005**).
12. A. J. L. Cooper, The Role of Glutathione in the Nervous System, edited by C. A. Shaw, Taylor and Francis, Washington (**1998**), pp. 91–115.
13. R. Dringen, P. G. Pawlowski, and J. Hirrlinger, Peroxide detoxification by brain cells. *J. Neurosci. Res.* 79, 157 (**2005**).
14. R. Dringen, The New Encyclopedia of Neuroscience, edited by L. Squire, T. Albright, F. Bloom, F. Gage, and N. Spitzer, Elsevier, Oxford (**2009**), pp. 733–737.
15. E. Tiffany-Castiglioni and Y. Qian, Astroglia as metal depots: Molecular mechanisms for metal accumulation, storage and release, *Neurotoxicology* 22, 577 (**2001**).
16. R. Dringen, G. M. Bishop, M. Koeppe, T. N. Dang, and S. R. Robinson, The pivotal role of astrocytes in the metabolism of iron in the brain, *Neurochem. Res.* 32, 1884 (**2007**).
17. T. Moos, T. Rosengren Nielsen, T. Skjørringe, and E. H. Morgan, Iron trafficking inside the brain. *J. Neurochem.* 103, 1730 (**2007**).
18. C. Au, L. Mutkus, A. Dobson, J. Riffle, J. Lalli, and M. Aschner, Effects of nanoparticles on the adhesion and cell viability on astrocytes. *Biol. Trace Elem. Res.* 120, 248 (**2007**).
19. T. R. Pisanic II, J. D. Blackwell, V. I. Shubayev, R. R. Finones, and S. Jin, Nanotoxicity of iron oxide nanoparticles internalization in growing neurons. *Biomaterials* 28, 2572 (**2007**).
20. B. Hamprecht and F. Löffler, Primary glial cultures as model for studying hormone action, *Methods Enzymol.* 109, 341 (**1985**).
21. J. Riemer, H. H. Hoepken, H. Czerwinska, S. R. Robinson, and R. Dringen, Colorimetric ferrozine-based assay for the quantification of iron in cultured cells. *Anal. Biochem.* 331, 370 (**2004**).
22. G. M. Bishop and S. R. Robinson, Quantitative analysis of cell death and ferritin expression in response to cortical iron: Implications for hypoxia-ischemia and stroke, *Brain Res.* 907, 175 (**2001**).
23. T. Moos and K. Mollgrad, A sensitive post-DAB enhancement technique for demonstration of iron in the central nervous system. *Histochemistry* 99, 471 (**1993**).
24. M. Grusch, D. Polgar, S. Gfatter, K. Leuhuber, S. Huettenbrenner, C. Leisser, G. Fuhrmann, F. Kassie, H. Steinkellner, K. Smid, G. J. Peters, H. N. Jayaram, W. Klepal, T. Szekeres, S. Knasmüller, and G. Krupitza, Maintenance of ATP favours apoptosis over necrosis triggered by benzamide riboside. *Cell Death Differ.* 9, 169 (**2002**).
25. R. Dringen, L. Kussmaul, and B. Hamprecht, Detoxification of endogenous hydrogen peroxide and organic hydroperoxides by cultured astroglia cells assessed by microtiter plate assay. *Brain Res. Protoc.* 2, 223 (**1998**).
26. O. H. Lowry, N. J. Rosebrough, A. L. Farr, and R. J. Randall, Protein measurements with the Folin phenol reagent. *J. Biol. Chem.* 193, 265 (**1951**).
27. D. Maity and D. C. Agrawal, Synthesis of iron oxide nanoparticles under oxidizing environment and their stabilization in aqueous and non-aqueous media. *J. Magn. Magn. Mater.* 308, 46 (**2007**).
28. A. K. Gupta and M. Gupta, Synthesis and surface engineering of iron oxide nanoparticles for biomedical applications. *Biomaterials* 26, 3995 (**2005**).
29. N. Fauconnier, J. N. Pons, J. Roger, and A. Bee, Thiolation of maghemite nanoparticles by dimercaptosuccinic acid. *J. Colloid Interface Sci.* 194, 427 (**1997**).
30. N. Fauconnier, A. Bee, J. Roger, and J. N. Pons, Synthesis of aqueous magnetic liquids by surface complexation of maghemite nanoparticles. *J. Mol. Liq.* 83, 233 (**1999**).
31. H. Pilgrimm, Superparamagnetic particles with increased R1 relaxivity, process for producing said particles and use thereof. U.S. Patent 6,634,494, October (**2003**).
32. A. Petri-Fink, B. Steitz, A. Finka, J. Salaklang, and H. Hofmann, Effect of cell media on polymer coated superparamagnetic iron oxide nanoparticles (SPIONs): Colloidal stability, cytotoxicity, and cellular uptake studies. *Eur. J. Pharm. Biopharm.* 86, 129 (**2008**).
33. N. Westergaard, U. Sonnewald, G. Unsgard, L. Peng, L. Hertz, and A. Schousboe, Uptake, release, and metabolism of citrate in neurons and astrocytes in primary cultures. *J. Neurochem.* 62, 1727 (**1994**).
34. H. H. Hoepken, T. Korten, S. R. Robinson, and R. Dringen, Iron accumulation, iron-mediated toxicity and altered levels of ferritin

Geppert et al.   Accumulation of Iron Oxide Nanoparticles by Cultured Brain Astrocytes

and transferrin receptor in cultured astrocytes during incubation with ferric ammonium citrate. *J. Neurochem.* 88, 1194 (**2004**).

35. A. Naveau, P. Smirnov, C. Ménager, F. Gazeau, O. Clément, A. Lafont, and B. Gogly, Phenotypic study of human gingival fibroplasts labeled with superparamagnetic anionic nanoparticles. *J. Periodontol.* 77, 238 (**2006**).

36. M. F. Falangola, S. P. Lee, R. A. Nixon, K. Duff, and J. A. Helpern, Histological co-localization of iron in Aβ plaques of PS/APP transgenic mice. *Neurochem. Res.* 30, 201 (**2005**).

37. J. R. Burdo, J. Martin, S. L. Menzies, K. G. Dolan, M. A. Romano, R. J. Fletcher, M. D. Garrick, L. M. Garrick, and J. R. Connor, Cellular distribution of iron in the brain of the Belgrade rat. *Neuroscience* 93, 1189 (**1999**).

38. D. J. Piñero and J. R. Connor, Iron in the brain: An important contributor in normal and diseased states. *Neuroscientist* 6, 435 (**2000**).

39. D. Trinder and E. Morgan, Mechanisms of ferric citrate uptake by human hepatoma cells. *Am. J. Physiol. Gastrointest. Liver. Physiol.* 275, 279 (**1998**).

40. Z. M. Qian, Q. K. Liao, Y. To, Y. Ke, Y. K. Tsoi, G. F. Wang, and K. P. Ho, Transferrin-bound and transferrin free iron uptake by cultured rat astrocytes. *Cell. Mol. Biol.* 46, 541 (**2000**).

41. D. R. Richardson, Iron and gallium increase iron uptake from transferrin by human melanoma cells: Further examination of the ferric ammonium citrate-derived iron uptake process, *Biochim. Biophys. Acta* 1536, 43 (**2001**).

42. M. Arreedondo, J. Kloosterman, S. Núñez, F. Segovia, V. Candia, S. Flores, S. Le Blanc, M. Olivares, and F. Pizarro, Heme iron uptake by Caco-2 cells is a saturable, temperature sensitive and modulated by extracellular pH and potassium. *Biol. Trace Elem. Res.* 125, 109 (**2008**).

43. J. S. Kim, T. J. Yoon, K. N. Yu, M. S. Noh, M. Woo, B. G. Kim, K. H. Lee, B. H. Sohn, S. B. Park, J. K. Lee, and M. H. Cho, Cellular uptake of magnetic nanoparticles is mediated through energy-dependent endocytosis in A549 cells. *J. Vet. Sci.* 7, 321 (**2006**).

44. A. Petri-Fink and H. Hoffmann, Superparamagnetic iron oxide nanoparticles (SPIONs): From synthesis to *in vivo* studies—a summary of the synthesis, characterization, *in vitro* and *in vivo* investigations of SPIONs with particular focus on surface and colloidal properties. *IEEE Transact. Nanobiosci.* 6, 289 (**2007**).

45. J. R. Liddell, H. H. Hoepken, P. J. Crack, S. R. Robinson, and R. Dringen, Glutathione peroxidase 1 and glutathione are required to protect mouse astrocytes from iron-mediated hydrogen peroxide toxicity. *J. Neurosci. Res.* 84, 578 (**2006**).

46. J. R. Liddell, S. R. Robinson, and R. Dringen, Endogenous glutathione and catalase protect cultured rat astrocytes from the iron-mediated toxicity of hydrogen peroxide. *Neurosci. Lett.* 364, 164 (**2004**).

47. A. Nel, T. Xia, L. Mädler, and L. Ning, Toxic potential of materials at the nanolevel. *Science* 311, 622 (**2006**).

2.2 Publication 2

Hohnholt, M. C., **Geppert, M.**, Nürnberger, S., von Byern, J., Grunwald, I. and Dringen R. (2010) Advanced Biomaterials: Accumulation of citrate-coated magnetic iron oxide nanoparticles by cultured brain astrocytes. *Adv Eng Mater* **12,** B690-694.

Contributions of M. Geppert:

- Synthesis of iron oxide nanoparticles
- Performance of the experiments for Figures 1 and 2

M. C. Hohnholt performed the Perls' staining (Figure 3), coordinated the sample preparation for electron microscopy and prepared the first draft of the manuscript. S. Nürnberger performed the electron microscopy and provided Figure 4.

ADVANCED BIOMATERIALS

Advanced Biomaterials Accumulation of Citrate-Coated Iron Oxide Nanoparticles by Cultured Brain Astrocytes**

By Michaela C. Hohnholt, Mark Geppert, Sylvia Nürnberger, Janek von Byern, Ingo Grunwald and Ralf Dringen*

Magnetic iron oxide nanoparticles (Fe-NP) are considered for various applications in the brain. However, little is known so far on the uptake and the metabolism of such nanoparticles in brain cells. Since astrocytes are strategically localized between capillaries and neurons, astrocytes are of particular interest concerning uptake and fate of nanoparticles in the brain. Using astrocyte-rich primary cultures as model system we have investigated the accumulation of citrate-coated Fe-NP by astrocytes. Viable cultured astrocytes accumulate iron from citrate-coated Fe-NP in a time-, concentration-, and temperature-dependent manner. The cellular iron content determined after 4 h of incubation increases proportional to the concentration of Fe-NP, if the particles were applied in concentrations of up to 1000×10^{-6} M of total iron. The iron accumulation from 500 or 1000×10^{-6} M iron as Fe-NP is significantly slowed by lowering the incubation temperature from 37 to 4 °C. Transmission electron microscopy of the cells revealed that most of the cellular Fe-NP are present in intracellular vesicles. These data demonstrate that astrocytes accumulate efficiently citrate-coated Fe-NP, most likely by an endocytotic pathway.

Magnetic iron oxide nanoparticles (Fe-NP) contain an iron oxide core (Fe_3O_4 or $\gamma\text{-}Fe_2O_3$) and a ligand shell which consists of small organic molecules, polymers, or proteins and is essential for the stable dispersion of such nanoparticles in physiological media.[1–3] Due to their small size Fe-NP are considered for many applications. Especially in medicine and brain cell biology, Fe-NP have already been used as contrast agent,[4] as carriers for drug delivery,[5] for magnetic hyperthermia approaches,[6] and for magnetic transfection of cells.[7] However, despite such important applications little is known so far about the uptake of Fe-NP into brain cells and on the fate of these particles in brain or in cultured brain cells.

The brain contains in addition to neurons also different types of glial cells. Among these glial cells, astrocytes are quantitatively the largest population of cells.[8] Astrocytes fulfill a variety of very important functions for the brain, e.g., in the regulation of ion, pH and transmitter homeostasis, in supporting synapse function and in giving metabolic support to other types of brain cells.[9–12] Endfeet of astrocytes are covering the surface of brain capillaries that consist of capillary endothelial cells which constitute the blood-brain barrier. Thus, astrocytes will be the first parenchymal brain cell type that encounters nanoparticles that have crossed the blood-brain barrier. Due to this strategically important location astrocytes can control the flow of metabolites and metal ions from the blood into the brain and vice versa.[9] Due to their potential to take up and release iron, astrocytes have been discussed to play an important role in the iron metabolism of the brain.[13] Thus, astrocytes should also be considered concerning the accumulation and the fate of Fe-NP in the brain. Application of different types of Fe-NP to

[*] Prof. R. Dringen, M. C. Hohnholt, M. Geppert
Center for Biomolecular Interactions Bremen and Center for Environmental Research and Sustainable Technology, University of Bremen,
PO. Box 330440, D-28334 Bremen, Germany
E-mail: ralf.dringen@uni-bremen.de
S. Nürnberger
Department of Traumatology, Medical University of Vienna, Waehringer Guertel 18-20, 1090 Vienna, Austria
Dr. J. von Byern
Faculty of Life Sciences, University of Vienna, Research Unit Cell Imaging and Ultrastructure
Althanstrasse 14, 1090 Vienna, Austria
Dr. I. Grunwald
Fraunhofer Institute for Manufacturing Technology and Applied Materials Research
Wiener Strasse, D-28359 Bremen, Germany

ADVANCED BIOMATERIALS

cultured astrocytes appears not to be acutely toxic to these cells.[7,14,15] These cells accumulate iron even better from Fe-NP than from identical amounts (100×10^{-6} M total iron) of low molecular weight iron sources.[14]

Here, we report that cultured astrocytes accumulate iron efficiently from citrate-coated Fe-NP in a time-, concentration-, and temperature dependent manner. Presence of cellular iron after exposure of astrocytes to Fe-NP was demonstrated by iron quantification, by cytochemical Perls' staining for iron as well as by transmission electron microscopy (TEM) of Fe-NP in the cells.

Experimental

Synthesis and Coating of Fe-NP

Magnetic Fe-NP were synthesized by using a wet chemical method as described previously[14] using the method initially described by Bee et al.[16]. The stock solution of Fe-NP in water (80×10^{-3} M total iron concentration) was diluted with an equal volume of 80×10^{-3} M freshly prepared aqueous tri-sodium citrate, resulting in an aqueous stable dispersion of citrate-coated Fe-NP that contained 40×10^{-3} M of total iron. The presence of the citrate as coating molecule on the surface of such Fe-NP has previously been demonstrated.[17,18] The dispersion of citrate-coated Fe-NP was sterile filtered and stored at $4\,^{\circ}$C. All concentrations of Fe-NP given here refer to the concentration of total iron in the diluted Fe-NP dispersions and not to the concentration of the nanoparticles.

Cell Culture and Experimental Incubations

Astrocyte-rich primary cultures in wells of 24-well plates were prepared from the brains of newborn Wistar rats and maintained as described previously.[14] Cells were exposed to citrate-coated Fe-NP in 1 mL incubation buffer (20×10^{-3} M HEPES, 145×10^{-3} M NaCl, 1.8×10^{-3} M CaCl$_2$, 5.4×10^{-3} M KCl, 1×10^{-3} M MgCl$_2$, 5×10^{-3} M glucose, 10×10^{-3} M tri-sodium citrate) that had been adjusted to pH 7.4 at the desired temperature. After the given incubation periods, the cells were washed twice with 1 mL of ice-cold phosphate-buffered saline (PBS: 10×10^{-3} M potassium phosphate buffer pH 7.4, containing 150×10^{-3} M NaCl) and dry cells were stored frozen until quantification of their iron and protein contents. Increasing the number of washing steps, washing the cells in presence of the iron chelator deferoxamine (10×10^{-3} M in PBS) or washing the cells with 10×10^{-3} M HCl did not lower the amount of detectable cellular iron after incubation with 1000×10^{-6} M Fe-NP for 4 h (data not shown), demonstrating that washing the cells twice with PBS is sufficient to remove all loosely bound Fe-NP from the cell membranes.

Determination of Cell Viability and Quantification of Cellular Contents of Protein and Iron

Cell viability was analyzed by comparison of the activities of extracellular and cellular lactate dehydrogenase (LDH) as described previously.[19,20] For quantification of the cellular protein content, cells were lysed in 400 µL 50×10^{-3} M NaOH and the protein content was determined according to the Lowry method [21] with bovine serum albumin as standard. Iron contents in media and cells were quantified by the ferrozine-based colorimetric assay [22] in the modification described previously.[14,19]

Visualization of Cellular Iron and Fe-NP by Perls' Staining and TEM

Cellular iron was visualized by the cytochemical Perls' staining [23] as described previously.[14,19] For TEM analysis, cells grown on Aclarfilm (Ted Pella, Redding, USA) in wells of 24-well dishes were incubated with 1000×10^{-6} M citrate-coated Fe-NP, washed with ice-cold PBS and prefixed with 2.5% w/v glutaraldehyde in 0.1 M sodium cacodylate buffer pH 7.3 for 60 min. After rinsing in prefixation buffer, fixation was carried out in 1% w/v osmium tetroxide and 1% w/v potassium ferrocyanide (in sodium cacodylate buffer) for 2 h. The samples were subsequently washed with cacodylate buffer, dehydrated in a graded series of increasing ethanol concentrations, infiltrated with Agar Low Viscosity Resin (Agar Scientific, Stansted, UK) and polymerized at $60\,^{\circ}$C. Ultrathin sections of 70 nm were stained with uranyl acetate and lead citrate. Sections were examined in an FEI Morgagni electron microscope (Eindhoven, Netherlands) operated at 80 kV. Results were documented with a Morada CCD-camera (Olympus, Vienna, Austria).

Presentation of Data

The data shown are means ± standard deviation from values obtained on three independently prepared cultures. Significance of differences between two sets of data was analyzed by paired t-test. $p > 0.05$ was considered as not significant.

Results

To test for the ability of astrocytes to accumulate iron from Fe-NP, astrocyte-rich primary cultures were incubated with citrate-coated Fe-NP (Fig. 1). While no alteration of the cellular iron content was observed for cells treated without Fe-NP at $37\,^{\circ}$C, the content of cell-associated iron increased almost linearly after exposure to Fe-NP from initial 18 ± 10 nmol iron/mg protein to 1075 ± 138 nmol mg^{-1} protein (500×10^{-6} M) and 1915 ± 93 nmol mg^{-1} protein (1000×10^{-6} M) [Fig. 1(A)]. Cells that were incubated with Fe-NP at $4\,^{\circ}$C under otherwise identical conditions contained at each time point investigated less iron than cells that had been incubated at $37\,^{\circ}$C [Fig. 1(A)]. The almost linear increases of the specific cellular iron contents between 1 and 6 h were used to calculate specific iron accumulation rates. For both Fe-NP concentrations used, the iron accumulation rate at $4\,^{\circ}$C was with $44.4 \pm 2.3\%$ (500×10^{-6} M) and $41.2 \pm 2.9\%$ (1000×10^{-6} M) significantly lower than that determined for $37\,^{\circ}$C [Fig. 1(B)], suggesting that a membrane dependent

M. C. Hohnholt et al./Advanced Biomaterials Accumulation of Citrate-Coated Magnetic . . .
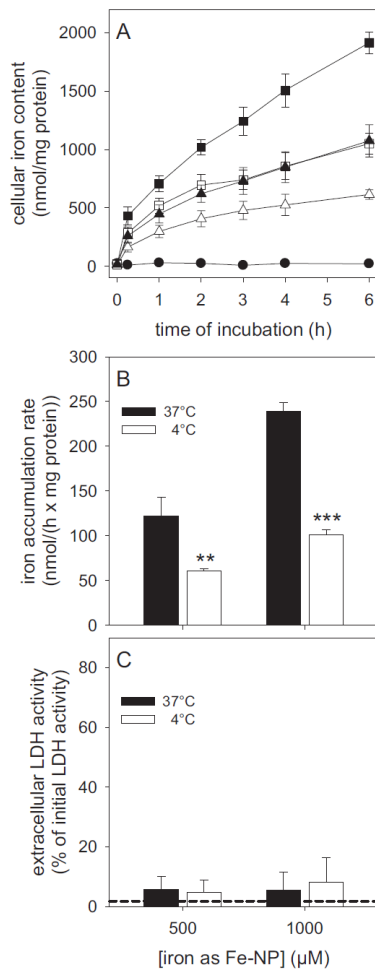

Fig. 1. (A) Time- and temperature-dependency of the accumulation of iron by cultured astrocytes after exposure to Fe-NP. The cells were incubated without (circles) or with 500×10^{-6} M (triangles) or 1000×10^{-6} M (squares) iron as citrate-coated Fe-NP for up to 6 h at 37 °C (filled symbols) or 4 °C (open symbols). (B) Iron accumulation rates that were calculated from the almost linear increases of the cellular iron contents between 1 and 6 h of incubation. (C) Extracellular LDH activity after 6 h of incubation as indicator for cell viability. Stars in B indicate the significance of differences between the values obtained for incubation at 37 and 4 °C (**$p < 0.01$, ***$p < 0.001$). The dashed line in C represents the extracellular LDH activity of cells that had been incubated without Fe-NP.
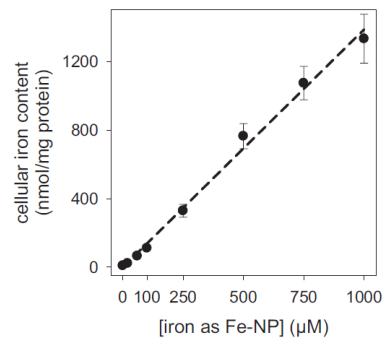

Fig. 2. Concentration dependency of the accumulation of iron from Fe-NP by cultured astrocytes. The cells were incubated for 4 h at 37 °C with iron supplied as citrate-coated Fe-NP in the indicated concentrations. Linear regression of the data revealed a correlation of 0.995.

The strong accumulation of iron from citrate-coated Fe-NP by cultured astrocytes was confirmed by cytochemical Perls' staining for iron (Fig. 3). Astrocytes that had been exposed to 1000×10^{-6} M citrate-coated Fe-NP for 4 h at 37 °C showed an intense dark staining [Fig. 3(C)] which was not detectable for cells that were incubated without Fe-NP [Fig. 3(A)]. The staining was punctuated and predominantly located around the cell nuclei [Fig. 3(C)]. In contrast, when cells were incubated at 4 °C hardly any Perls' staining was detectable both for cells that were incubated without or with citrate-coated Fe-NP [Fig. 3(B,D)].

To investigate whether the measured cell-associated iron represents intracellular Fe-NP, the cells were analyzed by TEM after incubation for 4 h with 1000×10^{-6} M citrate-coated Fe-NP at 37 °C (Fig. 4). Cells exposed to Fe-NP contained electron-dense particles that were predominately located as aggregates in intracellular membrane vesicle and to a lesser extent in the cytosol of the cells [Fig. 4(A,B)]. In addition,

uptake process is involved in iron accumulation from Fe-NP. None of the conditions used compromised cell viability, since after 6 h of incubation no significant increases in extracellular LDH activity were observed [Fig. 1(C)].

To investigate the concentration dependency of the iron accumulation from Fe-NP, astrocyte cultures were incubated with citrate-coated Fe-NP of various concentrations for 4 h (Fig. 2). The content of cell-associated iron increased almost linearly with the concentration of citrate-coated Fe-NP in the concentration range of 0–1000×10^{-6} M iron (Fig. 2).
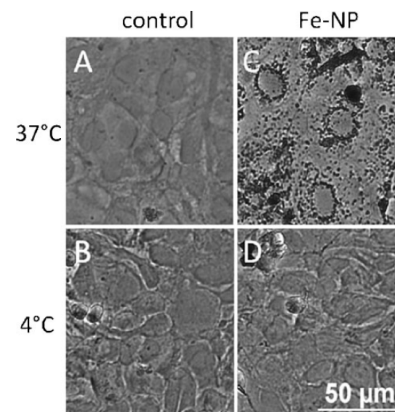

Fig. 3. Perls' iron staining of cultured astrocytes after exposure to Fe-NP. The cells were incubated without (control) or with 1000×10^{-6} M citrate-coated Fe-NP at 37 °C or at 4 °C. The size bar in D applies to all panels.
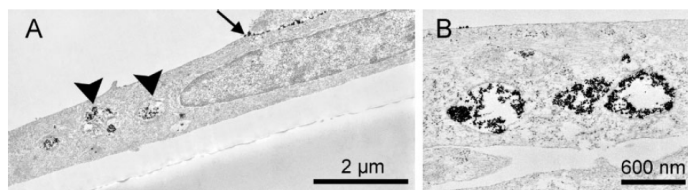
59

ADVANCED BIOMATERIALS

Fig. 4. TEM images of cultured astrocytes after exposure to Fe-NP. The cells were incubated at 37 °C with 1000×10^{-6} M iron as citrate-coated Fe-NP. Electron-dense particles are predominately visible in intracellular vesicles (A, arrowhead) and at the cell surface between cells (A, arrow).

electron-dense material was observed to be present between cells [Fig. 4(A), arrow].

Discussion

Exposure of cultured astrocytes to citrate-coated magnetic Fe-NP did not cause any acute damage, confirming published data for the exposure of astrocytes with different types of coated Fe-NP.[7,14] Cultured astrocytes accumulated iron efficiently to yield high specific iron contents of up to 2 μmol iron/mg protein within 6 h. This demonstrates the high capacity of astrocytes to accumulate iron from Fe-NP and is in line with the observation that astrocytes accumulate iron better from Fe-NP than from low molecular weight iron.[14] The concentration dependency of iron accumulation was almost linear for concentrations up to 1000×10^{-6} M Fe-NP, indicating that at least in this range the iron accumulation from citrate-coated Fe-NP is not saturable.

The iron quantification method used cannot discriminate between intracellular iron and iron that is extracellularly bound as Fe-NP to cell membranes. To discriminate between these two options, the iron accumulation from citrate-coated Fe-NP at 37 °C was compared to that at 4 °C, since membrane dependent uptake processes are strongly slowed by lowering the incubation temperature. Results from such experiments suggest that after exposure of astrocytes to Fe-NP around 40% of the cell-associated iron represents extracellularly bound iron, while around 60%, calculated as difference of the cellular iron contents determined after incubations at 37 and 4 °C, had been taken up into the cells. The view that cell-associated iron represents the sum of intracellular iron plus extracellularly bound iron is strongly supported by TEM images of astrocytes after exposure to Fe-NP, which revealed presence of Fe-NP in cells as well as between cells and on the cell surface. The temperature dependency of iron accumulation from 1000×10^{-6} M citrate-coated Fe-NP resembles results obtained for the cellular uptake of low molecular weight iron,[24–26] hemine iron,[27] or a low concentration (100×10^{-6} M) of citrate-coated Fe-NP.[14] Also in these studies, the amounts of cell-associated iron determined after incubation at 4 °C was considered to reflect extracellularly bound material.

Most of the electron-dense material observed by TEM for Fe-NP-treated astrocytes was localized within vesicle-like structures, confirming previous reports.[7,14] This observation

suggests that astrocytes internalize Fe-NP by an endocytotic uptake process, as it has been suggested for non-phagocytotic cells.[28] In addition, the Perls' iron staining of astrocytes that had been exposed to citrate-coated Fe-NP at 37 °C revealed presence of substantial amounts of iron in the cells, while cells that were incubated at 4 °C were not Perls'-positive. These data support the view that the temperature dependent part of the cellular iron reflects the amount of iron that has been taken up into the cells after exposure to citrate-coated Fe-NP, whereas the amount of cell-associated iron determined for cells that were incubated at 4 °C represents predominantly Fe-NP that had bound extracellularly to cell membranes. The absence of Perls' staining from cells that were exposed to Fe-NP at 4 °C is likely to be a consequence of the known poor sensitivity of this assay.[14]

In summary, cultured brain astrocytes are highly efficient to accumulate iron from citrate-coated Fe-NP in a time-, concentration-, and temperature dependent manner into intracellular vesicles by a mechanism that is likely to involve endocytosis, a process which is well known to occur in astrocytes in vitro.[29–31] However, further studies are required to investigate whether the observed accumulation of Fe-NP in cultured astrocytes is also a property of astrocytes in brain. Since astrocytes have important functions for the iron homeostasis of the brain,[13] the fate of the internalized Fe-NP particles will be interesting to study. If the iron of the accumulated Fe-NP is available for the cellular metabolism, it could support iron-dependent processes or, alternatively, induce iron-mediated toxicity in brain cells.

[1] S. Laurent, D. Forge, M. Port, A. Roch, C. Robic, L. Vander Elst, R. N. Muller, *Chem. Rev.* **2008**, *108*, 2064.

[2] A. H. Lu, E. L. Salabas, F. Schuth, *Angew. Chem, Int. Ed. Engl.* **2007**, *46*, 1222.

[3] B. Samanta, H. Yan, N. O. Fischer, J. Shi, D. J. Jerry, V. M. Rotello, *J. Mater. Chem.* **2008**, *18*, 1204.

[4] J. S. Weinstein, C. G. Varallyay, E. Dosa, S. Gahramanov, B. Hamilton, W. D. Rooney, L. L. Muldoon, E. A. Neuwelt, *J. Cereb. Blood Flow Metab.* **2010**, *30*, 15.

[5] B. Chertok, B. A. Moffat, A. E. David, F. Yu, C. Bergemann, B. D. Ross, V. C. Yang, *Biomaterials* **2008**, *29*, 487.

[6] A. Jordan, R. Scholz, K. Maier-Hauff, F. K. van Landeghem, N. Waldoefner, U. Teichgraeber, J. Pinkernelle, H. Bruhn, F. Neumann, B. Thiesen, A. von Deimling, R. Felix, *J. Neurooncol.* **2006**, *78*, 7.

ADVANCED BIOMATERIALS

M. C. Hohnholt et al./Advanced Biomaterials Accumulation of Citrate-Coated Magnetic . . .

[7] M. Pickard, D. Chari, *Nanomedicine (Lond)* **2010**, *5*, 217.

[8] M. Nedergaard, B. Ransom, S. A. Goldmann, *Trends Neurosci.* **2003**, *26*, 523.

[9] M. V. Sofroniew, H. V. Vinters, *Acta Neuropathol.* **2010**, *119*, 7.

[10] J. Hirrlinger, R. Dringen, *Brain Res. Rev.* **2010**, *63*, 177.

[11] M. M. Halassa, P. G. Haydon, *Annu. Rev. Physiol.* **2010**, *72*, 335.

[12] C. Giaume, A. Koulakoff, L. Roux, D. Holcman, N. Rouach, *Nat. Rev. Neurosci.* **2010**, *11*, 87.

[13] R. Dringen, G. M. Bishop, M. Koeppe, T. N. Dang, S. R. Robinson, *Neurochem. Res.* **2007**, *32*, 1884.

[14] M. Geppert, M. Hohnholt, L. Gaetjen, I. Grunwald, M. Baumer, R. Dringen, *J. Biomed. Nanotechnol.* **2009**, *5*, 285.

[15] C. Au, L. Mutkus, A. Dobson, J. Riffle, J. Lalli, M. Aschner, *Biol. Trace Elem. Res.* **2007**, *120*, 248.

[16] A. Bee, R. Massart, S. Neveu, *J. Magn. Magn. Mater.* **1995**, *149*, 6.

[17] N. Fauconnier, A. Bee, R. Massart, F. Dardoize, *J. Liq. Chromatogr. Relat. Technol.* **1996**, *19*, 783.

[18] N. Fauconnier, A. Bee, J. Roger, J. N. Pons, *Prog. Colloid Polym. Sci.* **1996**, *100*, 212.

[19] M. Hohnholt, M. Geppert, R. Dringen, *Neurochem. Res.* **2010**, *35*, 1259.

[20] R. Dringen, L. Kussmaul, B. Hamprecht, *Brain Res. Protoc.* **1998**, *2*, 223.

[21] O. H. Lowry, N. J. Rosebrough, A. L. Farr, R. J. Randall, *J. Biol. Chem.* **1951**, *193*, 265.

[22] J. Riemer, H. H. Hoepken, H. Czerwinska, S. R. Robinson, R. Dringen, *Anal. Biochem.* **2004**, *331*, 370.

[23] M. Perls, *Virchows Arch.* **1867**, *39*, 42.

[24] Z. M. Qian, Q. K. Liao, Y. To, Y. Ke, Y. K. Tsoi, G. F. Wang, K. P. Ho, *Cell Mol. Biol. (Noisy-le-grand)* **2000**, *46*, 541.

[25] D. R. Richardson, *Biochim. Biophys. Acta* **2001**, *1536*, 43.

[26] D. Trinder, E. Morgan, *Am. J. Physiol.* **1998**, *275*, G279.

[27] T. N. Dang, G. M. Bishop, R. Dringen, S. R. Robinson, *Glia* **2010**, *58*, 55.

[28] J. Rejman, V. Oberle, I. S. Zuhorn, D. Hoekstra, *Biochem. J.* **2004**, *377*, 159.

[29] W. Noske, H. Letzen, K. Lange, K. Keller, *Exp. Cell Res.* **1982**, *142*, 437.

[30] L. Megias, C. Guerri, E. Fornas, I. Azorin, E. Bendala, M. Sancho-Tello, J. M. Duran, M. Tomas, M. J. Gomez-Lechon, J. Reanu-Piqueras, *Int. J. Dev. Biol.* **2000**, *44*, 2009.

[31] M. Jiang, G. Chen, *J. Neurosci.* **2009**, *29*, 8063.

2.3 Publication 3

Geppert, M., Hohnholt, M. C., Thiel, K., Nürnberger, S., Grunwald, I., Rezwan, K. and Dringen R. (2011) Uptake of dimercapto-succinate-coated magnetic iron oxide nanoparticles in cultured brain astrocytes. *Nanotechnology* **22,** 145101.

Contributions of M. Geppert:

- Synthesis of iron oxide nanoparticles
- Performance of experiments for Table 1 and Figures 2, 3, 5 and 6
- Preparation of a first draft of the manuscript

M. C. Hohnholt performed the Perls' staining (Figure 4) and coordinated the sample preparation for the electron microscopy. K. Thiel performed electron microscopy and energy dispersive X-ray spectroscopy of the nanoparticles and generated Figure 1. S. Nürnberger performed the electron microscopy and provided Figures 5 and 6.

Uptake of dimercaptosuccinate-coated magnetic iron oxide nanoparticles by cultured brain astrocytes

Mark Geppert[1,2]**, Michaela C Hohnholt**[1,2]**, Karsten Thiel**[3]**,
Sylvia Nürnberger**[4,5]**, Ingo Grunwald**[3]**, Kurosch Rezwan**[6] **and
Ralf Dringen**[1,2,7,8]

[1] Center for Biomolecular Interactions Bremen, University of Bremen, PO Box 330440,
D-28334 Bremen, Germany
[2] Center for Environmental Research and Sustainable Technology, Leobener Strasse, D-28359
Bremen, Germany
[3] Fraunhofer Institute for Manufacturing Technology and Advanced Materials, Wiener Strasse
12, D-28359 Bremen, Germany
[4] Department of Traumatology, Medical University of Vienna, Waehringer Guertel 18-20,
1090 Vienna, Austria
[5] Ludwig Boltzmann Institute for Clinical and Experimental Traumatology, Austrian Cluster
for Tissue Regeneration, 1200 Vienna, Austria
[6] Advanced Ceramics, University of Bremen, Am Biologischen Garten 2, D-28359 Bremen,
Germany
[7] School of Psychology and Psychiatry, Monash University, Wellington Road, Clayton,
Victoria 3800, Australia

E-mail: ralf.dringen@uni-bremen.de

Abstract
Magnetic iron oxide nanoparticles (Fe-NP) are currently considered for various diagnostic and
therapeutic applications in the brain. However, little is known on the accumulation and
biocompatibility of such particles in brain cells. We have synthesized and characterized
dimercaptosuccinic acid (DMSA) coated Fe-NP and have investigated their uptake by cultured brain
astrocytes. DMSA-coated Fe-NP that were dispersed in physiological medium had an average
hydrodynamic diameter of about 60 nm. Incubation of cultured astrocytes with these Fe-NP caused a
time- and concentration-dependent accumulation of cellular iron, but did not lead within 6 h to any cell
toxicity. After 4 h of incubation with 100–4000 μM iron supplied as Fe-NP, the cellular iron content
reached levels between 200 and 2000 nmol mg^{-1} protein. The cellular iron content after exposure of
astrocytes to Fe-NP at 4 °C was drastically lowered compared to cells that had been incubated at 37 °C.
Electron microscopy revealed the presence of Fe-NP-containing vesicles in cells that were incubated
with Fe-NP at 37 °C, but not in cells exposed to the nanoparticles at 4 °C. These data demonstrate that
cultured astrocytes efficiently take up DMSA-coated Fe-NP in a process that appears to be saturable
and strongly depends on the incubation temperature.

1. Introduction

Magnetic iron oxide nanoparticles (Fe-NP) are available
with various functionalizations and have a wide range of

[8] Address for correspondence: Center for Biomolecular Interactions Bremen,
University of Bremen, PO Box 330440, D-28334 Bremen, Germany.

potential applications [1–3]. Among these, the most important
applications for biology and medicine are the utilization of Fe-
NP as contrast agents in magnetic resonance imaging [4, 5],
as carrier for drug delivery or transfection [6–8] and as
therapeutic agents in cancer therapy by magnetic field-
mediated hyperthermia [9]. Fe-NP contain an iron oxide core

1

(Fe_3O_4 or γ-Fe_2O_3) that is surrounded by a ligand shell which consists of small organic or inorganic molecules, polymers or proteins. These ligand shells are essential for the stabilization of the nanoparticles in physiological media [2, 3, 10].

Astrocytes are the most abundant cells in the brain [11]. They have a strategically very important localization between the blood vessels and neurons [11]. Thus, astrocytes are the first cells in brain that encounter substances which have passed the blood–brain barrier. Astrocytes have a variety of essential functions in the brain that include the uptake and release of transmitters [12, 13] and the supply of metabolites to neurons [14]. In addition, astrocytes contribute substantially to the antioxidative defense of the brain [14] and to the regulation of iron homeostasis [15].

Very recently it was shown that peripherally applied Fe-NP are able to pass the blood–brain barrier [16]. However, despite the promising potential of Fe-NP for brain-related approaches, surprisingly little is known about the consequences of an exposure of brain cells to Fe-NP. Such particles appear not to be acutely toxic to cultured astrocytes [8, 17, 18] or oligodendroglial cells [19], while PC12 cells, a frequently used cell model system for neurons, show an altered morphology and a severe loss in cell viability after exposure to Fe-NP [20]. In addition, cultured astrocytes have been shown to accumulate carboxyl-modified fluorescent Fe-NP [21] and citrate-coated Fe-NP [18, 22].

To investigate the characteristics of the uptake of Fe-NP into astrocytes in more detail, we have synthesized and characterized Fe-NP that were coated with dimercaptosuccinic acid (DMSA) and have used astrocyte-rich primary cultures as cell model system. DMSA-coated Fe-NP (D-Fe-NP) remained dispersed in physiological media after complete removal of unbound DMSA and could be applied to the cells for many hours without inducing toxicity. During the exposure, cultured astrocytes accumulated D-Fe-NP efficiently in a time-, concentration- and temperature-dependent manner.

2. Materials and methods

2.1. Materials

Fetal calf serum (FCS) and penicillin/streptomycin solution were obtained from Biochrom (Berlin, Germany). Dulbecco's modified Eagle's medium (DMEM) was from Gibco (Karlsruhe, Germany). Bovine serum albumin and NADH were purchased from Applichem (Darmstadt, Germany). All other chemicals of the highest purity available were from Sigma (Steinheim, Germany), Fluka (Buchs, Switzerland), Merck (Darmstadt, Germany) or Riedel-de Haen (Seelze, Germany). 96-well microtiter plates were from Nunc (Wiesbaden, Germany) and 24-well cell culture plates from Sarstedt (Nümbrecht, Germany).

2.2. Synthesis and coating of Fe-NP

Magnetic Fe-NP (γ-Fe_2O_3) were synthesized using a wet chemical method as described previously [18, 23]. In six independent experiments, the average yield of the synthesis regarding iron content was $68 \pm 7\%$. To disperse the

synthesized Fe-NP in physiological media, the nanoparticles were coated with DMSA as previously described [20, 24]. Briefly, 0.13 g of DMSA was dissolved in 150 ml pure water and added under vigorous stirring to 100 ml of an aqueous dispersion of Fe-NP (40 mM total iron concentration). After 30 min, the resulting precipitate was centrifuged (5 min; $800g$) and resuspended in 80 ml of pure water. The pH value was adjusted with NaOH to pH 10 and the solution was stirred for an additional 30 min before lowering the pH to 7.4 by adding HCl. To remove larger aggregates, the nanoparticle dispersion was centrifuged (10 min, $1000g$) and sterile filtered through a 0.2 μm filter. The solution was diluted with water to a final iron concentration of 40 mM (3.5 g particle l^{-1}) before storing the solution at 4 °C. Concentrations of D-Fe-NP are given as concentration of the iron present in the nanoparticle dispersion used and not as concentration of particles.

2.3. Transmission electron microscopy (TEM)

Preparation of TEM samples was done by dropping 1 μl of a diluted solution of D-Fe-NP (1 mM total iron) onto a carbon-coated copper-grid. After airdrying at room temperature, TEM imaging was carried out using a FEI Tecnai F20 S-TWIN (Hillsboro, Oregon, USA) operated at 200 kV. Images were recorded using a GATAN GIF2001 SSC-CCD camera. Element analysis by energy dispersive x-ray spectrometry (EDX) was carried out while operating the microscope in scanning mode (STEM) at a spatial resolution of about 1 nm. STEM images were recorded using a high-angle-annular-dark-field (HAADF)-STEM detector. EDX analysis was performed using an EDAX r-TEM-EDX-Detector with an energy resolution of 136 eV. Preparation for TEM analysis of cultured astrocytes that had been incubated without or with D-Fe-NP was performed as previously described [22].

2.4. Determination of the hydrodynamic diameter and the zeta-potential of the particles

The hydrodynamic diameter of the Fe-NP in solution was determined by dynamic light scattering at a scattering angle of 90° using a L.i.SA light scattering machine (Fraunhofer IFAM, Bremen, Germany). The zeta-potential and hydrodynamic particle diameter at a scattering angle of 165° were determined with a Delsa™ Nano C Analyzer (Beckmann Coulter, Krefeld, Germany).

2.5. Cell cultures and experimental incubations

Astrocyte-rich primary cultures were prepared from the brains of newborn Wistar rats and cultured to confluency as described previously [18, 25]. For incubation with D-Fe-NP, the cells were washed twice with 1 ml pre-warmed (37 °C) or cold (4 °C) incubation buffer (IB: 20 mM HEPES, 145 mM NaCl, 1.8 mM $CaCl_2$, 5.4 mM KCl, 1 mM $MgCl_2$, 5 mM glucose, adjusted to pH 7.4 at the desired temperature). Subsequently, the cells were incubated at the indicated temperature with 1 ml of IB containing D-Fe-NP. After the desired incubation period, the media were collected and the cells were washed twice with 1 ml each of ice-cold phosphate-buffered saline (PBS: 10 mM
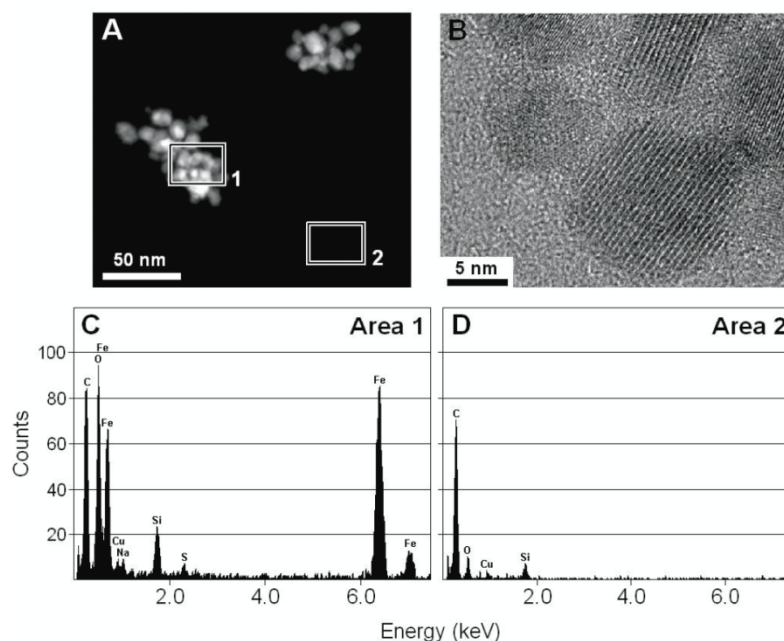
2

Figure 1. TEM-EDX analysis of DMSA-coated Fe-NP. The nanoparticles were diluted with water to a final concentration of 1 mM total iron, dried and investigated by TEM ((A), (B)). The EDX profiles of the contents of the frames 1 and 2 in (A) are presented as panels (C) and (D), respectively.

potassium phosphate buffer pH 7.4, containing 150 mM NaCl). The dry cells were stored frozen until determination of their iron and protein contents.

2.6. Iron quantification and histochemical Perls' staining for iron

The total iron content of the incubation buffers and cells was determined by a modification of the ferrozine-based colorimetric iron assay [26] as described previously [18]. Specific cellular iron contents were obtained by normalizing the total cellular iron content per well to the total cellular protein content per well. Ferric iron was visualized in cells by a modification of the histochemical Perls' iron staining as described previously [18, 19].

2.7. Determination of cell viability and protein content

Cell viability was analyzed by determining the activity of lactate dehydrogenase (LDH) in the incubation buffers using the microtiter plate assay described previously [27] with the modification that 20 μl of lysates or incubation buffers were used. The protein content per well was determined according to the Lowry method [28] after solubilization of the cells in 400 μl 50 mM NaOH, using bovine serum albumin as a standard.

2.8. Presentation of data

If not stated otherwise, the data are presented as means $\pm$ SD of values from at least three experiments that were performed on independently prepared cultures. Significance of difference between two sets of data was analyzed by the paired t-test; analysis of significance between groups of data was performed by ANOVA followed by the Bonferroni *post hoc* tests. $p >$ 0.05 was considered as not significant.

3. Results

3.1. Characterization of the synthesized DMSA-coated Fe-NP

The D-Fe-NP were synthesized as described in section 2. TEM of the nanoparticles revealed the presence of spherical particles with a diameter of about 5–20 nm which formed larger agglomerates of up to 70 nm diameter (figure 1(A)). High resolution TEM confirmed [3, 29] the presence of monocrystalline nanoparticles (figure 1(B)). By EDX analysis of the particles intensive signals for iron and oxygen as well as a small signal for sulfur were detected (figure 1(C)), which were not present in areas of the TEM grid that did not contain nanoparticles (figure 1(D)).

Investigation of diluted solutions (1 mM total iron in water) of uncoated or DMSA-coated Fe-NP by dynamic light scattering revealed for both types of particles a monomodal particle size distribution with d_{50} values of around 60 nm (table 1). Diluting the D-Fe-NP with incubation buffer (IB) did

3

not cause any significant change in the average hydrodynamic particle diameter (table 1), whereas dilution of uncoated Fe-NP in IB led immediately to aggregation and precipitation of the particles (table 1). Measurements of the zeta-potential of the nanoparticles revealed a positive value of 43 ± 14 mV for uncoated nanoparticles in water and negative values of -77 ± 18 mV and -26 ± 3 mV for DMSA-coated nanoparticles in water and IB, respectively. Uncoated nanoparticles aggregated in IB as expected for particles that show a zeta-potential of around zero (table 1).

3.2. Accumulation of iron from DMSA-coated Fe-NP by cultured astrocytes

To test for the ability of astrocytes to accumulate iron from Fe-NP, astrocyte cultures were incubated with D-Fe-NP and the amount of cell-associated iron was quantified for incubation periods of up to 6 h (figure 2). The cells accumulated iron as a function of time and concentration. After a 6 h incubation with 500 and 1000 μM D-Fe-NP, the specific cellular iron content had increased from an initial value of 18 ± 10 nmol mg^{-1} to 1232 ± 122 and 2151 ± 198 nmol mg^{-1} cellular protein, respectively (means $\pm$ SD of data from six experiments). The cellular iron content increased almost linearly between 1

Table 1. Hydrodynamic particle diameter and zeta-potential of uncoated and DMSA-coated Fe-NP. (Note: uncoated or DMSA-coated Fe-NP were dispersed in either water or incubation buffer (IB) to a final concentration of 1 mM total iron and the hydrodynamic particle diameter (at scattering angles of 90° or 165°) as well as the zeta-potential were measured. The numbers in brackets represent the number of measurements performed on individually prepared Fe-NP dispersions.)

Coating	Solvent	Hydrodynamic particle diameter (nm)		Zeta-potential (mV)
		90°	165°	
Uncoated	H$_2$O	64 ± 32 (5)	53 ± 6 (3)	$+43 \pm 14$ (3)
Uncoated	IB	>1000 (3)	>1000 (3)	-1 ± 1 (3)
DMSA	H$_2$O	59 ± 9 (4)	51 ± 7 (3)	-77 ± 18 (3)
DMSA	IB	74 ± 10 (12)	64 ± 14 (3)	-26 ± 3 (3)

and 6 h after application of D-Fe-NP (figure 2(A)), whereas the cellular iron content was not altered during incubation of the cells in the absence of nanoparticles (data not shown). The linear increase in the cellular iron content of D-Fe-NP-treated astrocytes between 1 and 6 h was used to calculate iron accumulation rates. Astrocytes that were exposed to 500 and 1000 μM D-Fe-NP accumulated iron with rates of 122 ± 16
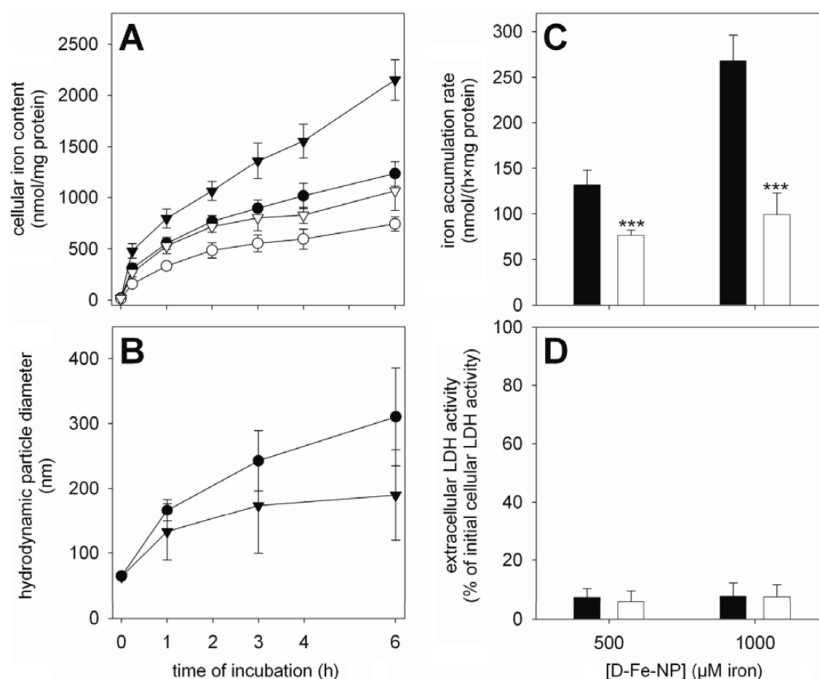

Figure 2. Time- and temperature-dependence of the iron accumulation of cultured astrocytes after exposure to DMSA-coated Fe-NP. The cells were incubated with 500 μM (circles in (A) and (B)) or 1000 μM (triangles in (A) and (B)) D-Fe-NP for up to 6 h at 37 °C (filled symbols and bars) or 4 °C (open symbols and bars) and the cellular iron content (A) and the hydrodynamic particle diameter (B) were determined. The iron accumulation rates (C) were calculated from the linear increases of the cellular iron contents between 1 and 6 h incubation. Extracellular LDH activity (D) was determined after 6 h of incubation as an indicator for a potential loss in cell viability. The extracellular LDH activities of cells incubated in the absence of D-Fe-NP were $5.5 \pm 4.9\%$ (37 °C) and $4.3 \pm 1.7\%$ (4 °C) of the initial cellular LDH activity. The data shown represent mean values $\pm$ SD of 3–6 experiments performed on independently prepared cultures. The stars in (C) indicate the significance of differences between the values obtained for incubation at 37 and 4 °C (*** $p < 0.001$).
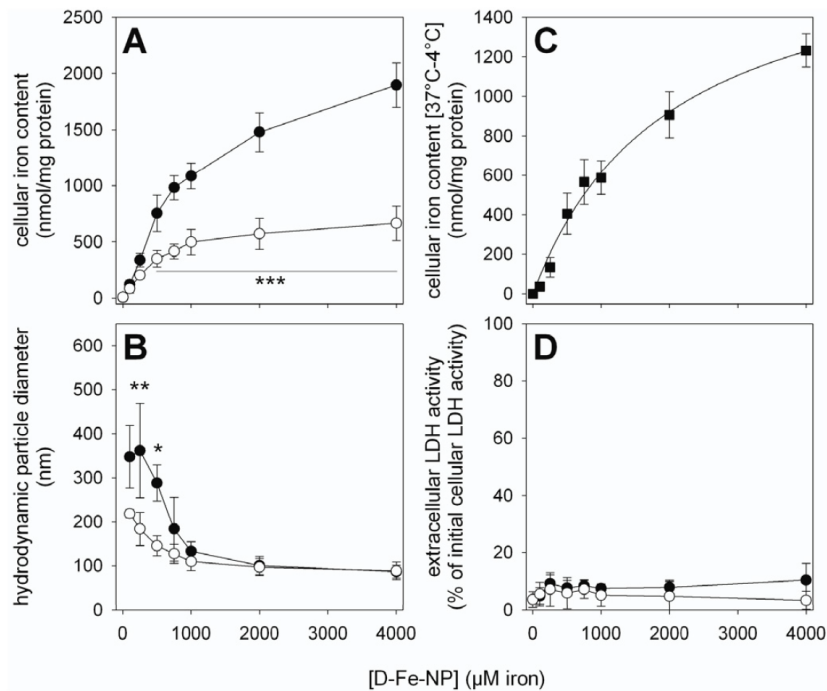
4

Figure 3. Concentration- and temperature-dependence of the iron accumulation from DMSA-coated Fe-NP by cultured astrocytes. The cells were incubated for 4 h with D-Fe-NP containing the indicated concentrations of iron at 37 °C (filled circles) or at 4 °C (open circles) and the cellular iron content (A), the hydrodynamic diameter of the nanoparticles in the supernatant (B) and the extracellular LDH activity (D) were measured. (C) shows the difference of cellular iron contents of cells that were exposed to Fe-NP at 37 °C and at 4 °C. Hyperbolic regression of the data shown in (C) using the Michaelis Menten equation gave a correlation of 0.989. The data represent means ± SD of values obtained in 3–4 experiments performed on independently prepared cultures. The significance of differences between the values obtained for cells that were incubated at 37 °C and at 4 °C is indicated (*$p < 0.05$; **$p < 0.01$; ***$p < 0.001$).

and 268 ± 28 nmol/(h × mg protein), respectively (figure 2(C)). Compared to incubation at 37 °C, astrocytes that were exposed at 4 °C to 500 and 1000 μM D-Fe-NP accumulated iron slower (figure 2(A)) with significantly lower rates that accounted for 58 ± 4 % and 37 ± 9 %, respectively, of the values calculated for the 37 °C conditions (figure 2(C)). Cell viability was not affected for these conditions, as indicated by the absence of any significant increase in extracellular LDH activity (figure 2(D)).

During incubation of cells with 500 and 1000 μM D-Fe-NP for 6 h, the average hydrodynamic diameter of the particles in the incubation medium increased significantly from an initial value of 66 ± 5 nm to values of 310 ± 75 (500 μM D-Fe-NP; $p < 0.01$) and 190 ± 70 nm (1000 μM D-Fe-NP; $p < 0.05$) (figure 2(B)). In contrast, incubation of D-Fe-NP under identical incubation conditions in the absence of cells did not lead to an increase in hydrodynamic particle diameter (data not shown).

To investigate the concentration- and temperature-dependence of the iron accumulation from D-Fe-NP as well as the agglomeration of the particles in the presence of cells in more detail, astrocyte cultures were incubated for 4 h with up to 4000 μM D-Fe-NP at 37 °C or at 4 °C (figure 3). While at 4 °C the amount of cell-associated iron already reached a plateau

of about 600 nmol mg^{-1} cellular protein after incubation for 4 h with around 1000 μM D-Fe-NP, significantly higher cellular iron contents were observed for cells that had been incubated at 37 °C with D-Fe-NP in concentrations above 200 μM (figure 3(A)). Specific cellular iron contents reached after incubation with 4000 μM D-Fe-NP values of around 1900 nmol iron mg^{-1} protein. None of these conditions affected cell viability as indicated by the lack of any significant increase in extracellular LDH activity (figure 3(D)).

The temperature-sensitive part of the iron accumulation from D-Fe-NP was calculated as the difference of the cellular iron contents determined for cells that were incubated at 37 and 4 °C. The temperature-sensitive iron accumulation increased hyperbolically with the concentration of D-Fe-NP applied (figure 3(C)). Analysis of these data by hyperbolic regression demonstrated that the cellular accumulation of iron from D-Fe-NP followed an apparent Michaelis Menten kinetic with apparent K_M and V_{Max} values of 2.1 ± 0.6 mM and 1871 ± 231 nmol iron/(mg × 4 h) (means ± SD of four independent experiments).

The average hydrodynamic diameter of the D-Fe-NP in the media was increased during the incubation with cells. While the diameter of the nanoparticles was at best slightly
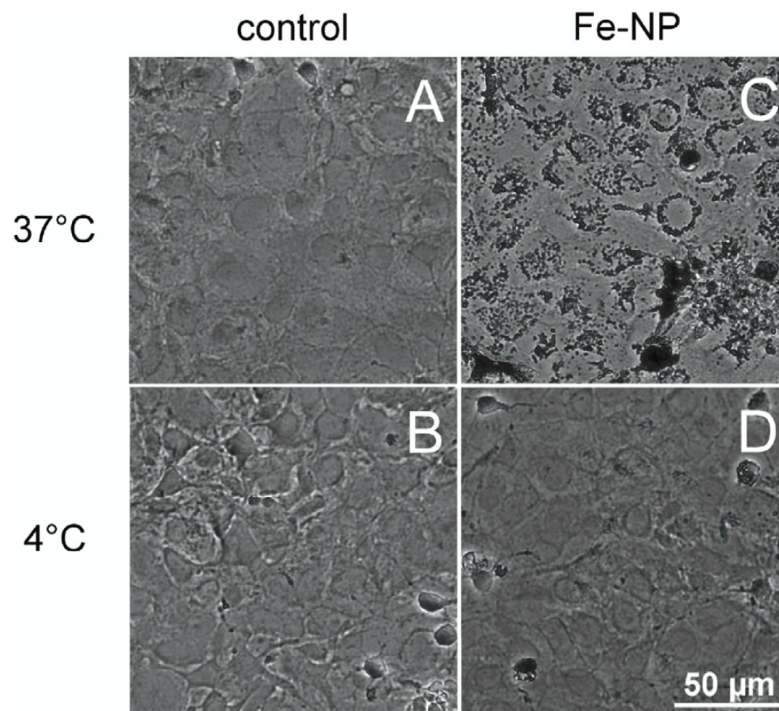
Figure 4. Perls' iron staining of cultured astrocytes after exposure to DMSA-coated Fe-NP. Cultured astrocytes were incubated without (control) or with 1000 μM of iron as D-Fe-NP at 37 °C or at 4 °C. The size bar in (D) applies to all panels.

increased from an initial value of 68 ± 4 to 87 ± 17 nm (37 °C) or 89 ± 20 nm (4 °C) during a 4 h incubation of cells with 4000 μM D-Fe-NP, their size increased significantly to 348 ± 71 nm (37 °C; $p < 0.01$) and 218 ± 19 nm (4 °C; $p < 0.01$) when cells were exposed to only 100 μM D-Fe-NP (figure 3(B)). At low D-Fe-NP concentrations of 200 and 500 μM the hydrodynamic diameter of nanoparticles that were exposed to cells at 37 °C was significantly larger than that of particles incubated with cells at 4 °C (figure 3(B)). In contrast, incubation of D-Fe-NP in media in the absence of cells did not cause any alteration of the hydrodynamic diameter during incubation at 4 or 37 °C (data not shown).

Cellular iron accumulation after exposure of astrocytes to D-Fe-NP was also investigated by the cytochemical Perls' staining which visualizes the presence of large amounts of cellular iron as black precipitate (figure 4). While cells that were incubated without D-Fe-NP were not Perls' positive (figures 4(A) and (B)), exposure of cells for 4 h with 1000 μM D-Fe-NP led to an intense staining for iron that was indicated by the dark color, especially visible around the nuclei of the cells (figure 4(C)). In contrast, when the cells were exposed to D-Fe-NP at 4 °C, hardly any cellular iron was detectable by Perls' staining (figure 4(D)).

3.3. Detection of intracellular Fe-NP by TEM

To investigate whether intact nanoparticles are present in the cells after exposure of astrocytes to D-Fe-NP, the cells were analyzed by TEM after incubation for 4 h without or with 1000 μM D-Fe-NP at 37 or 4 °C (figures 5 and 6). Control cells that were incubated in the absence of D-Fe-NP showed the normal medium electron density of all cellular structures, whereas hardly any dark electron-dense particles were present intra- or extracellularly (figure 5(A)). In contrast, cells exposed to D-Fe-NP at 37 °C contained large vesicles loosely or densely filled with electron-dense particles (figure 5(B) arrowheads; figure 6). Some vesicles contained additionally cellular residuals between the particles (figure 6(C)). In contrast to an incubation at 37 °C, hardly any intracellular vesicles that contained electron-dense material were observed for astrocytes that were incubated with D-Fe-NP at 4 °C (figure 5(C)). However, after exposure to D-Fe-NP at both 37 °C (figure 5(B)) and 4 °C (figure 5(C)), the cells were contoured with nanoparticles at their surface and between the cells.

4. Discussion

Magnetic D-Fe-NP were synthesized with good yield and reproducibility, using a modification of a previously published wet chemical method [18, 23]. The particles were spherical and polydisperse with an average diameter of about 10 nm observed by TEM, confirming previously published results [18]. The synthesized nanoparticles contained large amounts of iron and oxygen, as shown by TEM-EDX analysis,
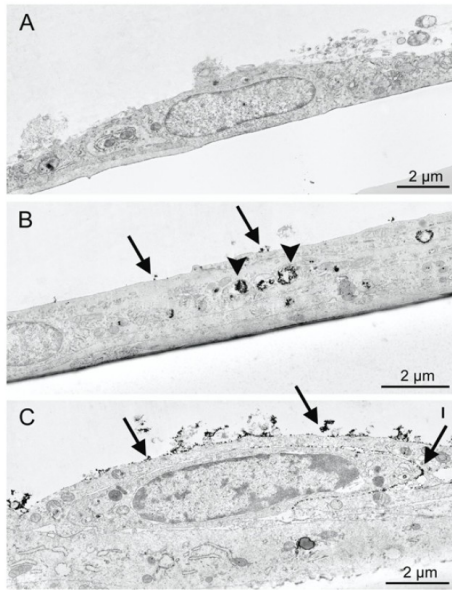
6

Figure 5. TEM images of astrocytes that were incubated with DMSA-coated Fe-NP. The cells were incubated at 37 °C ((A), (B)) or 4 °C (C) for 4 h without (A) or with ((B), (C)) 1000 μM of iron as D-Fe-NP. Electron-dense particles are visible in intracellular vesicles ((B), arrowhead) and contour the cell surface ((B) and (C), arrows) and the intercellular space (arrow labeled I in (C)).

as well as sulfur, which demonstrates that the particles are indeed coated with the sulfur containing DMSA. This treatment of the synthesized Fe-NP with DMSA allowed stable dispersion of the nanoparticles at physiological pH, as indicated by the absence of any increase in hydrodynamic particle diameter of the diluted D-Fe-NP. Thus, in contrast to citrate-coated Fe-NP [18], the presence of an excess of ligand was not required for dispersion of D-Fe-NP in physiological media, excluding potential side effects of an excess of the ligand DMSA on cells. Binding of the carboxyl groups of DMSA to the nanoparticle surface and formation of disulfide bridges between adsorbed DMSA molecules to form a cage-like structure around the Fe-NP core has been discussed as a mechanism of the DMSA stabilization [30]. The importance of the suggested formation of disulfide bridges for the stabilization of Fe-NP by DMSA is strongly supported by the observation that monomercaptosuccinate was unable to stabilize Fe-NP in physiological media (data not shown).

Uncoated and DMSA-coated nanoparticles showed a monomodal size distribution with average hydrodynamic particle diameters around 60 nm, and thus are substantially larger than the diameter of the individual particles observed by TEM. These agglomerates of Fe-NP are most likely formed due to magnetostatic interactions between the individual particles [31, 32]. However, even with an average diameter of around 60 nm the small agglomerates of dispersed D-Fe-NP were considered as well suited to investigate the uptake of nanoparticles by astrocytes. The zeta-potential of uncoated nanoparticles in water indicates a positively charged surface
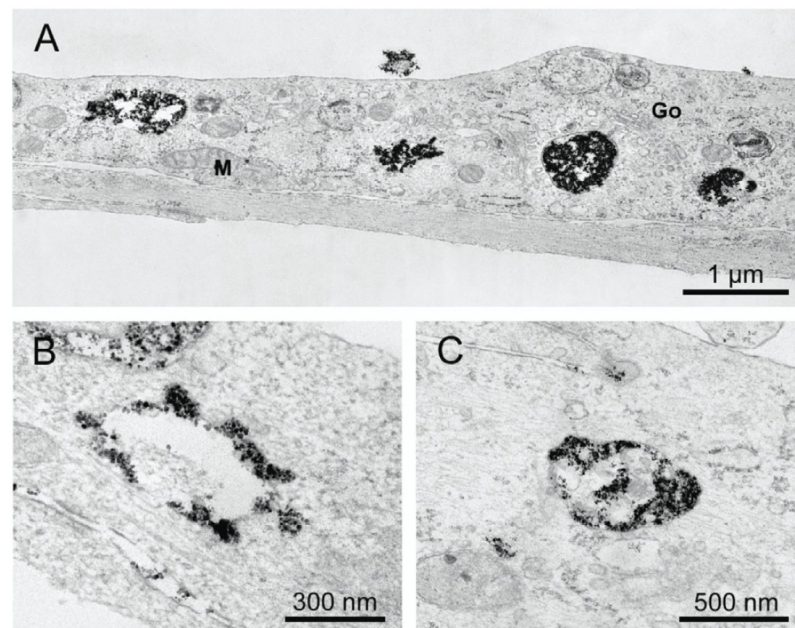
Figure 6. TEM images of astrocytes after treatment with DMSA-coated Fe-NP. The cells were incubated for 4 h with 1000 μM iron as D-Fe-NP at 37 °C. (A) shows a cross section through a cell showing four vesicles filled with electron-dense particles at different densities. Intact mitochondria (M) and the golgi apparatus (Go) are indicated. (B) Nanoparticle containing vesicles that may have fused with a larger vesicle. (C) Vesicle containing heterogeneous cellular debris and Fe-NP.

7

which is in line with the suggested stabilization by protonated surface hydroxyl groups at acidic pH [23]. This positive charge is removed after dispersion in physiological buffer, thereby changing the zeta-potential to around zero which subsequently causes the particles to flocculate out. The DMSA-coat stabilizes D-Fe-NP at physiological pH [23, 24, 33] by introducing a negative surface charge as indicated by the negative zeta-potential.

Incubation of astrocyte cultures with D-Fe-NP did not lead to acute cell death within 6 h, which confirms previously published results for citrate-coated Fe-NP [18, 22] and commercially available Fe-NP [8, 17]. The almost linear increase of cellular iron content observed during 6 h of incubation of cultured astrocytes with D-Fe-NP to values of up to 2000 nmol iron mg^{-1} protein demonstrates the high capacity of these cells to accumulate iron from D-Fe-NP, confirming that astrocytes accumulate iron better from Fe-NP than from low molecular weight iron complexes [18, 34, 35]. The amounts of iron accumulated from D-Fe-NP by cultured astrocytes are similar to those reported for citrate-coated Fe-NP [18, 22]. However, the use of D-Fe-NP has the strong advantage that presence of unbound DMSA is not required for dispersion of D-Fe-NP in physiological media. This contrasts with the situation for citrate-coated Fe-NP [22], since these nanoparticles require for their stability the presence of a high molar excess of the ligand citrate. Such high concentrations of citrate are likely to affect the properties of the cultured astrocytes [36], for example by chelation of extracellular Ca^{2+}-ions. Therefore, especially if higher concentrations of Fe-NP have to be applied to cells, D-Fe-NP appear to be better suited to investigation of the consequences of a treatment of cells with Fe-NP than citrate-coated particles.

After application of D-Fe-NP, the amount of cellular iron increased drastically. To test whether the cell-associated iron is intracellular or extracellularly bound to the cell surface, the iron accumulation from D-Fe-NP at 37 °C was compared to that at 4 °C. Iron accumulation at 4 °C was significantly lower than that observed at 37 °C, suggesting that a temperature-dependent transport process is involved in the iron accumulation from D-Fe-NP in astrocytes. However, the amounts of cell-associated iron that were still found after incubation at 4 °C demonstrate that a substantial part of the cell-associated iron represents extracellularly bound iron. Similar temperature dependences of metal uptake have also been reported for low molecular weight iron [37–39], for hemine iron [40], and for copper [41] as well as for citrate- or silica-coated Fe-NP [18, 22, 42]. Also in these studies the amounts of cell-associated metals determined after incubation at 4 °C were considered to reflect extracellularly bound material. For D-Fe-NP this hypothesis was experimentally confirmed by TEM images of astrocytes that were exposed to the nanoparticles. While, after incubation at both 37 and 4 °C, D-Fe-NP were found decorating the cell membrane extracellularly, the presence of large amounts of intracellular vesicles that contained D-Fe-NP was only observed for the 37 °C condition. In addition, also the Perls' iron staining of astrocytes that had been exposed to D-Fe-NP at 37 °C revealed the presence of substantial amounts of iron in the cells, while

cells that were incubated at 4 °C were not Perls'-positive. These data demonstrate that indeed the temperature-dependent part of the cellular iron reflects the amount of iron that has been taken up into the cells after exposure to D-Fe-NP, whereas the amount of cell-associated iron determined for cells that were incubated at 4 °C represents predominantly the amount of D-Fe-NP that had bound extracellularly to cell membranes. The absence of large, nanoparticle-filled vesicles in the 4 °C condition is in accord with the reduced physiological activity of vesicle transport systems at low temperatures [42].

While the amounts of cellular iron after incubation with D-Fe-NP at 37 °C increased at least up to a concentration of 4000 μM, the cellular iron accumulation at 4 °C already reached a plateau after incubation of the cells with around 1000 μM D-Fe-NP. This suggests a limited capacity of the cells to bind D-Fe-NP extracellularly, whereas the maximum of the uptake of D-Fe-NP into the cells at 37 °C has not been reached even after application of 4000 μM D-Fe-NP. The difference of the iron contents of cells treated with D-Fe-NP at 37 °C versus 4 °C was calculated to get further information on the temperature-dependent transport process that leads to the occurrence of intracellular D-Fe-NP. Uptake of D-Fe-NP appears to be saturable with apparent K_M and V_{Max} values of 2.1 ± 0.6 mM and 1871 ± 231 nmol iron/(mg × 4 h), respectively. Considering the fact that each nanoparticle contains at least several thousand iron atoms, it has to be expected that the apparent K_M value for iron accumulation from D-Fe-NP differs by orders of magnitude from those reported for example for ferrous iron which is taken up into astrocytes with K_M values of about 1 μM [37].

Uptake of D-Fe-NP into astrocytes is likely to involve a membrane-dependent uptake process. Free diffusion of D-Fe-NP through the plasma membrane is unlikely to occur, since the particles are negatively charged as indicated by their zeta-potential. The cellular localization of D-Fe-NP in astrocytes by TEM revealed that these cells contained large vesicles filled with substantial amounts of electron-dense nanoparticles. The presence of Fe-NP in intracellular vesicles in astrocytes confirms previous reports for other types of Fe-NP in astrocytes [18, 21, 22] and suggests that endocytotic mechanisms [43, 44] are involved in the uptake process. Indeed, inhibitors of endocytosis have been reported to lower cellular uptake of fluorescent Fe-NP into astrocytes [21]. The occurrence of several large aggregates of Fe-NP in one vesicle is likely to be a consequence of fusion of several endosomes.

During the incubation of D-Fe-NP with astrocytes, but not in the absence of cells, a significant increase in the hydrodynamic diameter of the particles in the medium was observed. Interestingly, this increase was strongest when D-Fe-NP were applied in low concentrations. In addition, the increase in hydrodynamic diameter was significantly lowered by a decrease in the incubation temperature to 4 °C. These observations suggest that compound(s) that are released from astrocytes in a temperature-dependent manner at limited amounts foster the agglomeration of the dispersed D-Fe-NP to larger aggregates. Thus, regarding the interactions of nanoparticles with astrocytes, not only binding to and uptake of nanoparticles into cells have to be considered, but also the

8

alteration of the properties of the dispersed nanoparticles by cell-derived compounds.

5. Conclusions

DMSA-coated iron oxide nanoparticles (D-Fe-NP) were efficiently taken up into cultured astrocytes and were found predominately in intracellular vesicles, which supports literature data [21] that endocytotic uptake mechanisms are involved in Fe-NP uptake. Since incubation with D-Fe-NP at 4 °C prevented the occurrence of Fe-NP in intracellular vesicles, this temperature control appears to be well suited to determine the amount of Fe-NP that is bound extracellularly to cell membranes. This allows us to discriminate the amount of Fe-NP that is attached to the cells from the amount of Fe-NP that has been internalized into the cells. Astrocytes are highly efficient at strongly increasing their iron content after application of D-Fe-NP. If astrocytes are able to liberate iron from Fe-NP, this iron would be available for the cells and could subsequently be used for iron-dependent processes. Alternatively, since iron can be liberated from Fe-NP under conditions that resemble the intracellular environment [45], cell damage by iron-mediated radical formation could also be a consequence of a long time exposure of astrocytes to Fe-NP. Thus, further studies are also required to investigate the fate of D-Fe-NP in astrocytes, especially in the context of the suggested supply and regulatory function of astrocytes in the iron homeostasis of the brain [15].

Acknowledgments

References

[1] Gupta A K and Gupta M 2005 Synthesis and surface engineering of iron oxide nanoparticles for biomedical applications *Biomaterials* **26** 3995–4021

[2] Laurent S, Forge D, Port M, Roch A, Robic C, Elst L V and Muller R N 2008 Magnetic iron oxide nanoparticles: synthesis, stabilization, vectorization, physicochemical characterizations, and biological applications *Chem. Rev.* **108** 2064–110

[3] Lu A H, Salabas E L and Schuth F 2007 Magnetic nanoparticles: synthesis, protection, functionalization, and application *Angew. Chem. Int. Edn* **46** 1222–44

[4] Corot C, Robert P, Idee J M and Port M 2006 Recent advances in iron oxide nanocrystal technology for medical imaging *Adv. Drug Deliv. Rev.* **58** 1471–504

[5] Weinstein J S, Varallyay C G, Dosa E, Gahramanov S, Hamilton B, Rooney W D, Muldoon L L and Neuwelt E A 2010 Superparamagnetic iron oxide nanoparticles: diagnostic magnetic resonance imaging and potential therapeutic applications in neurooncology and central nervous system inflammatory pathologies, a review *J. Cereb. Blood Flow Metab.* **30** 15–35

[6] Chertok B, Moffat B A, David A E, Yu F Q, Bergemann C, Ross B D and Yang V C 2008 Iron oxide nanoparticles as a drug delivery vehicle for MRI monitored magnetic targeting of brain tumors *Biomaterials* **29** 487–96

[7] Jain T K, Morales M A, Sahoo S K, Leslie-Pelecky D L and Labhasetwar V 2005 Iron oxide nanoparticles for sustained delivery of anticancer agents *Mol. Pharmacol.* **2** 194–205

[8] Pickard M and Chari D 2010 Enhancement of magnetic nanoparticle-mediated gene transfer to astrocytes by 'magnetofection': effects of static and oscillating fields *Nanomedicine* **5** 217–32

[9] Jordan A et al 2006 The effect of thermotherapy using magnetic nanoparticles on rat malignant glioma *J. Neurooncol.* **78** 7–14

[10] Samanta B, Yan H, Fischer N O, Shi J, Jerry D J and Rotello V M 2008 Protein-passivated Fe(3)O(4) nanoparticles: low toxicity and rapid heating for thermal therapy *J. Mater. Chem.* **18** 1204–8

[11] Sofroniew M V and Vinters H V 2010 Astrocytes: biology and pathology *Acta Neuropathol.* **119** 7–35

[12] Eulenburg V and Gomeza J 2010 Neurotransmitter transporters expressed in glial cells as regulators of synapse function *Brain Res. Rev.* **63** 103–12

[13] Parpura V and Zorec R 2010 Gliotransmission: exocytotic release from astrocytes *Brain Res. Rev.* **63** 83–92

[14] Hirrlinger J and Dringen R 2010 The cytosolic redox state of astrocytes: maintenance, regulation and functional implications for metabolite trafficking *Brain Res. Rev.* **63** 177–88

[15] Dringen R, Bishop G M, Koeppe M, Dang T N and Robinson S R 2007 The pivotal role of astrocytes in the metabolism of iron in the brain *Neurochem. Res.* **32** 1884–90

[16] Wang J et al 2010 Pharmacokinetic parameters and tissue distribution of magnetic Fe_3O_4 nanoparticles in mice *Int. J. Nanomed.* **5** 861–6

[17] Au C, Mutkus L, Dobson A, Riffle J, Lalli J and Aschner M 2007 Effects of nanoparticles on the adhesion and cell viability on astrocytes *Biol. Trace Elem. Res.* **120** 248–56

[18] Geppert M, Hohnholt M, Gaetjen L, Grunwald I, Bäumer M and Dringen R 2009 Accumulation of iron oxide nanoparticles by cultured brain astrocytes *J. Biomed. Nanotechnol.* **5** 285–93

[19] Hohnholt M, Geppert M and Dringen R 2010 Effects of iron chelators, iron salts and iron oxide nanoparticles on the proliferation and the iron content of oligodendroglial OLN-93 cells *Neurochem. Res.* **35** 1259–68

[20] Pisanic T R II, Blackwell J D, Shubayev V I, Finones R R and Jin S 2007 Nanotoxicity of iron oxide nanoparticle internalization in growing neurons *Biomaterials* **28** 2572–81

[21] Pickard M R, Jenkins S I, Koller C J, Furness D N and Chari D M 2010 Magnetic nanoparticle labeling of astrocytes derived for neural transplantation *Tissue Eng.* C *Methods* **17** 89–99

[22] Hohnholt M C, Geppert M, Nürnberger S, von Byern J, Grunwald I and Dringen R 2010 Advanced biomaterials: accumulation of citrate-coated magnetic iron oxide nanoparticles by cultured brain astrocytes *Adv. Eng. Mater.* **12** B690–4

[23] Bee A, Massart R and Neveu S 1995 Synthesis of very fine maghemite particles *J. Magn. Magn. Mater.* **149** 6–9

9

[24] Fauconnier N, Pons J N, Roger J and Bee A 1997 Thiolation of maghemite nanoparticles by dimercaptosuccinic acid *J. Colloid Interface Sci.* **194** 427–33

[25] Hamprecht B and Löffler F 1985 Primary glial cultures as a model for studying hormone action *Methods Enzymol.* **109** 341–5

[26] Riemer J, Hoepken H H, Czerwinska H, Robinson S R and Dringen R 2004 Colorimetric ferrozine-based assay for the quantitation of iron in cultured cells *Anal. Biochem.* **331** 370–5

[27] Dringen R, Kussmaul L and Hamprecht B 1998 Detoxification of exogenous hydrogen peroxide and organic hydroperoxides by cultured astroglial cells assessed by microtiter plate assay *Brain Res. Prot.* **2** 223–8

[28] Lowry O H, Rosebrough N J, Farr A L and Randall R J 1951 Protein measurement with the Folin phenol reagent *J. Biol. Chem.* **193** 265–75

[29] Petri-Fink A and Hofmann H 2007 Superparamagnetic iron oxide nanoparticles (SPIONs): from synthesis to *in vivo* studies—a summary of the synthesis, characterization, *in vitro*, and *in vivo* investigations of SPIONs with particular focus on surface and colloidal properties *IEEE Trans. Nanobiosci.* **6** 289–97

[30] Valois C R, Braz J M, Nunes E S, Vinolo M A, Lima E C, Curi R, Kuebler W M and Azevedo R B 2010 The effect of DMSA-functionalized magnetic nanoparticles on transendothelial migration of monocytes in the murine lung via a beta2 integrin-dependent pathway *Biomaterials* **31** 366–74

[31] Chantrell R W, Bradbury A, Popplewell J and Charles S W 1982 Agglomerate formation in a magnetic fluid *J. Appl. Phys.* **53** 2742–4

[32] Maity D and Agrawal D C 2007 Synthesis of iron oxide nanoparticles under oxidizing environment and their stabilization in aqueous and non-aqueous media *J. Magn. Magn. Mater.* **308** 46–55

[33] Fauconnier N, Bee A, Roger J and Pons J N 1999 Synthesis of aqueous magnetic liquids by surface complexation of maghemite nanoparticles *J. Mol. Liq.* **83** 233–42

[34] Hoepken H H, Korten T, Robinson S R and Dringen R 2004 Iron accumulation, iron-mediated toxicity and altered levels of ferritin and transferrin receptor in cultured astrocytes during incubation with ferric ammonium citrate *J. Neurochem.* **88** 1194–202

[35] Tulpule K, Robinson S R, Bishop G M and Dringen R 2010 Uptake of ferrous iron by cultured rat astrocytes *J. Neurosci. Res.* **88** 563–71

[36] Westergaard N, Sonnewald U, Unsgard G, Peng L, Hertz L and Schousboe A 1994 Uptake, release, and metabolism of citrate in neurons and astrocytes in primary cultures *J. Neurochem.* **62** 1727–33

[37] Qian Z M, Liao Q K, To Y, Ke Y, Tsoi Y K, Wang G F and Ho K P 2000 Transferrin-bound and transferrin-free iron uptake by cultured rat astrocytes *Cell. Mol. Biol.* **46** 541–8

[38] Richardson D R 2001 Iron and gallium increase iron uptake from transferrin by human melanoma cells: further examination of the ferric ammonium citrate-activated iron uptake process *Biochim. Biophys. Acta* **1536** 43–54

[39] Trinder D and Morgan E 1998 Mechanisms of ferric citrate uptake by human hepatoma cells *Am. J. Physiol. Gastrointest. Liver Physiol.* **275** G279–86

[40] Dang T N, Bishop G M, Dringen R and Robinson S R 2010 The putative heme transporter HCP1 is expressed in cultured astrocytes and contributes to the uptake of hemin *Glia* **58** 55–65

[41] Scheiber I F, Mercer J F and Dringen R 2010 Copper accumulation by cultured astrocytes *Neurochem. Int.* **56** 451–60

[42] Kim J S *et al* 2006 Cellular uptake of magnetic nanoparticle is mediated through energy-dependent endocytosis in A549 cells *J. Vet. Sci.* **7** 321–6

[43] Kumari S, Mg S and Mayor S 2010 Endocytosis unplugged: multiple ways to enter the cell *Cell. Res.* **20** 256–75

[44] Megías L, Guerri C, Fornas E, Azorin I, Bendala E, Sancho-Tello M, Durán J M, Tomás M, Gomez-Lechon M J and Renau-Piqueras J 2000 Endocytosis and transcytosis in growing astrocytes in primary culture. Possible implications in neural development *Int. J. Dev. Biol.* **44** 209–21

[45] Levy M, Lagarde F, Maraloiu V A, Blanchin M G, Gendron F, Wilhelm C and Gazeau F 2010 Degradability of superparamagnetic nanoparticles in a model of intracellular environment: follow-up of magnetic, structural and chemical properties *Nanotechnology* **21** 395103

10

2.4 Publication 4

Lamkowsky, M. C., **Geppert, M.**, Schmidt, M. M. and Dringen, R. (2012) Magnetic field-induced acceleration of the accumulation of magnetic iron oxide nanoparticles by cultured brain astrocytes. *J Biomed Mater Res A,* **100,** 323-334.

Contributions of M. Geppert:

- Synthesis of iron oxide nanoparticles
- Supervision of the experiments that lead to the generation of Table 2 and Figures 2, 4 and 5
- Performance of the experiments for Table 3 and Figures 3 and 6
- Preparation of a first draft of the manuscript

M. C. Lamkowsky obtained the data given in Table 2 and Figures 2, 4 and 5 during her Bachelor Thesis. M. M. Schmidt provided Figure 3.

Society For
Biomaterials

Magnetic field-induced acceleration of the accumulation of magnetic iron oxide nanoparticles by cultured brain astrocytes

Marie-Christin Lamkowsky,[1] Mark Geppert,[1,2] Maike M. Schmidt,[1,2,3] Ralf Dringen[1,2,4]

[1]Centre for Biomolecular Interactions Bremen, University of Bremen, Bremen, Germany
[2]Centre for Environmental Research and Sustainable Technology, University of Bremen, Bremen, Germany
[3]Advanced Ceramics, University of Bremen, Germany
[4]School of Psychology and Psychiatry, Monash University, Clayton, Australia

Abstract: Magnetic iron oxide nanoparticles (Fe-NPs) are considered for various biomedical and neurobiological applications that involve the presence of external magnetic fields. However, little is known on the effects of a magnetic field on the uptake of such particles by brain cells. Cultured brain astrocytes accumulated dimercaptosuccinate-coated Fe-NP in a time-, temperature-, and concentration-dependent manner. This accumulation was strongly enhanced by the presence of the magnetic field generated by a permanent neodymium iron boron magnet that had been positioned below the cells. The magnetic field-induced acceleration of the accumulation of Fe-NP increased almost proportional to the strength of the magnetic field applied, increasing the cellular-specific iron content from an initial 10 nmol/mg protein within 4 h of incubation at 37°C to up to 12,000 nmol/mg protein. However, presence of a magnetic field also increased the amounts of iron that attached to the cells during incubation with Fe-NP at 4°C. These results suggest that the presence of an external magnetic field promotes in cultured astrocytes both the binding of Fe-NP to the cell membrane and the internalization of Fe-NP. © 2011 Wiley Periodicals, Inc. J Biomed Mater Res Part A: 100A: 323–334, 2012.

Key Words: astrocytes, iron, magnet, nanoparticles, transport

---

INTRODUCTION

Magnetic iron oxide nanoparticles (Fe-NPs) contain a core of magnetic iron oxide (Fe_3O_4 or γ-Fe_2O_3) that is surrounded by a ligand shell, which is important for the stabilization of the particles in physiological media.[1,2] Such NPs are considered for various biomedical and neurobiological applications,[2,3] for example for targeted drug delivery and transfection,[2,4–6] as contrast agent in magnetic resonance imaging[7,8] or for the elimination of tumors by magnetic field-mediated hyperthermia.[9,10] For all these applications, the magnetic properties of Fe-NP are crucial.

Astrocytes are the most abundant cells in the brain that tile the entire central nervous system forming an extensive glial network and possess a large number of essential functions for the brain.[11–13] This cell type plays an important role in the uptake and release of nutrients[14] and neurotransmitters,[15,16] the detoxification of reactive oxygen species and xenobiotics,[17–19] and the regulation of the metal homeostasis.[20,21] In the brain, astrocytes have a strategically very important localization, covering almost completely the brain capillaries with their endfeet.[22] As it has been shown recently that Fe-NP are capable to pass the blood-brain barrier,[23] astrocytes will be the first cells that encounter these particles in brain. Thus, the consequences of an exposure of astrocytes to Fe-NP are of special importance.

Various types of Fe-NP have been reported to be taken up into cultured brain cells, including astrocytes.[6,24–29] Although cultured astrocytes efficiently accumulate Fe-NP, their viability is not compromised despite of large amounts of iron accumulated by the cells.[6,24,25,27,28] The presence of a magnetic field strongly increased the uptake of polymer-coated Fe-NP by Hela cells and of silica-coated Fe-NP by different cell lines by factors of 2–5, depending on the cell type investigated, on the type of magnet used, and on the distance of the magnet from the cells.[30,31] To our knowledge, the consequences of a magnetic field on the accumulation of Fe-NP have not been reported so far for any type of brain cells. However, as the transfection of cells by NP-mediated gene transfer in a magnetic field[32–34] has recently been demonstrated to work also for cultured astrocytes,[6] the uptake of Fe-NP into astrocytes is expected to be increased by the presence of a strong magnetic field.

Exposure of cultured astrocytes to dimercaptosuccinate (DMSA)-coated Fe-NP leads to a strong increase in the cellular iron content, which represents both internalized Fe-NP and particles that are extracellularly attached to the cells.[25] To investigate how the presence of an external static magnetic field affects Fe-NP uptake into and binding of Fe-NP to astrocytes, we have exposed primary astrocyte cell cultures

Correspondence to: R. Dringen; e-mail: ralf.dringen@uni-bremen.de

323

TABLE I. Physical Data of the Magnets Used

Magnet Thickness (mm)	Adhesive Force		Remanence (T)	Magnetic Flux Density (B-Field)	
	kg	N		Surface (T)	1 mm above (T)
1	0.5	4.9	1.17	0.115	0.102
2	1.2	11.8	1.29	0.239	0.205
3	1.8	17.7	1.29	0.331	0.275
5	2.6	25.5	1.29	0.454	0.367
10	3.9	38.3	1.32	0.588	0.469

The table summarizes physical properties of the NdFeB-magnets used in this study as given by the supplier (Webcraft, Uster, Switzerland). The cylindrical magnets had a diameter of 10 mm and a thickness of 1–10 mm as indicated. Their corresponding adhesive force is given in kg and in N and their remanence in Tesla (T). Magnetic flux densities (B-Fields) were calculated for the surface of the magnet and for a distance of 1 mm above the surface which corresponds to the distance between cells and magnet.

to DMSA-coated Fe-NP in the presence or absence of a magnetic field that was generated by positioning permanent neodymium iron boron (NdFeB)-magnets underneath the cells. Our data demonstrate that the presence of a static magnetic field strongly accelerates both the temperature-dependent uptake of the particles into the cells as well as the extracellular adsorbance of Fe-NP to the cell membrane.

MATERIALS AND METHODS

Materials

Fetal calf serum (FCS) and penicillin/streptomycin solution were obtained from Biochrom (Berlin, Germany). Dulbecco's modified Eagle's medium (DMEM) was from Gibco (Karlsruhe, Germany). Bovine serum albumin and NADH were purchased from Applichem (Darmstadt, Germany). All other chemicals of the highest purity available were from Sigma (Steinheim, Germany), Fluka (Buchs, Switzerland), Merck (Darmstadt, Germany), or Riedel-de Haen (Seelze, Germany). Ninety-six-well microtiter plates were purchased from Nunc (Wiesbaden, Germany) and 24-well cell culture plates from Sarstedt (Nümbrecht, Germany).

Magnets

NdFeB-Magnets were purchased from Webcraft (Uster, Switzerland). The cylindrical magnets had a diameter of 10 mm and the strength of the magnets varies with its thickness. Table I lists the magnetic adhesive forces and additional

physical data of the magnets used for the present study. If not stated otherwise, a 5-mm-thick magnet was used that generates a magnetic adhesive force of $25.5N$ (2.6 kg). For the experiments with cells, the magnets were positioned in a polyvinylchloride-positioning plate [Fig. 1(A)], manufactured by the mechanical facility of the University of Bremen. The magnet-loaded plates positioned magnets directly underneath the centers of the wells of 24-well cell culture dishes. The magnet surface touched directly the bottom of the wells, leaving a 1 mm plastic space between the surface of the magnet and the cells. The data presented in Table II demonstrate that a magnetic field introduced by a magnet of an adhesive force of $25.5N$ does not affect iron accumulation from Fe-NP in neighboring wells. To prevent such an effect also for magnets of an adhesive force of $38.3N$ (3.9 kg), the magnet-exposed wells were separated by a row of free wells from each other.

Iron oxide NPs

Fe-NPs were synthesized, stabilized by coating with DMSA, and characterized as previously described.[24,25,35] The aqueous dispersion of DMSA-coated Fe-NP was filtered sterile (200 nm filter; Sartorius, Göttingen, Germany), adjusted to a total iron content of 40 mM and stored at 4°C. Concentrations of Fe-NP are given here as concentration of the iron contained in the NP dispersion, not as concentration of particles. The hydrodynamic diameter of Fe-NP in solution was
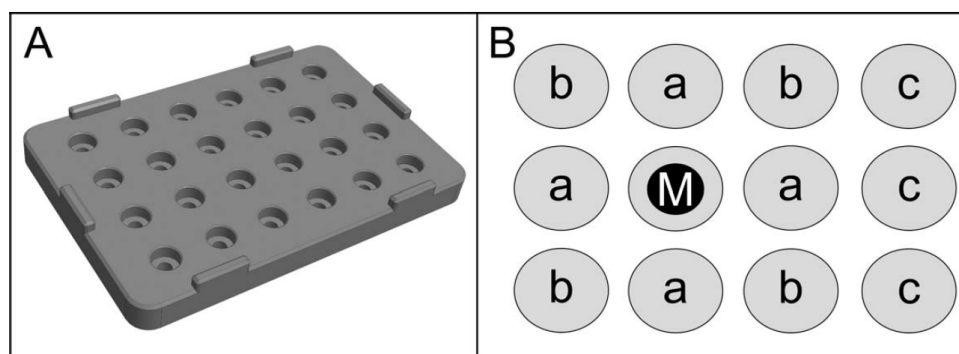

FIGURE 1. Arrangement of magnets under wells of cultured astrocytes. (A) magnet positioning plate. (B) positioning of a single NdFeB-magnet (M) under one central well of an array of 12 wells of astrocyte cultures.

TABLE II. Magnetic Field-Dependent Fe-NP Accumulation by Cultured Astrocytes

	Time (h)	M	a	b	c
Extracellular LDH Activity	0	0 ± 0	0 ± 0	0 ± 0	0 ± 0
	0.5	4 ± 6	3 ± 1	4 ± 2	2 ± 2
(% of initial cellular	1	4 ± 7	3 ± 1	3 ± 3	3 ± 3
LDH activity)	4	3 ± 2	3 ± 1	5 ± 1	4 ± 5
	0	144 ± 14	144 ± 14	144 ± 14	144 ± 14
Cellular protein content	0.5	133 ± 17	123 ± 17	129 ± 20	126 ± 20
(µg/well)	1	126 ± 13	124 ± 18	127 ± 21	128 ± 19
	4	121 ± 17	123 ± 17	127 ± 17	127 ± 16
	0	1 ± 0	1 ± 0	1 ± 0	1 ± 0
Cellular iron content	0.5	213 ± 31***	60 ± 7	56 ± 9	54 ± 6
(nmol/well)	1	247 ± 5***	96 ± 10	94 ± 12	86 ± 4
	4	371 ± 12***	181 ± 14	178 ± 13	168 ± 9

Cells in wells of a 24-well cell culture plate were incubated for up to 4 h with 1 mM Fe-NP. During the incubation, a single NdFeB-magnet was positioned underneath the well M [see Fig. 1(B)]. After the indicated time periods the extracellular LDH activity, the cellular protein content and the cellular iron content were determined for all 12 wells of the array depicted in Figure 1(B). The data were obtained in three experiments performed on individually prepared cultures. For each experiment, the data obtained for wells within one group (a, b, or c) were merged to obtain one value. Indicated are the significances of differences between the values obtained for the well with the magnet (M) and the wells representing a given distance (a, b or c) to the magnet (***$p < 0.001$). The values obtained for a, b, and c positions in the array did not differ significantly from each other.

determined by dynamic light scattering according to a method described previously[36] with a Li.S.A. light scattering machine (Fraunhofer IFAM, Bremen, Germany). Dispersed in incubation medium, the negatively charged DMSA-coated NPs had a monomodal particle size distribution [Fig. 6(C,D)] with a d_{50} value of 58 ± 1 nm and a zeta-potential of -26 ± 3 mV.[25]

Cell cultures
Astrocyte-rich primary cultures were prepared from the brains of newborn Wistar rats according to a method originally described by Hamprecht and Löffler.[37] Three hundred thousand viable cells were seeded in 1 mL culture medium (90% DMEM, 10% FCS, 1 mM pyruvate, 20 U/mL penicillin G, and 20 µg/mL streptomycin sulfate) in wells of 24-well plates. The cultures were kept in a humidified atmosphere of a Sanyo (Osaka, Japan) incubator with 10% CO_2, and the culture medium was renewed every seventh day. After 7 days incubation, the glucose concentration of the culture medium was lowered from 22 mM to around 10 mM. The 7 day feeding paradigm did not cause any starvation of the cells or any obvious alterations in cell morphology or cell metabolism (data not shown). The confluent cultures were used for experiments at a culture age between 15 and 22 days. As demonstrated by immunocytochemical characterization for cell-type specific markers, astrocyte-rich primary cultures contain predominately (more than 90%) astrocytes and only small amounts of oligodendroglial, ependymal, and microglial cells but no neurons.[38–40]

Experimental incubation
The cells were washed twice with 1 mL prewarmed (37°C) or ice-cold (4°C) phosphate-free incubation buffer (IB: 20 mM HEPES, 145 mM NaCl, 1.8 mM CaCl$_2$, 5.4 mM KCl, 1 mM MgCl$_2$, 5 mM glucose, adjusted to pH 7.4 at the desired temperature) and then incubated with 1 mL IB containing Fe-NP and/or other substances as given in the legends of the individual figures and tables in the absence or presence

of a magnet. The incubation media did not contain any FCS or protein. After the desired incubation period, the media were collected and the cells were washed twice with ice-cold phosphate-buffered saline (PBS: 10 mM potassium phosphate buffer pH 7.4, containing 150 mM NaCl). After aspiration of the PBS, dry cells were stored frozen until determination of protein and iron contents.

Iron quantification and staining
Cellular and extracellular iron contents were quantified using a modification[24] of the previously published ferrozine-based iron assay.[41] Staining for iron was performed by the Perls' method using a modification of a previously described protocol.[24] Briefly, cells were washed thrice with 1 mL ice-cold PBS, fixed in 500 µL 4% paraformaldehyde in 0.1M potassium phosphate buffer pH 7.2 (PB) for 30 min and washed again thrice with 1 mL PB. To perform the Perls' reaction, cells were incubated in 500 µL 5% (w/v) potassium ferrocyanide and 5% HCl in PB for 30 min. Subsequently, the stained cells were washed thrice with 1 mL of PB for 10 min, the cell nuclei stained with 4′,6-diamidino-2-phenylindole dihydrochloride (DAPI, 1 µg/mL water) for 5 min, the cells washed again thrice with 1 mL PB and incubated at 4°C over night in 1 mL PBS to clear the staining, before it was documented in bright-field using the Eclipse TS2000U microscope (Nikon, Düsseldorf, Germany).

Determination of cell viability and protein content
Cell viability was measured by determining the activity of lactate dehydrogenase (LDH) using a microtiter-plate assay.[42] Briefly, 20 µL of cell medium or 20 µL of cell lysate (100% control) that was obtained by a 30 min incubation of astroglial cultures with 1 mL of 1% (v/v) Triton X-100 in IB were diluted with 340 µL reaction mixture to obtain final concentrations of 1.8 mM pyruvate, 0.2 mM NADH, 200 mM NaCl, and 80 mM Tris/HCl buffer, pH 7.2. The decrease of absorbance at 340 nm due to the oxidation of NADH to NAD^+ was followed over 5 min. Loss of viability correlates

with an increase in the extracellular activity of the cellular enzyme LDH and is expressed as percental amount of extracellular LDH activity compared to the initial cellular LDH activity of untreated cultures. Cellular protein content was determined according to the Lowry method[43] using bovine serum albumin as a standard.

Presentation of data

The data are presented as means ± SD of values derived from at least three independent experiments that were performed on individually prepared primary astrocyte cultures. Analysis of the significance between two sets of data was performed by the paired t-test. The significance between groups of data was analyzed by ANOVA followed by Bonferroni's *post hoc* test. $p > 0.05$ was considered as not significant.

RESULTS

Establishment of experimental conditions for magnetic field exposure of astrocytes

Magnets in polyvinylchloride-positioning plates [Fig. 1(A)] were used to investigate the effects of an external magnetic field on the accumulation of Fe-NP by cultured astrocytes. To test whether a magnetic field generated by a single magnet positioned underneath one well would only affect the iron accumulation by cells in the well directly above the magnet but not that of cells cultured in the adjacent wells, the positioning plate [Fig. 1(A)] was equipped with one magnet (adhesive force of 25.5N, Table I) underneath the well M [Fig. 1(B)] of an array of 12 wells with cultured astrocytes. This array defines in addition to the well M three groups of wells with cells (a, b, and c) that differed in their distance to the center of the magnet, which generates the magnetic field [Fig. 1(B)]. The cells of all 12 wells were incubated for up to 4 h with 1 mM Fe-NP at 37°C. Treatment of the cells with Fe-NP caused in none of the wells, irrespective of the distance to the magnet, any significant increase in extracellular LDH activity or any alteration in the cellular protein content per well (Table II). In contrast, the iron content of the cells incubated in the well directly above the magnet increased significantly stronger than that of the cells in the other wells investigated. After 4 h of incubation with Fe-NP, the iron content of cells that were incubated in the well directly above the magnet was twice as high (371 ± 12 nmol/well) than that of cells in the neighboring wells (around 180 nmol/well). The iron contents of cells incubated in different distances to the magnet (positions a–c) did not differ significantly ($p > 0.05$) for the incubation periods investigated (Table II). These data demonstrate that the magnet positioned underneath one well does not provide a magnetic field that significantly influences Fe-NP accumulation by the cells in neighboring wells.

Time, temperature, and concentration dependency of the Fe-NP accumulation

To study the effects of an external magnetic field on the accumulation of Fe-NP by cultured astrocytes in more detail, the cells were incubated for up to 4 h at 37 or 4°C with 1 or 4 mM iron as Fe-NP in absence or presence of a magnet

underneath the cells (Fig. 2). None of these conditions caused any increase in extracellular LDH activity nor a loss of cell protein from the dish (data not shown), demonstrating that the cell viability was not compromised. In addition, the cellular morphology in the cultures appeared not to be obviously altered by incubation of astrocytes for 4 h with Fe-NP in concentrations of up to 4 mM, neither in the absence or the presence of a magnetic field (data not shown).

The cellular iron content increased strongly after exposure of the cells to Fe-NP from an initial value of 9.3 ± 4.6 nmol/mg protein to values between about 1700 and 10,000 nmol/mg protein, depending on the experimental condition [Fig. 2(A)]. After 4 h of incubation with 1 or 4 mM Fe-NP in the absence of a magnet cellular iron contents of 1695 ± 111 and 2499 ± 157 nmol/mg were determined, respectively. Already after 15 min incubation, exposure to Fe-NP in presence of a magnet led to cellular iron values that were significantly ($p < 0.05$) higher than those obtained by incubations without magnet, reaching after 4 h of incubation 4784 ± 516 nmol/mg protein (1 mM) and 9940 ± 424 nmol/mg protein [4 mM; Fig. 2(A)]. At an incubation temperature of 4°C [Fig. 2(B)], the increase in cellular iron content was lower than that of cells incubated with Fe-NP at 37°C [Fig. 2(A)]. After 4 h of incubation at 4°C with Fe-NP, the contents of cell-associated iron accounted for 58 ± 8% (1 mM, without magnet), 52 ± 5% (4 mM, without magnet), 61 ± 5% (1 mM, with magnet), and 65 ± 3% (4 mM, with magnet) of the values determined for the respective 37°C incubation condition [Fig. 2(A,B)].

As endocytotic uptake of Fe-NP hardly occurs at 4°C,[28,44] the iron values determined for cells incubated at 4°C represent almost exclusively material that had bound extracellularly to the cells.[25,45] Thus, the difference of the iron values of cells treated at 37 and 4°C (ΔFe) represents the amount of Fe-NP that had been internalized by the cells.[25] The ΔFe values increased between 30 min and 4 h of incubation almost linearly for cells that were exposed to 1 or 4 mM Fe-NP in absence or presence of a magnetic field [Fig. 2(C)]. Iron accumulation rates calculated from the linear increases of the ΔFe values were almost identical for cells that had been exposed to 1 mM (3.2 ± 0.6 nmol/(min × mg protein)) or 4 mM Fe-NP (4.2 ± 0.4 nmol/(min × mg protein)) in the absence of the magnet [Fig. 2(D)]. However, presence of a magnet underneath the cells significantly increased the iron accumulation rates by 165% (1 mM) and 270% [4 mM; Fig. 2(D)].

Perls' staining was used to visualize cellular iron after exposure of astrocytes to Fe-NP under various conditions. Astrocytes that had been incubated without Fe-NP were almost Perls' negative [Fig. 3(A,D,G,J)] and cultures that had been exposed to 1 mM Fe-NP at 4°C in the absence of the magnet showed a weak Perls' iron staining [Fig. 3(B)] that was slightly increased after incubation with 4 mM Fe-NP [Fig. 3(C)]. The presence of a magnet during incubation of the cells with Fe-NP at 4°C increased the intensity of the Perls' staining [Fig. 3(E,F)]. In contrast, incubation of the cells at 37°C in the presence of Fe-NP (without a magnet) resulted in a substantially stronger staining [Fig. 3(H,I)]
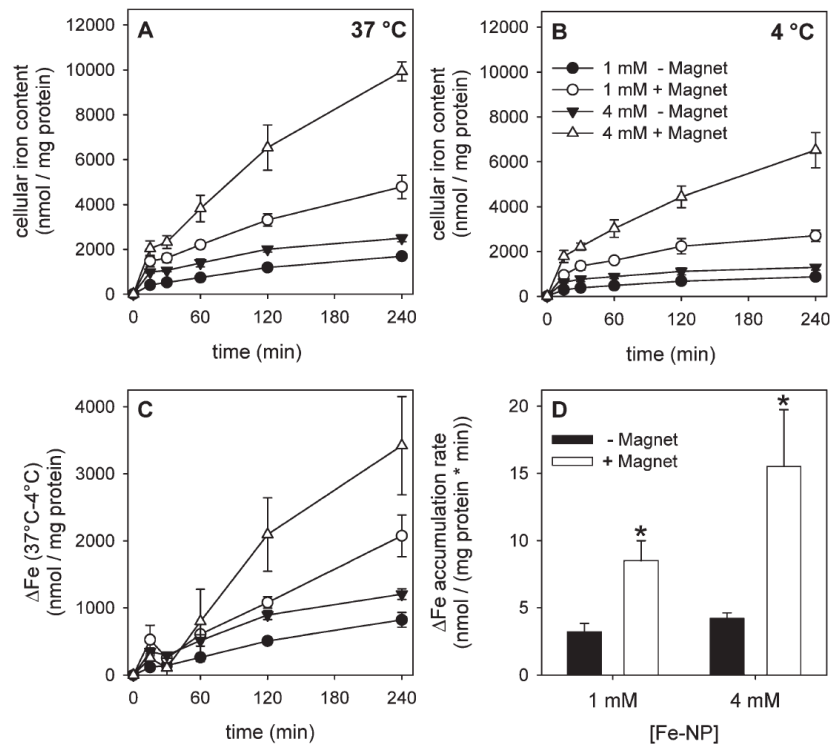
FIGURE 2. Effects of a magnetic field on the Fe-NP accumulation by astrocytes. The cells were incubated for up to 4 h at 37°C (A) or 4°C (B) with 1 or 4 mM Fe-NP in the absence or the presence of an external magnetic field (for conditions see panel B). Quantification of extracellular LDH activity and of the cellular protein content revealed that none of the conditions used compromised cell viability (data not shown). C shows the calculated differences ΔFe of the iron contents determined for cells incubated at 37°C minus those of cells incubated at 4°C. D shows the iron accumulation rates calculated from the almost linear increases in ΔFe values given in C between 30 and 240 min of incubation. Indicated in D are the significances between incubation conditions with and without magnets (*$p < 0.05$).

compared with the respective 4°C control [Fig. 3(B,C)]. The presence of a magnetic field during the incubation of the cells with 1 mM Fe-NP at 37°C [Fig. 3(K)] strongly intensified the Perls' staining, which was even more prominent after incubation with 4 mM Fe-NP [Fig. 3(L)]. Costaining of nuclei with DAPI confirmed that the cells were intensively stained for iron by the Perls' method (data not shown).

To investigate the concentration dependency of the iron accumulation in more detail, cultured astrocytes were incubated for 4 h with up to 4 mM iron as Fe-NP in presence or absence of a magnetic field at 37 or 4°C (Fig. 4). None of these conditions compromised cell viability as indicated by the absence of any increase in extracellular LDH activity [Fig. 4(A)] and of any change in cellular protein content per well [Fig. 4(B)]. The cellular accumulation of iron after exposure to Fe-NP depended strongly on the temperature and on the concentration of the Fe-NP applied. In the absence of a magnet, the cellular iron content increased with the Fe-NP concentration applied, reaching maximal values of about 2500 nmol/mg protein after exposure to 2 mM Fe-NP. Presence of a magnet underneath the cells significantly ($p<0.05$) increased the amount of cellular iron for most concentrations of Fe-NP applied [Fig. 4(C)], while incubation at 4°C

resulted for each concentration of Fe-NP in a lower cellular iron content compared with the respective 37°C incubation [Fig. 4(C)]. Calculation of the ΔFe values revealed that the temperature-dependent iron accumulation was saturable in the absence of a magnetic field, reaching maximal values at around 2 mM [Fig. 4(D)]. In contrast, the presence of the magnet increased ΔFe substantially to values that were about four times higher at 4 mM Fe-NP than those observed in the absence of a magnet [Fig. 4(D)]. However, also for the magnet condition a saturation of the iron accumulation with Fe-NP in concentration of around 2 mM cannot be excluded, as the values observed for the iron contents of cells treated with Fe-NP in concentrations above 1 mM did not differ significantly from each other [Fig. 4(D)].

Fe-NP accumulation depends on the strength of the magnetic field
To test for the influence of the strength of the magnetic field on the iron accumulation, cultured astrocytes were incubated with 4 mM iron as Fe-NP for 4 h at 37 or 4°C in presence of NdFeB-magnets that possessed adhesive magnetic forces between 0 (control without magnet) and 38.3N (Fig. 5). None of these conditions caused an increase in
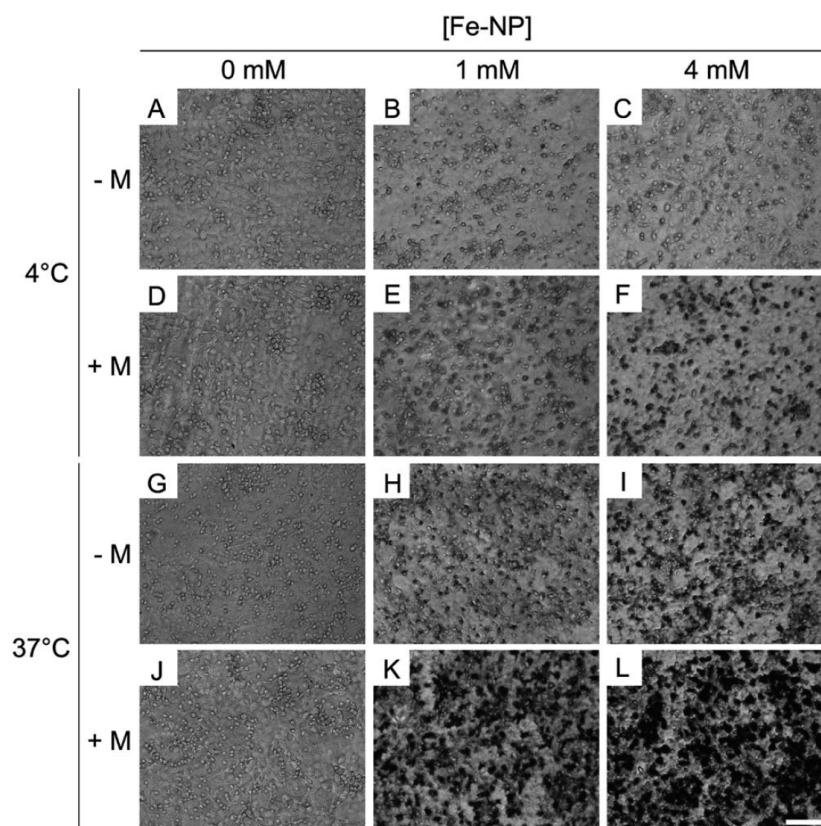
FIGURE 3. Perls' staining of iron in astrocytes. The cells had been incubated for 4 h without (0 mM) or with 1 or 4 mM Fe-NP at 4 or 37°C in absence (-M) or presence (+M) of a magnetic field. The scale bar in L represents 50 μm and applies to all panels.

extracellular LDH activity [Fig. 5(A)] or a decrease in the cellular protein content per well [Fig. 5(B)]. The cellular iron content determined after 4 h incubation at 37°C with Fe-NP increased almost proportional with the increase in magnetic force from 2907 ± 857 nmol/mg protein (control without magnet) to 11,981 ± 2504 nmol/mg protein. However, also an incubation with Fe-NP at 4°C led to an increase in the cellular iron contents with increasing magnetic field strength [Fig. 5(C)]. For all magnets applied, the cellular iron content after incubation at 4°C represented about 50–60% of the cellular iron content determined for cells that had been incubated at 37°C [Fig. 5(C,D)].

Effects of the magnetic field on the diameter of dispersed Fe-NP
During incubation of cells without a magnet, the average hydrodynamic diameter of the NPs in the incubation medium increased slightly from 58 ± 1 nm to 77 ± 11 nm (37°C) and 72 ± 2 nm (4°C). In contrast, presence of a magnetic field during the incubation at both 37 and 4°C lowered the average hydrodynamic particle diameter in the supernatant, reaching around 40 nm after incubation with the strongest magnet [Fig. 6(A)]. A similar decline in the av-

erage hydrodynamic diameter of the particles in the supernatant was observed after 4 h incubation in the absence of cells at 37°C [Fig. 6(B)]. These observations were reflected by the size distribution of the Fe-NP. In the absence of cells and magnet, the size distribution of a Fe-NP dispersion remained constant [Fig. 6(D)], while presence of cells for 4 h caused a small shift in the size distribution curve towards higher diameters [Fig. 6(C)]. A magnet under the well caused for both the presence [Fig. 6(C)] and the absence [Fig. 6(D)] of cells a disappearance of the larger particles from the dispersion as demonstrated by the shift in size distribution towards smaller diameters [Fig. 6(C,D)].

Effects of endocytosis inhibitors on accumulation of Fe-NP by astrocytes
To investigate whether endocytotic pathways are involved in the cellular accumulation of Fe-NP, astrocyte cultures were incubated for 4 h with 1 mM Fe-NP in the absence or presence of magnetic fields without or with known inhibitors of different endocytotic pathways. Under the conditions used only chlorpromazine and 5-(N-ethyl-N-isopropyl)amiloride (EIPA) were investigated for their potential to lower iron accumulation from Fe-NP, since chloroquine, methyl-β-cyclodextrine,
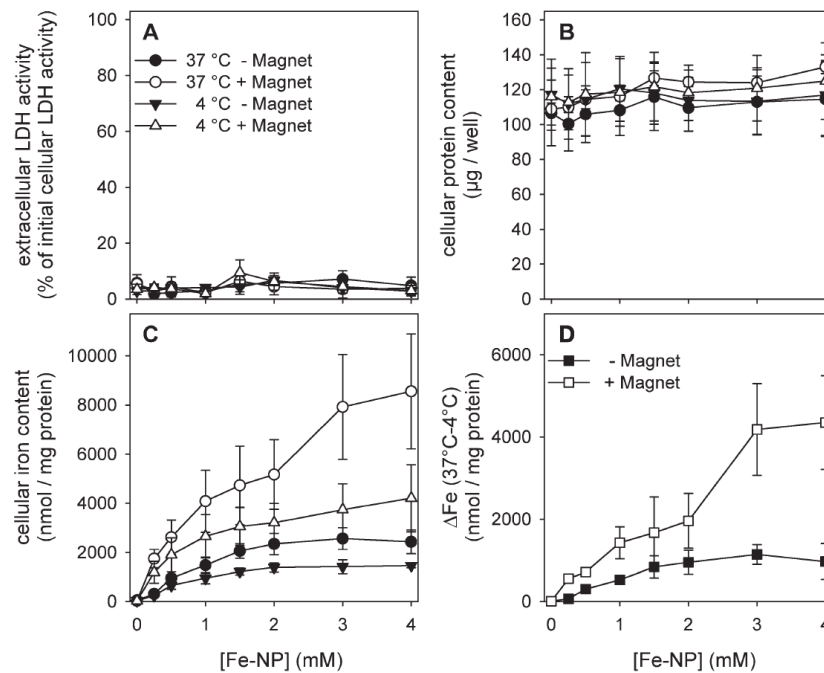
FIGURE 4. Concentration-dependency of Fe-NP accumulation by cultured astrocytes in absence or presence of a magnetic field. The cells were incubated for 4 h with Fe-NP in the indicated concentrations at 37 or 4°C in the absence or the presence of an external magnetic field. The extracellular LDH activity (A), the cellular protein content (B) and the specific cellular iron content (C) were determined. D shows the temperature-sensitive part of the iron accumulation (ΔFe) obtained by calculation of the differences of the iron contents of cells that had been incubated at 37 and 4°C.

dynasore and tyrphostin 23 caused aggregation and precipitation of the Fe-NP (data not shown). When compared with controls (absence of endocytosis inhibitors), the application of 20 μM chlorpromazine or 25 μM EIPA did not affect the cell viability or the accumulation of iron by astrocytes from Fe-NP at 4 or 37°C in the absence or the presence of a magnetic field (Table III). Higher concentrations of chlorpromazine or EIPA were not applied for these studies, since they caused cell death under the conditions used (data not shown).

DISCUSSION
Viability of astrocytes exposed to Fe-NP and magnets
Astrocytes in wells of 24-well culture dishes were incubated with DMSA-coated Fe-NP in presence of an external static magnetic field, generated by a permanent NdFeB-magnet placed underneath the cells. None of the conditions used here acutely compromised cell viability as indicated by the absence of any elevated LDH release from the cells and protein loss of the cultures. Thus, cultured astrocytes are able to deal successfully with an even 1000-fold elevated specific cellular iron content. The observed absence of any acute toxicity of Fe-NP-treated astrocytes is in accord with literature data on cultured astrocytes that had been exposed to DMSA-coated,[25] citrate-coated,[24,27] or other Fe-NP.[28,46] The high resistance of astrocytes against Fe-NP-mediated damage contrasts the situation observed for other cell types.

Cell damage as well as alterations in cell morphology during treatment with Fe-NP were reported for PC12 cells[29] and aortic endothelial cells.[47] In contrast, even astrocytes that had been maximally loaded for 4 h with Fe-NP neither show any obvious alterations in cell morphology nor alterations in the cellular distribution of cytoskeleton proteins (data not shown), which has been reported to be involved in morphology changes observed for Fe-NP-treated aortic endothelial cells.[47] Thus, under the acute 4 h incubation conditions used, the viability of cultured astrocytes was not compromised, allowing the analysis of the influence of a magnetic field on Fe-NP accumulation. In contrast, an extended incubation period of 24 h with 1 or 4 mM Fe-NP caused severe cell damage to cultured astrocytes that was not accelerated by the presence of a magnet under the cells (data not shown), demonstrating that the accumulation of large amounts of iron as Fe-NP has the potential to damage cultured astrocytes.

Accumulation of Fe-NP by astrocytes
In the absence of magnets, cultured astrocytes accumulated Fe-NP efficiently in a time-, temperature-, and concentration-dependent manner, leading to specific iron contents similar to those recently published,[25] confirming that the capacity of these cells to accumulate iron as Fe-NP is higher than their capacity to take up iron in low molecular weight
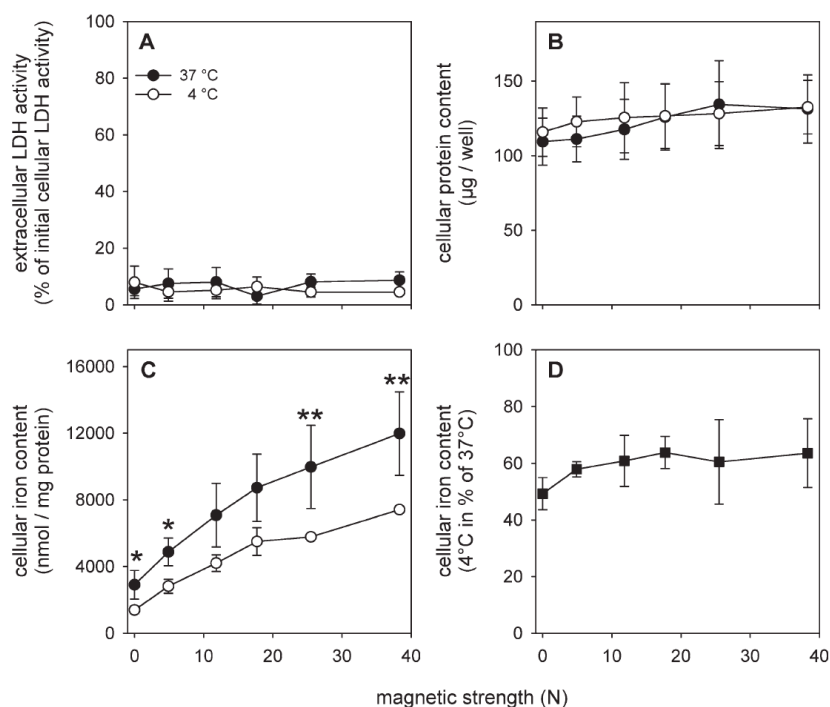
FIGURE 5. Fe-NP accumulation by astrocytes depends on the strength of the magnetic field. The cells were incubated for 4 h at 37 or 4°C with 4 mM Fe-NP in the absence or the presence of a magnetic field that was generated by NdFeB-magnets of the indicated adhesive strength. The extracellular LDH activity (A), the cellular protein content (B) and the specific cellular iron content (C) were determined. D shows the specific iron content of cells that had been incubated at 4°C with Fe-NP, given as percent of the values obtained for cells incubated at 37°C. Indicated in C are the significances of differences between the 37 and 4°C conditions (*$p < 0.05$; **$p < 0.01$).

form.[24,48,49] The quantification of cellular iron does not allow to discriminate between Fe-NP that had been internalized by the cells and Fe-NP that had bound extracellularly to the cell membrane. However, as membrane-dependent transport processes are strongly temperature dependent and internalization of NPs is almost completely prevented at a temperature of 4°C,[25,45] the amount of iron detected after exposure of cells at 4°C is considered to represent pre-

dominantly extracellularly bound material.[25,27,45] Thus, the ΔFe values, calculated as difference between iron contents of cells that had been incubated at 37°C minus the contents of cells incubated at 4°C, can be considered to reflect the material internalized by the cells. This view is confirmed by data from Perls' stainings of Fe-NP-treated astrocytes. After incubation of the cells with Fe-NP at 4°C at best a weak Perls' staining was observed as previously reported.[25] The

TABLE III. Effects of Endocytosis Inhibitors on the Fe-NP Accumulation by Cultured Astrocytes

Temperature	Inhibitor	Extracellular LDH Activity (% of initial)		Specific Cellular Iron Content (nmol/mg)	
		− magnet	+ magnet	− magnet	+ magnet
37°C	Control (DMSO)	4.8 ± 3.1	4.4 ± 3.6	1558 ± 295	4643 ± 708
	Chlorpromazine	5.3 ± 1.9	8.2 ± 3.3	1553 ± 273	4565 ± 786
	EIPA	5.6 ± 2.9	4.6 ± 2.1	1606 ± 213	4558 ± 895
4°C	Control (DMSO)	5.5 ± 2.1	4.7 ± 1.6	820 ± 213	1563 ± 264
	Chlorpromazine	3.4 ± 2.3	4.2 ± 2.9	815 ± 119	1471 ± 362
	EIPA	4.2 ± 2.8	3.7 ± 2.5	800 ± 147	1566 ± 497

The cells were incubated for 4 h with 1 mM Fe-NP at 37 or 4°C in absence or presence of an external magnetic field in IB without (control; 0.1% dimethyl sulfoxide, DMSO) or with 20 μM chlorpromazine or 25 μM 5-(N-ethyl-N-isopropyl)amiloride (EIPA) and the extracellular LDH activity and cellular iron content were determined. The differences in the cellular iron contents between incubations at 37 and 4°C or between conditions with and without magnet were statistically significant ($p < 0.05$). However, no statistical significance could be observed between control and inhibitory conditions.
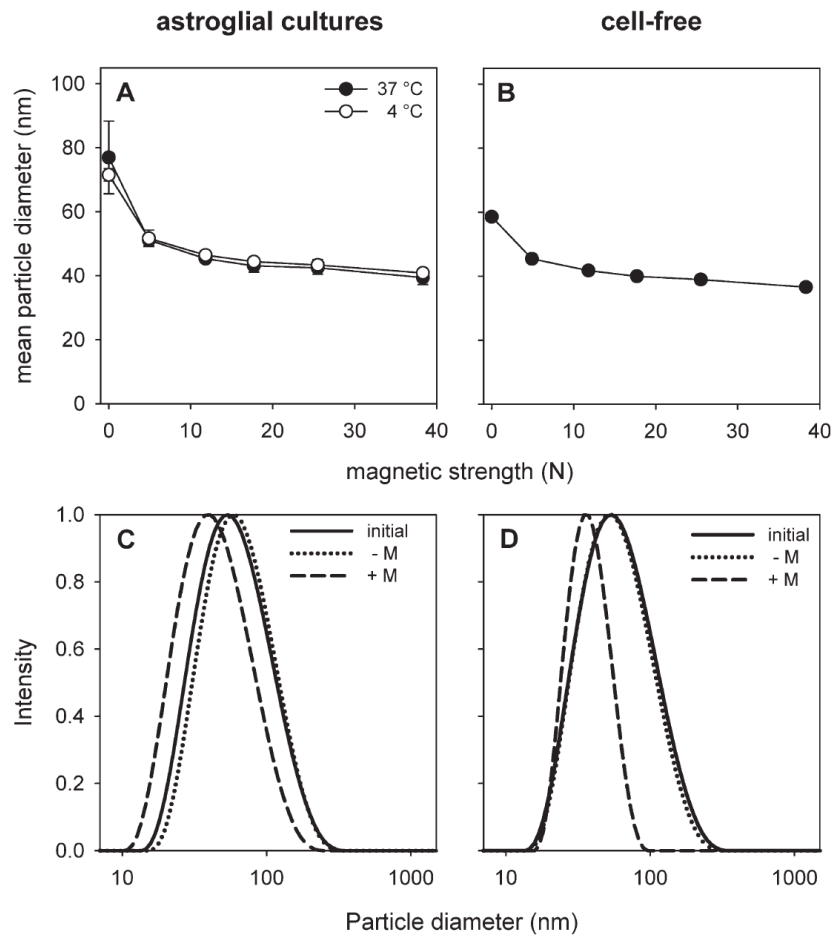
astroglial cultures   **cell-free**

FIGURE 6. Effects of a magnetic field on the size distribution of Fe-NP in incubation buffer in the presence or absence of astroglial cultures. Fe-NP were dispersed in IB to a final concentration of 4 mM total iron and the mean hydrodynamic particle diameter was determined after 4 h incubation at 37 or 4°C with (A) or without (B) cells in the presence of a magnetic field that was generated by NdFeB-magnets of the indicated adhesive strength. The panels C and D show the particle size distributions of Fe-NP dispersed in IB before (initial) or after 4 h at incubation at 37°C without (-M) or with (+M) a NdFeB-magnet (25.5N adhesive force) in the presence (C) or the absence (D) of cells.

harsh washing procedures used during the staining process remove most of the Fe-NP that had attached extracellularly to the cell membrane, leaving almost only the intracellular iron to be detectable by the Perls' staining. The temperature-sensitive uptake of DMSA-coated-Fe-NP was saturable as indicated by the maximal ΔFe value observed after incubation with more than 1.5 mM Fe-NP, suggesting that a protein-dependent process is involved in the uptake of Fe-NP into astrocytes. This is consistent with the reported contribution of endocytotic pathways in the uptake of Fe-NP into astrocytes.[28]

Magnetic field-dependent Fe-NP accumulation in cultured astrocytes
The effects of the field generated by a single NdFeB-magnet were limited to a single well of the culture dish, demon-strating that the experimental setup was suitable for the investigation of the effects of magnetic fields on the iron accumulation from Fe-NP by cultured astrocytes. The presence of a magnet underneath cultured astrocytes significantly increased the amounts of cellular iron up to fourfold. Similar stimulations by a magnetic field on the uptake of polymer-coated or silica-coated Fe-NP have been reported for various cell lines.[30,31] In addition, the observed enhancement of the Fe-NP accumulation of astrocytes that were incubated in the presence of magnets of increasing magnetic field is consistent with literature data on the uptake of Fe-NP into cell lines.[30,31]

For all conditions used, the amount of cell-associated iron determined for 4°C-incubated cells was between 50 and 60% of the values observed for cells exposed to Fe-NP at 37°C, demonstrating that the presence of a magnetic field

increases both Fe-NP uptake into astrocytes as well as association of Fe-NP to the cell membrane. This view is supported by the low number of Perls' positive cells in cultures that had been incubated with Fe-NP at 4°C in a magnetic field, while cells treated at 37°C under otherwise identical conditions were strongly Perls' positive.

Effects of endocytosis inhibitors on the accumulation of Fe-NP by astrocytes

As demonstrated by TEM, astrocytes that have been exposed to Fe-NP at 37°C contain electron-dense NPs predominately in large vesicles, while such vesicles were not observed for the 4°C condition.[25] This predominant occurrence of Fe-NP in vesicles suggested that endocytotic pathways contribute to the uptake of Fe-NP into astrocytes as recently described.[28] Although the specificity of individual inhibitors for defined endocytic pathways is a matter of debate,[50] we used several known inhibitors of endocytotic pathways[51–53] to investigate the involvement of endocytosis in the Fe-NP accumulation by astrocytes. Many of the inhibitors applied caused aggregation and precipitation of Fe-NP under the conditions used, but at least chlorpromazine and EIPA did not cause any significant increase in the average hydrodynamic particle diameter (data not shown) of Fe-NP in the incubation medium. However, presence of chlorpromazine and EIPA did not alter the astrocytic iron accumulation from Fe-NP, suggesting that clathrin-dependent endocytosis and macropinocytosis, respectively,[51–54] do not play a major role in Fe-NP accumulation under the conditions used in the present study. A contribution of macropinocytosis has recently been reported for the accumulation of carboxyl-modified fluorescent Fe-NP by cultured astrocytes.[28] Likely reasons for the discrepancy of this finding compared with our results are the differences in the size (average diameter of 200–390 nm) and in the coating of the NPs used as well as different incubation conditions. For example, in order to avoid alterations of surface properties of Fe-NP that are likely to affect binding to and uptake into cells, we did not incubate the cells with Fe-NP in presence of FCS, as serum doubled the average hydrodynamic particle diameter of DMSA-coated Fe-NP (data not shown). In serum-containing medium, the accumulation of Fe-NP into astrocytes is indeed lowered by 20–30% by chlorpromazine and EIPA (data not shown), demonstrating that these inhibitors in the concentrations applied affect particle uptake into astrocytes and that their inhibitory potential depends strongly on the incubation conditions.

Effects of the magnetic field on the diameter of dispersed Fe-NP

The DMSA-coated Fe-NP applied to cells showed in dynamic light scattering a monomodal size distribution with an average diameter of around 60 nm. However, the incubation of astrocytes with Fe-NP was accompanied by the disappearance of larger Fe-NP from the incubation medium which resulted in a decrease in the average hydrodynamic diameter of the Fe-NP in the supernatant of the cells, which depended on the strength of the magnetic field. As the mag-

netic field accelerates the sedimentation of larger particles in the population of Fe-NP stronger toward the magnet than smaller particles,[55] presence of a magnet underneath the cells will increase the likelihood that cells encounter and bind larger Fe-NP, which contain more iron. Thus, even with an unchanged number of binding events, more cellular iron would be detected in cells that were incubated above a magnet due to the enrichment of larger particles in the vicinity of the cells. This view is supported by the comparable magnetic field-dependent decline in the size distribution and in the average hydrodynamic diameter observed for Fe-NP that were incubated without cells but under otherwise identical conditions. However, we can currently not exclude that the presence of a magnetic field can also accelerate the uptake of NPs of a defined size compared to the uptake of such particles in the absence of the magnet, thereby contributing to the increased cellular iron content of cultured astrocytes that were incubated with Fe-NP above a magnet.

CONCLUSIONS

Viable cultured astrocytes are able to accumulate large amounts of DMSA-coated magnetic Fe-NP in a time-, concentration-, and temperature-dependent process that is strongly accelerated by the presence of a magnetic field. This effect of an external static magnetic field on the uptake of Fe-NP into astrocytes is consistent with the observed increased transfection efficiency of plasmid-bound Fe-NP in astrocytes.[6] The presence of a static magnetic field increased both the extracellular adsorbance of Fe-NP to the cell membrane as well as the uptake of Fe-NP into cells. Further studies are required to elucidate the fate of the Fe-NP that had bound to the cell membrane or had been taken up into the cells as well as the mechanisms involved in the delayed toxicity observed for astrocytes that were treated with Fe-NP for 24 h. The observation that even a 1000fold increase in the specific iron contents is not acutely toxic for cultured astrocytes suggests that these cells do not liberate iron from the Fe-NP accumulated at a rate that can quickly harm the cells and/or that astrocytes have sufficient antioxidative mechanisms to at least transiently survive an iron-mediated oxidative stress after exposure to Fe-NP.

REFERENCES

1. Laurent S, Forge D, Port M, Roch A, Robic C, Elst LV, Muller RN. Magnetic iron oxide nanoparticles: Synthesis, stabilization, vectorization, physicochemical characterizations, and biological applications. Chem Rev 2008;108:2064–2110.

ORIGINAL ARTICLE

2. Lu AH, Salabas EL, Schuth F. Magnetic nanoparticles: Synthesis, protection, functionalization, and application. Angew Chem Int Ed Engl 2007;46:1222–1244.

3. Stark WJ. Nanoparticles in biological systems. Angew Chem Int Ed Engl 2011;50:1242–1258.

4. Chertok B, Moffat BA, David AE, Yu FQ, Bergemann C, Ross BD, Yang VC. Iron oxide nanoparticles as a drug delivery vehicle for MRI monitored magnetic targeting of brain tumors. Biomaterials 2008;29:487–496.

5. Dilnawaz F, Singh A, Mohanty C, Sahoo SK. Dual drug loaded superparamagnetic iron oxide nanoparticles for targeted cancer therapy. Biomaterials 2010;31:3694–3706.

6. Pickard M, Chari D. Enhancement of magnetic nanoparticle-mediated gene transfer to astrocytes by 'magnetofection': Effects of static and oscillating fields. Nanomedicine 2010;5:217–232.

7. Corot C, Robert P, Idee JM, Port M. Recent advances in iron oxide nanocrystal technology for medical imaging. Adv Drug Deliv Rev 2006;58:1471–1504.

8. Weinstein JS, Varallyay CG, Dosa E, Gahramanov S, Hamilton B, Rooney WD, Muldoon LL, Neuwelt EA. Superparamagnetic iron oxide nanoparticles: Diagnostic magnetic resonance imaging and potential therapeutic applications in neurooncology and central nervous system inflammatory pathologies, a review. J Cereb Blood Flow Metab 2010;30:15–35.

9. Johannsen M, Thiesen B, Wust P, Jordan A. Magnetic nanoparticle hyperthermia for prostate cancer. Int J Hyperthermia 2010; 26:790–795.

10. Jordan A, Scholz R, Maier-Hauff K, van Landeghem FK, Waldoefner N, Teichgraeber U, Pinkernelle J, Bruhn H, Neumann F, Thiesen B, von Deimling A, Felix R. The effect of thermotherapy using magnetic nanoparticles on rat malignant glioma. J Neurooncol 2006; 78:7–14.

11. Kimelberg HK. Functions of mature mammalian astrocytes: A current view. Neuroscientist 2010;16:79–106.

12. Markiewicz I, Lukomska B. The role of astrocytes in the physiology and pathology of the central nervous system. Acta Neurobiol Exp (Wars) 2006;66:343–358.

13. Sofroniew MV, Vinters HV. Astrocytes: Biology and pathology. Acta Neuropathol 2010;119:7–35.

14. Barros LF, Deitmer JW. Glucose and lactate supply to the synapse. Brain Res Rev 2010;63:149–159.

15. Eulenburg V, Gomeza J. Neurotransmitter transporters expressed in glial cells as regulators of synapse function. Brain Res Rev 2010;63:103–112.

16. Parpura V, Zorec R. Gliotransmission: Exocytotic release from astrocytes. Brain Res Rev 2010;63:83–92.

17. Dringen R, Pawlowski PG, Hirrlinger J. Peroxide detoxification by brain cells. J Neurosci Res 2005;79:157–165.

18. Hirrlinger J, Dringen R. The cytosolic redox state of astrocytes: Maintenance, regulation and functional implications for metabolite trafficking. Brain Res Rev 2010;63:177–188.

19. Schmidt M, Dringen R. Glutathione synthesis and metabolism. In: R. Gruetter, I.Y. Choi, editors. Advances in Neurobiology. New York: Springer Science, in press.

20. Dringen R, Bishop GM, Koeppe M, Dang TN, Robinson SR. The pivotal role of astrocytes in the metabolism of iron in the brain. Neurochem Res 2007;32:1884–1890.

21. Tiffany-Castiglioni E, Qian YC. Astroglia as metal depots: Molecular mechanisms for metal accumulation, storage and release. Neurotoxicology 2001;22:577–592.

22. Nedergaard M, Ransom B, Goldman SA. New roles for astrocytes: Redefining the functional architecture of the brain. Trends Neurosci 2003;26:523–530.

23. Wang J, Chen Y, Chen B, Ding J, Xia G, Gao C, Cheng J, Jin N, Zhou Y, Li X, et al. Pharmacokinetic parameters and tissue distribution of magnetic Fe_3O_4 nanoparticles in mice. Int J Nanomed 2010;5:861–866.

24. Geppert M, Hohnholt M, Gaetjen L, Grunwald I, Bäumer M, Dringen R. Accumulation of iron oxide nanoparticles by cultured brain astrocytes. J Biomed Nanotechnol 2009;5:285–293.

25. Geppert M, Hohnholt MC, Thiel K, Nürnberger S, Grunwald I, Rezwan K, Dringen R. Uptake of dimercaptosuccinate-coated magnetic iron oxide nanoparticles by cultured brain astrocytes. Nanotechnology 2011;22:145101–145110.

26. Hohnholt M, Geppert M, Dringen R. Effects of iron chelators, iron salts, and iron oxide nanoparticles on the proliferation and the iron content of oligodendroglial OLN-93 cells. Neurochem Res 2010;35:1259–1268.

27. Hohnholt MC, Geppert M, Nürnberger S, von Byern J, Grunwald I, Dringen R. Advanced biomaterials: Accumulation of citrate-coated magnetic iron oxide nanoparticles by cultured brain astrocytes. Adv Eng Mater 2010;12:B690–B694.

28. Pickard MR, Jenkins SI, Koller CJ, Furness DN, Chari DM. Magnetic nanoparticle labeling of astrocytes derived for neural transplantation. Tissue Eng Part C Methods 2011;17:89–99.

29. Pisanic TR, II, Blackwell JD, Shubayev VI, Finones RR, Jin S. Nanotoxicity of iron oxide nanoparticle internalization in growing neurons. Biomaterials 2007;28:2572–2581.

30. Petri-Fink A, Hofmann H. Superparamagnetic iron oxide nanoparticles (SPIONs): From synthesis to in vivo studies—A summary of the synthesis, characterization, in vitro, and in vivo investigations of SPIONs with particular focus on surface and colloidal properties. IEEE Trans Nanobiosci 2007;6:289–297.

31. Prijic S, Scancar J, Romih R, Cemazar M, Bregar VB, Znidarsic A, Sersa G. Increased cellular uptake of biocompatible superparamagnetic iron oxide nanoparticles into malignant cells by an external magnetic field. J Membr Biol 2010;236:167–179.

32. Kamau SW, Hassa PO, Steitz B, Petri-Fink A, Hofmann H, Hofmann-Amtenbrink M, von Rechenberg B, Hottiger MO. Enhancement of the efficiency of non-viral gene delivery by application of pulsed magnetic field. Nucleic Acids Res 2006;34:e40.

33. Plank C, Anton M, Rudolph C, Rosenecker J, Krotz F. Enhancing and targeting nucleic acid delivery by magnetic force. Exp Opin Biol Ther 2003;3:745–758.

34. Scherer F, Anton M, Schillinger U, Henke J, Bergemann C, Kruger A, Gansbacher B, Plank C. Magnetofection: Enhancing and targeting gene delivery by magnetic force in vitro and in vivo. Gene Ther 2002;9:102–109.

35. Bee A, Massart R, Neveu S. Synthesis of very fine maghemite particles. J Magn Magn Mater 1995;149:6–9.

36. Aberle LB, Kleemeier M, Hennemann OD, Burchard W. Selection of single scattering from multiple scattering systems by 3D cross-correlation. 2. Concentrated polymer solutions. Macromolecules 2002;35:1877–1886.

37. Hamprecht B, Löffler F. Primary glial cultures as a model for studying hormone action. Methods Enzymol 1985;109:341–345.

38. Dang TN, Bishop GM, Dringen R, Robinson SR. The putative heme transporter HCP1 is expressed in cultured astrocytes and contributes to the uptake of hemin. Glia 2010;58:55–65.

39. Gutterer JM, Dringen R, Hirrlinger J, Hamprecht B. Purification of glutathione reductase from bovine brain, generation of an antiserum, and immunocytochemical localization of the enzyme in neural cells. J Neurochem 1999;73:1422–1430.

40. Reinhart PH, Pfeiffer B, Spengler S, Hamprecht B. Purification of glycogen phosphorylase from bovine brain and immunocytochemical examination of rat glial primary cultures using monoclonal antibodies raised against this enzyme. J Neurochem 1990;54: 1474–1483.

41. Riemer J, Hoepken HH, Czerwinska H, Robinson SR, Dringen R. Colorimetric ferrozine-based assay for the quantitation of iron in cultured cells. Anal Biochem 2004;331:370–375.

42. Dringen R, Kussmaul L, Hamprecht B. Detoxification of exogenous hydrogen peroxide and organic hydroperoxides by cultured astroglial cells assessed by microtiter plate assay. Brain Res Brain Res Protoc 1998;2:223–228.

43. Lowry OH, Rosebrough NJ, Farr AL, Randall RJ. Protein measurement with the Folin phenol reagent. J Biol Chem 1951;193: 265–275.

44. Kim JS, Yoon TJ, Yu KN, Noh MS, Woo N, Kim BG, Lee KH, Sohn BH, Park SB, Lee JK, Cho MH. Cellular uptake of magnetic nanoparticles is mediated through energy-dependent endocytosis in A549 cells. J Vet Sci 2006;7:321–326.

45. Wilhelm C, Gazeau F. Universal cell labelling with anionic magnetic nanoparticles. Biomaterials 2008;29:3161–3174.

46. Au C, Mutkus L, Dobson A, Riffle J, Lalli J, Aschner M. Effects of nanoparticles on the adhesion and cell viability on astrocytes. Biol Trace Elem Res 2007;120:248–256.

47. Buyukhatipoglu K, Clyne AM. Superparamagnetic iron oxide nanoparticles change endothelial cell morphology and mechanics via reactive oxygen species formation. J Biomed Mater Res A 2011;96:186–195.

48. Bishop GM, Dang TN, Dringen R, Robinson SR. Accumulation of Non-transferrin-bound iron by neurons. Astrocytes, and microglia. Neurotox Res 2011;19:443–451.

49. Tulpule K, Robinson SR, Bishop GM, Dringen R. Uptake of ferrous iron by cultured rat astrocytes. J Neurosci Res 2010;88: 563–571.

50. Ivanov AI. Pharmacological inhibition of endocytic pathways: Is it specific enough to be useful? Methods Mol Biol 2008;440:15–33.

51. Dausend J, Musyanovych A, Dass M, Walther P, Schrezenmeier H, Landfester K, Mailander V. Uptake mechanism of oppositely

charged fluorescent nanoparticles in HeLa cells. Macromol Biosci 2008;8:1135–1143.

52. Huth US, Schubert R, Peschka-Suss R. Investigating the uptake and intracellular fate of pH-sensitive liposomes by flow cytometry and spectral bio-imaging. J Control Release 2006;110:490–504.

53. Rejman J, Oberle V, Zuhorn IS, Hoekstra D. Size-dependent internalization of particles via the pathways of clathrin- and caveolae-mediated endocytosis. Biochem J 2004;377:159–169.

54. Gekle M, Freudinger R, Mildenberger S. Inhibition of Na^+-H^+ exchanger-3 interferes with apical receptor-mediated endocytosis via vesicle fusion. J Physiol 2001;531:619–629.

55. Arsianti M, Lim M, Marquis CP, Amal R. Assembly of polyethylenimine-based magnetic iron oxide vectors: insights into gene delivery. Langmuir 2010;26:7314–7326.

2.5   Publication/Manuscript 5

Geppert, M. and Dringen, R. (2012) Presence of serum alters the properties of iron oxide nanoparticles and lowers their accumulation by cultured brain astrocytes. *Submitted for publication*.

Contributions of M. Geppert:

- Performance of all experimental work
- Preparation of a first draft of the manuscript

Publication/Manuscript 5

Presence of serum alters the properties of iron oxide nanoparticles and lowers their accumulation by cultured brain astrocytes

Mark Geppert[1,2] and Ralf Dringen[1,2]

[1]*Centre for Biomolecular Interactions Bremen, University of Bremen, Bremen, Germany*

[2]*Centre for Environmental Research and Sustainable Technology, University of Bremen, Bremen, Germany*

Address correspondence to:

Dr. Ralf Dringen

Centre for Biomolecular Interactions Bremen

University of Bremen

P.O. Box 330440

28334 Bremen, Germany

Telephone: +49-421-21863230

Facsimile: +49-421-21863244

email: Ralf Dringen (ralf.dringen@uni-bremen.de)

homepage: http://www.fb2.uni-bremen.de/en/dringen

Abstract

Iron oxide nanoparticles (IONPs) are considered for various diagnostic and therapeutic applications. Such particles are able to cross the blood-brain barrier and are taken up into brain cells. To test whether serum components affect properties of IONPs and/or their uptake into brain cells, we have incubated dimercaptosuccinate-coated magnetic IONPs without and with fetal calf serum (FCS) and have exposed cultured brain astrocytes with IONPs in the absence or presence of FCS. Incubation with FCS caused a concentration-dependent increase in the average hydrodynamic diameter of the particles and of their zeta-potential. In presence of 10% FCS the diameter of the IONPs was increased from 57 ± 2 nm to 107 ± 6 nm and the zeta-potential of the particles from -22 ± 5 mV to -9 ± 1 mV. FCS affected also strongly the uptake of IONPs by cultured astrocytes. The efficient time- and temperature-dependent cellular accumulation of IONPs was lowered with increasing concentration of FCS by up to 90%. In addition, in the absence of serum, endocytosis inhibitors did not alter the IONP accumulation by astrocytes, while chlorpromazine or wortmannin lowered significantly the accumulation of IONPs in the presence of FCS, suggesting that clathrin-mediated endocytosis and macropinocytosis are involved in astrocytic IONP uptake from serum-containing medium. These data demonstrate that presence of FCS strongly affects the properties of IONPs as well as their accumulation by cultured brain cells.

Key words:

albumin, brain, endocytosis, fetal calf serum, IONPs

Abbreviations: ANOVA, analysis of variance; BSA, bovine serum albumin, DMEM, Dulbecco's modified Eagle's medium; DMSA, dimercaptosuccinic acid; DMSO, dimethyl sulfoxide; EIPA, 5-(N-ethyl-N-isopropyl)amiloride; FCS, fetal calf serum; HEPES, 2-(4-(2-hydroxyethyl)-1-piperazinyl)-ethansulfonic acid; IB, incubation buffer; IONPs, iron oxide nanoparticles; LDH, lactate dehydrogenase; NADH, nicotinaminde adenine dinucleotide (reduced); PBS, phosphate buffered saline; SD, standard deviation

1.   Introduction

Magnetic iron oxide nanoparticles (IONPs) with various types of functionalizations are tools for a wide range of biomedical and therapeutical applications in the brain, such as targeted drug delivery (Laurent et al. 2008; Yang et al. 2011; Chertok et al. 2008), contrast enhancement in magnetic resonance imaging (Weinstein et al. 2010; Yang 2010), for cell labeling (Bhirde et al. 2011; Mahmoudi et al. 2011) or treatment of tumors via magnetic field-mediated hyperthermia (Jordan et al. 2006; Thiesen and Jordan 2008). Recent studies have shown, that peripherally applied IONPs are able to cross the blood brain barrier (Wang et al. 2010). Since astrocytes cover with their endfeet almost completely the brain capillaries, they have a strategically very important location being the first cells that encounter substances which have crossed the blood-brain barrier (Sofroniew and Vinters 2010). In the brain, astrocytes outnumber neurons almost fivefold (Sofroniew and Vinters 2010) and have many important functions, including the supply of metabolic nutrients (Barros and Deitmer 2010), the uptake and release of neurotransmitters (Eulenburg and Gomeza 2010; Parpura and Zorec 2010), the regulation the cytosolic redox potential (Hirrlinger and Dringen 2010) and the regulation of iron homeostasis (Dringen et al. 2007).

The stability and the aggregation behaviour of IONPs depend on the coating as well as on the composition of the incubation media (Chen et al. 2008; Eberbeck et al. 2010; Petri-Fink et al. 2008). Especially the proteins present in the fetal calf serum (FCS), which is a common component of culture media, interact with the nanoparticle surface and form a protein corona around the particles, thereby affecting their properties (Nel et al. 2009; Wiogo et al. 2011). The stabilization by FCS prevents precipitation of IONPs and allows efficient uptake of FCS-treated IONPs into some cell lines (Chen et al. 2008).

Several reports have demonstrated that cultured brain astrocytes take up IONPs both in the absence (Geppert et al. 2009; Geppert et al. 2011; Hohnholt et al. 2010; Lamkowsky et al. 2011) and in the presence (Pickard et al. 2011) of serum. For the serum condition, endocytotic mechanisms have been demonstrated to be involved in IONP uptake (Pickard et al. 2011), while inhibitors of endocytotic pathways did not lower IONP

accumulation in the absence of serum (Lamkowsky et al. 2011). This discrepancy suggests that presence of serum affects the mechanisms of IONP uptake into astrocytes.

A direct comparison of IONP accumulation by brain cells in absence or presence of serum as well as a detailed study on the consequences of the presence of serum on properties of IONPs have to our knowledge not been reported so far. Therefore, we have addressed such questions by investigating properties of dimercaptosuccinate (DMSA)-coated IONPs as well as their accumulation by cultured astrocytes in the absence or the presence of FCS. Here we report that presence of FCS strongly increases the size and the zeta-potential of IONPs and severely lowers the accumulation of the particles by cultured astrocytes. In addition, we demonstrate that endocytosis inhibitors lower IONP accumulation only in the presence of serum, but not in serum-free conditions. These data demonstrate that properties of IONPs as well as the extent of IONP accumulation by astrocytes and its mechanism depend strongly on the absence or presence of serum components. These results should be considered for experimental and biomedical applications of IONPs.

2.   Materials and Methods

2.1   Materials

Penicillin/streptomycin solution was obtained from Biochrom (Berlin, Germany). Dulbecco's modified Eagle´s medium (DMEM) was from Gibco (Karlsruhe, Germany). Bovine serum albumin (BSA) and NADH were purchased from Applichem (Darmstadt, Germany). All other chemicals of the highest purity available were from Sigma (Steinheim, Germany), Fluka (Buchs, Switzerland), Merck (Darmstadt, Germany) or Riedel-de Haen (Seelze, Germany). 96-well microtiter plates were from Nunc (Wiesbaden, Germany) and 24-well cell culture plates from Sarstedt (Nümbrecht, Germany).

Magnetic iron oxide nanoparticles (IONPs) were synthesized using an earlier described wet chemical method that involves co-precipitation of ferrous and ferric iron in an alkaline environment with subsequent oxidation via nitric acid and ferric nitrate (Bee et al. 1995; Geppert et al. 2009). To disperse the synthesized IONPs in the incubation buffers used, they were coated with dimercaptosuccinic acid (DMSA) as described earlier (Fauconnier et al. 1997; Geppert et al. 2011). The DMSA-coated IONPs used in this work consist of spherical particles with a monomodal size distribution and a mean hydrodynamic diameter of about 60 nm (Geppert et al. 2011). The IONP concentrations given represent the concentrations of total iron in the dispersions and not the concentration of particles.

Fetal calf serum (FCS) was purchased from Biochrom (Berlin, Germany). This serum contained 1.33 mM phosphate as stated by the supplier. Heated FCS was obtained by incubation of FCS for 20 min at 90°C. Protein-free FCS was obtained by filtration of the FCS using Spin-X^{R}6 5k MWCO concentrators (Corning, Lowell, Massachusetts) for 20 min at 4000 g which lowered the protein content from 45.0 ± 8.6 mg/mL to 0.20 ± 0.08 mg/mL in the filtrate.

2.2   Determination of particle size and zeta-potential of IONPs

The hydrodynamic diameters of IONPs were determined by dynamic light scattering using the Li.S.A detector (Fraunhofer IFAM, Bremen, Germany) as described earlier (Geppert et al. 2011). Zeta-potential of the IONPs was determined with a Delsa™Nano C Analyzer (Beckmann Coulter, Krefeld, Germany).

2.3   Cell cultures and experimental incubations

Astrocyte-rich primary cultures were prepared from the brains of newborn Wistar rats as described earlier (Hamprecht and Löffler 1985). 300.000 viable cells were seeded in 1 mL culture medium (90% DMEM, 10% FCS, 1 mM pyruvate, 20 units/mL penicillin G and 20 μg/mL streptomycin sulphate) in wells of 24-well cell culture plates (Sarstedt, Nümbrecht, Germany) and the medium was changed every seventh day. For experiments, cultures at an age between 15 and 22 days were used.

Cells in 24-well dishes were washed twice with 1 mL pre-warmed (37°C) or ice-cold (4°C) incubation buffer (IB: 20 mM HEPES, 145 mM NaCl, 1.8 mM $CaCl_2$, 5.4 mM KCl, 1 mM $MgCl_2$, 5 mM glucose, adjusted to pH 7.4 at the desired temperature) and then incubated with 1 mL IB containing 0 or 1 mM IONPs and the indicated amounts of FCS and/or other compounds as indicated in the figures and tables. After incubation, the media were collected and the cells were washed twice with 1 mL ice-cold phosphate buffered saline (PBS: 10 mM potassium phosphate buffer pH 7.4, containing 150 mM NaCl). Dry cells were stored frozen until further investigation of their iron and protein contents.

2.4   Determination of cell viability, protein content and iron content

Cell viability was assessed by measuring the extracellular activity of lactate dehydrogenase (LDH) as previously described (Dringen et al. 1998) with the modification that 30 μL of incubation buffers and/or lysates were used in the assay. Protein contents were determined with the Lowry method (Lowry et al. 1951) using bovine serum albumin as a standard. Iron was quantified using the previously published

ferrozine-based iron assay (Riemer et al. 2004) which was slightly modified for the quantification of iron from IONPs (Geppert et al. 2009).

2.5   Presentation of data

If not stated otherwise, all experiments were performed at least three times, the cell experiments on three individually prepared cultures. The data given in the figures and the tables represent mean values ± standard deviation (SD). Statistical analysis for two sets of data was performed using the *t*-test. Analysis between groups of data was performed using ANOVA with the Bonferroni *post hoc* test. $p > 0.05$ was considered as not significant.

3.   Results

3.1   Effects of FCS on properties of IONPs

The synthesized DMSA-coated IONPs used in the present study had a monomodal size distribution with an average hydrodynamic diameter of 57 ± 2 nm. Incubation of IONPs with FCS for 4 h strongly increased the diameter of the particles as indicated by the shift in the size distribution curve (Fig. 1a) and by the increase in average diameter (Fig. 1b) compared to IONPs incubated without FCS. While FCS in a low concentration of 1% increased the mean hydrodynamic particle diameter to a maximal value of 207 ± 6 nm, higher concentrations of FCS were less efficient to increase the diameter of the particles (Fig. 1b). IONPs that had been incubated in presence of 10% FCS had an average diameter of 107 ± 6 nm (Fig. 1b).

Dispersed in serum-free incubation buffer, DMSA-coated IONPs have a zeta-potential of -26 ± 3 mV (Geppert et al. 2011). This value was not significantly altered by incubation of the particles for 4 h in IB as demonstrated by the detection of a zeta-potential of -22 ± 5 mV (Fig. 1c). However, incubation of the particles in serum-containing IB increased the zeta-potential significantly in a concentration-dependent manner. While incubation with 1% FCS increased the zeta-potential already significantly to -12 ± 1 mV, a treatment of the particles with 10% FCS increased the zeta-potential further to -9 ± 1 mV (Fig. 1c).

3.2   Presence of serum lowers the accumulation of IONPs by astrocytes

Cultured astrocytes are known to efficiently accumulate IONPs under serum-free incubation conditions (Geppert et al. 2011). To test for the consequences of the presence of FCS on the accumulation of IONPs by cultured astrocytes, the cells were incubated for up to 6 h with 1 mM iron as IONPs without (control) or with 1, 3 or 10% FCS (Fig. 2). None of these conditions caused any significant increase in extracellular LDH activity (Fig. 2c), indicating that the viability of the cells was not compromised under the conditions used. In the absence of FCS, the specific cellular iron content increased within 6 h from an initial value of 12 ± 4 nmol/mg protein to 1717 ± 86 nmol/mg (Fig. 2a). This increase in specific iron content was substantially lowered, if the cells were

incubated with IONPs in presence of FCS, as clearly demonstrated by specific iron contents of 756 ± 96 (1% FCS), 439 ± 33 (3% FCS) and 234 ± 26 (10% FCS) nmol/mg protein that were determined after 6 h of incubation. For all these conditions a rapid initial increase of cellular iron was observed for the first 15 min of incubation, after which the iron accumulation remained almost linear for up to 6 h. From these linear increases between 15 min and 6 h, iron accumulation rates were calculated (Fig. 2b). In absence of FCS, the cells accumulate IONPs with a rate of 215 ± 30 nmol iron/(h $\times$ mg protein). This accumulation rate was significantly lowered in presence of FCS by 58%, 80% and 89% to 90 ± 6 (1% FCS), 44 ± 3 (3% FCS) and 24 ± 4 (10% FCS) nmol iron/(h $\times$ mg protein), respectively (Fig. 2b).

To investigate the concentration-dependent effects of FCS on IONP accumulation in more detail, the cells were incubated for 4 h with 1 mM IONPs in presence of different concentrations of FCS. To discriminate between cell-associated and internalized IONPs these incubations were performed at 37°C and at 4°C, since IONP internalization is prevented during incubation at 4°C (Geppert et al. 2011). None of the incubation conditions used caused a loss in cell viability as indicated by the absence of any significant increase in extracellular LDH activity (data not shown). If cells were incubated with IONPs at 37°C in the absence of FCS, their cellular iron content increased during 4 h to 1412 ± 128 nmol/mg protein (Fig. 3a). This value was significantly lowered in a concentration-dependent manner by presence of FCS during the incubation, resulting in as little as 171 ± 4 nmol iron/mg protein after incubation of the cells with IONPs at 37°C with 10% FCS (Fig. 3a). Compared to the 37°C conditions, incubation of astrocytes with IONPs at 4°C resulted in significantly ($p<0.05$) lower cellular iron contents for both the serum and serum-free conditions (Fig. 3a). The data obtained for cellular iron contents of cells incubated at 4°C ranged between 679 ± 146 nmol/mg (incubation without FCS) and 65 ± 9 nmol/mg (presence of 10% FCS) (Fig. 3a). The amount of cell-associated iron detected at 4°C accounted for all serum concentrations applied to about 40-50% of the amount of cellular iron determined for cells that had been incubated with IONPs at 37°C. The differences between the cellular iron contents obtained after incubation at 37°C and at 4°C (ΔFe-values) represent the amounts of internalized IONPs (Geppert et al. 2011). These values

demonstrate that FCS caused a concentration-dependent decrease in the amount of internalized IONPs (Fig. 3b).

Investigation of the concentration-dependent effect of FCS on the hydrodynamic particle diameter in the supernatant of cells exposed to 1 mM IONPs at 37°C (Fig. 3c) revealed a maximally elevated average diameter for IONP that had been incubated with cells in presence of around 1% FCS (Fig. 3c). In contrast, compared to the control condition (absence of FCS) incubation in presence of 10% FCS did not increase the hydrodynamic diameter of the IONPs. For both the control conditions (absence of FCS) as well as for the serum conditions the IONPs in the medium of cells had a substantially increased diameter (Fig. 3c) compared to the values obtained for respective incubations in the absence of cells (Fig. 1b). The average hydrodynamic diameter of IONPs in IB without, with 1% serum and with 10% serum increased significantly during incubation with cells from 57 ± 2 to 173 ± 9 nm, from 207 ± 6 to 231 ± 3 nm and from 107 ± 6 to 140 ± 10, respectively (Figs. 1B and 3C).

3.3   Effects of endocytosis inhibitors on the cellular IONP accumulation

IONP exposed astrocytes contain IONPs in intracellular vesicles (Geppert et al. 2011; Pickard et al. 2011), suggesting that endocytotic pathways are involved in IONP uptake. To investigate the mechanism of the IONP uptake in absence or presence of FCS, cultured astrocytes were incubated for 4 h with 1 mM IONPs in the absence or the presence of 10% FCS and/or compounds that have been described to affect endocytotic pathways (Dausend et al. 2008; Greulich et al. 2011; Huth et al. 2006; Luther et al. 2011; Pickard et al. 2011; Rejman et al. 2004) (Tab. 1). None of the conditions applied caused a loss in cell viability, as indicated by the absence of any significant increase in the extracellular LDH activity (Tab. 1). In absence of endocytosis inhibitors, the cellular iron contents increased within 4 h incubation in the absence and presence of 10% FCS to about 1300 nmol/mg and 180 nmol/mg, respectively, as expected from the data presented in Figs. 2 and 3. These values were significantly lowered by incubation at 4°C for both the serum-free and the serum condition by 50 to 70% compared to the values obtained for the respective 37°C conditions (Tab. 1). While during incubation with IONPs in the absence of serum none of the applied endocytosis inhibitors altered

significantly the cellular iron content, the IONP accumulation in presence of serum was significantly lowered by chlorpromazine and wortmannin. IONP accumulation in the presence of serum was not affected by 3-methyladenine, but a 20% reduction in iron accumulation was observed in presence of EIPA, although this alteration did not reach the level of significance. Compared to controls, the application of a mixture of chlorpromazine, wortmannin and EIPA lowered IONP accumulation by about 50% in presence of 10% FCS, but did not affect IONP accumulation by astrocytes incubated under serum-free conditions (Tab. 1).

3.4 Effects of serum proteins on the diameter of IONPs and on their accumulation by astrocytes

To elucidate whether the proteins in FCS may be responsible for the observed effects of FCS on properties of IONPs and on their accumulation by cells, cultured astrocytes were incubated for 4 h with 1 mM IONP in IB containing untreated FCS or FCS that had either been heated to denature proteins or had been filtered to remove proteins. Alternatively, to test for protein-dependent effects the cells were exposed to IONPs in presence of the proteins BSA or ovalbumin. None of the conditions used caused any loss in cell-viability as indicated by the absence of any increase in extracellular LDH activity (Tab. 2). Presence of protein-free FCS during the incubation of astrocytes with 1 mM IONPs caused aggregation and precipitation of the particles as demonstrated by the strong increase in their hydrodynamic diameter (Tab. 2). Under this condition, the lowering effect of FCS on the accumulation of IONPs by astrocytes was completely abolished (Tab. 2). In contrast, denaturing of proteins by heating increased the particle diameter only to a small extent and did not prevent the inhibitory potential of FCS on IONP accumulation (Tab. 2). Similarly, BSA and ovalbumin, if applied in concentrations corresponding to the total protein content present in the 10% FCS condition, did not significantly alter the diameter of the particles compared to controls (none), but significantly lowered IONP accumulation by astrocytes, to values similar to those found after treatment with 10% FCS (Tab. 2).
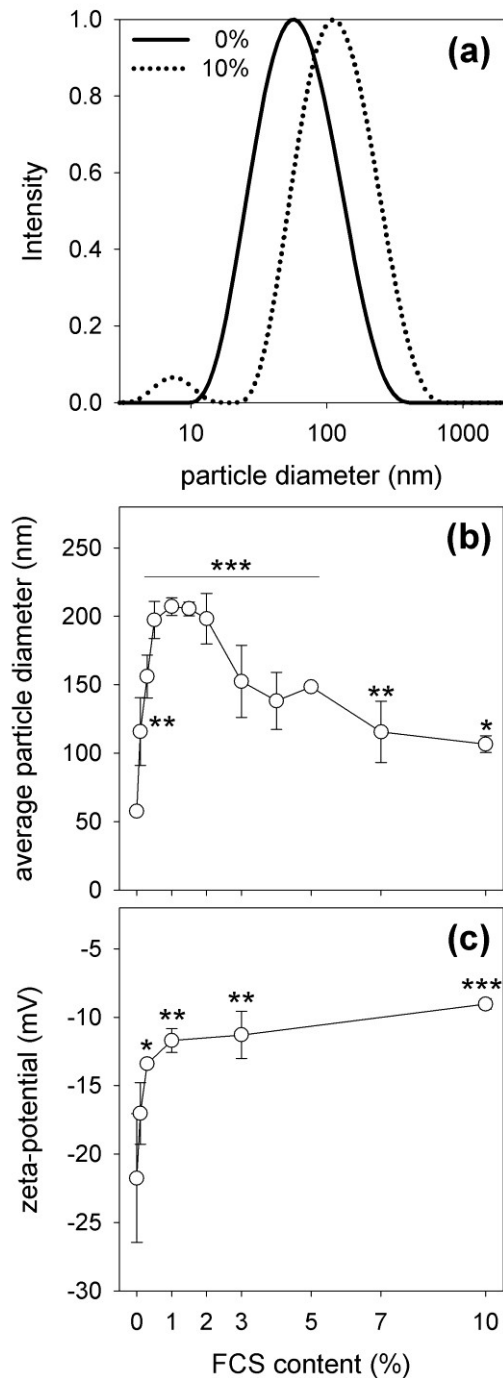
Figure 1: Effects of FCS on the hydrodynamic diameter (a,b) and on the zeta-potential (c) of IONPs. 1 mM iron as IONPs was incubated for 4 h at 37°C with IB containing the indicated concentrations of FCS before the hydrodynamic particle diameter (a,b) and the zeta-potential (c) were determined. Stars in b and c indicate the significance of differences between the controls (absence of FCS) and the FCS-containing conditions with *$p<0.05$, **$p<0.01$ and ***$p<0.001$.
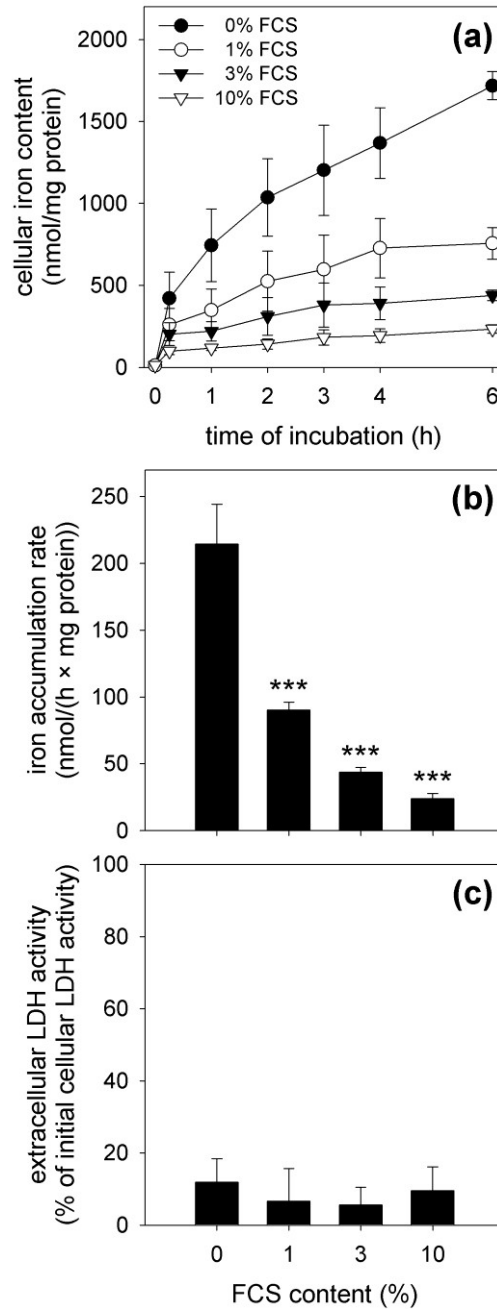
Figure 2: Time dependence of the iron accumulation from IONPs in cultured astrocytes. The cells were incubated for up to 6 h with 1 mM iron as IONPs in presence of the indicated concentrations of FCS. The cellular iron content (a) and the extracellular LDH activity after 6 h (c) were measured. The iron accumulation rates (b) were calculated from the almost linear increases of the cellular iron contents between 15 min and 6 h. In b, the significance of differences of data compared to the control (absence of FCS) is indicated with ***$p<0.001$.
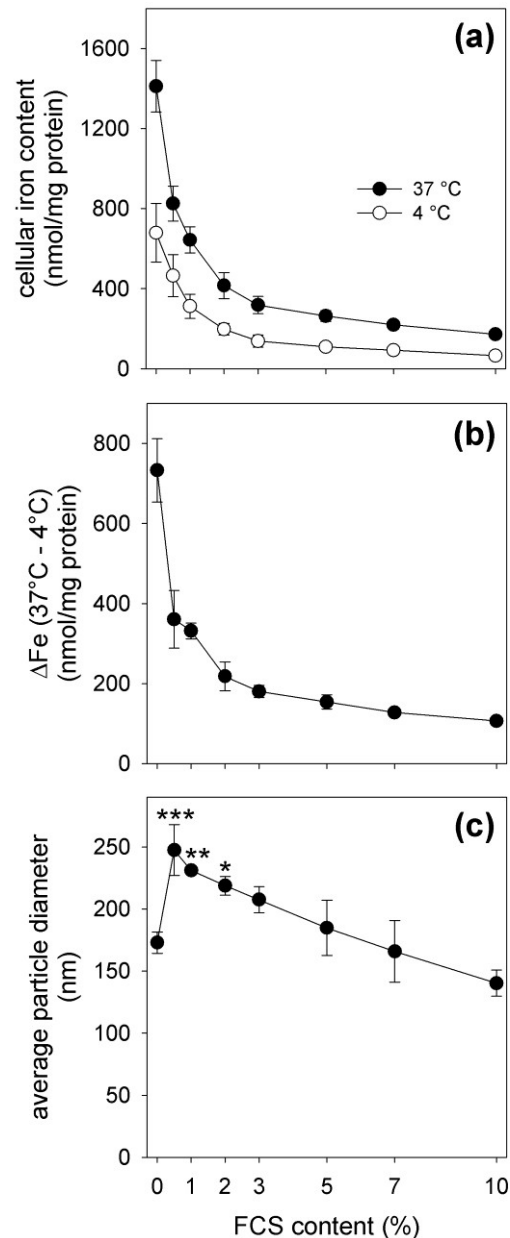
Figure 3: Serum- and temperature-dependence of the iron accumulation from IONPs by cultured astrocytes and of the hydrodynamic diameter of the particles. The cells were incubated for 4 h with 1 mM iron as IONP in IB containing the indicated concentrations of FCS at 37°C or at 4°C. The cellular iron content (a) was measured, b shows the difference of the cellular iron contents obtained after incubation of cells at 37°C minus that at 4°C, and c gives the average hydrodynamic diameter of the IONPs in the supernatant. In a and b, the values obtained for all serum-treated samples were significantly ($p < 0.05$) lower than those measured for the control (absence of serum). In a, the values obtained for all 4°C incubations were significantly lower ($p < 0.05$) than those for the respective 37°C conditions. In c, the significance of differences of data compared to the control (absence of FCS) is indicated with $*p < 0.05$, $**p < 0.01$ and $***p < 0.001$.

Table 1: Effects of endocytosis inhibitors on the iron accumulation from IONPs by cultured astrocytes in the absence or presence of FCS.

Substance	concentration	no FCS		10% FCS	
		extracellular LDH activity (% of initial)	specific cellular iron content (nmol/mg protein)	extracellular LDH activity (% of initial)	specific cellular iron content (nmol/mg protein)
Control		5 ± 5	1329 ± 27	2 ± 1	180 ± 15
3-Methyladenine	2.5 mM	8 ± 5	1252 ± 123	2 ± 1	190 ± 15
4 °C		4 ± 0	583 ± 26 ***	3 ± 3	61 ± 5 ***
Control (DMSO)	0.1%	4 ± 1	1333 ± 154	1 ± 0	191 ± 24
Chlorpromazine	20 µM	6 ± 3	1190 ± 126	3 ± 3	137 ± 7 **
EIPA	25 µM	6 ± 4	1155 ± 34	3 ± 1	157 ± 8
Wortmannin	100 nM	7 ± 1	1277 ± 29	4 ± 2	139 ± 9 **
Control (DMSO)	0.3%	8 ± 3	1253 ± 46	3 ± 1	182 ± 15
Inhibitor mixture		14 ± 4	1327 ± 119	7 ± 2	99 ± 6 ***

The cells were incubated for 4 h with 1 mM iron as IONPs without or with 10% FCS in absence or presence of the indicated endocytosis inhibitors and the cellular iron content as well as the extracellular LDH activity were measured. Dimethyl sulfoxide (DMSO) was used to pre-dissolve some of the inhibitors. "Inhibitor mixture" represents a mixture of 20 µM Chlorpromazine, 25 µM 5-(N-ethyl-N-isopropyl)amiloride (EIPA) and 100 nM Wortmannin. The significance of differences of data compared to the respective control is indicated by ** $p < 0.01$ and *** $p < 0.001$.

Table 2: Effects of FCS and proteins on the diameter of IONPs in the incubation medium and on the accumulation of IONPs by astrocytes.

Compound	concentration	extracellular LDH-activity (% of initial)	cellular iron content (nmol/mg)	hydrodynamic particle diameter (nm)
None		2 ± 2	1732 ± 174	163 ± 23
FCS	10% (v/v)	3 ± 3	289 ± 112 ***	141 ± 10
protein-free FCS	10% (v/v)	2 ± 3	2602 ± 394 **	> 1000 ***
heated FCS	10% (v/v)	3 ± 3	222 ± 74 ***	278 ± 77 *
BSA	5 mg/mL	3 ± 3	585 ± 113 ***	202 ± 14
Ovalbumin	5 mg/mL	6 ± 1	522 ± 117 ***	130 ± 10

Cultured astrocytes were incubated with 1 mM iron as IONPs for 4 h in the absence (none) or presence of the indicated compounds and the extracellular LDH activity, the specific cellular iron content and the hydrodynamic particle diameter in the supernatant were determined. The data represent mean values ± SD of three experiments performed on individually prepared cultures. Indicated are the significances of differences to control values (none) as *$p<0.05$, **$p<0.01$ and ***$p<0.001$.

4.   Discussion

4.1   Alteration of IONP properties by serum

Presence of serum causes substantial alterations of the properties of IONPs as clearly demonstrated by the concentration-dependent increases in the average hydrodynamic diameter as well as of the zeta-potential of the particles. The negative zeta-potential of -22 mV of DMSA-coated IONPs in serum-free IB indicates a negatively charged surface, as expected from the carboxyl groups of the DMSA-coat (Fauconnier et al. 1997). The increase in zeta potential to -9 ± 1 mV in presence of FCS demonstrates a loss of negative charges from the surface, which is likely to be a consequence of adsorption of proteins on the IONP surface which form a protein corona around the particles (Lynch and Dawson 2008; Nel et al. 2009; Wiogo et al. 2011). DMSA forms a cage-like structure around IONP (Fauconnier et al. 1997; Valois et al. 2010) that is crosslinked by disulfide bridges and has carboxylate and thiol groups at the surface. Thus, in addition to electrostatic interactions between positive surface charges of serum proteins with the carboxylate groups of the DMSA-coat, also disulfide bridge formation between thiol and disulfide groups of DMSA-coat and proteins may be involved in the binding of a protein layer around DMSA-coated IONPs that caused the positivation of their zeta-potential in presence of FCS. Although already as little as 1% FCS substantially increased the zeta-potential of the particles, a further positivation of the potential was observed by increasing the FCS concentration to up to 10%, indicating that coverage of the particles by serum proteins was not complete in presence of low serum concentrations.

In contrast to the continuous increase of the zeta-potential with increasing concentrations of FCS, the dependence of the IONP diameter on the FCS concentration followed a bell shaped curve that showed a maximal particle diameter in the presence of around 1% FCS. This behaviour is likely to be a consequence of the simultaneous presence of compounds in the serum-containing medium that stabilize IONPs and/or induce their aggregation, i.e., ions that cause particle agglomeration and proteins that stabilize nanoparticles (Lynch and Dawson 2008; Wiogo et al. 2011). The proteins in FCS have been discussed to stabilize IONPs by preventing their interactions with low molecular weight ions that cause aggregation and precipitation of IONPs (Wiogo et al.

2011). This view of a stabilizing function of serum proteins is strongly supported by the observation that removal of the proteins from FCS by filtration caused immediate aggregation of IONPs. Since incubation media contain large concentrations of salt ions, a given threshold amount of protein is required to stabilize the IONPs against aggregation, explaining that at least 4% serum is required to stabilize carboxyl-functionalized IONPs (Wiogo et al. 2011) and that presence of 10% FCS prevented at least in part the increase in diameter of IONPs that was observed for the 1% FCS condition. This explanation is also in accord with the observation that presence of 1% FCS does not lead to a maximal increase in zeta-potential. Thus, with 1% FCS protein coverage appears not to be maximal and presence of higher amounts of serum protein will improve the coverage, thereby shielding the particles away from ions and at least in part prevent interactions between particles and aggregation.

During incubation of cells with DMSA-coated IONPs both in absence and presence of serum, the average diameter of the particles in the incubation buffer was significantly increased, confirming literature data (Geppert et al. 2011; Lamkowsky et al. 2011). Thus, compounds released from astrocytes are likely to induce some aggregation of the particles. Since the average hydrodynamic diameter of serum-treated IONPs was significantly higher after incubation with cells compared to control incubations without cells, the aggregation induced by cell-derived factors appears not to be abolished by high serum concentrations.

4.2   Presence of serum affects the accumulation of IONPs by cultured astrocytes

Viable cultured astrocytes have the capacity to accumulate large amounts of DMSA-coated IONPs which increases the specific cellular iron content 100fold, confirming literature data (Geppert et al. 2011; Lamkowsky et al. 2011). This efficient IONP accumulation was severely affected by the presence of FCS. Serum lowered the increase in cellular iron content by almost 90%, if the cells were incubated with IONPs in presence of 10% FCS. This observation is consistent with recent literature data, demonstrating that presence of serum lowered also the uptake of negatively charged carboxyl-modified polystyrene nanoparticles into macrophages (Lunov et al. 2011).

Of the various components present in serum, the proteins are most likely to be responsible for the lowering of IONP accumulation in astrocytes, since removal of the proteins from FCS abolished the FCS-mediated reduction in IONP accumulation. Since albumin is the predominant protein in FCS and known to bind to the surface of IONPs mainly by electrostatic interactions (Yang et al. 2009), this protein is highly likely to bind to the particle surface, thereby lowering the uptake of IONPs by astrocytes. Indeed, application of pure BSA also lowered astrocytic IONP accumulation by 70%, confirming literature data reported for HeLa cells (Wilhelm et al. 2003). It is unlikely that the observed FCS-induced inhibition of IONP uptake is a specific property of albumin, since presence of the unrelated protein ovalbumin lowered IONP accumulation to a similar extent. However, the mixture of proteins present in FCS appears to be even more efficient to lower IONP accumulation by astrocytes than an identical concentration of pure BSA, suggesting that other serum proteins than BSA are modulating IONP surface properties and cellular uptake. This is consistent with a recent report describing that other serum-proteins bind more strongly to the surface of IONPs than BSA (Wiogo et al. 2011).

Potential reasons for the drastic inhibition of astrocytic IONP-uptake by FCS could be the altered surface charge that enables the particles to efficiently bind to cell membranes as well as the increased size of the particles in presence of serum. The positive or negative surface charge of nanoparticles is considered to play a major role in their interaction with cell membranes and in their cellular uptake (Chen et al. 2011; Yue et al. 2011). For the conditions used here, the FCS-mediated lowering of the negative surface charge is likely to reduce the binding of IONPs to the cells, thereby slowing also their uptake. Indeed, both the adsorbance of IONPs to the cells, determined as cellular iron content after incubation at 4°C, as well as the internalization of the particles, as calculated as difference of the iron values determined for cells that had been exposed to IONPs at 37°C and at 4°C (Geppert et al. 2011), were lowered by the same factor, supporting the view that binding and uptake of IONPs are simultaneously lowered in presence of FCS.

Since nanoparticle size can influence their uptake into cells (Huang et al. 2010), also the increased size of FCS-treated IONPs could contribute to the observed reduction in IONP uptake in presence of serum. However, the diameter of DMSA-coated IONPs increased also rapidly in serum-free incubation buffer due to factors released from the cells (Geppert et al. 2011; Lamkowsky et al. 2011). In addition, presence of 10% FCS lowered the IONP accumulation by astrocytes much stronger than presence of 1% FCS, although the particle diameter determined for 10% FCS was only half of that of particles incubated with 1% FCS. Thus, the increased size of FCS-treated IONPs appears not to substantially contribute to the lower IONP accumulation from serum-containing medium compared to serum-free conditions.

4.3   Effects of endocytosis-inhibitors on IONP accumulation by cultured astrocytes

After incubation of astrocytes with IONPs the particles are present in intracellular vesicles (Geppert et al. 2011). This suggests that IONPs are taken up into astrocytes by endocytotic pathways. Indeed, for serum-containing incubation conditions some endocytosis inhibitors lowered significantly the uptake of IONPs, confirming previous results on the uptake of fluorescent IONPs in serum-containing medium (Pickard et al. 2011). The partial inhibition of IONP accumulation in serum-containing medium by wortmannin and chlorpromazine, which are known inhibitors for macropinocytosis and clathrin-mediated endocytosis (Greulich et al. 2011; Huth et al. 2006), respectively, as well as the additive effects observed for a mixture of different endocytosis inhibitors indicate that more than one endocytotic pathway is involved in IONP uptake by astrocytes. This view is supported also by recent results on the uptake of silver nanoparticles into cultured astrocytes in serum-containing medium, which appears to involve macropinocytosis and the endosomal pathway (Luther et al. 2011). In contrast, for serum-free conditions none of the endocytosis inhibitors applied here or previously (Lamkowsky et al. 2011) lowered astrocytic IONP accumulation. Thus, in addition to the known endocytotic pathways which appear to be predominately involved in the uptake of serum-treated IONPs in astrocytes, another quantitatively very efficient mechanism of uptake for IONPs appears to be present in astrocytes that mediates most of the uptake of IONPs in absence of serum.

4.4   Conclusions

Presence of serum strongly affects the properties and the accumulation of IONPs by cultured astrocytes. Although protein components of serum stabilize IONPs in dispersion, they also increase the diameter of the particles, strongly lower the rate of accumulation and alter the mechanisms involved in IONP uptake. These serum effects highlight the importance of clearly defined experimental conditions to understand and predict IONP accumulation by cells. In addition, these data are of high relevance for the interpretation and comparison of literature data on consequences of a treatment of cultured cells with IONPs. For the *in vivo* situation, our data suggest that IONPs applied to the blood are likely to be strongly affected by the presence of serum components. Since peripherally applied IONPs can cross the blood-brain barrier (Wang et al. 2010), brain cells are likely to encounter IONPs that carry serum proteins which may also *in vivo* lower their uptake into brain cells. Such a scenario should be considered for the development of further strategies to apply IONPs to the brain or to brain cells for experimental or medical reasons.

References

Barros LF, Deitmer JW (2010) Glucose and lactate supply to the synapse. Brain Res Rev 63:149-159. doi:10.1016/j.brainresrev.2009.10.002

Bee A, Massart R, Neveu S (1995) Synthesis of very fine maghemite particles. J Magn Magn Mater 149:6-9. doi:10.1016/0304-8853(95)00317-7

Bhirde A, Xie J, Swierczewska M, Chen X (2011) Nanoparticles for cell labeling. Nanoscale 3:142-153. doi:10.1039/c0nr00493f

Chen L, McCrate JM, Lee JC, Li H (2011) The role of surface charge on the uptake and biocompatibility of hydroxyapatite nanoparticles with osteoblast cells. Nanotechnology 22:105708. doi:10.1088/0957-4484/22/10/105708

Chen ZP, Zhang Y, Xu K, Xu RZ, Liu JW, Gu N (2008) Stability of hydrophilic magnetic nanoparticles under biologically relevant conditions. J Nanosci Nanotechnol 8:6260-6265. doi:10.1166/jnn.2008.343

Chertok B, Moffat BA, David AE, Yu FQ, Bergemann C, Ross BD, Yang VC (2008) Iron oxide nanoparticles as a drug delivery vehicle for MRI monitored magnetic targeting of brain tumors. Biomaterials 29:487-496. doi:10.1016/j.biomaterials.2007.08.050

Dausend J, Musyanovych A, Dass M, Walther P, Schrezenmeier H, Landfester K, Mailander V (2008) Uptake mechanism of oppositely charged fluorescent nanoparticles in HeLa cells. Macromol Biosci 8:1135-1143. doi:10.1002/mabi.200800123

Dringen R, Bishop GM, Koeppe M, Dang TN, Robinson SR (2007) The pivotal role of astrocytes in the metabolism of iron in the brain. Neurochem Res 32:1884-1890. doi:10.1007/s11064-007-9375-0

Dringen R, Kussmaul L, Hamprecht B (1998) Detoxification of exogenous hydrogen peroxide and organic hydroperoxides by cultured astroglial cells assessed by microtiter plate assay. Brain Res Brain Res Protoc 2:223-228. doi:10.1016/S1385-299X(97)00047-0

Eberbeck D, Kettering M, Bergemann C, Zirpel P, Hilger I, Trahms L (2010) Quantification of the aggregation of magnetic nanoparticles with different polymeric coatings in cell culture medium. J Phys D Appl Phys 43:405002-405010. doi:10.1088/0022-3727/43/40/405002

Eulenburg V, Gomeza J (2010) Neurotransmitter transporters expressed in glial cells as regulators of synapse function. Brain Res Rev 63:103-112. doi:10.1016/j.brainresrev.2010.01.003

Fauconnier N, Pons JN, Roger J, Bee A (1997) Thiolation of maghemite nanoparticles by dimercaptosuccinic acid. J Colloid Interface Sci 194:427-433. doi:CS975125

Geppert M, Hohnholt M, Gaetjen L, Grunwald I, Bäumer M, Dringen R (2009) Accumulation of iron oxide nanoparticles by cultured brain astrocytes. J Biomed Nanotechnol 5:285-293. doi:10.1166/jbn.2009.1033

Geppert M, Hohnholt MC, Thiel K, Nürnberger S, Grunwald I, Rezwan K, Dringen R (2011) Uptake of dimercaptosuccinate-coated magnetic iron oxide nanoparticles by cultured brain astrocytes. Nanotechnology 22:145101. doi:10.1088/0957-4484/22/14/145101

Greulich C, Diendorf J, Simon T, Eggeler G, Epple M, Koller M (2011) Uptake and intracellular distribution of silver nanoparticles in human mesenchymal stem cells. Acta Biomater 7:347-354. doi:10.1016/j.actbio.2010.08.003

Hamprecht B, Löffler F (1985) Primary glial cultures as a model for studying hormone action. Methods Enzymol 109:341-345

Hirrlinger J, Dringen R (2010) The cytosolic redox state of astrocytes: Maintenance, regulation and functional implications for metabolite trafficking. Brain Res Rev 63:177-188. doi:10.1016/j.brainresrev.2009.10.003

Hohnholt MC, Geppert M, Nürnberger S, von Byern J, Grunwald I, Dringen R (2010) Advanced Biomaterials: Accumulation of citrate-coated magnetic iron oxide nanoparticles by cultured brain astrocytes. Adv Eng Mater 12:B690-B694. doi:10.1002/adem.201080055

Huang J, Bu L, Xie J, Chen K, Cheng Z, Li X, Chen X (2010) Effects of nanoparticle size on cellular uptake and liver MRI with polyvinylpyrrolidone-coated iron oxide nanoparticles. ACS Nano 4:7151-7160. doi:10.1021/nn101643u

Huth US, Schubert R, Peschka-Suss R (2006) Investigating the uptake and intracellular fate of pH-sensitive liposomes by flow cytometry and spectral bio-imaging. J Control Release 110:490-504. doi:10.1016/j.jconrel.2005.10.018

Jordan A, Scholz R, Maier-Hauff K, van Landeghem FK, Waldoefner N, Teichgraeber U, Pinkernelle J, Bruhn H, Neumann F, Thiesen B, von Deimling A, Felix R (2006) The effect of thermotherapy using magnetic nanoparticles on rat malignant glioma. J Neurooncol 78:7-14. doi:10.1007/s11060-005-9059-z

Lamkowsky M, Geppert M, Schmidt MM, Dringen R (2011) Magnetic field-induced acceleration of the accumulation of magnetic iron oxide nanoparticles by cultured brain astrocytes. J Biomed Mater Res A:*in press*

Laurent S, Forge D, Port M, Roch A, Robic C, Elst LV, Muller RN (2008) Magnetic iron oxide nanoparticles: Synthesis, stabilization, vectorization, physicochemical characterizations, and biological applications. Chem Rev 108:2064-2110. doi:10.1021/Cr068445e

Lowry OH, Rosebrough NJ, Farr AL, Randall RJ (1951) Protein measurement with the Folin phenol reagent. J Biol Chem 193:265-275

Lunov O, Syrovets T, Loos C, Beil J, Delacher M, Tron K, Nienhaus GU, Musyanovych A, Mailander V, Landfester K, Simmet T (2011) Differential uptake of functionalized polystyrene nanoparticles by human macrophages and a monocytic cell line. ACS Nano 5:1657-1669. doi:10.1021/nn2000756

Luther EM, Koehler Y, Diendorf J, Epple M, Dringen R (2011) Accumulation of silver nanoparticles by cultured primary brain astrocytes. Nanotechnology 22:375101-375111. doi:10.1088/0957-4484/22/37/375101

Lynch I, Dawson KA (2008) Protein-nanoparticle interactions. Nano Today 3:40-47

Mahmoudi M, Hosseinkhani H, Hosseinkhani M, Boutry S, Simchi A, Journeay WS, Subramani K, Laurent S (2011) Magnetic resonance imaging tracking of stem cells in vivo using iron oxide nanoparticles as a tool for the advancement of clinical regenerative medicine. Chem Rev 111:253-280. doi:10.1021/cr1001832

Nel AE, Madler L, Velegol D, Xia T, Hoek EM, Somasundaran P, Klaessig F, Castranova V, Thompson M (2009) Understanding biophysicochemical interactions at the nano-bio interface. Nat Mater 8:543-557. doi:10.1038/nmat2442

Parpura V, Zorec R (2010) Gliotransmission: Exocytotic release from astrocytes. Brain Res Rev 63:83-92. doi:10.1016/j.brainresrev.2009.11.008

Petri-Fink A, Steitz B, Finka A, Salaklang J, Hofmann H (2008) Effect of cell media on polymer coated superparamagnetic iron oxide nanoparticles (SPIONs): Colloidal stability, cytotoxicity, and cellular uptake studies. Eur J Pharm Biopharm 68:129-137. doi:10.1016/j.ejpb.2007.02.024

Pickard MR, Jenkins SI, Koller CJ, Furness DN, Chari DM (2011) Magnetic nanoparticle labeling of astrocytes derived for neural transplantation. Tissue Eng Part C Methods 17:89-99. doi:10.1089/ten.TEC.2010.0170

Rejman J, Oberle V, Zuhorn IS, Hoekstra D (2004) Size-dependent internalization of particles via the pathways of clathrin- and caveolae-mediated endocytosis. Biochem J 377:159-169. doi:10.1042/BJ20031253

Riemer J, Hoepken HH, Czerwinska H, Robinson SR, Dringen R (2004) Colorimetric ferrozine-based assay for the quantitation of iron in cultured cells. Anal Biochem 331:370-375. doi:10.1016/j.ab.2004.03.049

Sofroniew MV, Vinters HV (2010) Astrocytes: biology and pathology. Acta Neuropathol 119:7-35. doi:10.1007/s00401-009-0619-8

Thiesen B, Jordan A (2008) Clinical applications of magnetic nanoparticles for hyperthermia. Int J Hyperther 24:467-474. doi:10.1080/02656730802104757

Valois CR, Braz JM, Nunes ES, Vinolo MA, Lima EC, Curi R, Kuebler WM, Azevedo RB (2010) The effect of DMSA-functionalized magnetic nanoparticles on transendothelial migration of monocytes in the murine lung via a β_2 integrin-dependent pathway. Biomaterials 31:366-374. doi:10.1016/j.biomaterials.2009.09.053

Wang J, Chen Y, Chen B, Ding J, Xia G, Gao C, Cheng J, Jin N, Zhou Y, Li X, Tang M, Wang XM (2010) Pharmacokinetic parameters and tissue distribution of magnetic Fe_3O_4 nanoparticles in mice. Int J Nanomedicine 5:861-866. doi:10.2147/IJN.S13662

Weinstein JS, Varallyay CG, Dosa E, Gahramanov S, Hamilton B, Rooney WD, Muldoon LL, Neuwelt EA (2010) Superparamagnetic iron oxide nanoparticles: diagnostic magnetic resonance imaging and potential therapeutic applications in neurooncology and central nervous system inflammatory pathologies, a review. J Cereb Blood Flow Metab 30:15-35. doi:10.1038/jcbfm.2009.192

Wilhelm C, Billotey C, Roger J, Pons JN, Bacri JC, Gazeau F (2003) Intracellular uptake of anionic superparamagnetic nanoparticles as a function of their surface coating. Biomaterials 24:1001-1011. doi:S0142961202004404

Wiogo HTR, Lim M, Bulmus V, Yun J, Amal R (2011) Stabilization of magnetic iron oxide nanoparticles in biological media by fetal bovine serum (FBS). Langmuir 27:843-850. doi:10.1021/La104278m

Yang H (2010) Nanoparticle-mediated brain-specific drug delivery, imaging, and diagnosis. Pharm Res 27:1759-1771. doi:10.1007/s11095-010-0141-7

Yang QQ, Liang JG, Han HY (2009) probing the interaction of magnetic iron oxide nanoparticles with bovine serum albumin by spectroscopic techniques. J Phys Chem B 113:10454-10458. doi:10.1021/Jp904004w

Yang X, Hong H, Grailer JJ, Rowland IJ, Javadi A, Hurley SA, Xiao Y, Yang Y, Zhang Y, Nickles RJ, Cai W, Steeber DA, Gong S (2011) cRGD-functionalized, DOX-conjugated, and ^{64}Cu-labeled superparamagnetic iron oxide nanoparticles for targeted anticancer drug delivery and PET/MR imaging. Biomaterials 32:4151-4160. doi:10.1016/j.biomaterials.2011.02.006

Yue ZG, Wei W, Lv PP, Yue H, Wang LY, Su ZG, Ma GH (2011) Surface charge affects cellular uptake and intracellular trafficking of chitosan-based nanoparticles. Biomacromolecules 12:2440-2446. doi:10.1021/bm101482r

2.6 Publication/Manuscript 6

Geppert, M., Hohnholt, M. C., Nürnberger, S. and Dringen, R. (2012) Ferritin upregulation and transient ROS production in cultured brain astrocytes after loading with iron oxide nanoparticles. *Submitted for publication*.

Contributions of M. Geppert:

- Performance of all experimental incubations
- Generation of data given in Table 1 and Figures 2 and 3
- Preparation of a first draft of the manuscript

M. C. Hohnholt obtained the data given in Figures 5 and 6 and prepared samples for electron microscopy. S. Nürnberger provided electron microscopical pictures given in Figures 1 and 4.

Publication/Manuscript 6

Ferritin upregulation and transient ROS production in cultured brain astrocytes after loading with iron oxide nanoparticles

Mark Geppert[1,2], Michaela C. Hohnholt[1,2], Sylvia Nürnberger[3,4] and Ralf Dringen[1,2]

[1]Centre for Biomolecular Interactions Bremen, University of Bremen, Bremen, Germany

[2]Centre for Environmental Research and Sustainable Technology, University of Bremen, Bremen, Germany

[3]Medical University of Vienna, Department of Traumatology, 1090 Vienna, Austria

[4]Ludwig Boltzmann Institute for Clinical and Experimental Traumatology, Austrian Cluster for Tissue Regeneration, 1200 Vienna, Austria

Email:
Mark Geppert: mgeppert@uni-bremen.de
Michaela C. Hohnholt: hohnholt@uni-bremen.de
Sylvia Nürnberger: sylvia.nuernberger@meduniwien.ac.at

Address correspondence to:
Dr. Ralf Dringen
Centre for Biomolecular Interactions Bremen
University of Bremen
P.O. Box 330440
28334 Bremen, Germany
Telephone: +49-421-21863230
Facsimile: +49-421-21863244
email: Ralf Dringen (ralf.dringen@uni-bremen.de)
homepage: http://www.fb2.uni-bremen.de/en/dringen

Abstract

To investigate the cellular consequences of a prolonged cellular presence of large amounts of iron oxide nanoparticles (IONPs) as well as the fate of such particles in brain cells, cultured primary astrocytes were loaded for 4 h with dimercaptosuccinate-coated IONPs. Subsequently, the IONP-treated cells were incubated for up to 7 d in IONP-free medium and the cell viability, metabolic parameters as well as the iron metabolism of the cells were investigated. Despite of an up to 100-fold elevated specific cellular iron content, IONP-loaded cells remained viable throughout the 7 d main incubation and did not show any substantial alteration in glucose and glutathione metabolism. During the incubation the high cellular iron content of IONP-loaded astrocytes remained almost constant. Electron microscopy revealed that after 7 d of incubation most of the cellular iron was still present in IONP-filled vesicles. However, the transient appearance of reactive oxygen species as well as a strong increase in cellular levels of the iron storage protein ferritin suggest that at least some low molecular weight iron was liberated from the accumulated IONPs. These results demonstrate that even the prolonged presence of large amounts of accumulated IONPs does not harm astrocytes and that these cells store IONP-derived iron in ferritin.

Key words:

brain; ferritin; glutathione; iron metabolism; oxidative stress

1.   Introduction

Due to their small size and their magnetic properties iron oxide nanoparticles (IONPs) are considered for a wide range of therapeutical and biological applications, for example as tool for magnetic hyperthermia, as contrast agent in magnetic resonance imaging (MRI), for cell labelling or for targeted drug delivery [1-6]. Also for neurobiological applications IONPs are considered as promising tool [7, 8]. Although IONPs have been shown to enter the brain by either crossing the blood-brain barrier [9] or by the olfactory neuronal pathway [10], little is currently known on the acute or chronic consequences of a presence of IONPs in brain cells. IONPs which have crossed the blood-brain barrier will encounter astrocytes as first parenchymal brain cells, since these cells cover with their endfeet almost completely the brain capillaries [11].

Astrocytes are of special interest regarding the uptake and metabolism of IONPs, since these cells are known to take up IONPs *in vivo* [12, 13] and *in vitro* [14-18] and since astrocytes are considered to play an important role in the iron homeostasis of the brain [19]. Astrocytes are the most abundant cell type in the brain [20] and have a variety of important functions in brain, including the supply of metabolic nutrients to neurons and the protection of the brain against metal toxicity and oxidative stress [21-23].

The acute consequences of an exposure of cultured astrocytes for a few hours to IONPs have recently been described. Primary viable astrocytes efficiently accumulate IONPs in a time-, concentration- and temperature-dependent manner [14-18]. Fluorescence and electron microscopy revealed that IONP-exposed astrocytes contain accumulated IONPs in intracellular vesicles, but showed also that substantial amounts of IONPs are attached extracellularly to the cell membrane [14-16, 18]. These observations as well as the reported reduction of IONP accumulation by endocytosis inhibitors [18] suggest that endocytotic processes are involved in the uptake of IONPs by astrocytes.

In brain, IONPs applied acutely for therapeutical and analytical purposes such as cancer treatment via hyperthermia [5, 24] or MRI [8] remain at the sites of instillation and are taken up by phagocytic cells and astrocytes where they are detectable at least for up to 7 d [12, 13]. Although molecular interactions of IONPs with cells and within cells have raised concerns for potential long-term effects of IONPs [25, 26] and of IONP-derived

iron [27, 28], the consequences of a prolonged presence of IONPs on metabolism and functions of brain cells have to our knowledge not been reported so far. To address such questions, we have loaded cultured astrocytes with IONPs and have subsequently monitored for a prolonged incubation of up to 7 d in IONP-free media the cell viability and several metabolic parameters including the iron metabolism.

IONP-loaded astrocytes which contained up to 100fold elevated specific iron contents compared to untreated cells remained viable during 7 d of incubation and contained large amounts of IONPs in intracellular vesicles. However, the transient increase in the production of reactive oxygen species (ROS) and the strong upregulation of the iron storage protein ferritin suggest that some iron was released from the vesicular IONPs into the cytosol. The data presented here demonstrate that cultured astrocytes cope very well even for a prolonged time with large amounts of intracellular IONPs that had been accumulated during a short bolus application of IONPs.

2.   Materials and Methods

2.1   Materials

Dulbecco's modified Eagle's medium (DMEM) was from Gibco (Karlsruhe, Germany). Fetal calf serum (FCS) and penicillin/streptomycin solution were obtained from Biochrom (Berlin, Germany). Bovine serum albumin and NADH were purchased from Applichem (Darmstadt, Germany). The goat anti-L-ferritin antibody and horseradish peroxidase-conjugated anti-goat-IgG were obtained from Dianova (Hamburg, Germany). All other chemicals of the highest purity available were obtained from Merck (Darmstadt, Germany), Sigma (Steinheim, Germany), Fluka (Buchs, Switzerland), or Riedel-de Haen (Seelze, Germany). 24-well cell culture plates were from Sarstedt (Nümbrecht, Germany), 96-well microtiter plates and 6 cm dishes from Nunc (Wiesbaden, Germany).

2.2   Iron oxide nanoparticles

Dimercaptosuccinic acid (DMSA)-coated magnetic iron oxide nanoparticles (IONPs) with a core-size of about 10 nm in diameter were synthesized in a wet chemical process and characterized as described earlier [14, 15]. Dispersed in incubation buffer (IB; 20 mM HEPES, 145 mM NaCl, 1.8 mM $CaCl_2$, 5.4 mM KCl, 1 mM $MgCl_2$, 5 mM glucose, adjusted to pH 7.4), DMSA-coated IONPs have an average hydrodynamic diameter of 60 nm and a zeta-potential of -26 mV [15]. The given concentrations of IONPs represent the concentrations of iron in the IONP-dispersion and not the concentration of particles.

2.3   Cell cultures and experimental incubation

Astrocyte-rich primary cultures were prepared from the brains of newborn Wistar rats according to a published method [29]. For Western blot experiments, 3 000 000 viable cells were seeded in 5 mL culture medium (90% DMEM, 10% FCS, 1 mM pyruvate, 20 U/mL penicillin G and 20 µg/mL streptomycin sulfate) in 6 cm dishes. For all other experiments, 300 000 viable cells were seeded in 1 mL culture medium in wells of 24-well dishes. For electron microscopy, the cells were seeded on Aclar film (EMS,

Hatfield, PA, USA) in wells of 24-well dishes. Cells were cultured at 37°C in a humidified atmosphere with 10% CO_2 in a cell incubator (Sanyo, Osaka, Japan) and the medium was renewed every 7th day. Experimental incubations were performed on cultures at an age between 15 and 21 days.

To load cells with IONPs, the cells were washed twice with 1 mL (24-well plates) or 5 mL (6 cm dishes) sterile filtered pre-warmed (37°C) IB, and than loaded for 4 h at 37°C in a humidified atmosphere of a CO_2-free incubator in 1 mL (24-well plates) or 5 mL (6 cm dishes) IB containing IONPs in the indicated concentrations. After 4 h of IONP-exposure, the incubation media were collected, the cells were washed twice with 1 mL (24-well plates) or 5 mL (6 cm dishes) culture medium and subsequently incubated in culture medium for further 20 h (1 d), 68 h (3 d) or 164 h (7 d). At the indicated time-points, the incubation media were collected and the cells were washed twice with ice-cold phosphate-buffered saline (PBS: 10 mM potassium phosphate buffer, containing 150 mM NaCl, pH 7.4) for analysis of cellular compounds.

2.4   Determination of cell viability and protein content

Cell viability was assessed by determining the activity of lactate dehydrogenase (LDH) and the cellular accumulation of Neutral Red (NR). Cellular and extracellular LDH activities were determined as previously described [30] and extracellular LDH activities were expressed as percentage of total (cellular + extracellular) LDH activity. NR accumulation was measured as recently described [31] and is expressed as percent of the specific initial NR uptake. Cellular protein contents were determined according to the Lowry method [32] using bovine serum albumin as a standard.

2.5   Determination of iron, glutathione and lactate contents

Iron contents of cells and media samples were quantified using a ferrozine-based iron assay [33] which was slightly modified for the quantification of iron from IONPs [14]. Total cellular glutathione (GSx = amount of glutathione (GSH) plus twice the amount of glutathione disulfide (GSSG)) and GSSG contents were determined using the colorimetric Tietze method [34] which was adapted to microtiter plates [35]. For all

conditions investigated here, the cellular GSSG content remained in the range of the detection limit of the assay used. Extracellular lactate contents were measured as previously described [36, 37] with the modification that 5 µL of media samples were used for determination.

2.6   Staining for reactive oxygen species

Intracellular reactive oxygen species were detected by a modification of a recently published method [38]. Briefly, after the experimental incubation cells were washed twice with IB at 37°C and subsequently incubated in 0.5 mL IB containing 5 µg/mL dihydrorhodamine 123 for 30 min at 37°C. Subsequently, the cells were washed twice with IB and fixed with 4% (w/v) paraformaldehyde in 0.1 M potassium phosphate buffer (pH 7.2). After washing three times with PBS, the cells were analyzed for fluorescence using a Nikon (Düsseldorf, Germany) TS2000U microscope.

2.7   Western blotting and transmission electron microscopy (TEM)

The cellular content of the ferritin protein was determined by Western blotting as described recently [38]. Briefly, cells incubated on 6 cm dishes were scraped off and centrifuged for 1 min at 12 000g. The cell pellet was lysed in water and 40 µg lysate protein was separated on a 12.5% polyacrylamide gel and subsequently electroblotted to a nitrocellulose membrane. The membranes were incubated overnight at 4°C with goat anti-L-ferritin antibody (1:500) in TBST (10 mM Tris-HCl, 150 mM NaCl, 0.1% (w/v) Tween 20, pH 7.3) containing 5% (w/v) milk powder. After washing three times with TBST, the membrane was exposed to horseradish peroxidase-conjugated anti-goat-IgG (1:10 000) diluted in TBST/5% milk powder for 1 h at room temperature. The membranes were washed three times with TBST and protein bands were visualized by enhanced chemiluminescence (GE Healthcare, Buckinghamshire, UK).

The intracellular presence of IONPs was investigated by transmission electron microscopy (TEM) as published previously [15]. After the indicated experimental incubation of cells grown on Aclar film, the cells were washed twice with 1 mL PBS, fixed with 2.5% glutaraldehyde in 0.1 M sodium cacodylate buffer pH 7.3 for 1 h at

room temperature, washed trice with cacodylate buffer and postfixed with 1% (w/v) osmium tetroxide in cacodylate buffer for 2 h at room temperature. Dehydration was accomplished by incubation of the cells in solutions of increasing ethanol concentrations (up to 100%) followed by an incubation in acetonitrile. Finally, the cells were embedded in the low viscosity resin (Agar Scientific, Stansted, United Kingdom) and sliced with a microtome (Ultracut UCT, Leica, Germany). After staining of the slices with uranyl acetate and lead citrate, they were analyzed using a FEI Morgagni electron microscope (Eindhoven, Netherlands) operated at 80 kV.

2.8   Presentation of data

The data given in the figures and the table represent means ± standard deviations (SD) of values from at least three independent experiments that were performed on independently prepared cultures. Figures showing cell staining and Western blots are from representative experiments. Statistical analysis between groups of data was carried out using ANOVA with the Dunnett's *post hoc* test.

3.   Results

3.1   Loading of astrocytes with IONPs

To load cultured astrocytes with IONPs the cultures were exposed for 4 h to IONPs in concentrations of up to 4 mM iron. During the loading phase, the viability of the cells was not compromised as indicated by the absence of any significant increase in the extracellular LDH activity and by the absence of any significant loss of protein (Table 1). Also metabolic parameters such as he NR accumulation and the specific lactate production by the cells during exposure to IONPs for 4 h were not significantly altered, while the specific GSx values were lowered in a concentration-dependent manner in IONP-treated cells by up to 25% for cells exposed to 4 mM IONPs (Table 1). However, IONP-treatment did not increase the specific content of the GSH oxidation product GSSG in the cells (Table 1).

Exposure of astrocytes for 4 h to IONPs caused a concentration-dependent significant increase in the total and in the specific cellular iron contents (Table 1). The specific iron contents increased from 18 ± 3 nmol/mg to 366 ± 90 nmol/mg, 1086 ± 101 nmol/mg and 1507 ± 137 nmol/mg after application of 0.25 mM, 1 mM and 4 mM iron as IONPs, respectively (Table 1). TEM images of cells that had been exposed for 4 h to 4 mM IONPs (Fig. 1) revealed that in the cells electron-dense IONPs were almost exclusively found in vesicles localized close to the cell membrane (Fig. 1A,B). Most of these vesicles were partly filled (Fig. 1B,C) and only a few were densely filled (Fig. 1C,D) with IONP aggregates. High magnification revealed that the size of the individual particles was quite regular and most of them had diameters between 8 and 14 nm (Fig. 1D). In addition to intracellular IONPs, electron-dense particles were attached to the surface of the cells either as individual particles or as particle aggregates (Fig. 1A,B) and were found in the space between cells (Fig. 1A) or between the cell processes (Fig. 1C).

After loading astrocytes for 4 h with IONPs, the cells were washed and subsequently incubated for up to 7 d in IONP-free culture medium. The following result paragraphs compare data obtained for IONP-loaded cells with those obtained for control cells that had been incubated during the loading phase without IONPs.

3.2   Viability of cells

The viability of astrocytes that had been loaded with IONPs in concentrations of up to 4 mM was not substantially compromised during the main incubation (Fig. 2). Only after 7 d of incubation, the extracellular LDH activity was slightly but significantly elevated in cells treated with 1 mM or 4 mM IONPs compared to control cells (Fig. 2A). This was accompanied by a small but not significant increase in the total protein contents per well of cultures that had been treated with 1 mM or 4 mM IONPs (Fig. 2B). Furthermore, the ability of IONP-treated cells to accumulate NR (Fig. 2C) and to produce and release lactate (Fig. 2D) was not altered compared to control cells.

3.3   IONPs and iron in cells and media

Loading of astrocytes with 0.25 mM, 1 mM and 4 mM iron as IONPs resulted in specific cellular iron levels that were elevated compared to that of control cells by 20-fold, 60-fold and 100-fold, respectively (Table 1). These cellular iron contents remained almost constant during the 7 d main incubation period (Fig. 3A). Compared to the initial values, only cells loaded with 1 mM or 4 mM IONPs showed a small but not significant ($p>0.05$) drop in the cellular iron content after the first day of incubation that was accompanied by a small significant ($p<0.05$) increase in the extracellular iron content (Fig. 3B). In contrast, no further alterations in cellular and extracellular iron contents were observed for IONP-treated cultures during incubation for more than 1 d (Fig. 3A,B).

TEM analysis of astrocytes that had been loaded with 4 mM IONPs and were subsequently incubated for 7 d revealed that, in contrast to cells that had been fixed directly after the loading with IONPs (Fig. 1), electron-dense IONPs were not detectable anymore extracellularly attached to the cell membrane, but were exclusively localized in densely packed vesicular structures (Fig. 4). The vesicular aggregates of IONPs had an irregular shape and contained some cell debris that was deposited between the particles (Fig. 4B,C). The size of the individual IONPs was regular (Fig. 4D) and did not differ from that found for intracellular IONPs directly after loading of the cells with IONPs (Fig. 1D).

3.4   Glutathione content and ROS production

Treatment of the cells with IONPs led to small but significant concentration-dependent loss in cellular GSx (Table 1). After application of culture medium to IONP-loaded cells, the GSx contents increased within 1 d to up to 60 nmol/mg, which was even higher than the initial GSx content of the cells (Fig. 3C). During longer incubation the specific cellular GSx contents declined to less than 30 nmol/mg during 7 d (Fig. 3C), but the GSx contents of the IONP-treated cultures did not differ from that of control cells (loading period without IONPs) (Fig. 3C). For all conditions and time points investigated, the specific cellular GSSG content remained lower than 2 nmol GSx/mg (Fig. 3D).

Since cellular liberation of iron from accumulated IONPs can lead to enhanced ROS formation [39, 40], the occurrence of ROS was investigated for IONP-treated astrocytes by using the rhodamine 123 staining (Fig. 5). Control cells (loading period without IONPs) showed only low staining intensity for ROS during incubation of up to 7 d (Fig. 5A-D). In contrast, a transient increase of the rhodamine 123 fluorescence signal was found for cells loaded with IONPs (Fig. 5E) which became even more prominent 1 d after exposure to the IONPs (Fig. 5F). However, 3 d or 7 d after the IONP-loading, no obvious difference in rhodamine 123 staining intensity was observed anymore between control cells (Fig. 5C,D) and cells that had been loaded with IONPs (Fig. 5G,H).

3.5   Ferritin content of IONP-treated astrocytes

Incubation of cultured astrocytes with low molecular weight iron induces the synthesis of the iron storage protein ferritin [41]. Since ferritin synthesis requires the presence of an excess of low molecular weight iron in cells [42], an increase in cellular ferritin levels in IONP-treated cells is considered as evidence that iron is liberated from accumulated IONPs [38]. Therefore, ferritin levels were investigated by Western blotting of the proteins in cell homogenates of control cells and of cells that had been loaded with IONPs and were subsequently incubated for up to 7 d (Fig. 6). Hardly any signal for ferritin was observed for untreated astrocyte cultures (0 h) and for control cells that had not been exposed to IONPs (Fig. 6). In contrast, a strong ferritin signal

was observed for IONP-treated astrocytes already 1 d after exposure to IONPs and the signal was even further intensified after incubation for 3 d or 7 d (Fig. 6).
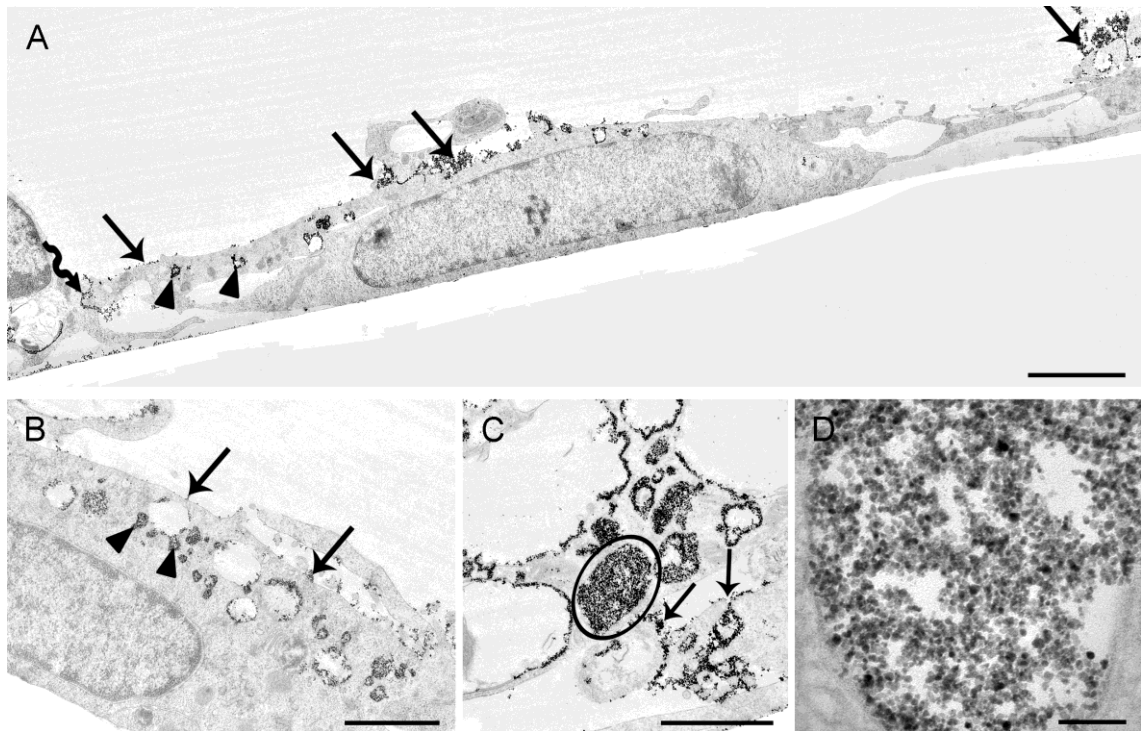
Figure 1: TEM images of cultured astrocytes after loading IONPs for 4 h. A: Cross section through the cell-monolayer shows IONPs on the cellular surface (arrows), between cells (curved arrow) and in cells (arrowheads). B: Image of a cell containing many vesicles with IONP aggregates. In some cases smaller vesicles seem to have fused (arrowheads). IONPs are also present on the surface of the cell membrane (arrows). C: Detail image of a cell containing large, almost empty and smaller densely packed (circle) vesicles. Note the IONPs between the cell processes of one or several cells (arrows). D shows the densely IONP-packed vesicles in high magnification. The scale bars represent 5 (A), 1 (B,C) and 0.1 (D) µm.
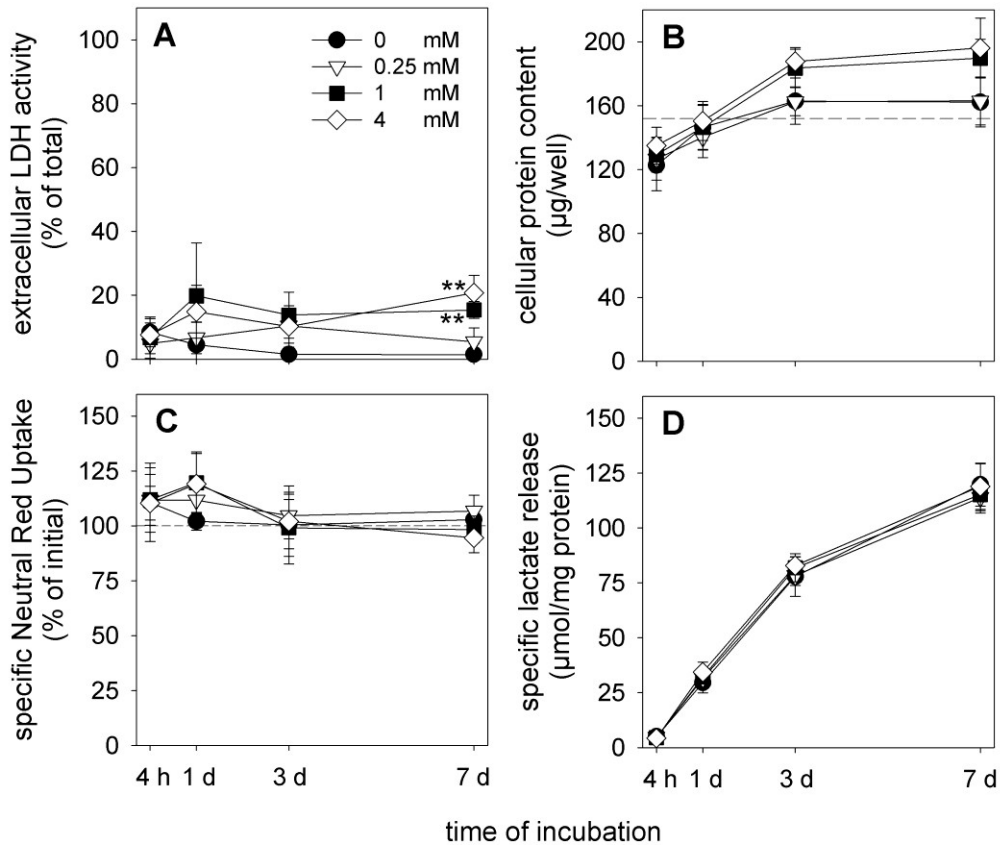
Figure 2: Effects of IONPs on cell viability and lactate production by astrocytes.
The cells were loaded for 4 h with IONPs in the indicated (A) concentrations and then incubated in culture medium for up to 7 d. The extracellular LDH activity (A), the cellular protein content (B), the NR accumulation (C) and the lactate production (D) were determined. The initial values of protein content and NR accumulation are given in Table 1 and are indicated by the dashed lines in B and C. Stars show the significance of differences compared to values obtained for controls (0 mM IONPs) with **$p<0.01$.
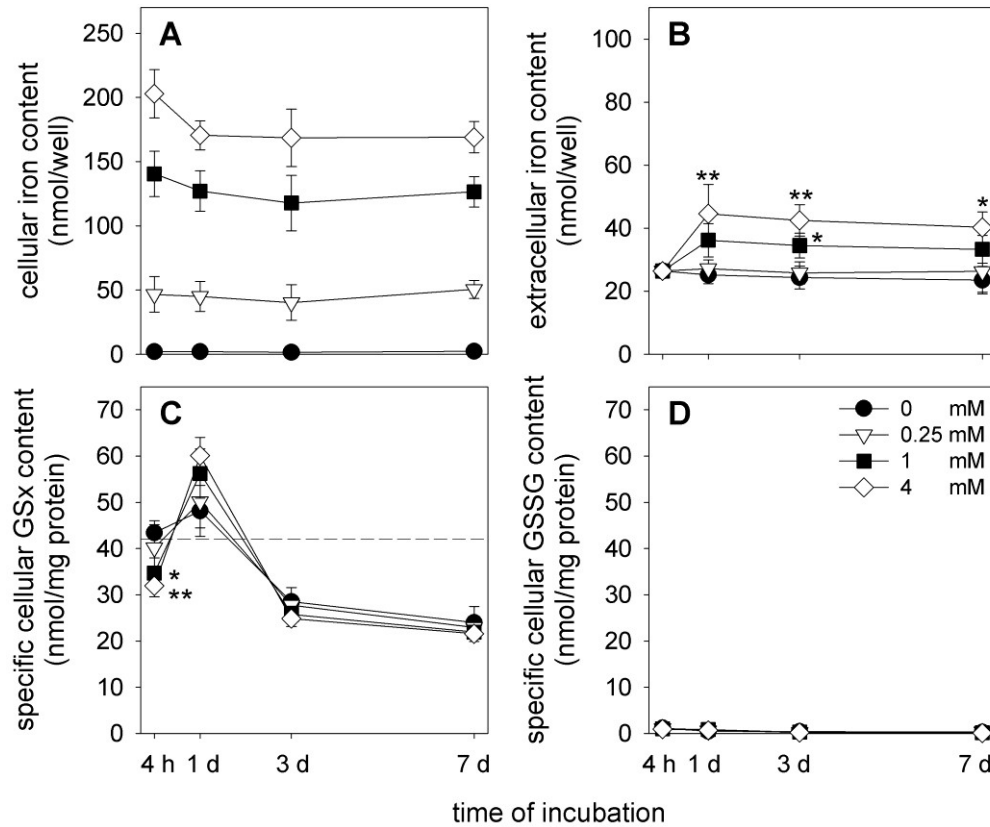
Figure 3: Effects of IONPs on the contents of iron and glutathione in astrocytes.
The cells were loaded for 4 h with IONPs in the concentrations indicated (D) and then incubated in culture medium for up to 7 d. The cellular iron content (A), the extracellular iron content (B), the cellular GSx content (C) and the cellular GSSG content (D) were determined. Iron values are given as nmol per well (A,B), GSx and GSSG contents as specific values normalized on the cellular protein content as nmol/mg. The initial value for the specific cellular GSx content is given in Table 1 and is indicated by the dashed line in C. Stars indicate the significance of differences compared to controls (0 mM IONPs) with *$p<0.05$ and **$p<0.01$.
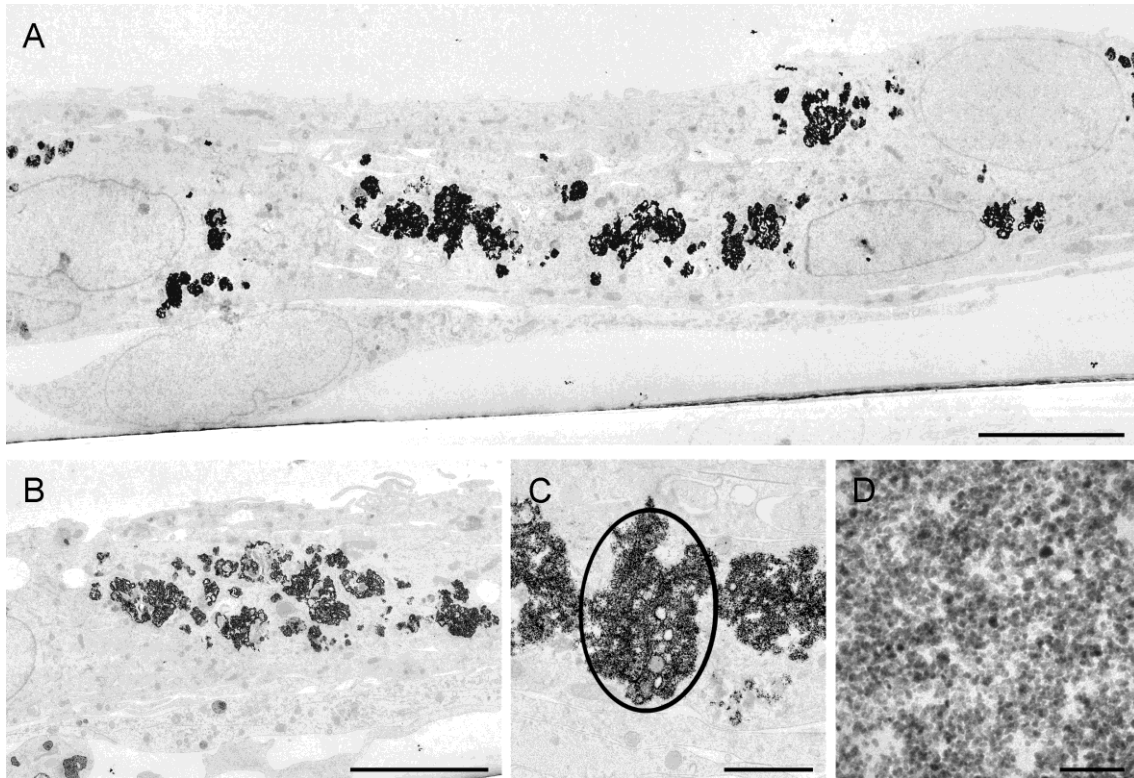
Figure 4: TEM images of cultured astrocytes 7 d after loading with IONPs. A: Cross section through the cell shows that IONPs are not anymore detectable on the cell surface but are exclusively accumulated in intracellular vesicles. B: Astrocyte containing many vesicles densely filled with IONPs and some cell debris. C: Detailed images of a densely packed vesicle with irregular outline (circle). D: High resolution image of the IONPs inside the vesicles. The scale bars represent 5 (A, B), 1 (C) and 0.1 (D) μm.

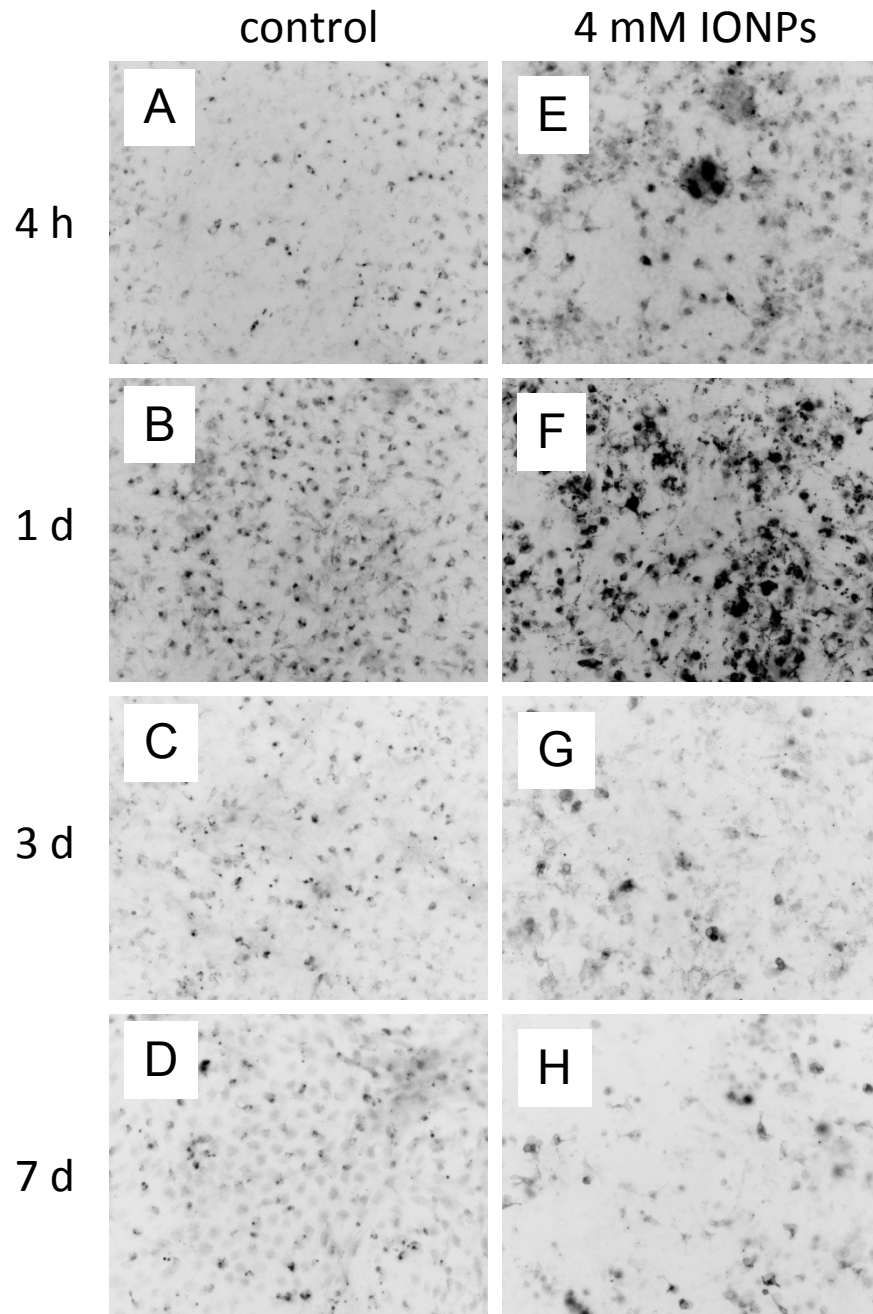control   4 mM IONPs

Figure 5: ROS-staining of cultured astrocytes after exposure to IONPs. The cells were loaded for 4 h without (control) or with 4 mM IONPs and then further incubated without IONPs in culture medium for up to 7 d.
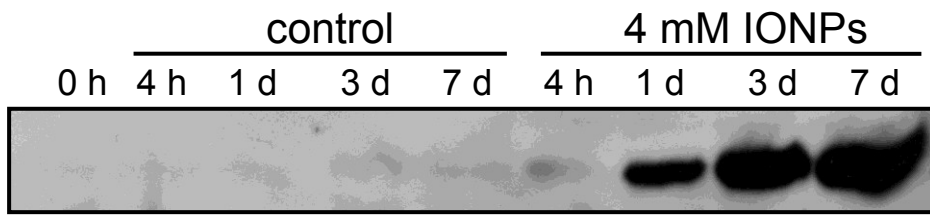
Figure 6: Western blot for the iron storage protein ferritin. The cells were loaded for 4 h without (control) or with 4 mM IONPs and then incubated without IONPs in culture medium for up to 7 d. Cell lysates containing 40 µg protein were loaded to each lane, separated by electrophoresis and analyzed for ferritin content by Western blotting.

Table 1: Short-time effects of IONPs on the viability, the iron content and the metabolism of cultured astrocytes.

Investigated parameter	Initial	Control (0 mM)	After 4 h incubation with IONPs		
			0.25 mM	1 mM	4 mM
Extracellular LDH activity (% of total)	–	8 ± 4	5 ± 3	7 ± 6	8 ± 4
Cellular protein content (µg/well)	152 ± 12	123 ± 16	127 ± 13	129 ± 11	135 ± 11
Specific Neutral Red accumulation (% of initial)	100 ± 9	111 ± 18	112 ± 15	112 ± 12	110 ± 8
Cellular iron content (nmol/well)	2 ± 0	2 ± 0	47 ± 14**,#	141 ± 18**,##	203 ± 19**,##
Specific cellular iron content (nmol/mg)	16 ± 3	18 ± 3	366 ± 90**,##	1086 ± 101**,##	1507 ± 137**,##
Specific extracellular lactate content (µmol/mg)	–	5.0 ± 1.0	4.8 ± 0.7	4.4 ± 1.0	4.3 ± 1.1
Specific cellular GSx content (nmol/mg)	43 ± 2	43 ± 3	40 ± 5	35 ± 3*,#	32 ± 2**,##
Specific cellular GSSG content (nmol/mg)	0.6 ± 0.3	1.2 ± 0.6	1.0 ± 0.6	1.0 ± 0.8	0.9 ± 0.4

The cells were incubated for 4 h with IONPs in the indicated concentrations. Indicated are the significances of differences of data compared to the initial values (*$p<0.05$; **$p<0.01$) or to control values (#$p<0.05$; ##$p<0.01$).

4.   Discussion

To investigate long-time consequences of a short exposure of cultured astrocytes to IONPs, the cells were loaded for 4 h with DMSA-coated IONPs. This treatment increased the specific cellular iron content by up to 100-fold, but did not compromise cell viability. Also basal metabolic parameters such as the accumulation of NR and the production of lactate by the cells were not altered during exposure to IONPs, demonstrating a remarkable resistance of cultured astrocytes towards any acute toxicity of IONPs. TEM revealed that a substantial amount of cell-associated IONPs had been taken up into the cells within the 4 h loading period but that another part of the IONPs were attached extracellularly to the cells. These data are consistent with the recently reported membrane adsorption and efficient internalization of IONPs by viable cultured astrocytes [15, 17].

Treatment of cultured astrocytes with 1 mM or 4 mM IONPs caused a small but significant reduction in cellular GSH contents, as previously reported also for MRC-5 cells [43] and OLN-93 cells [40] and. This loss of up to 25% of the cellular GSH after IONP-treatment of astrocytes is likely to be mediated by conjugation of GSH to the DMSA-coat of the IONPs, since only DMSA-coated IONPs, but not citrate-coated IONPs, lower the GSH content of OLN-93 cells [40]. The ability of DMSA-coated IONPs to directly react with GSH is also supported by the disappearance of detectable GSH, but not of GSSG, in cell-free incubations with DMSA-IONPs (data not shown), strongly suggesting that the thiol group of GSH reacts with the disulfide bridges that stabilize the DMSA-coat [44, 45] of the IONPs used in our study. The small loss in cellular GSH levels after IONP-loading of astrocytes was fully compensated by synthesis of GSH during a subsequent incubation in the amino acid-containing culture medium, demonstrating that cellular presence of IONPs does not prevent GSH synthesis.

Presence of up to a 100-fold elevated cellular iron content of IONP-treated astrocytes did not compromise cell viability during a subsequent prolonged incubation for up to 7 d, as indicated by the low activity of extracellular LDH and by the absence of any loss in cellular protein. Also cellular processes such as NR accumulation or glycolytic

lactate production were not altered in IONP-containing cells, contrasting for example the situation reported for astrocytes that were treated with copper [31].

Exposure of cultured astrocytes to IONPs induced ROS formation in astrocytes, as recently reported for other types of neural cells [40, 46]. The generation of ROS is likely to be a result of the iron-catalyzed Fenton reaction, which can either occur on the surface of IONPs [25, 47] or is catalyzed by iron liberated from accumulated IONPs [27]. The elevated ROS production in IONP-treated astrocytes was transient and most prominent 1 d after IONP-loading, but completely disappeared after incubation for 3 d or 7 d. A likely reason for this observation is the strong upregulation of ferritin synthesis in IONP-loaded astrocytes, which will sequester IONP-derived low molecular weight iron and store it in redox-inactive form, thereby preventing iron-mediated ROS formation [41]. Despite of the transient elevated ROS production, the viability of IONP-containing astrocytes was not substantially compromised nor were cellular GSSG levels increased, suggesting that IONP-treated astrocytes do not suffer from severe oxidative stress. This contrasts the situation of astrocytes that encounter oxidative stress due to the presence of metal ions or hydrogen peroxide [41, 48-50].

The high resistance of astrocytes against IONP-mediated toxicity, contrasts literature reports that show severe toxicity of MRC-5 lung fibroblasts [43] or PC12 cells [51] after exposure to IONPs. However, a high resistance against metal- and nanoparticle-induced toxicity [15, 50, 52, 53] appears to be a special feature of astrocytes that is consistent with the proposed function of this cell type as regulator of metal metabolism in brain [19, 23]. Molecular mechanisms that could contribute to a high resistance of astrocytes against metal- and nanoparticle-induced toxicity include the upregulation of metal storage and binding proteins such as ferritin [41, 54] or metallothioneins [55, 56] and the endocytotic uptake of nanoparticles into vesicular compartments [15, 18, 53].

After loading of cultured astrocytes with IONPs, the cellular iron content remained almost constant. Only during the first day of incubation a low increase in the amounts of extracellular iron was found for cells treated with high concentrations of IONPs, which may be the consequence of desorption of some of the membrane-adsorbed IONPs that were visible in the TEM pictures of IONP-treated cultures after 4 h. Membrane-

adsorbed IONPs represent around 50% of the cell-associated iron determined directly after loading of astrocytes with IONPs [15], but the total cellular (internalised and membrane-attached) iron content was only lowered by around 10% during the first day of incubation and remained constant during further incubation. Cell-attached electron-dense material was not detected anymore after 7 d of incubation, suggesting that the majority of the membrane-associated IONPs observed by TEM for acutely loaded astrocytes had been internalized. After 7 d of incubation the cellular IONPs were densely packed in large vesicles, but no obvious alteration in the size of the individual particles was found. Some of the IONP-containing vesicles observed in the cells may be lysosomes, since the low pH of these organelles has been discussed to contribute to the liberation of iron from accumulated IONPs [27].

The presence of large IONP aggregates in astrocytes 7 d after exposure to the particles suggests that a large part of the accumulated IONPs remain deposited as electron-dense IONP-aggregates in cellular vesicles. However, the upregulation of ferritin in IONP-treated astrocytes demonstrates that some iron was liberated from the accumulated IONPs into the cytosol, since this processes requires the presence of low molecular weight iron [38, 40, 42, 57]. The relative stability of IONP-aggregates in vesicles as well as the strong upregulation of ferritin are likely reasons for the high resistance of astrocytes against potential IONP-toxicity. Slow release of iron from accumulated IONPs as well as effective storage of IONP-derived iron in ferritin explains also the absence of any substantial iron release from IONP-containing astrocytes during prolonged incubation, although this cell type is known to have the capacity to release low molecular weight iron [58].

5. Conclusions

The data presented demonstrate that the presence of large iron contents in astrocytes that had been exposed for a short time to IONPs does not compromise cell viability and metabolism during a subsequent prolonged incubation. Although IONPs were found densely packed in intracellular vesicles after 7 d of incubation, some iron was also liberated from the accumulated IONPs, at least in amounts that induced a strong

upregulation of ferritin in astrocytes. These data suggest that vesicular deposition of accumulated IONPs as well as efficient storage of IONP-derived low molecular weight iron in ferritin contribute to the resistance of astrocytes against potential toxicity of IONP-derived iron. Such processes are likely to enable also astrocytes in brain, which are known to take up IONPs after a bolus application for therapeutical or diagnostic reason [12, 13], to deal successfully with accumulated IONPs and with its iron content for a prolonged time.

Acknowledgements

References

[1] Amstad E, Textor M, Reimhult E. Stabilization and functionalization of iron oxide nanoparticles for biomedical applications. Nanoscale 2011;3:2819-43.

[2] Chertok B, Moffat BA, David AE, Yu FQ, Bergemann C, Ross BD, et al. Iron oxide nanoparticles as a drug delivery vehicle for MRI monitored magnetic targeting of brain tumors. Biomaterials 2008;29:487-96.

[3] Huang SH, Juang RS. Biochemical and biomedical applications of multifunctional magnetic nanoparticles: a review. J Nanopart Res 2011;13:4411-30.

[4] Mahmoudi M, Stroeve P, Milani AS, Arbab AS. Superparamagnetic iron oxide nanoparticles: synthesis, surface engineering, cytotoxicity and biomedical applications. New York: Nova Science Publishers, Inc.; 2011.

[5] Maier-Hauff K, Ulrich F, Nestler D, Niehoff H, Wust P, Thiesen B, et al. Efficacy and safety of intratumoral thermotherapy using magnetic iron-oxide nanoparticles

combined with external beam radiotherapy on patients with recurrent glioblastoma multiforme. J Neurooncol 2011;103:317-24.

[6] Yang X, Hong H, Grailer JJ, Rowland IJ, Javadi A, Hurley SA, et al. cRGD-functionalized, DOX-conjugated, and (64)Cu-labeled superparamagnetic iron oxide nanoparticles for targeted anticancer drug delivery and PET/MR imaging. Biomaterials 2011;32:4151-60.

[7] Weinstein JS, Varallyay CG, Dosa E, Gahramanov S, Hamilton B, Rooney WD, et al. Superparamagnetic iron oxide nanoparticles: diagnostic magnetic resonance imaging and potential therapeutic applications in neurooncology and central nervous system inflammatory pathologies, a review. J Cereb Blood Flow Metab 2010;30:15-35.

[8] Winer JL, Kim PE, Law M, Liu CY, Apuzzo ML. Visualizing the future: enhancing neuroimaging with nanotechnology. World Neurosurg 2011;75:626-37.

[9] Wang J, Chen Y, Chen B, Ding J, Xia G, Gao C, et al. Pharmacokinetic parameters and tissue distribution of magnetic Fe_3O_4 nanoparticles in mice. Int J Nanomedicine 2010;5:861-6.

[10] Kwon JT, Hwang SK, Jin H, Kim DS, Minai-Tehrani A, Yoon HJ, et al. Body distribution of inhaled fluorescent magnetic nanoparticles in the mice. Journal of occupational health 2008;50:1-6.

[11] Mathiisen TM, Lehre KP, Danbolt NC, Ottersen OP. The perivascular astroglial sheath provides a complete covering of the brain microvessels: an electron microscopic 3D reconstruction. Glia 2010;58:1094-103.

[12] van Landeghem FK, Maier-Hauff K, Jordan A, Hoffmann KT, Gneveckow U, Scholz R, et al. Post-mortem studies in glioblastoma patients treated with thermotherapy using magnetic nanoparticles. Biomaterials 2009;30:52-7.

[13] Murillo TP, Sandquist C, Jacobs PM, Nesbit G, Manninger S, Neuwelt EA. Imaging brain tumors with ferumoxtran-10, a nanoparticle magnetic resonance contrast agent. Therapy 2005;2:871-82.

[14] Geppert M, Hohnholt M, Gaetjen L, Grunwald I, Bäumer M, Dringen R. Accumulation of iron oxide nanoparticles by cultured brain astrocytes. J Biomed Nanotechnol 2009;5:285-93.

[15] Geppert M, Hohnholt MC, Thiel K, Nürnberger S, Grunwald I, Rezwan K, et al. Uptake of dimercaptosuccinate-coated magnetic iron oxide nanoparticles by cultured brain astrocytes. Nanotechnology 2011;22:145101.

[16] Hohnholt MC, Geppert M, Nürnberger S, von Byern J, Grunwald I, Dringen R. Advanced Biomaterials: Accumulation of citrate-coated magnetic iron oxide nanoparticles by cultured brain astrocytes. Adv Eng Mater 2010;12:B690-B4.

[17] Lamkowsky MC, Geppert M, Schmidt MM, Dringen R. Magnetic field-induced acceleration of the accumulation of magnetic iron oxide nanoparticles by cultured brain astrocytes. J Biomed Mater Res A 2012;100:323-34.

[18] Pickard MR, Jenkins SI, Koller CJ, Furness DN, Chari DM. Magnetic nanoparticle labeling of astrocytes derived for neural transplantation. Tissue Eng Part C Methods 2011;17:89-99.

[19] Dringen R, Bishop GM, Koeppe M, Dang TN, Robinson SR. The pivotal role of astrocytes in the metabolism of iron in the brain. Neurochem Res 2007;32:1884-90.

[20] Sofroniew MV, Vinters HV. Astrocytes: biology and pathology. Acta Neuropathol 2010;119:7-35.

[21] Hirrlinger J, Dringen R. The cytosolic redox state of astrocytes: Maintenance, regulation and functional implications for metabolite trafficking. Brain Res Rev 2010;63:177-88.

[22] Parpura V, Heneka MT, Montana V, Oliet SH, Schousboe A, Haydon PG, et al. Glial cells in (patho)physiology. J Neurochem 2012:*in press*.

[23] Tiffany-Castiglioni E, Hong S, Qian Y. Copper handling by astrocytes: Insights into neurodegenerative diseases. Int J Dev Neurosci 2011;29:811-8.

[24] Thiesen B, Jordan A. Clinical applications of magnetic nanoparticles for hyperthermia. Int J Hyperther 2008;24:467-74.

[25] Nel A, Xia T, Madler L, Li N. Toxic potential of materials at the nanolevel. Science 2006;311:622-7.

[26] Winer JL, Liu CY, Apuzzo ML. The Use of Nanoparticles as Contrast Media in Neuroimaging: A Statement on Toxicity. World Neurosurg 2011:*in press*.

[27] Levy M, Lagarde F, Maraloiu VA, Blanchin MG, Gendron F, Wilhelm C, et al. Degradability of superparamagnetic nanoparticles in a model of intracellular environment: follow-up of magnetic, structural and chemical properties. Nanotechnology 2010;21:395103.

[28] Levy M, Luciani N, Alloyeau D, Elgrabli D, Deveaux V, Pechoux C, et al. Long term in vivo biotransformation of iron oxide nanoparticles. Biomaterials 2011;32:3988-99.

[29] Hamprecht B, Löffler F. Primary glial cultures as a model for studying hormone action. Methods Enzymol 1985;109:341-5.

[30] Dringen R, Kussmaul L, Hamprecht B. Detoxification of exogenous hydrogen peroxide and organic hydroperoxides by cultured astroglial cells assessed by microtiter plate assay. Brain Res Brain Res Protoc 1998;2:223-8.

[31] Scheiber IF, Dringen R. Copper accelerates glycolytic flux in cultured astrocytes. Neurochem Res 2011;36:894-903.

[32] Lowry OH, Rosebrough NJ, Farr AL, Randall RJ. Protein measurement with the Folin phenol reagent. J Biol Chem 1951;193:265-75.

[33] Riemer J, Hoepken HH, Czerwinska H, Robinson SR, Dringen R. Colorimetric ferrozine-based assay for the quantitation of iron in cultured cells. Anal Biochem 2004;331:370-5.

[34] Tietze F. Enzymic method for quantitative determination of nanogram amounts of total and oxidized glutathione: applications to mammalian blood and other tissues. Anal Biochem 1969;27:502-22.

[35] Dringen R, Hamprecht B. Glutathione content as an indicator for the presence of metabolic pathways of amino acids in astroglial cultures. J Neurochem 1996;67:1375-82.

[36] Dringen R, Gebhardt R, Hamprecht B. Glycogen in astrocytes: possible function as lactate supply for neighboring cells. Brain Res 1993;623:208-14.

[37] Schmidt MM, Dringen R. Differential effects of iodoacetamide and iodoacetate on glycolysis and glutathione metabolism of cultured astrocytes. Front Neuroenergetics 2009;1:1-10.

[38] Hohnholt MC, Geppert M, Dringen R. Treatment with iron oxide nanoparticles induces ferritin synthesis but not oxidative stress in oligodendroglial cells. Acta Biomater 2011;7:3946-54.

[39] Buyukhatipoglu K, Clyne AM. Superparamagnetic iron oxide nanoparticles change endothelial cell morphology and mechanics via reactive oxygen species formation. J Biomed Mater Res A 2011;96:186-95.

[40] Hohnholt MC, Dringen R. Iron-dependent formation of reative oxygen species and glutathione depletion after accumulation of magnetic iron oxide nanoparticles by oligodendroglial cells. J Nanopart Res 2011;13:6761-74.

[41] Hoepken HH, Korten T, Robinson SR, Dringen R. Iron accumulation, iron-mediated toxicity and altered levels of ferritin and transferrin receptor in cultured

astrocytes during incubation with ferric ammonium citrate. J Neurochem 2004;88:1194-202.

[42] Arosio P, Ingrassia R, Cavadini P. Ferritins: a family of molecules for iron storage, antioxidation and more. Biochim Biophys Acta 2009;1790:589-99.

[43] Radu M, Munteanu MC, Petrache S, Serban AI, Dinu D, Hermenean A, et al. Depletion of intracellular glutathione and increased lipid peroxidation mediate cytotoxicity of hematite nanoparticles in MRC-5 cells. Acta biochimica Polonica 2010;57:355-60.

[44] Fauconnier N, Pons JN, Roger J, Bee A. Thiolation of maghemite nanoparticles by dimercaptosuccinic acid. J Colloid Interface Sci 1997;194:427-33.

[45] Valois CR, Braz JM, Nunes ES, Vinolo MA, Lima EC, Curi R, et al. The effect of DMSA-functionalized magnetic nanoparticles on transendothelial migration of monocytes in the murine lung via a β_2 integrin-dependent pathway. Biomaterials 2010;31:366-74.

[46] Soenen SJ, Himmelreich U, Nuytten N, De Cuyper M. Cytotoxic effects of iron oxide nanoparticles and implications for safety in cell labelling. Biomaterials 2011;32:195-205.

[47] Voinov MA, Sosa Pagan JO, Morrison E, Smirnova TI, Smirnov AI. Surface-mediated production of hydroxyl radicals as a mechanism of iron oxide nanoparticle biotoxicity. J Am Chem Soc 2011;133:35-41.

[48] Bishop GM, Dringen R, Robinson SR. Zinc stimulates the production of toxic reactive oxygen species (ROS) and inhibits glutathione reductase in astrocytes. Free Radic Biol Med 2007;42:1222-30.

[49] Liddell JR, Zwingmann C, Schmidt MM, Thiessen A, Leibfritz D, Robinson SR, et al. Sustained hydrogen peroxide stress decreases lactate production by cultured astrocytes. J Neurosci Res 2009;87:2696-708.

[50] Scheiber IF, Schmidt MM, Dringen R. Zinc prevents the copper-induced damage of cultured astrocytes. Neurochem Int 2010;57:314-22.

[51] Pisanic TR, 2nd, Blackwell JD, Shubayev VI, Finones RR, Jin S. Nanotoxicity of iron oxide nanoparticle internalization in growing neurons. Biomaterials 2007;28:2572-81.

[52] Tulpule K, Robinson SR, Bishop GM, Dringen R. Uptake of ferrous iron by cultured rat astrocytes. J Neurosci Res 2010;88:563-71.

[53] Luther EM, Koehler Y, Diendorf J, Epple M, Dringen R. Accumulation of silver nanoparticles by cultured primary brain astrocytes. Nanotechnology 2011;22:375101.

[54] Dang TN, Bishop GM, Dringen R, Robinson SR. The metabolism and toxicity of hemin in astrocytes. Glia 2011;59:1540-50.

[55] Aschner M, Cherian MG, Klaassen CD, Palmiter RD, Erickson JC, Bush AI. Metallothioneins in brain – the role in physiology and pathology. Toxicol Appl Pharmacol 1997;142:229-42.

[56] Lee SJ, Koh JY. Roles of zinc and metallothionein-3 in oxidative stress-induced lysosomal dysfunction, cell death, and autophagy in neurons and astrocytes. Mol brain 2010;3:30.

[57] Pawelczyk E, Arbab AS, Pandit S, Hu E, Frank JA. Expression of transferrin receptor and ferritin following ferumoxides-protamine sulfate labeling of cells: implications for cellular magnetic resonance imaging. NMR Biomed 2006;19:581-92.

[58] Jeong SY, David S. Glycosylphosphatidylinositol-anchored ceruloplasmin is required for iron efflux from cells in the central nervous system. J Biol Chem 2003;278:27144-8.

Part 3

Summarizing discussion

3.   Summarizing discussion

Magnetic iron oxide nanoparticles (IONPs) are considered for a wide range of therapeutical and diagnostic applications in the brain (Yang 2010, Winer *et al.* 2011, Yigit *et al.* 2012). Such particles are able to cross the blood-brain barrier (Wang *et al.* 2010) or can enter the brain via the olfactory neuronal pathway (Kwon *et al.* 2008). IONPs which have been injected into the brain are taken up by macrophages and astrocytes and remain at the site of injection for at least 7 d (Murillo *et al.* 2005, van Landeghem *et al.* 2009). However, data about the effects of IONPs on brain cells are limited so far.

This thesis investigated the effects of IONPs on cultured brain astrocytes as a model system for astrocytes in the brain. Viable cultured astrocytes accumulated large amounts of citrate- or dimercaptosuccinate (DMSA)-coated IONPs and stored them in intracellular vesicles. The uptake rates of IONPs depended strongly on the experimental incubation conditions, such as time, temperature, IONP-concentration, composition of the incubation medium and the presence of external magnetic fields. For none of the conditions investigated, the presence of extracellular or intracellular IONPs compromised cell viability or altered metabolic parameters. However, a transient formation of reactive oxygen species (ROS) and a strong upregulation of the iron storage protein ferritin suggest that low molecular weight iron is liberated in astrocytes from accumulated IONPs.

3.1   Iron oxide nanoparticles

3.1.1 Synthesis and coating

IONPs were synthesized according to a previously published method (Bee *et al.* 1995) which was slightly modified (Geppert 2008). The resulting magnetic fluid contained polydisperse IONPs with a mean diameter of 8 nm as observed by transmission electron microscopy (TEM), which is consistent with literature data (Bee *et al.* 1995). The used synthesis method for IONPs showed a good reproducibility regarding size, shape and

the iron content of the resulting IONP-dispersions. In a total number of nine experiments, the average yield of the synthesis was 71 ± 12% regarding the total iron content of the dispersion.

IONPs were coated either with citric acid or with DMSA to stabilize them in the incubation buffers used for cell-experiments. Both compounds have been described in the literature as suitable for stabilization of IONPs in biological media (Fauconnier *et al.* 1997, Racuciu *et al.* 2006). Since citrate-coated IONPs were only stable in incubation buffer in presence of a high excess of citrate (Publications 1 and 2) which at least in millimolar concentrations is likely to affect cellular functions (Westergaard *et al.* 1994), the majority of the studies of this thesis were undertaken using DMSA-coated IONPs. These IONPs were extensively characterized regarding their core-size, elemental composition, hydrodynamic size distribution and surface charge.

3.1.2 Characterization

DMSA-coated IONPs contain a core of iron oxide which is surrounded by a shell of DMSA molecules that are cross-linked via disulfide bridges and thus form a cage-like structure around the core (Fauconnier *et al.* 1997, Valois *et al.* 2010). The presence of the DMSA-coating of the here used IONPs was confirmed by the detection of sulfur via energy dispersive X-ray spectroscopy (EDX), since DMSA was the only sulfur-containing compound present during the IONP-preparation (Publication 3).

Dispersed in water, uncoated IONPs as well as citrate- or DMSA-coated IONPs had an average hydrodynamic diameter of about 60 nm as determined by dynamic light scattering (DLS). This large increase in particle size compared to the results obtained by TEM demonstrates that the IONPs form small agglomerates in dispersion probably due to magnetostatic interactions (Chantrell *et al.* 1982, Maity & Agrawal 2007).

The uncoated IONPs dispersed in water had an acidic pH-value and a positive zeta-potential as expected due to their positive surface charge that is caused by protonated hydroxyl groups at the surface of IONPs (Cheng *et al.* 2005). Thus, IONPs are stabilized in water by electrostatic repulsive forces between equally charges particles

(Laurent *et al.* 2008). After dispersion in incubation buffer at a physiological pH-value, the surface hydroxyl groups are deprotonated and thus loose their positive charges. These uncharged particles are not electrostatically stabilized anymore and rapidly aggregate and precipitate at physiological pH. In contrast, DMSA-coated IONPs have a negative zeta-potential at physiological pH due to the negatively charged carboxylate groups of the coating material, thereby maintaining the stabilization via electrostatic repulsive forces and keeping the particles dispersed in physiological incubation buffers.

Fetal calf serum (FCS) is often added as supplement for cell culture media and has been described to stabilize IONPs (Wiogo *et al.* 2011). However, presence of 10% FCS or other proteins such as bovine serum albumin (BSA) or ovalbumin in the incubation buffer lead to a 2-3 fold increase of the hydrodynamic diameter of dispersed DMSA-coated IONPs and to a positivation of their zeta-potential. This can be explained by binding of such proteins to the IONP surface forming a protein-corona as previously described (Lynch & Dawson 2008, Nel *et al.* 2009, Wiogo *et al.* 2011). A similar increase of the hydrodynamic IONP-diameter was observed for IONPs after incubation with cultured astrocytes in incubation buffer (Publication 3) or in astrocyte preconditioned medium (Chatterjee 2011). This effect was concentration dependent (stronger increase in IONP-size at lower IONP-concentrations) but independent of the presence or absence of FCS in the incubation buffer (Publication 3; Publication/Manuscript 5). These observations suggest that substances released by the astrocytes into the medium are causing IONP-agglomeration. Indeed, serine protease 40, a protein that is released from cultured astrocytes, has been identified to be bound on the IONP surface (Chatterjee 2011).

3.2 Uptake and biocompatibility of iron oxide nanoparticles in cultured astrocytes

Citrate- and DMSA-coated IONPs were used to study the uptake and biocompatibility of IONPs in cultured astrocytes. However, since DMSA seemed to be the better surface coating-material as it allowed to obtain stable IONPs in the absence of any free coating-material, only initial studies were performed for citrate-coated IONPs and most of the studies were carried out with DMSA-coated IONPs. Uptake of IONPs was quantified by

measuring the total cellular iron content and visualized by Perl's staining and electron microscopy. Acute effects of IONPs on cultured astrocytes were studied during an exposure of the cells to IONPs for up to 6 h. In addition, long term consequences of the cellular presence of IONPs were investigated for up to 7 d after loading of the cells for 4 h with IONPs.

3.2.1 Quantification of the iron accumulation

Only very recently was demonstrated that cultured astrocytes are able to take up IONPs (Ding *et al.* 2010, Pickard & Chari 2010, Pickard *et al.* 2011, Yiu *et al.* 2011). However, the first detailed quantitative analysis of the iron accumulation by cultured astrocytes from IONPs is provided by the publications and manuscripts of the present thesis. Details are given in the individual chapters of this thesis. A summary on the consequences of alterations of experimental incubation parameters on the cellular iron accumulation is given in Table 3.1.

Table 3.1: Modulation of the accumulation of IONPs in cultured astrocytes

Changed experimental parameter	Cellular iron content		n
	(nmol/mg)	**(% of control)**	
Control (4 h, 1 mM DMSA-IONPs, 37°C)	1375 ± 260	100 ± 19	28
Elongation of incubation time to 6 h	2151 ± 198	156 ± 14	6
Increase of IONP concentration to 4 mM	2209 ± 385	161 ± 28	10
Lowering incubation temperature to 4°C	726 ± 214	53 ± 16	19
Addition of 10% FCS	182 ± 24	13 ± 2	9
Application of an external magnetic field	4411 ± 1062	321 ± 77	6
Use of citrate-coated IONPs	1507 ± 142	110 ± 10	6

The table shows how the indicated alterations of the experimental conditions affect the cellular iron content of IONP-exposed astrocytes. Basis for the calculation are the data given in the publications/manuscripts in the chapters 2.2 to 2.6 of this thesis. Iron contents were given as specific values normalized on the cellular protein content and as percentage of the control. A 4 h incubation of astrocytes with 1 mM DMSA-coated IONPs at 37°C is defined as control condition.

Cultured astrocytes effectively accumulated both, citrate- and DMSA-coated IONPs as shown by a strong increase in the cellular iron content exceeding the initial iron content by more than 100-fold. The cellular iron contents of IONP-treated astrocytes were even five to ten times higher than the cellular iron contents resulting from incubation with low molecular weight ferric ammonium citrate (FAC) (Hoepken *et al.* 2004, Riemer *et al.* 2004, Tulpule *et al.* 2010, Bishop *et al.* 2011). However, for none of the conditions applied, any acute loss in cell viability was observed, indicating that astrocytes are remarkably resistant to IONPs and are able to safely store these large amounts of accumulated iron.

The accumulation of citrate-coated IONPs did not significantly differ to the accumulation of DMSA-coated IONPs by astrocytes under otherwise identical experimental conditions. This was expected since both types of IONPs have almost identical core sizes, hydrodynamic diameters and negative surface charges (Publications 2, 3) (Bee *et al.* 1995, Fauconnier *et al.* 1997). TEM revealed that this increase in iron content of IONP-treated astrocytes is a result of uptake and membrane association of IONPs or IONP-aggregates (Publication 3). Lowering the incubation temperature to 4°C lowered the iron accumulation to around 50% of the amount obtained at 37°C. For the 4°C condition, only extracellular membrane bound IONPs/IONP-aggregates were observed by TEM (Publication 3), as expected, since membrane transport processes are strongly reduced at 4°C (Kim *et al.* 2006, Wilhelm & Gazeau 2008). Thus, ΔFe-values that represent the difference between cellular iron contents obtained at 37°C and 4°C give the amount of iron internalized due to IONP-uptake. It should be kept in mind that the ΔFe represents only about 50% of the iron content observed at 37°C for all experiments performed to investigate IONP-accumulation. The second half of the specific iron content represents extracellularly adsorbed IONPs.

In addition to a temperature dependency, IONP-accumulation was time and concentration dependent. Over time, no maximal IONP-accumulation was observed for the conditions investigated in this thesis. However, cellular iron contents were only determined for up to 6 h incubation of astrocytes with IONPs, since long incubations of the cells with IONPs in incubation buffer for 24 h compromise cell viability (data not shown). The concentration dependency of IONP-accumulation showed a saturation in

IONP-uptake for high concentrations. This saturation was observed for incubations at 37°C and 4°C, indicating that IONP-uptake and membrane association are saturable processes. Analysis of the IONP internalization (ΔFe-values) after 4 h for DMSA-IONP-concentrations of up to 4 mM revealed a Michaelis-Menten like kinetic with apparent K_M- and V_{max}-values of 2.1 ± 0.6 mM and 1871 ± 231 nmol iron/(mg × 4 h), respectively (Publication 3). This represents the first description of kinetic parameters of IONP-uptake into cells.

IONP-uptake was strongly enhanced in the presence of an external magnetic field that was generated by positioning NdFeB-magnets underneath the cells. The observed cellular iron contents at 37°C and 4°C increased by about 3-fold compared to the respective conditions without magnets, demonstrating that both the IONP-internalization and the membrane association of IONPs were increased due to the magnetic field. This leads to even more cellular iron than expected from the saturation found in the concentration dependency of IONP-accumulation by astrocytes. Potential reason for this observation could be the formation and accumulation of larger IONP-aggregates in the magnetic field (Chantrell *et al.* 1982). Such an increase in IONP-accumulation was previously described for various cell lines (Petri-Fink & Hofmann 2007, Prijic *et al.* 2010) and also for magnetic-nanoparticle mediated gene-transfer in astrocytes (Pickard & Chari 2010). However, a detailed time-, concentration- and temperature-dependent analysis of magnetic-field induced IONP-uptake in astrocytes was first described in the context of this thesis (Publication 4).

Presence of FCS in the incubation buffer led to a strong reduction in IONP-uptake in cultured astrocytes. Proteins of FCS are likely to bind to the surface of the IONPs (Wiogo *et al.* 2011) forming a so-called protein corona (Nel *et al.* 2009) around DMSA-IONPs. This results in an increase in particle size and in a positivation of their zeta-potential (Publication/Manuscript 5) which is likely to influence the interactions between the IONPs and the cell membranes and subsequently results in reduction in IONP-uptake. The strong effect of presence of serum or other proteins on IONP-uptake into brain cells was shown for the first time in this thesis. However, effects of serum on the uptake of different types of IONPs by various cell lines have been previously reported. Depending on the cell-type, the medium and the type of IONPs used, presence

of serum either decreased or increased IONP-uptake (Chen *et al.* 2008, Petri-Fink *et al.* 2008).

3.2.2 Mechanisms of particle uptake

IONPs which have been taken up by astrocytes were found to be incorporated in intracellular vesicles as shown by TEM (Publications 2,3). This strongly suggests the involvement of endocytotic pathways in IONP-uptake. Astrocytes in culture are known to have an active endocytotic system and to express proteins involved in different endocytotic pathways (Megias *et al.* 2000). However, because of the large number of different endocytotic pathways (Kumari *et al.* 2010, Platta & Stenmark 2011, Sandvig *et al.* 2011) the identification of the pathways involved in IONP-uptake in cultured astrocytes is quite complicated. In this context, it has to be noted that the specificity of substances that have been described to modulate and inhibit these pathways (Rejman *et al.* 2004, Huth *et al.* 2006, Dausend *et al.* 2008, Greulich *et al.* 2011, Luther *et al.* 2011, Pickard *et al.* 2011) is a matter of debate (Ivanov 2008).

For serum-containing conditions, macropinocytosis and clathrin-mediated endocytosis appear to contribute to IONP-uptake into cultured astrocytes (Publication/Manuscript 5; Figure 3.1). This confirms data reported by Pickard and colleagues who incubated astrocytes with larger (0.20-0.39 µm) carboxyl-modified fluorescent IONPs (Pickard *et al.* 2011). However, macropinocytosis and clathrin-mediated endocytosis seem not to be the only pathways involved in IONP-uptake in astrocytes since the ΔFe-values of the inhibitory conditions are still higher than the 4°C control which represents extracellular bound IONPs. In contrast, for serum-free conditions none of the inhibitors applied lead to a significant reduction in cellular iron content of IONP-treated astrocytes (Publication 4; Publication/Manuscript 5) suggesting that especially IONPs coated by serum-proteins but not DMSA-IONPs are taken up by macropinocytosis and clathrin-mediated endocytosis into astrocytes. Since incubation of cultured astrocytes with DMSA-IONPs in serum-free buffer lead to an about 8 times higher cellular iron content, a highly effective pathway has to be responsible for IONP-uptake under serum-free conditions which remains to be identified. Figure 3.1 shows the mechanisms which may be responsible for IONP-uptake in cultured astrocytes.
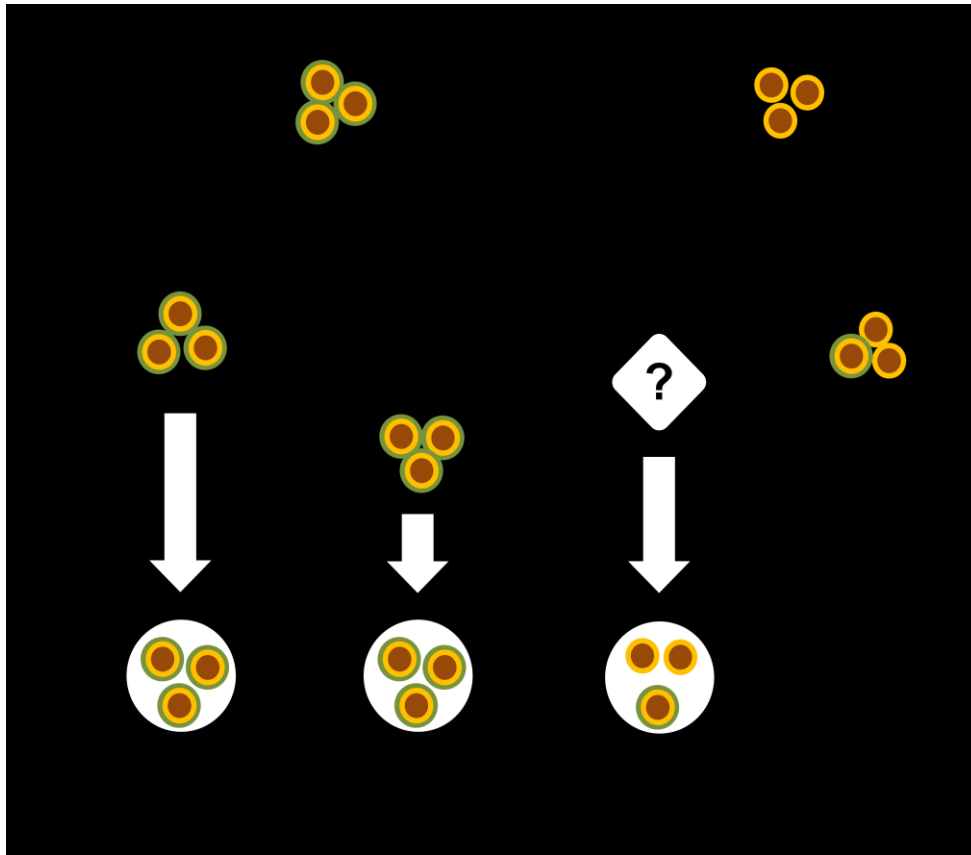
Figure 3.1: Mechanisms of IONP-uptake into cultured astrocytes. Substantial amounts of IONPs will attach extracellularly to the cell membrane. Cultured astrocytes take up IONPs in serum containing medium by macropinocytosis and by clathrin-mediated endocytosis. In addition, another unknown pathway is likely to be involved in particle uptake. For serum-free conditions, the uptake-mechanism could not be identified so far.

3.2.3 Consequences of a prolonged presence of particles

IONPs, which are applied for diagnostic or therapeutic reasons into the brain will be accumulated by macrophages and astrocytes and remain there for at least 7 d (Murillo *et al.* 2005, van Landeghem *et al.* 2009). However, data about the long term consequences of the presence of IONPs in brain cells have not been reported so far. This thesis presents an analysis of the metabolic effects of a prolonged presence of large amounts of IONPs following a bolus application to cultured astrocytes. This experimental paradigm is considered as a model-system for studying the consequences of cellular presence of IONPs and for the fate of IONPs in brain cells.

The experimental setup composed of a 4 h loading phase of astrocytes with up to 4 mM IONPs in incubation buffer and a subsequent up to 7 d main incubation in culture medium. These conditions did neither compromise the cell viability, nor affect glycolytic lactate production or the cellular glutathione/glutathione disulfide (GSH/GSSG)-ratio (Publication/Manuscript 6). Only a slight decrease of cellular GSx after the loading phase was observed, which is a likely result of conjugate formation between GSH and the DMSA-coating since citrate-coated IONPs did not cause such an effect (Hohnholt & Dringen 2011). A summary of the pathways involved in handling of intracellular IONPs by astrocytes is given in Figure 3.2.
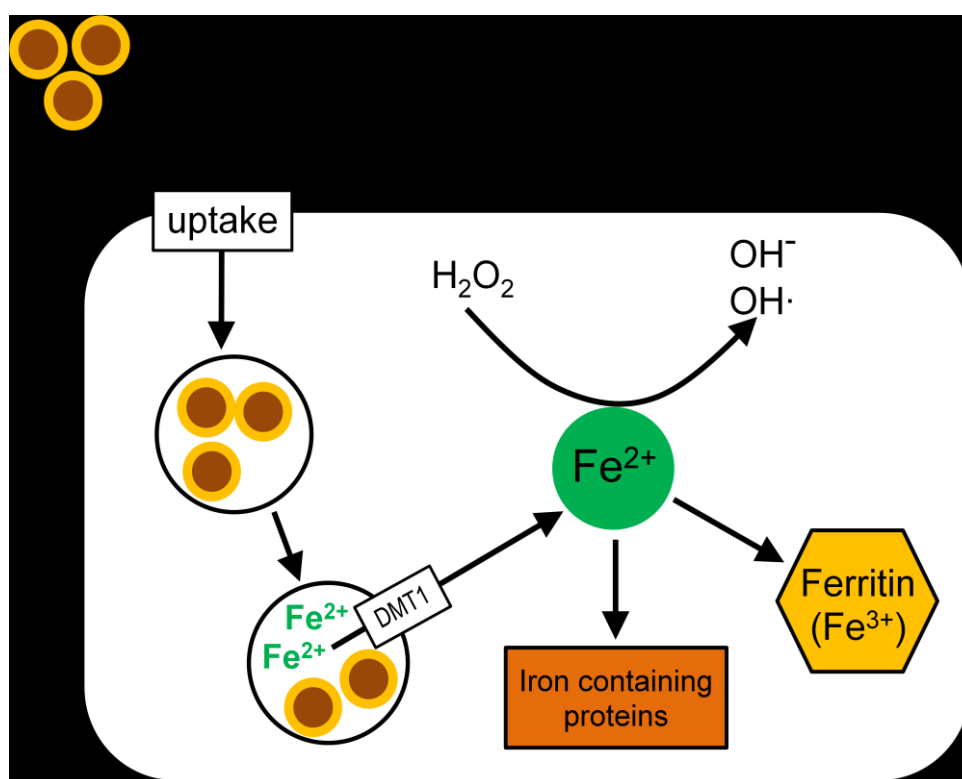

Figure 3.2: Cellular fate considered for IONPs in cultured astrocytes. After uptake, the nanoparticles may be directed to the lysosomes. Due to the acidic pH low molecular weight iron is liberated from the IONPs which is than exported into the cytosol via the divalent metal transporter 1 (DMT1). Here it enters the labile iron pool and can either induce the formation of hydroxyl radicals, be stored as ferric iron in ferritin or be incorporated in iron containing proteins.

After the 4 h loading-phase of cultured astrocytes with IONPs, a large amount of cellular IONPs was decorating the cell membrane, while 7 d after the loading IONPs were exclusively detected in intracellular vesicles (Publication/Manuscript 6). This

suggests that membrane associated IONPs were incorporated during this time frame. A significant export of iron or IONPs was not detectable during 7 d, underlining the role of astrocytes to function as metal depots (Tiffany-Castiglioni & Qian 2001, Dringen *et al.* 2007, Tiffany-Castiglioni *et al.* 2011). IONPs and/or their containing iron seemed to be stored safely in the astrocytes even though it is known, that cultured astrocytes express the iron exporter ferroportin (Wu *et al.* 2004, Dringen *et al.* 2007, Garrick & Garrick 2009).

Presence of IONPs led to a transient formation of ROS and to a delayed upregulation of the iron storage protein ferritin in cultured astrocytes. While ROS are likely to be generated by the Fenton reaction either on the surface of IONPs (Voinov *et al.* 2011) or due to the liberation of low molecular weight ferrous iron from the particles (Levy *et al.* 2010), ferritin upregulation requires intracellular low molecular iron (Arosio *et al.* 2009). Therefore, at least the upregulation of ferritin indicates liberation of low molecular weight iron from the IONPs in the cells. Such a liberation may occur in the lysosomes since their acidic pH is likely to foster IONP-degradation (Levy *et al.* 2010). Ferrous iron is than exported into the cytosol via the divalent metal transporter 1 (DMT1) which is expressed in cultured astrocytes (Burdo *et al.* 2001, Tulpule *et al.* 2010), where it is entering the labile iron pool. Here it can be stored in ferritin (as ferric iron), induce ROS-generation or it can even be used for cell metabolism, for example for proliferation as recently published for OLN93-cells (Hohnholt *et al.* 2010, Hohnholt *et al.* 2011). Nevertheless, it has to be mentioned that for the time frame investigated only a small amount of the total internalized particles appears to have been degraded to low molecular weight iron, since TEM-pictures showed vesicles densely packed with IONPs 7 days after loading. Furthermore, a complete dissolution of the IONPs uptaken by the cells would lead to an intracellular iron concentration of 526 ± 92 mM (4 h incubation with 4 mM IONPs at 37°C), which would rapidly induce osmotic cell death.

3.3   Conclusions and future perspectives

This thesis investigated the synthesis and characterization of citrate- and DMSA-coated IONPs as tools for studying uptake, reactivity and biocompatibility of IONPs in brain cells. The cells in astrocyte-rich primary cultures efficiently took up citrate- and

DMSA-coated IONPs without any acute loss in their viability. Even prolonged presence of IONPs in the cells did neither compromise cell viability nor substantially alter cellular metabolism. However, a transient formation of ROS and a strong upregulation of ferritin indicate liberation of low molecular weight iron from accumulated IONPs. In summary, the results of this thesis suggest that IONPs at least for the conditions investigated can be considered as save tool for biomedical and clinical applications and could even be a useful and safe iron source.

IONPs were taken up and stored in intracellular vesicles. In further studies, a detailed analysis of the subcellular localization of the particles in cells should be done. Such questions could be addressed by fractioning of cells via differential and density gradient centrifugation (Aronson & Touster 1974, Ozols 1990, Tedelind *et al.* 2010) after incubation with IONPs and quantifying the iron content of the different fractions. However, it has been shown that such a cell-fractionation is complicated due to the high density of the IONPs (Petters 2010). More detailed information about the subcellular fate of the IONPs could be gained by immunogold labeling of the vesicles combined with electron microscopy (Mayhew 2011). Furthermore, the use of fluorescent IONPs will simplify studying the intracellular fate of such particles. DMSA-coated fluorescent IONPs were successfully synthesized (Kaltz 2011) and at least are taken up by cultured OLN93-cells (Bulcke 2012).

The mechanism of IONP-uptake – especially under serum-free conditions – is another unsolved aspect of this thesis. Additional experiments with other types of endocytosis inhibitors under varying experimental conditions could help to reveal these yet unknown pathways. A potential reason for the unclear results of the inhibitor studies could be that the large size distributions of the IONP-dispersions address several endocytotic mechanisms. These may contribute together to the IONP-uptake, since it is known that endocytotic uptake mechanisms strongly depend on the particle size (Rejman *et al.* 2004). In addition, the use of fluorescently labeled IONPs could help to address the unsolved questions for the IONP-uptake mechanism(s).

IONPs accumulated by cultured astrocytes liberate iron which is intracellularly stored in ferritin as shown by Western Blotting. However, ferritin molecules were not detected

via TEM. Such an electron microscopic detection of ferritin has been shown (Lopez-Castro *et al.* 2011) and could be an additional prove for the release of low molecular weight iron from the IONPs in astrocytes. Furthermore, immunocytochemical detection of cellular ferritin could be undertaken in future. A better quantification of the ratio of intracellular IONPs, low molecular weight iron and ferritin will be an important task for further studies. One method to quantify intracellular low molecular weight iron could be the use of fluorescent dyes like Phen Green^{TM} or calcein (Kakhlon & Cabantchik 2002, Petrat *et al.* 2002).

The purity of the used cultures is another important task that should be considered for future studies. The here used astrocyte-rich primary cultures contain mainly, but not exclusively, astrocytes. Small amounts of oligodendrocyte precursor cells, ependymal and microglia cells which are present in these cultures (Reinhart *et al.* 1990, Gutterer *et al.* 1999, Dang *et al.* 2010) are able to also contribute to the observed IONP-uptake. The use of secondary cultures could be a possibility to obtain purer astrocyte-cultures that hardly contain any other type of cells. In addition, studies on the uptake of IONPs in cultures enriched in oligodendrocytes, ependymal cells or microglia will give estimates on how efficient these cell-types take up IONPs.

Since IONPs were already clinical used in the brain, *in vivo* studies will be a key issue to address the fate of such particles in the brain. A recent report by Wang and colleagues investigated the distribution and clearance of IONPs infused into the rat striatum (Wang *et al.* 2011) with the result that dextran-coated IONPs freely diffuse through the interstitial space of the brain and were cleared from the site of infusion in about 2 weeks. Detailed analysis of the metabolic effects of such particles on the different types of brain cells are not given so far and represent thus a big challenge for future investigations of consequences of the presence of IONPs in the brain.

3.4   References

Aronson, N. N., Jr. and Touster, O. (1974) Isolation of rat liver plasma membrane fragments in isotonic sucrose. *Methods Enzymol,* **31,** 90-102.

Arosio, P., Ingrassia, R. and Cavadini, P. (2009) Ferritins: a family of molecules for iron storage, antioxidation and more. *Biochim Biophys Acta,* **1790,** 589-599.

Bee, A., Massart, R. and Neveu, S. (1995) Synthesis of very fine maghemite particles. *J Magn Magn Mater,* **149,** 6-9.

Bishop, G. M., Dang, T. N., Dringen, R. and Robinson, S. R. (2011) Accumulation of non-transferrin-bound iron by neurons, astrocytes, and microglia. *Neurotox Res,* **19,** 443-451.

Bulcke, F. (2012) *Characterization and accumulation of fluorescent iron oxide nanoparticles by oligodendroglial cells*, Master Thesis, University of Bremen.

Burdo, J. R., Menzies, S. L., Simpson, I. A., Garrick, L. M., Garrick, M. D., Dolan, K. G., Haile, D. J., Beard, J. L. and Connor, J. R. (2001) Distribution of divalent metal transporter 1 and metal transport protein 1 in the normal and Belgrade rat. *J Neurosci Res,* **66,** 1198-1207.

Chantrell, R. W., Bradbury, A., Popplewell, J. and Charles, S. W. (1982) Agglomerate formation in a magnetic fluid. *J Appl Phys,* **53,** 2742-2744.

Chatterjee, A. (2011) *Interactions between iron oxide nanoparticles and proteins released by astrocytes*, Master Thesis, University of Bremen.

Chen, Z. P., Zhang, Y., Xu, K., Xu, R. Z., Liu, J. W. and Gu, N. (2008) Stability of hydrophilic magnetic nanoparticles under biologically relevant conditions. *J Nanosci Nanotechnol,* **8,** 6260-6265.

Cheng, F. Y., Su, C. H., Yang, Y. S., Yeh, C. S., Tsai, C. Y., Wu, C. L., Wu, M. T. and Shieh, D. B. (2005) Characterization of aqueous dispersions of Fe_3O_4 nanoparticles and their biomedical applications. *Biomaterials,* **26,** 729-738.

Dang, T. N., Bishop, G. M., Dringen, R. and Robinson, S. R. (2010) The putative heme transporter HCP1 is expressed in cultured astrocytes and contributes to the uptake of hemin. *Glia,* **58,** 55-65.

Dausend, J., Musyanovych, A., Dass, M., Walther, P., Schrezenmeier, H., Landfester, K. and Mailander, V. (2008) Uptake mechanism of oppositely charged fluorescent nanoparticles in HeLa cells. *Macromol Biosci,* **8,** 1135-1143.

Ding, J., Tao, K., Li, J., Song, S. and Sun, K. (2010) Cell-specific cytotoxicity of dextran-stabilized magnetite nanoparticles. *Colloids Surf B Biointerfaces,* **79,** 184-190.

Dringen, R., Bishop, G. M., Koeppe, M., Dang, T. N. and Robinson, S. R. (2007) The pivotal role of astrocytes in the metabolism of iron in the brain. *Neurochem Res,* **32,** 1884-1890.

Fauconnier, N., Pons, J. N., Roger, J. and Bee, A. (1997) Thiolation of maghemite nanoparticles by dimercaptosuccinic acid. *J Colloid Interface Sci,* **194,** 427-433.

Garrick, M. D. and Garrick, L. M. (2009) Cellular iron transport. *Biochim Biophys Acta,* **1790,** 309-325.

Geppert, M. (2008) *Synthese und Charakterisierung von Eisenoxid-Nanopartikeln und Untersuchung ihrer Biokompatibilität an Zellkulturen*, Diploma Thesis, University of Bremen.

Greulich, C., Diendorf, J., Simon, T., Eggeler, G., Epple, M. and Koller, M. (2011) Uptake and intracellular distribution of silver nanoparticles in human mesenchymal stem cells. *Acta Biomater,* **7,** 347-354.

Gutterer, J. M., Dringen, R., Hirrlinger, J. and Hamprecht, B. (1999) Purification of glutathione reductase from bovine brain, generation of an antiserum, and immunocytochemical localization of the enzyme in neural cells. *J Neurochem,* **73,** 1422-1430.

Hoepken, H. H., Korten, T., Robinson, S. R. and Dringen, R. (2004) Iron accumulation, iron-mediated toxicity and altered levels of ferritin and transferrin receptor in cultured astrocytes during incubation with ferric ammonium citrate. *J Neurochem,* **88,** 1194-1202.

Hohnholt, M., Geppert, M. and Dringen, R. (2010) Effects of iron chelators, iron salts and iron oxide nanoparticles on the proliferation and the iron content of oligodendroglial OLN-93 cells. *Neurochem Res,* **35,** 1259-1268.

Hohnholt, M. C. and Dringen, R. (2011) Iron-dependent formation of reative oxygen species and glutathione depletion after accumulation of magnetic iron oxide nanoparticles by oligodendroglial cells. *J Nanopart Res,* **13,** 6761-6774.

Hohnholt, M. C., Geppert, M. and Dringen, R. (2011) Treatment with iron oxide nanoparticles induces ferritin synthesis but not oxidative stress in oligodendroglial cells. *Acta Biomater,* **7,** 3946-3954.

Huth, U. S., Schubert, R. and Peschka-Suss, R. (2006) Investigating the uptake and intracellular fate of pH-sensitive liposomes by flow cytometry and spectral bio-imaging. *J Control Release,* **110,** 490-504.

Ivanov, A. I. (2008) Pharmacological inhibition of endocytic pathways: is it specific enough to be useful? *Methods Mol Biol,* **440,** 15-33.

Kakhlon, O. and Cabantchik, Z. I. (2002) The labile iron pool: characterization, measurement, and participation in cellular processes. *Free Radic Biol Med,* **33,** 1037-1046.

Kaltz, A. (2011) *Herstellung und Charakterisierung von fluoreszenzmarkierten Eisenoxid-Nanopartikeln*, Bachelor Thesis, University of Bremen.

Kim, J. S., Yoon, T. J., Yu, K. N., Noh, M. S., Woo, N., Kim, B. G., Lee, K. H., Sohn, B. H., Park, S. B., Lee, J. K. and Cho, M. H. (2006) Cellular uptake of magnetic nanoparticles is mediated through energy-dependent endocytosis in A549 cells. *J Vet Sci,* **7,** 321-326.

Kumari, S., Mg, S. and Mayor, S. (2010) Endocytosis unplugged: multiple ways to enter the cell. *Cell Res,* **20,** 256-275.

Kwon, J. T., Hwang, S. K., Jin, H., Kim, D. S., Minai-Tehrani, A., Yoon, H. J., Choi, M., Yoon, T. J., Han, D. Y., Kang, Y. W., Yoon, B. I., Lee, J. K. and Cho, M. H. (2008) Body distribution of inhaled fluorescent magnetic nanoparticles in the mice. *J Occup Health,* **50,** 1-6.

Laurent, S., Forge, D., Port, M., Roch, A., Robic, C., Elst, L. V. and Muller, R. N. (2008) Magnetic iron oxide nanoparticles: Synthesis, stabilization, vectorization, physicochemical characterizations, and biological applications. *Chem Rev,* **108,** 2064-2110.

Levy, M., Lagarde, F., Maraloiu, V. A., Blanchin, M. G., Gendron, F., Wilhelm, C. and Gazeau, F. (2010) Degradability of superparamagnetic nanoparticles in a model of intracellular environment: follow-up of magnetic, structural and chemical properties. *Nanotechnology,* **21,** 395103.

Lopez-Castro, J. D., Maraloiu, A. V., Delgado, J. J., Calvino, J. J., Blanchin, M. G., Galvez, N. and Dominguez-Vera, J. M. (2011) From synthetic to natural nanoparticles: monitoring the biodegradation of SPIO (P904) into ferritin by electron microscopy. *Nanoscale,* **3,** 4597-4599.

Luther, E. M., Koehler, Y., Diendorf, J., Epple, M. and Dringen, R. (2011) Accumulation of silver nanoparticles by cultured primary brain astrocytes. *Nanotechnology,* **22,** 375101.

Lynch, I. and Dawson, K. A. (2008) Protein-nanoparticle interactions. *Nano Today,* **3,** 40-47.

Maity, D. and Agrawal, D. C. (2007) Synthesis of iron oxide nanoparticles under oxidizing environment and their stabilization in aqueous and non-aqueous media. *J Magn Magn Mater,* **308,** 46-55.

Mayhew, T. M. (2011) Mapping the distributions and quantifying the labelling intensities of cell compartments by immunoelectron microscopy: progress towards a coherent set of methods. *J Anat,* **219,** 647-660.

Megias, L., Guerri, C., Fornas, E., Azorin, I., Bendala, E., Sancho-Tello, M., Duran, J. M., Tomas, M., Gomez-Lechon, M. J. and Renau-Piqueras, J. (2000) Endocytosis and transcytosis in growing astrocytes in primary culture. Possible implications in neural development. *Int J Dev Biol,* **44,** 209-221.

Murillo, T. P., Sandquist, C., Jacobs, P. M., Nesbit, G., Manninger, S. and Neuwelt, E. A. (2005) Imaging brain tumors with ferumoxtran-10, a nanoparticle magnetic resonance contrast agent. *Therapy,* **2,** 871-882.

Nel, A. E., Madler, L., Velegol, D., Xia, T., Hoek, E. M., Somasundaran, P., Klaessig, F., Castranova, V. and Thompson, M. (2009) Understanding biophysicochemical interactions at the nano-bio interface. *Nat Mater,* **8,** 543-557.

Ozols, J. (1990) Preparation of membrane fractions. *Methods Enzymol,* **182,** 225-235.

Petrat, F., de Groot, H., Sustmann, R. and Rauen, U. (2002) The chelatable iron pool in living cells: a methodically defined quantity. *Biol Chem,* **383,** 489-502.

Petri-Fink, A. and Hofmann, H. (2007) Superparamagnetic iron oxide nanoparticles (SPIONs): from synthesis to in vivo studies – a summary of the synthesis, characterization, in vitro, and in vivo investigations of SPIONs with particular focus on surface and colloidal properties. *IEEE Trans Nanobioscience,* **6,** 289-297.

Petri-Fink, A., Steitz, B., Finka, A., Salaklang, J. and Hofmann, H. (2008) Effect of cell media on polymer coated superparamagnetic iron oxide nanoparticles (SPIONs): Colloidal stability, cytotoxicity, and cellular uptake studies. *Eur J Pharm Biopharm,* **68,** 129-137.

Petters, C. (2010) *Investigations on the subcellular localization of iron oxide nanoparticles in cultured astrocytes*, Master Thesis, University of Bremen.

Pickard, M. and Chari, D. (2010) Enhancement of magnetic nanoparticle-mediated gene transfer to astrocytes by 'magnetofection': effects of static and oscillating fields. *Nanomedicine,* **5,** 217-232.

Pickard, M. R., Jenkins, S. I., Koller, C. J., Furness, D. N. and Chari, D. M. (2011) Magnetic nanoparticle labeling of astrocytes derived for neural transplantation. *Tissue Eng Part C Methods,* **17,** 89-99.

Platta, H. W. and Stenmark, H. (2011) Endocytosis and signaling. *Curr Opin Cell Biol,* **23,** 393-403.

Prijic, S., Scancar, J., Romih, R., Cemazar, M., Bregar, V. B., Znidarsic, A. and Sersa, G. (2010) Increased cellular uptake of biocompatible superparamagnetic iron oxide nanoparticles into malignant cells by an external magnetic field. *J Membr Biol,* **236,** 167-179.

Racuciu, M., Creanga, D. E. and Airinei, A. (2006) Citric-acid-coated magnetite nanoparticles for biological applications. *Eur Phys J E Soft Matter,* **21,** 117-121.

Reinhart, P. H., Pfeiffer, B., Spengler, S. and Hamprecht, B. (1990) Purification of glycogen phosphorylase from bovine brain and immunocytochemical examination of rat glial primary cultures using monoclonal antibodies raised against this enzyme. *J Neurochem,* **54,** 1474-1483.

Rejman, J., Oberle, V., Zuhorn, I. S. and Hoekstra, D. (2004) Size-dependent internalization of particles via the pathways of clathrin- and caveolae-mediated endocytosis. *Biochem J,* **377,** 159-169.

Riemer, J., Hoepken, H. H., Czerwinska, H., Robinson, S. R. and Dringen, R. (2004) Colorimetric ferrozine-based assay for the quantitation of iron in cultured cells. *Anal Biochem,* **331,** 370-375.

Sandvig, K., Pust, S., Skotland, T. and van Deurs, B. (2011) Clathrin-independent endocytosis: mechanisms and function. *Curr Opin Cell Biol,* **23,** 413-420.

Tedelind, S., Poliakova, K., Valeta, A., Hunegnaw, R., Yemanaberhan, E. L., Heldin, N. E., Kurebayashi, J., Weber, E., Kopitar-Jerala, N., Turk, B., Bogyo, M. and Brix, K. (2010) Nuclear cysteine cathepsin variants in thyroid carcinoma cells. *Biol Chem,* **391,** 923-935.

Tiffany-Castiglioni, E., Hong, S. and Qian, Y. (2011) Copper handling by astrocytes: insights into neurodegenerative diseases. *International journal of developmental neuroscience : the official journal of the International Society for Developmental Neuroscience,* **29,** 811-818.

Tiffany-Castiglioni, E. and Qian, Y. C. (2001) Astroglia as metal depots: Molecular mechanisms for metal accumulation, storage and release. *Neurotoxicology,* **22,** 577-592.

Tulpule, K., Robinson, S. R., Bishop, G. M. and Dringen, R. (2010) Uptake of ferrous iron by cultured rat astrocytes. *J Neurosci Res,* **88,** 563-571.

Valois, C. R., Braz, J. M., Nunes, E. S., Vinolo, M. A., Lima, E. C., Curi, R., Kuebler, W. M. and Azevedo, R. B. (2010) The effect of DMSA-functionalized magnetic nanoparticles on transendothelial migration of monocytes in the murine lung via a beta2 integrin-dependent pathway. *Biomaterials,* **31,** 366-374.

van Landeghem, F. K., Maier-Hauff, K., Jordan, A., Hoffmann, K. T., Gneveckow, U., Scholz, R., Thiesen, B., Bruck, W. and von Deimling, A. (2009) Post-mortem studies in glioblastoma patients treated with thermotherapy using magnetic nanoparticles. *Biomaterials,* **30,** 52-57.

Voinov, M. A., Sosa Pagan, J. O., Morrison, E., Smirnova, T. I. and Smirnov, A. I. (2011) Surface-mediated production of hydroxyl radicals as a mechanism of iron oxide nanoparticle biotoxicity. *J Am Chem Soc,* **133,** 35-41.

Wang, F. H., Kim, D. K., Yoshitake, T., Johansson, S. M., Bjelke, B., Muhammed, M. and Kehr, J. (2011) Diffusion and clearance of superparamagnetic iron oxide nanoparticles infused into the rat striatum studied by MRI and histochemical techniques. *Nanotechnology,* **22,** 015103.

Wang, J., Chen, Y., Chen, B., Ding, J., Xia, G., Gao, C., Cheng, J., Jin, N., Zhou, Y., Li, X., Tang, M. and Wang, X. M. (2010) Pharmacokinetic parameters and tissue distribution of magnetic Fe_3O_4 nanoparticles in mice. *Int J Nanomedicine,* **5,** 861-866.

Westergaard, N., Sonnewald, U., Unsgard, G., Peng, L., Hertz, L. and Schousboe, A. (1994) Uptake, release, and metabolism of citrate in neurons and astrocytes in primary cultures. *J Neurochem,* **62,** 1727-1733.

Wilhelm, C. and Gazeau, F. (2008) Universal cell labelling with anionic magnetic nanoparticles. *Biomaterials,* **29,** 3161-3174.

Winer, J. L., Kim, P. E., Law, M., Liu, C. Y. and Apuzzo, M. L. (2011) Visualizing the future: enhancing neuroimaging with nanotechnology. *World Neurosurg,* **75,** 626-637.

Wiogo, H. T. R., Lim, M., Bulmus, V., Yun, J. and Amal, R. (2011) Stabilization of magnetic iron oxide nanoparticles in biological media by fetal bovine serum (FBS). *Langmuir,* **27,** 843-850.

Wu, L. J., Leenders, A. G., Cooperman, S., Meyron-Holtz, E., Smith, S., Land, W., Tsai, R. Y., Berger, U. V., Sheng, Z. H. and Rouault, T. A. (2004) Expression of the iron transporter ferroportin in synaptic vesicles and the blood-brain barrier. *Brain Res,* **1001,** 108-117.

Yang, H. (2010) Nanoparticle-mediated brain-specific drug delivery, imaging, and diagnosis. *Pharm Res,* **27,** 1759-1771.

Yigit, M. V., Moore, A. and Medarova, Z. (2012) Magnetic Nanoparticles for Cancer Diagnosis and Therapy. *Pharm Res, in press*.

Yiu, H. H., Pickard, M. R., Olariu, C. I., Williams, S. R., Chari, D. M. and Rosseinsky, M. J. (2011) Fe_3O_4-PEI-RITC Magnetic Nanoparticles with Imaging and Gene Transfer Capability: Development of a Tool for Neural Cell Transplantation Therapies. *Pharm Res, in press*.

<u>Part 4</u>

Appendix

4.1 Curriculum vitae

Personal Information:

Name:	Mark Geppert
Date of birth:	28th of August 1982
Place of birth:	Bremen, Germany
Marital status:	Unmarried
Parents:	Uwe Geppert; self-employed businessman Bärbel Geppert; retail sales clerk
Brothers and sisters:	One brother, Marius, date of birth: 28th of August 1982

Education:

06/2002	**Abitur (general qualification for university entrance)** Gymnasium Syke, Germany
10/2002 – 07/2008	**Studies of chemistry** University of Bremen, Germany
14th of July 2008	**Diploma**
Since 12/2008	**Doctoral thesis in neurochemistry**
	Topic: „Synthesis and characterization of iron oxide nanoparticles and investigation of their biocompatibility on astrocyte cultures"

Voluntary services:

1997 – 2011	Member of the **Federal Agency for Technical Relief (THW)** local association Syke, Germany
Since 02/2002	Board member (THW)

Other Memberships:

Since 08/2010	Member of the **European Society for Neurochemistry (ESN)**

4.2   List of publications

Geppert, M., Hohnholt, M. C., Gaetjen, L., Grunwald, I., Bäumer, M., Dringen, R. (2009) Accumulation of iron oxide nanoparticles by cultured brain astrocytes. *J Biomed Nanotechnol* **5,** 285-293.

Hohnholt, M. C., **Geppert, M.**, Dringen, R. (2010) Effects of iron chelators, iron salts, and iron oxide nanoparticles on the proliferation and the iron content of oligodendroglial OLN-93 cells. *Neurochem Res* **35,** 1259-1268.

Hohnholt, M. C., **Geppert, M.**, Nürnberger, S., von Byern, J., Grunwald, I., Dringen, R. (2010) Accumulation of citrate-coated magnetic iron oxide nanoparticles by cultured brain astrocytes. *Adv Eng Mater* **12,** B690-694.

Geppert, M., Hohnholt, M. C., Thiel, K., Nürnberger, S., Grunwald, I., Rezwan, K., Dringen, R. (2011) Uptake of dimercaptosuccinate-coated magnetic iron oxide nanoparticles in cultured brain astrocytes. *Nanotechnology* **22,** 145101.

Lamkowsky, M., **Geppert, M.**, Schmidt, M. M., Dringen, R. (2011) Magnetic field-induced acceleration of the accumulation of magnetic iron oxide nanoparticles by cultured brain astrocytes. *J Biomed Mater Res* A, **100,** 323-334.

Hohnholt, M. C., **Geppert, M.**, Dringen, R. (2011) Treatment with iron oxide nanoparticles induces ferritin synthesis but not oxidative stress in oligodendroglial cells. *Acta Biomater*, **7,** 3946-3954.

Geppert, M., Dringen, R. (2012) Presence of serum alters the properties of iron oxide nanoparticles and lowers their accumulation by cultured brain astrocytes. *Submitted for publication*.

Geppert, M., Hohnholt, M. C., Nürnberger, S., Dringen, R. (2012) Ferritin upregulation and transient ROS production in cultured brain astrocytes after loading with iron oxide nanoparticles. *Submitted for publication*.